Ökomorphologische Diversität und Funktion des Klebfangapparates mitteleuropäischer *Stenus*-Arten (Coleoptera, Staphylinidae)

Dissertation

der Mathematisch-Naturwissenschaftlichen Fakultät
der Eberhard Karls Universität Tübingen
zur Erlangung des Grades eines
Doktors der Naturwissenschaften
(Dr. rer. nat.)

vorgelegt von
Lars Koerner
aus Berlin

Tübingen
2020

Gedruckt mit Genehmigung der Mathematisch-Naturwissenschaftlichen Fakultät der Eberhard Karls Universität Tübingen.

Tag der mündlichen Qualifikation:	15.07.2020
Dekan:	Prof. Dr. Wolfgang Rosenstiel
1. Berichterstatter:	Prof. Dr. O. Betz
2. Berichterstatter:	PD Dr. Michael Heethoff

Inhalt

Übersicht über Publikationen (vollständige Publikationsliste siehe Kapitel 10 „Lebenslauf“) sowie Anteil der Autoren:

Publikationen als Erstautor

Publikation I:

Functional morphology and adhesive performance of the stick-capture apparatus of the rove beetles *Stenus* spp. (Coleoptera, Staphylinidae)

Lars Koerner, Stanislav N Gorb, Oliver Betz (2012). *Zoology* 115: 117–127.

Publikation II

Adhesive performance of the stick-capture apparatus of rove beetles of the genus *Stenus* (Coleoptera, Staphylinidae) toward various surfaces

Lars Koerner, Stanislav N Gorb, Oliver Betz (2012). *Journal of Insect Physiology* 58: 155–163.

Publikation III

Divergent morphologies of adhesive predatory mouthparts of *Stenus* species (Coleoptera, Staphylinidae) explain differences in adhesive performance and resulting prey-capture success

Lars Koerner, László Zsolt Garamszegi, Michael Heethoff, Oliver Betz (2017). *Zoological Journal of the Linnean Society*, 181: 500–518.

Publikation IV

The labial adhesive pads of rove beetles of the genus *Stenus* (Coleoptera: Staphylinidae) as carriers of bacteria

Lars Koerner, Volkmar Braun, Oliver Betz (2016). *Entomologia Generalis* 36: 33–41.

Publikation V

Loss of the sticky harpoon—COI sequences indicate paraphyly of *Stenus* with respect to *Dianous* (Staphylinidae, Steninae)

Lars Koerner, Michael Laumann, Oliver Betz, Michael Heethoff (2013). *Zoologischer Anzeiger* 252: 337–347.

Anteil der Autoren an den vorgelegten Publikationen:

Lars Koerner: Design und Durchführung der Experimente und Studien, Feldprobenahme, Datenerfassung und -analyse, Vorbereitung und Verfassen der Manuskripte zur Veröffentlichung

Oliver Betz: Betreuung der gesamten Arbeit

Stanislav N. Gorb: Mitarbeit bei der Versuchsplanung, methodische Unterstützung, Diskussion der Manuskripte (Publikationen I und II)

Michael Heethoff: Methodische Unterstützung und Beteiligung an der Versuchsplanung und Datenanalyse, Diskussion der Manuskripte (Publikation III und V)

Michael Laumann: Methodische Unterstützung und Beteiligung an der Versuchsplanung und Datenanalyse, Diskussion des Manuskriptes (Publikation V)

László Zsolt Garamszegi: Methodische Unterstützung und Beteiligung an der Datenanalyse und Diskussion des Manuskriptes (Publikation III)

Volkmar Braun: Methodische Unterstützung und Beteiligung an der Datenanalyse und Diskussion des Manuskriptes (Publikation IV)

Zusammenfassung

Mit mehr als 3000 beschriebenen Arten bildet die Gattung *Stenus* die artenreichste Tiergattung überhaupt (Puthz, pers. Mitt.). Innerhalb der Familie der Staphylinidae gelten sie als die einzigen Vertreter, die ein stabförmig verlängertes Fanglabium aufweisen, das durch Hämolymphdruck innerhalb weniger Millisekunden hervorgeschnellt werden kann. Bleibt ein Beutetier an den zu Haftpolstern umgebildeten Paraglossen haften, wird die Beute durch Retraktion des Labiums zwischen die Mandibeln gebracht und kann gefressen werden. Die beim Beutefang auftretenden Haftkräfte wurden bislang nur theoretisch bestimmt (Kölsch 2000), während die beim Ausschleudern des Labiums auftretenden Druckkräfte noch völlig unbekannt sind.

Zentraler Teil der vorliegenden Arbeit ist die Bestimmung der über den Klebfangmechanismus erzeugten Druck- und Zugkraft. Dazu wurde eine Messmethode, mit der es erstmals möglich ist, den genauen zeitlichen Verlauf der entwickelten Kräfte zu verfolgen und statistisch auszuwerten. Die Tiere sind visuell orientiert und "schießen" mit ihren Klebzungen auf einen sich bewegenden Insektennadelkopf, der mit einem Kraftmessgerät verbunden ist (**Publikationen I-III**). Umfangreiche Studien von Betz (1996) an verschiedenen *Stenus*-Arten zeigten, dass größere und strukturell komplexere Haftpolster zu einem erhöhtem Fangerfolg führen. Diese Schlussfolgerung wird durch die neuen Experimente unterstützt und mit der Integration der Performanzmessungen kann nun erstmalig ein direkter Zusammenhang zwischen der Morphologie der Haftpolster, deren Haftperformanz und dem Beutefangerfolg hergestellt werden.

Die während des Klebfanges entstehenden Druck- (beim Auftreffen der Klebpolster auf eine Beuteattrappe) und Adhäsionskräfte (beim Rückzug der Klebpolster von der Attrappe) wurden bei 14 mitteleuropäischen Vertretern der Gattung *Stenus* bestimmt (**Publikation III**). Mit Werten zwischen 0.28 mN bei *S. morio* und 1.08 mN bei *S. bimaculatus* zeigen vor allem die Adhäsionskräfte signifikante interspezifische Unterschiede, welche auf die unterschiedliche Größe und die Komplexität der Haftpolster (d.h. der Anzahl an Hafthaaren und Haftkontakten) zurückzuführen sind (**Publikation III**). Die durchschnittlichen Druckkräfte während des Fangschlages erreichten Werte zwischen 0.05 mN bei *S. biguttatus* und 0.18 mN bei *S. juno* und waren somit um eine Größenordnung niedriger als die Adhäsionskräfte. Außerdem konnte gezeigt werden, dass ein signifikanter Zusammenhang zwischen Druckkraft und Zug- (Adhäsions-)kraft besteht, d.h., je größer die Kraft mit der die Klebpolster auf ein Beuteobjekt auftreffen, desto größer ist auch die Adhäsion zwischen Klebpolstern und Beute. Dieses Ergebnis weist auf einen druckempfindlichen Haftmechanismus bei *Stenus* hin.

Die phylogenetisch-vergleichenden Analysen zeigten weiterhin, dass sich die Zugfestigkeit (Haftkraft pro Haftposterfläche) mit zunehmender Haftpolsterfläche verringert, sodass *Stenus*-Arten mit

kleineren Haftpolstern zwar geringere absolute Adhäsionskräfte erzeugen, aber insgesamt höhere Zugfestigkeiten erreichen und somit adhäsiv effizientere Haftpolster besitzen. Die berechneten Werte für die Zugfestigkeit lagen dabei zwischen 51.9 kPa bei *S. bimaculatus* und 153.2 kPa bei *S. humilis* (**Publikation I, III**). Die negative Korrelation von Zugfestigkeit und Haftpolsterfläche zeigt, dass das Haftsekret, welches während des Fangschlages über die Fläche des Haftpolsters verteilt wird, einen sehr großen Beitrag zur Haftfähigkeit des Fangapparates leistet. Dadurch sind auch Arten mit kleineren Haftpolstern befähigt, eine relativ gute Haftperformanz zu erreichen.

Die während des Fangschlages auftretenden Kräfte können in Bezug mit Daten über den Fangerfolg bei verschiedenen Beutegrößen gesetzt werden. Bei diesen Fangversuchen wurden verschiedene einheimische *Stenus*-Arten mit Springschwänzen (*Heteromurus nitidus*) verschiedener Größen- (bzw. Gewichts-)klassen konfrontiert und die Anwendungshäufigkeiten beider Fangtechniken (Labium/Mandibel) sowie der Fangerfolg analysiert. Die Analysen zeigten, dass eine höhere Adhäsionskraft der Klebpolster zu einem höheren Fangerfolg gegenüber Collembolen der Art *H. nitidus* führt. Dieser Effekt war beim Fang größerer Collembolen wesentlich stärker ausgeprägt ($p < 0.001$) als beim Fang kleiner Collembolen ($p < 0.1$) (**Publikation III**).
Außerdem wurde die Haftleistung der Klebzunge auf Oberflächen unterschiedlicher Rauigkeit und Oberflächenenergie untersucht (**Publikation II**). Dazu wurden unterschiedliche Oberflächen am Insektennadelkopf angebracht und die Haftperformanz bestimmt (**Publikation II**). Es stellte sich heraus, dass die Haftleistung der Klebpolster von *S. juno* und *S. bimaculatus* selbst auf sehr rauen Oberflächen nicht vermindert ist. Diese Beobachtung weist darauf hin, dass es sich bei dem Haftsekret der Käfer um einen echten Klebstoff handelt, da auch diese eine gleichbleibende bzw. bessere Klebfestigkeit auf rauen Oberflächen erreichen. Die Bedeutung rauer Oberflächen für die Haftkraft liegt einerseits in der besseren Verzahnung von Klebstoff und Oberfläche und andererseits in der Vergrößerung der Kontaktfläche zwischen Klebstofffilm und Substrat und damit in der Steigerung der spezifischen Adhäsionskräfte. Des Weiteren konnte gezeigt werden, dass sich die Haftkräfte auf Oberflächen mit unterschiedlichen Oberflächenenergien nur geringfügig voneinander unterscheiden **(Publikation II)**. Auf Oberflächen mit geringer Oberflächenenergie (hydrophobe Oberfläche) ist die Haftleistung zwar vermindert, kann jedoch wahrscheinlich infolge der Zusammensetzung des Haftsekretes aus hydrophilen und hydrophoben Komponenten kompensiert werden.

Die Klebpolster bestehen aus mehreren Funktionselementen, die synergistisch während des Beutefangprozesses zusammenwirken (**Publikation I**). Das Netzwerk aus weichen endokutikularen Fasern stabilisiert das Haftpolsterinnere und verleiht der gesamten Struktur Flexibilität und Elastizität (in Verbindung mit dem elastischen Protein Resilin), so dass sie sich an die speziellen Formen und Oberflächenunregelmäßigkeiten der Beutetiere anpassen kann. Das dichte Netz aus kutikulären Fasern unterstützt beim Fangschlag mechanisch die eigentliche Kleboberfläche, die in zahlreiche Hafthaare

strukturiert ist. Diese Hafthaare sind während des Fangschlages fast vollständig mit dem Sekret benetzt werden - lediglich deren terminale Verzeigungen ragen aus dem Sekret. Die Unterteilung der Haftkontakte in viele Einzelelemente ist verantwortlich für den optimalen Haftkontakt zwischen den Haftpolstern und den unvorhersehbaren Oberflächenstrukturen der Beutetiere (in Kombination mit dem Haftsekret). Außerdem ermöglichen derartige endständige Verzweigungsstrukturen generell eine höhere Packungsdichte der Hafthaare, da die endständigen Verzweigungen ein Verkleben benachbarter Hafthaare verhindern. Die histochemischen Färbungen ergaben, dass es sich bei dem Haftsekret um ein komplexes Gemisch aus mehr als nur einer chemischen Phase handelt, d.h. aus einer Emulsion aus wasserlöslichen (Zucker: Mucopolysacchariden; Proteine) und fettlöslichen (Lipide) Komponenten. Die meisten in der Natur vorkommenden Haftsysteme basieren ebenfalls auf proteinösen sowie zuckerhaltigen Komponenten (siehe Scherge & Gorb, 2001). Wie für das Tarsalsekret von Heuschrecken (siehe Scherge & Gorb, 2001) vermutet, könnte eine solche Emulsion für die effektive Verteilung des Sekrets über verschiedene Oberflächentypen (hydrophil und lipophil) von Vorteil sein. Die große Sekretmenge, die hohe Viskosität des Sekretes sowie die Tatsache, dass deren Haftwirkung bei hoher Geschwindigkeit auftritt, lassen vermuten, dass der Adhäsionsmechanismus vor allem auf den viskosen Eigenschaften des Sekrets basiert (Stefan-Adhäsion). Die hohe Viskosität konnte durch Hochgeschwindigkeits-Videoaufnahmen belegt werden, auf denen das Zurückziehen der Klebpolster von einer Oberfläche zu sehen ist: wie bei kommerziell verfügbaren Haftklebstoffen dehnt sich das Sekret dabei aus und gliedert sich in lange parallele Fasern (Fibrillation) auf, bevor es schließlich an der Kontaktzone mit dem Substrat abreißt. Diese Eigenschaft des Haftsekretes steht im Zusammenhang mit einer hohen inneren Festigkeit, sodass die Verbindung nicht innerhalb des Sekretes bricht (hohe kohäsive Kräfte). Zusammenfassend lässt sich folgern, dass es sich bei dem Beutefangapparat der Gattung *Stenus* um ein hierarchisch aufgebautes System handelt, bei dem ein multiphasisches Haftsekret mit der spezifischen Struktur terminal verzweigter Hafthaare kombiniert ist.

Zwischen den Hafthaaren im Sekret befinden sich zahlreiche Bakterien, deren Funktion bisher unbekannt ist. Über die Sequenzierung des ribosomalen 16S rRNA-Gens wurden diese Bakterien identifiziert (**Publikation IV**). Die Analyse ergab eine vielfältige Bakterienzusammensetzung: die meisten dieser Bakterien konnten den Gruppen der Actinomycetales (*Arthrobacter*, *Microbacterium*, *Rhodococcus*) und Pseudomonadales (*Acinetobacter*, *Pseudomonas*) zugeordnet werden. Die Bakteriendiversität innerhalb des Haftsekretes ist wahrscheinlich sogar noch größer, da nur Arten identifiziert wurden, die *in vitro* auf Agarplatten kultiviert werden konnten. Die Bakterien leben als Kommensalen im Haftsekret bei *Stenus* und nutzen möglicherweise die verschiedenen Komponenten des Haftsekretes als Nahrungsquelle (Mucopolysaccharide, Proteine, Lipide).

Zusammenfassung

Der Klebfangapparat wurde bisher als prominenteste Autapomorphie der Gattung *Stenus* angesehen und galt als wesentliches Abgrenzungsmerkmal für die Monophylie dieser Gattung gegenüber der Schwestergattung *Dianous*. Im Vergleich zu *Stenus* zeigt das Labium der Gattung *Dianous* allerdings den gleichen Grundbauplan, nur in verkürzter Form, wobei die Paraglossen bei *Dianous* nicht zu Haftpolstern differenziert sind. Bisher wurde davon ausgegangen, dass das morphologisch einfach gebaute, verkürzte Labium von *Dianous* den plesiomorphen, und das vorschnellbare Fanglabium mit den modifizierten Paraglossen von *Stenus* den apomorphen Zustand darstellt. Diese Vermutung wurde in einem weiteren Teil der Dissertation mit Hilfe molekularer Sequenzdaten von 41 Arten der Gattung *Stenus* sowie 13 Arten der Gattung *Dianous* analysiert (**Publikation V**). Die Analyse des Cytochrom Oxidase I (COI)-Gens zeigte interessanterweise, dass die untersuchten *Dianous*-Arten eine monophyletische Gruppe innerhalb der Gattung *Stenus* bilden, wobei Arten der Untergattung *Stenus* s. str. (*S. ater*-, *clavicornis*-, *humilis*- und *guttula*-Gruppe) dabei eine Nachbarposition zu *Dianous* einnehmen. Aus Konsequenz der phylogenetischen Untersuchungen ist allerdings eine sekundäre Reduktion des ehemals komplexeren Fangapparates bei *Dianous* wahrscheinlich. Diese Aussage wird durch (i) Untersuchungen der Gensequenzabschnitte COI, 16S rRNA, Histon H3 (Lang et al. 2015) und 18S rDNA (Grebennikov & Newton 2009), (ii) chemische Analysen des Pygidialdrüsensekretes (Lang et al. 2015) sowie (iii) bisher unveröffentlichte Studien zur Kopfmorphologie (Gold, unpublizierte Diplomarbeit) bestätigt. Allerdings sind weitergehende morphologische und phylogenetische Untersuchungen mit einer größeren Artenzahl sowie anderen Genen nötig, um ein genaueres Bild über die Verwandtschaftsbeziehungen der „Schwestergattungen“ *Stenus* und *Dianous* zu geben.

Summary

The genus *Stenus* Latreille, 1796 (Coleoptera, Staphylinidae) is one of the largest beetle genera, comprising more than 3000 species widely distributed throughout the world (Puthz, pers. comm.). Within the family Staphylinidae they are the only representatives that are characterized by an elongated labium which can be protruded towards the potential prey extremely rapidly (within 1–3 ms) by haemolymph pressure. The paraglossae at the distal end of the rod-like prementum are modified into adhesive pads, whose surface is differentiated into terminally branched outgrowths. As soon as the prey adheres to these sticky pads, the labium is instantly retracted and the beetle can seize the prey with its mandibles. To date, the adhesive forces generated during the predatory strike of these beetles have only been estimated theoretically (Kölsch 2000) while the impact (compressive) forces of the labium hitting the prey are completely unknown.

A central part of the present dissertation was the identification of both the compressive and adhesive forces during the predatory strike of *Stenus* beetles. Using micro force sensors I succeeded in measuring, graphically displaying and statistically analyzing the temporal course of the adhesive and compressive force values. These measurements were carried out with the head of an insect pin which was used as a prey dummy. *Stenus* beetles are visually oriented predators and the strike at the dummy causes force sensor deflection that was digitally recorded and later processed (**Publications I-III**). Extensive studies by Betz (1996, 1998a) revealed that larger surface areas of the adhesive pads and more adhesive outgrowths and adhesive contacts lead to improved adhesion and consequently increased capture success. My experimental approach supports this conclusion and demonstrates for the first time a direct functional relationship between the morphology of the prey-capture device of *Stenus* beetles and its adhesive performance in a natural behavioural context.

The compressive and adhesive forces generated during the beetles' predatory strike were determined in 14 species of this genus which cover a representative size range of Central European *Stenus* species (**Publication III**). The measurements revealed strong interspecific differences in the adhesive forces generated during the predatory attack, which varied from 0.28 mN in *S. morio* to 1.08 mN in *S. bimaculatus*. The variations in the adhesive efficiency are functionally correlated with the morphology of the adhesive pads, e.g. their surface area and their number of adhesive outgrowths, and divergences in the compressive forces generated during the predatory strike, ranging from 0.05 mN in *S. biguttatus* to 0.18 mN in *S. juno*. Thus, the experiments strongly suggest that the involved adhesive mechanism is pressure-sensitive, i.e. that higher compressive forces result in better adhesive performances.

The mean tenacity, as calculated by dividing the mean adhesive force by the mean surface areas of both adhesive pads, amounted to between 51.9 kPa in *S. bimaculatus* and 153.2 kPa in *S. humilis*.

Allometric analyses revealed that the tenacity shows negative correlations with the surface area of the adhesive pad and the size parameters, i.e. pronotum length and body mass. Thus, although species with smaller adhesive pads (which usually corresponded to smaller body sizes) generated lower absolute values of the adhesive forces, they attained higher tenacities and therefore had more adhesively efficient pads (**Publications I, III**). These negative relationships might mean that the action of the adhesive secretion alone plays a more important role than the size and morphological complexity of the adhesive pads, i.e. the adhesive strength of the secretion probably overrides the adhesive impact of the pad size and the inter-correlated number of adhesive contacts. This would be an important functional feature, especially for species with smaller adhesive pads, since it enables them to achieve a relatively high adhesive performance.

My approach reveals how interspecific differences in the adhesive pad morphology (i.e. their surface area and their number of adhesive outgrowths) lead to differences in the adhesive forces generated during the predatory attack and thus influences the prey-capture success towards springtails. The analysis revealed that the adhesive forces attained by the various pad morphologies influenced the prey-capture success towards large springtails of *Heteromurus nitidus* ($p < 0.001$), while this relationship was only almost significant ($p < 0.1$) for small springtails of this species. Thus, higher adhesive forces lead to higher prey-capture success rates in *Stenus* beetles; this effect was more pronounced towards large-sized springtails (**Publication III**).

Stenus species are polyphagous predators that consume a variety of prey species. Thus, their prey-capture apparatus should be able to adapt to a wide range of natural substrates with a variety of physico-chemical properties and surface topographies differing in dimensions by several orders of magnitude. Thus, the influence of both surface energy and roughness of the substrate on the adhesive performance of the prey-capture apparatus was investigated in two *Stenus* species (**Publication II**). The same experimental setup as described above was used to measure the adhesive forces generated during the predatory strike on (1) epoxy resin surfaces with defined roughness values and (2) hydrophobic versus hydrophilic glass surfaces. The results obtained by the force measurements demonstrate that the attachment efficiency of the adhesive pads is not affected by the surface roughness, since no critical surface roughness has been found such as that previously described for the tarsal adhesive organs of beetles and flies. The reason for this effect might be explained by (1) the small dimensions of the spherically shaped, terminal elements of their adhesive outgrowths and (2) the presence of a thick layer of adhesive secretion covering small substrate irregularities, thus increasing the real contact area with the non-smooth (prey) surface. Furthermore, the adhesive pads are able to attach to both hydrophobic and hydrophilic smooth surfaces. The latter effect might be explained by the multi-phasic composition of the adhesive secretion. Since, compared with the tarsal adhesive organs of insects, the reversibility of the adhesive bond probably does not represent a decisive

constraint in the functioning of the investigated prey-capture apparatus, the major selective advantage in this system might arise from its ability to adapt to a variety of prey surfaces. Thus, neither the surface roughness nor the surface energy significantly influences the attachment ability of the prey-capture apparatus and the prey-capture apparatus of *Stenus* beetles is therefore well adapted to adhere to the various unpredictable surfaces with diverse roughness and surface energy occurring in a wide range of potential prey.

The adhesive pads of *Stenus* beetles consist of different functional elements which work together synergistically during the prey-capture process (**Publication I**). The network of soft cuticular fibres stabilizes the interior of the adhesive pad and ensures that the entire structure is flexible and elastic, so it can adapt closely to the shape and surface irregularities of the prey. This functional feature is due to the adhesive pads being composed of a flexible, highly elastic cuticle containing resilin, an elastic protein. The dense network of endocuticular fibres provides mechanical support for the adhesive surface, which is made up of numerous, terminally branched adhesive outgrowths. During prey capture, the outgrowths are deeply immersed in the adhesive secretion, with only the tips of their terminal ramifications slightly protruding. The functional advantage of such a hierarchically organized structure lies in the break-up of the adhesive surface into a large number of independent elements that compensate for possible surface irregularities of the prey, although in the present case of a "flooded regime" (Bhushan, 2003; Mate, 2008), in which the adhesive contacts are deeply immersed within the secretion, the actual number of single contacts should be less important than the surface area of the entire adhesive pad. A branched morphology of the outgrowths is additionally advantageous, because these structures reduce the condensation between neighboring outgrowths, therefore allowing a higher packing density of the outgrowths. Histochemical tests revealed that the secretion is a complex mix of more than one chemical phases, i.e. droplets of a lipid-like substance are emulsified in a larger aqueous fraction (proteins and water-soluble sugars (mucopolysaccharides)). A possible advantage of such emulsion-like colloids consisting of both hydrophilic and hydrophobic compounds would be their effective spreading over surfaces of various surface energies (**Publication II**). The large quantity of adhesive secretion and the fact that its adhesive effect occurs at high speed make it plausible that Stefan adhesion based on the high viscosity of the secretion is the major mechanism involved in the investigated adhesive system. The high viscosity of the secretion is supported by high-speed video recordings during the retraction of the adhesive pad from a prey dummy surface: as in pressure-sensitive adhesives, the secretion elongates and splits into long fibres before finally breaking away from the contact area of the substrate. This observation is indicative of the high viscosity of the adhesive imparting a high cohesive strength which gives the secretion a high level of internal strength.

In summary, the prey-capture apparatus of beetles of the genus *Stenus* can be described as a hierarchical system in which a multi-phase adhesive secretion is combined with the specific structure

of adhesive outgrowths with terminal branches. Accordingly, the investigated adhesive system combines typical functional features of both wet and dry adhesive systems.

In some regions of the adhesive secretion, transmission electron microscopy revealed high densities of bacteria (**Publication IV**). Sequencing of the 16S ribosomal RNA gene identified a diverse bacterial composition with eight bacterial sequences being present in *S. bimaculatus* and five in *S. juno*. The majority of the bacteria belonged to the Actinomycetales (*Arthrobacter*, *Microbacterium*, *Rhodococcus*) and Pseudomonadales (*Acinetobacter*, *Pseudomonas*). Since freshly collected beetles in the field possess bacteria, we conclude that bacteria naturally occur within the adhesive secretion of *Stenus*, in which they might use the various components of the secretion (mucopolysaccharides, lipids, proteins) as a commensalic food source. The bacterial diversity within the secretion is probably even larger, since only those species that can be cultivated *in vitro* have been identified. Further microbiological characterization of the established bacteria might elucidate whether they influence the chemical composition of the secretion itself, as this might have an effect on the adhesive performance of the adhesive pads and thus the prey-capture success of the beetles.

The genus *Stenus* has been hypothesized to be monophyletic based on the possession of its protruding elongated labium. The labium of representatives of its sister genus *Dianous* is much shorter and also slightly eversible but lacks the adhesive pads of *Stenus*. Although the genus *Stenus* has been considered monophyletic on the basis of its possession of the labial adhesive capture apparatus and several other adult (mostly related to the prey-capture apparatus) and larval characters, the genus *Dianous* is not defined by any autapomorphies. Because of its simple labium and the developed paratergites at the abdomen, *Dianous* has always been considered more primitive than *Stenus*. Thus, it was hypothesized that the short and simple structured labium of *Dianous* represents the plesiomorphic, and the elongated labium of *Stenus* the apomorphic state. The aim of another part of the dissertation (**Publication V**) was to clarify the phylogenetic relationships of *Stenus* and *Dianous* on the basis of a molecular phylogeny using the barcoding gene cytochrome oxidase I (COI).

The most important result of the analysis of the COI gene in 41 *Stenus* and 13 *Dianous* species is the consistent position of the *Dianous* species of group II originating within *Stenus*, therefore rendering *Stenus* paraphyletic. All gene trees recovered a derived position of *Dianous* as a sister clade to one cluster of the subgenus *Stenus* s.str. (*S. ater*, *clavicornis*-, *humilis*- and *guttula*-group). This indicates the evolutionary origin of *Dianous* within *Stenus*, suggesting that the labial morphology of *Dianous* reflects a process of secondary reduction of the formerly more complex prey-capture apparatus rather than its precursor. The paraphyly of *Stenus* with respect to *Dianous* also corresponds to results based on (i) molecular analyses of 18S rDNA (Grebennikov & Newton 2009), COI, 16S rRNA und Histone H3 (Lang et al. 2015), (ii) chemotaxonomy of the pygidial gland secretion (Lang et al. 2015), and (iii)

previously unpublished data on the head morphology of *Stenus* and *Dianous* (Gold, unpublished diploma thesis). However, further investigations with a higher taxon sampling and other genes are needed to completely resolve the phylogenetic relationships of *Stenus* and *Dianous*.

1 Einleitung

1.1 Stand der Wissenschaft bezüglich des Klebfangapparates der Gattung *Stenus* Latreille, 1797

Die Untersuchung von Haftsystemen bei Insekten und anderen Arthropoden reicht zurück bis in das 19. Jahrhundert (z. B. Dewitz 1883). Die Thematik ist in den letzten dreißig Jahren wieder verstärkt aufgegriffen worden (z. B. Kendall 1970; Stork 1980; Dixon et al. 1990) und seit jüngster Zeit dank der Einführung neuester experimenteller und mikroskopischer Techniken in einen enormen Aufschwung begriffen (z. B. Attygalle et al. 2000; Federle et al. 2000; Jiao et al. 2000; Scherge & Gorb 2001). Dabei geht es um das Verständnis ganz unterschiedlicher Aspekte wie der generellen Morphologie und Ultrastruktur von Haftorganen (z. B. Gorb 2001), der chemischen Beschaffenheit tarsaler Haftsekrete (z. B. Attygalle et al. 2000), der Adhäsionsleistung von Haftstrukturen (z. B. Jiao et al. 2000) sowie der den Haftvorgängen zugrunde liegenden physikalischen Mechanismen (z. B. Dixon et al. 1990). Bei der vergleichenden Untersuchung der Vielfalt der Haftsysteme von Insekten zeigte sich, dass grundsätzlich zwei verschiedene Haftsysteme verwirklicht sind, nämlich entweder solche mit glatten oder solche mit behaarten Oberflächen (Beutel & Gorb 2001). Aufgrund ihrer hohen Flexibilität sind beide Systeme in der Lage, die Kontaktfläche zum Substrat unabhängig von dessen Rauigkeit zu maximieren. Dabei konnten in beiden Systemen (zum Teil nicht-lineare) Skalierungseffekte nachgewiesen und quantifiziert werden, die zeigen, wie die erzielbaren Haftkräfte von verschiedenen morphologischen Parametern der Haftstrukturen (zum Beispiel Anzahl und Fläche der Haftelemente) abhängen (Gorb 2001; Gorb et al. 2001; Arzt et al. 2003; Labonte & Federle 2015). Die den verschiedenen Haftsystemen zugrunde liegenden Mechanismen können von Fall zu Fall sehr unterschiedlich sein und werden in unterschiedlichem Ausmaß von van der Waals-, Kapillar-, Viskositäts- und Reibungskräften generiert (z.B. Israelachvili 1991; Scherge & Gorb 2001; Labonte & Federle 2015).

Adhäsionssysteme bei Insekten wurden in der Vergangenheit in erster Linie im Kontext von Lokomotionsvorgängen untersucht, bei welcher die Tarsen den Kontakt und die Haftung an Oberflächen unterschiedlicher Rauigkeit und Oberflächenenergie bewerkstelligen müssen (z. B. Stork 1980; Lees & Hardie 1988). Ein weiterer bislang wenig beachteter Aspekt, bei dem Haftstrukturen bei Insekten eine wichtige Rolle spielen, ist der Beutefang (Betz & Kölsch 2004). Hier spielen Haftprinzipien nicht nur in Form passiver Klebfallen (Beispiel Spinnennetze) eine Rolle, sondern können auch als aktive Systeme (zum Beispiel in Form von Fangbeinen) mit mobilen adhäsiven Strukturen auftreten, die auf der Beute appliziert werden. Dabei muss die Haftstruktur eine sehr rasche Verbindung eingehen können, die gleichsam im Moment des Kontaktes wirksam wird, damit die nach

dem Kontakt mit dem Räuber einsetzenden Fluchtbewegungen der Beute unwirksam bleiben. Auf der anderen Seite muss dieser Kontakt reversibel sein, da das Beutetier vor der Verdauung mit den Mundwerkzeugen und Beinen manipuliert werden muss.

Einen besonders interessanten Beutefangapparat besitzen Vertreter der Kurzflügelkäfergattung *Stenus* LATREILLE, 1797 (Coleoptera, Staphylinidae), die mit mehr als 3000 rezenten Arten (Puthz, pers. Mitt.) die artenreichste Tiergattung bildet. Die meisten dieser Arten leben in der feuchten Bodenstreu oder als Pflanzenkletterer in den Tropen und Subtropen, einige besiedeln sogar die Kronenzone tropischer Bäume (Puthz 1971). Die Imagines sind Räuber, die sich optisch mit großen, beinahe die gesamten Kopfseiten einnehmenden Komplexaugen orientieren (Abb. 1, 2A, 3A). Als besondere Apomorphie weisen die Vertreter dieser Gattung ein stabförmig verlängertes Fanglabium auf, das innerhalb weniger Millisekunden durch Hämolymphdruck aus dem Körper hervorgeschnellt werden kann (Abb.1, 2A, 3B). Bleibt ein Beutetier an den zwei zu Haftpolstern umgebildeten Paraglossen (Abb.2B) haften, wird dieses durch Retraktion des Labiums in den Bereich der Mandibeln gebracht und kann gefressen werden (Abb.1). Dieser Fangapparat stellte offenbar eine Schlüsselinnovation in der Evolution dieser Tiere dar, die deren hohen evolutiven Erfolg mitbegründet hat. Durch ihren Klebfangapparat sind die Käfer in der Lage, selbst ausgesprochen fluchtfähige Beutetiere wie Springschwänze (Collembola) effektiv zu erbeuten (vgl. Betz 1996, 1998a, b). Alternativ können die Vertreter vieler Arten Beuteobjekte aber auch direkt, ohne Einsatz des Fanglabiums, mit den Mandibeln ergreifen (Bauer & Pfeiffer 1991; Betz 1996). Die Struktur, Funktion und biologische Rolle dieses Fangapparates sind bereits in einer Reihe von Studien untersucht worden (Bauer & Pfeiffer 1991; Betz 1994, 1996, 1998a, b; Kölsch & Betz 1998; Kölsch 2000; Schmitz 1943; Weinreich 1968).

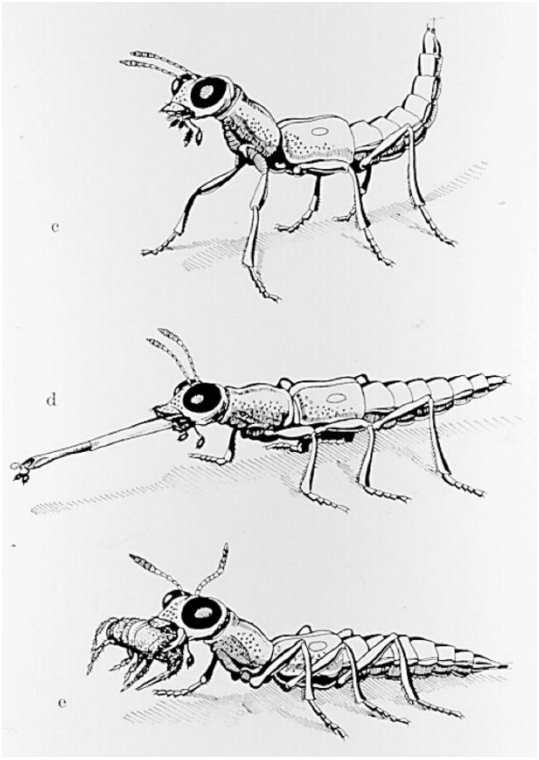

Abb.1: Beutefangsequenz bei *S. comma*. Nach Annäherung an die Beute auf Fangdistanz (oben) wird der Klebfangapparat blitzartig vorgeschnellt (Mitte) und das angeklebte Beuteobjekt in den Bereich der Mandibeln zurückgezogen (unten). Aus Weinreich (1968). Mit freundlicher Genehmigung des Springer Verlages, Heidelberg.

Demnach trägt das Labium an seiner Spitze ein Paar kutikulärer Haftpolster (die umgewandelten Paraglossae), deren Oberfläche in zahlreiche Hafttrichome differenziert ist (Abb.2B). Diese sind an ihrem Ende nochmals vielfach verzweigt, wodurch die Gesamtzahl an Kontaktpunkten deutlich erhöht wird (bis zu mehreren tausend). In ihrem Inneren bestehen die Haftpolster aus einem Geflecht elastischer Kutikulafasern (Betz 1996; Kölsch & Betz 1998). In Verbindung mit der flexiblen Außenwand der Haftpolster wird auf diese Weise offenbar ein elastisches System geschaffen, welches sich den Unregelmäßigkeiten der Beutetieroberfläche sehr genau anpassen kann.

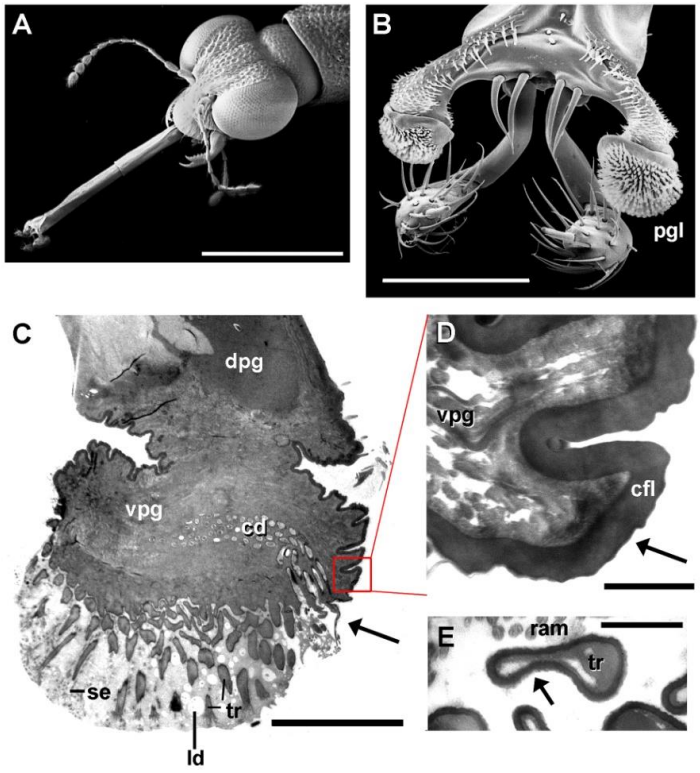

Abb.2: Der Klebfangapparat bei *Stenus* spp. **A-B** *S. comma*. Rasterelektronenmikroskopische (REM-) Aufnahmen. **C-E** *S. juno*. Transmissionselektronen-mikroskopische (TEM-)Aufnahmen. (**A)** Kopf mit vorgestrecktem Labium (**B)** Dorso-Frontalansicht der Spitze des Labiums mit zu Haftpolstern umgewandelten Paraglossen (pgl) (**C)** Querschnitt durch ein Haftpolster. Sekretkanäle (cd) leiten das Haftsekret seitlich aus (Pfeil), von wo es über die Zone der Hafttrichome (tr) verteilt wird. dpg dorsaler, vpg ventraler Abschnitt des Haftpolsters, ld Lipidtropfen, se proteinöses Sekret (**D)** Cuticula an den seitlichen Flanken (cfl) des ventralen Abschnitts eines Haftpolsters mit glatter Oberfläche (Pfeil) (**E)** Cuticula der Hafttrichome (tr) mit rauer Oberfläche (Pfeil). ram Terminale Verzweigungen eines Hafttrichoms. Maßstäbe: **A** 1 mm, **B** 100 µm, **C** 20 µm **D-E** 1 µm. Aus Betz und Kölsch (2004). Mit freundlicher Genehmigung von Elsevier.

Im Unterschied zu bei der Lokomotion an glatten Oberflächen bei Insekten eingesetzten Hafttarsen werden die Klebpolster bei *Stenus* spp. mit hohem Druck beim Ausschleudern des Fangapparates an die Beute angepresst, wobei die Haftwirkung bei der anschließenden Retraktion senkrecht zur Substratoberfläche entfaltet werden muss. Hieran ist ein Haftsekret beteiligt, welches in speziellen Kopfdrüsen produziert und in Kanalbündeln innerhalb des Labiums in die Haftpolster transportiert

wird (Abb.2C). Dieses Haftsekret wird vor dem Fangakt über die mit einer rauen Oberfläche versehenen Hafttrichome verteilt (Abb.2E), während die eine glatte Oberfläche aufweisenden lateralen Flankenhäute unbenetzt bleiben (Abb.2D). Wegen der großen Menge an abgegebenem Haftsekret beruht seine Wirkung vermutlich vor allem auf dem Mechanismus der Viskosität (Kölsch 2000; Betz 2006). Untersuchungen zur Ultrastruktur der Sekret-produzierenden Kopfdrüsen sowie des Sekretes selber weisen darauf hin, dass es sich um ein disperses System handelt, bei dem Lipidtröpfchen in einer mächtigeren proteinhaltigen wässrigen Fraktion emulgiert vorliegen (vgl. ld und se in Abb.2C) (Kölsch 2000; Betz & Kölsch 2004). Emulsionen sind sogenannte metastabile Kolloide aus zwei nicht mischbaren Flüssigkeiten (eine polare und eine weniger polare), wobei die eine Phase in der anderen dispergiert vorliegt. Mikro-Emulsionen, bei denen lipidartige Nanotröpchen fein verteilt in einer wasserlöslichen Komponente vorliegen ("Öl-in-Wasser"-Emulsion) oder umgekehrt ("Wasser-in-Öl"-Emulsion), werden auch im Zusammenhang mit dem Haftsekret tarsaler Haftsysteme bei Insekten diskutiert (Gorb 2001; Federle et al. 2002; Vötsch et al. 2002). Der Vorteil solcher Emulsionen könnte zum einen in verbesserten Benetzungseigenschaften gegenüber verschiedenen Substraten liegen, da sie sich sowohl mit hydrophilen als auch hydrophoben Oberflächen verbinden können. Zum anderen ließe sich darüber auch die Viskosität des Haftsekretes und damit seine Haftwirkung erhöhen und vielleicht sogar differenziert auf die jeweils erforderlichen Bindungskräfte einstellen.

1.2 Fragestellung und Zielsetzung der Dissertation

1.2.1 Untersuchung des Klebfangapparates der Gattung *Stenus*

Die Untersuchungen zur Gattung *Stenus* sind Teil eines ökomorphologischen Forschungskonzeptes, in dem versucht wird, die Wechselbeziehungen zwischen der Morphologie und Ökologie von Organismen in einem integrativen Ansatz zu verstehen (vgl. Reilly & Wainwright 1994; Lauder 2003; Herrel et al. 2005; Wainwright 1991). Im Mittelpunkt dieses Ansatzes steht der Versuch einer Verknüpfung zwischen der Morphologie eines Organismus und der Konsequenz seiner morphologischen Strukturen für seine Ökologie, Physiologie und Fitness. In diesem Ansatz wird die Morphologie mit experimentellen Untersuchungen sowie Tests zur maximalen Leistungsfähigkeit (Performanz) der betrachteten morphologischen Strukturen im Labor und (Halb-)Freiland verknüpft und so untersucht, welche Leistungen ein Organismus mit seinen morphologischen Strukturen erbringen kann. Die Untersuchung der maximalen Leistungsfähigkeit ist zentraler Teil der Ökomorphologie, da diese die Fähigkeit eines Organismus angibt, Ressourcen effektiv zu nutzen und entscheidende physiologische Funktionen zu erfüllen. Durch die Einbeziehung phylogenetischer Analysen lassen sich vermutete Anpassungen zudem in einen historischen Kontext einbetten, wodurch

sich interessante Hinweise auf von der Evolution gewählte Stellglieder ergeben können, die zu einer Leistungsverbesserung der untersuchten Systeme geführt haben.
Dem ökomorphologischen Forschungskonzept folgend untersuchte ich in meinem Dissertationsprojekt die Leistungsfähigkeit des Fangapparates der Kurzflügelkäfergattung *Stenus*. Laut Betz (1996) existieren bei den Arten der Gattung *Stenus* große interspezifische Unterschiede in der Morphologie der Haftpolster, vor allem hinsichtlich der Größe der distalen Haftpolsterflächen und der Anzahl der Haftkontakte (entspricht der Anzahl an Hafthaaren pro Klebpolster multipliziert mit der Anzahl an Verzweigungen pro Hafthaar). Diese Unterschiede korrelieren vermutlich mit der Nischendifferenzierung (erste Ansätze bei Betz 1994, 1996, 1998a), und es ist daher anzunehmen, dass sie mit der maximal noch zu bewältigenden Beutetiergröße in Bezug stehen. Betz (1996, 1998a, b) zeigte in Verhaltensexperimenten, dass die Haftpolster des Fangapparates von *Stenus* effektive Haftorgane sind, mit denen zum Teil sehr hohe Fangerfolge erzielt werden. Der Fangerfolg ist dabei umso höher, je größer die Haftpolster und je mehr Haftkontakte auf ihrer Oberfläche untergebracht sind. Größere Haftpolster besitzen demnach vermutlich eine stärkere Haftwirkung, sodass größere Beutetiere gefangen werden können. Bislang wurden die beim Beutefang der Gattung *Stenus* auftretenden Haftkräfte nur theoretisch bestimmt (Kölsch 2000), während die Kräfte beim Ausschleudern des Labiums noch völlig unbekannt sind. Laut Kölsch (2000) betrug die höchste theoretisch berechnete Haftkraft bei *Stenus comma* beruhend auf dem Mechanismus der Viskosität 66.4 µN, während die Kräfte beruhend auf dem Mechanismus der Oberflächenspannung (2.22 µN) oder van der Waals-Kräften (87.5 nN µN) wesentlich geringere Werte aufwiesen.

Vor diesem Hintergrund sollte ein Messverfahren für die experimentelle Bestimmung der Druck- und Haftkräfte des Klebfangapparates im natürlichen Verhaltenskontext (*in vivo* Kraftmessungen) entwickelt werden. Außerdem waren detaillierte vergleichende Untersuchungen der morphologischen Merkmale der Haftpolster, des Beutefangerfolges und -verhaltens erforderlich, um korrelative Zusammenhänge dieser Parameter mit den gemessenen Kräften aufzudecken. Um diese Parameter vor einem phylogenetischen Hintergrund diskutieren zu können, wurden außerdem molekular phylogenetische Analysen der untersuchten Arten durchgeführt. Erst bei Vorliegen solider Stammbaumhypothesen über die betrachteten Arten können die ökomorphologisch relevanten Merkmalszustände historisch interpretiert werden.

Folgende Fragestellungen sollten dabei umfassend untersucht werden:

- Unterscheiden sich die verschiedenen *Stenus*-Arten bezüglich ihrer Druck- und Haftkräfte? Welchen Einfluss hat die Druckkraft auf die resultierende Haftkraft?
- Welchen Einfluss hat die Struktur der Haftpolster (Anzahl und Dichte der Haftkontakte; Haftpolsterfläche) auf die erzielbaren Haftkräfte?

- Inwieweit unterscheidet sich die resultierende Zugfestigkeit (Haftkraft pro Klebpolsterfläche) bei den untersuchten *Stenus*-Arten und wie groß ist diese im Vergleich zu anderen Haftsystemen?
- Auf welchem Haftmechanismus beruht die Wirkung des Fangapparates bei *Stenus* (Viskosität, Kapillarität)?
- Korreliert die Haftkraft mit dem Beutefangerfolg? Lassen sich die Druck- und Haftkräfte ökomorphologisch im Hinblick auf ein bestimmtes Beutefangverhalten interpretieren?
- Welchen Einfluss haben Oberflächenrauheit und -energie auf die resultierende Haftkraft?
- Zusammenfassend sollten die funktionellen Grundprinzipien des *Stenus*-Haftsystems herausgearbeitet werden.

1.2.2 Phylogenie

Ein weiterer Teil der Dissertation sollte Fragen zur ökologisch-morphologischen Diversifizierung sowie zur Evolution ökologisch relevanter morphologischer Strukturen und Verhaltensweisen einiger mitteleuropäischer *Stenus*-Arten klären. Als Grundlage für diese Analysen wurden molekulare Sequenzdaten der Untereinheit 1 des mitochondrialen Cytochromoxidase (COI)-Gens erhoben. Bei der Auswertung dieser Sequenz-Daten stellte sich interessanterweise heraus, dass die ursprünglich als Außengruppe vorgesehene Schwestergattung *Dianous* Leach 1819 unabhängig von der phylogenetischen Analysemethode inmitten der Gattung *Stenus* clusterte. Aus diesem Grund wurde das Verwandtschaftsverhältnis beider Gattungen in einer eigenständigen Publikation thematisiert (Publikation V).

Die Gattungen *Stenus* und *Dianous* gehören zur Staphyliniden-Unterfamilie der Steninae, die nur diese beiden Gattungen beinhaltet. Die Monophylie der Steninae wird durch mehrere larvale und adulte Autapomorphien (Puthz 1981; Hansen 1997; Leschen & Newton 2003; Thayer 2005; Grebennikov & Newton 2009; Clarke & Grebennikov 2009) sowie durch molekulare Daten (Grebennikov & Newton 2009) gestützt. Eine bislang unbeschriebene Gattung, die einen Fangapparat ähnlich dem von *Stenus* besitzt, gehört möglicherweise auch in diese Unterfamilie (Leschen & Newton 2003; Betz & Kölsch 2004; Clarke & Grebennikov 2009). Während die Monophylie der Gattung *Stenus* aufgrund des apomorphen Fanglabiums und weiterer morphologischer Merkmale, die mit diesem im Zusammenhang stehen, bisher als gesichert galt (Puthz 1981; Clarke & Grebennikov 2009), ist die Gattung *Dianous* durch kein apomorphes Merkmal als Monophylum gekennzeichnet (Puthz 1981; Clarke & Grebennikov 2009). Laut Puthz (1981) ist die Gattung *Dianous* nur als „plesiomorphe, vielleicht paraphyletische Gruppe gekennzeichnet und damit, streng genommen, phylogenetisch nicht definiert“ und stellt somit eine „praktische klassifikatorische Verlegenheitslösung“ dar. In diesem Zusammenhang spricht er von der „Aporie des Stenologen“ (Puthz 1981).

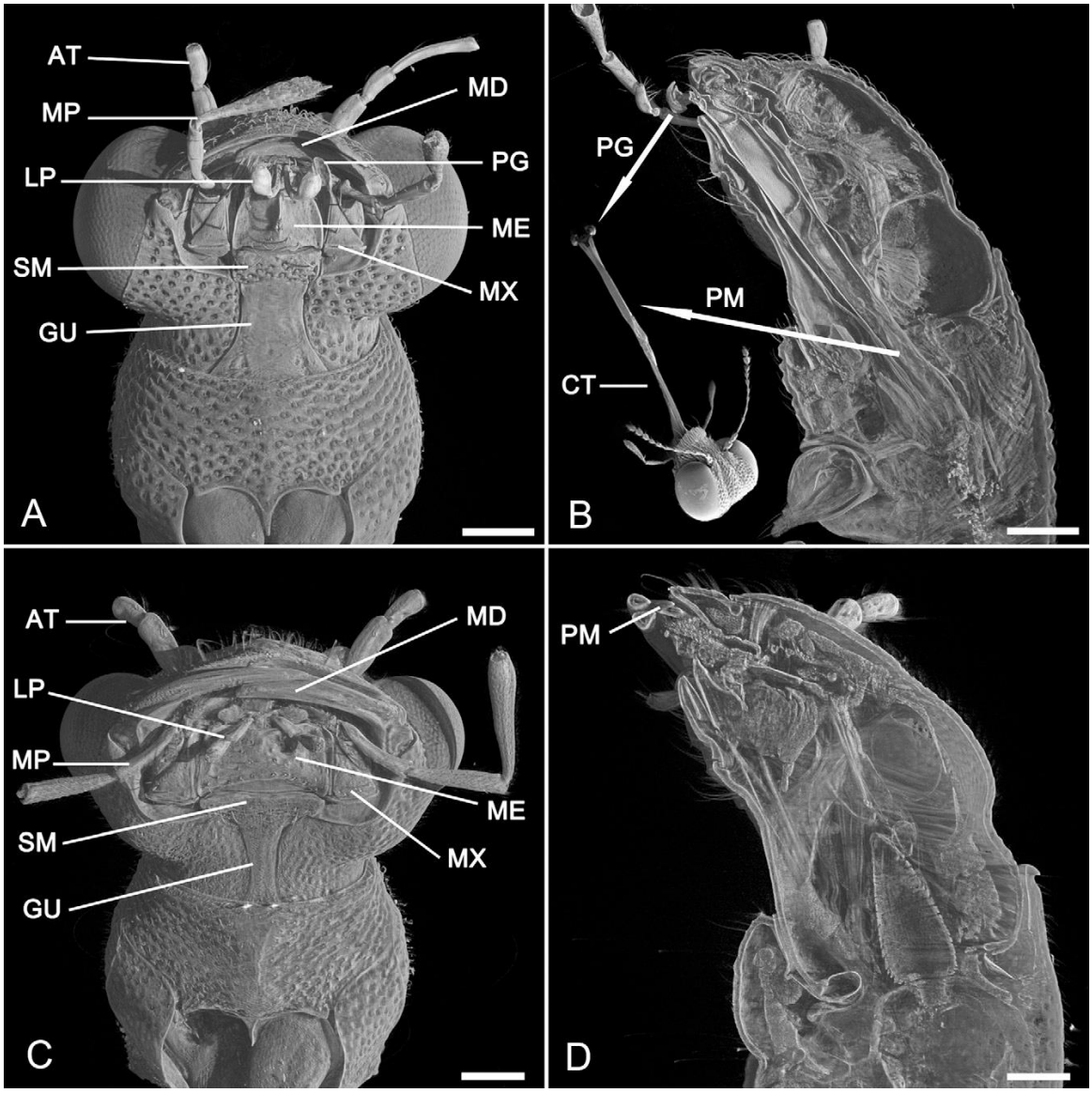

Abb.3: Kopfmorphologie von *Stenus cicindeloides* im Ruhezustand (**A**, **B**) and *Dianous coerulescens* (**C**, **D**) aus Synchrotron Mikro-Computertomographie Datensätzen. (**A**, **C**) 3-D-Modell des Kopfes (ventral); (**B**, **D**) virtueller Sagittalschnitt des Kopfes. Aus Publikation V. Mit freundlicher Genehmigung von Elsevier. Maßstabsskala = 0.2mm. Abkürzungen: AT, Antenne; CT, häutige Verbindungsmembran; GU, Gula; LP, Labialpalpus; MD, Mandibel; ME, Mentum; MP, Maxillarpalpus; MX, Maxille; PG, Paraglossa modifiziert in Haftploster; PM, Praementum; SM, Submentum.

Die Gattung *Dianous* ist mit bisher mehr als 210 beschriebenen Arten (Shi & Zhou 2009, 2011) in der Orientalis und Holarktis verbreitet, wobei das Verbreitungszentrum in China, Indien und Südostasien liegt (Puthz 1981; Shi & Zhou 2011). Ökologisch unterscheiden sich die meisten *Dianous*-Arten deutlich von den *Stenus*-Arten, da sie überwiegend stenök und streng hygrobiont sind (Puthz 1981, 2000). Im Vergleich zu *Stenus* zeigt das Labium von *Dianous* den gleichen Grundbauplan, nur in verkürzter Form: das Eulabium (Praementum) kann bei *Dianous* ebenfalls vorgestreckt und wieder

hinter das Mentum zurückgezogen werden (Weinreich 1968; Abb.3C, D). Im Unterschied zu *Stenus* sind die Paraglossen bei *Dianous* allerdings nicht zu Haftpolstern differenziert, bilden also keinen Klebfangapparat (Weinreich 1968). Beutetiere (z. B. Larven von Dipteren und Coleopteren) werden deshalb ausschließlich mit den Mandibeln gefangen (Pfeiffer 1989). Bisher wurde davon ausgegangen, dass das morphologisch einfach gebaute, verkürzte Labium von *Dianous* den plesiomorphen, und das vorschnellbare Fanglabium mit den modifizierten Paraglossen von *Stenus* den apomorphen Zustand darstellen würde.

Innerhalb der Gattung *Dianous* lassen sich zwei Artengruppen anhand des Stirnbaues unterscheiden (Puthz 1981, 2000; Shi and Zhou 2011; Tang et al. 2011; Puthz 2015a). Bei Artengruppe I (ca. 30 % aller *Dianous*-Arten) ist die Stirnmitte konkav eingesenkt, besitzt also keinen erhobenen Mittelteil: hierher gehören alle diejenigen Arten, die bisher zur Gattung *Stenus* gezählt wurden, wegen des Baues der Fangapparates jetzt jedoch zu *Dianous* gestellt werden. Bei Gruppe II besitzt die Stirn einen mehr oder weniger erhobenen Mittelteil. Die Arten der Gruppe I haben überdies sehr große Augen („*Stenus*-Augen“).

Die Gattung *Stenus* wurde traditionell in 6 Untergattungen (Subgenera) aufgeteilt, deren Namen verschiedentlich gewechselt haben und von denen gegenwärtig noch 5 nomenklatorisch gültig sind: *Stenus* s.str., *Hemistenus* Motschulsky 1860, *Hypostenus* Rey 1884, *Metatesnus* Adam 1987 and *Tesnus* Rey 1884 (Puthz 2001, 2008). Allerdings wurden bei dieser Einteilung nur nordhemisphärische Arten berücksichtigt – das Gros der *Stenus*-Arten lebt jedoch in der Südhemisphäre bzw. am Übergang zu den südlichen Faunenregionen (Puthz 2001, 2008).

Laut Puthz (2008) kommt erschwerend hinzu,

a) dass die traditionellen Untergattungen mit einer begrenzten Zahl von Merkmalen definiert wurden (die Gestalt der letzten Abdominalsklerite sowie Metatarsen; Genitalcharaktere und auch die Paraglossen spielten dabei überhaupt keine Rolle),

b) dass die zur Definition benutzten Merkmale nicht immer eindeutig identifiziert worden sind, und

c) dass diese Merkmale monophyletische Gruppen auseinander reißen, weil sie nah verwandte Arten in verschiedene Subgenera einordnen.

Demnach ist die traditionelle Untergattungs-Einteilung bei *Stenus* rein künstlich und wurde bisher aus praktischen (Bestimmungs- und Orientierungs-) Gründen weiter geführt; eine Auflösung der Untergattungen in eine große Anzahl an monophyletischen Gruppen wurde bereits umgesetzt (zusammengefasst in Puthz 2008). Die molekularen Untersuchungen des mitochondrialen Cytochromoxidase-Gens I (COI) geben einen ersten Überblick über die Verwandtschaftsbeziehungen sowohl innerhalb der Gattung *Stenus* als auch zwischen den Schwestergattungen *Stenus* und *Dianous* (Publikation V; Lang et al. 2015).

2 Ergebnisse und Diskussion

2.1 Vergleichende Untersuchungen zum Mechanismus des Klebfangapparates der Kurzflügelkäfergattung *Stenus* Latreille, 1797 (Coleoptera, Staphylinidae)

Publikation I: Functional morphology and adhesive performance of the stick-capture apparatus of the rove beetles *Stenus* spp. (Coleoptera, Staphylinidae). Lars Koerner, Stanislav N Gorb, Oliver Betz (2012). Zoology 115: 117-127.

Publikation II: Adhesive performance of the stick-capture apparatus of rove beetles of the genus *Stenus* (Coleoptera, Staphylinidae) toward various surfaces. Lars Koerner, Stanislav N Gorb & Oliver Betz (2012). Journal of Insect Physiology 58: 155-163.

Publikation III: Divergent morphologies of adhesive predatory mouthparts of *Stenus* species (Coleoptera, Staphylinidae) explain differences in adhesive performance and resulting prey-capture success. Lars Koerner, László Zsolt Garamszegi, Michael Heethoff & Oliver Betz (2017). Zoological Journal of the Linnean Society 181: 500-518.

Publikation IV: The labial adhesive pads of rove beetles of the genus *Stenus* (Coleoptera: Staphylinidae) as carriers of bacteria. Lars Koerner, Volkmar Braun & Oliver Betz (2016). Entomologia Generalis 36: 33-41.

2.1.1 Bestimmung der beim Klebfangmechanismus erzeugten Kräfte

Zentraler Teil der Dissertation war die experimentelle Bestimmung der über den Klebfangapparat erzeugten Kräfte (Druck- und Zugkraft) im natürlichen Verhaltenskontext. Hierfür wurde ein Messverfahren für *in vivo* Kraftmessungen entwickelt, mit dem es möglich war, den zeitlichen Verlauf der entwickelten Kräfte zu verfolgen und statistisch auszuwerten (Abb.4). Der Käfer wird dabei in eine Arena gesetzt. Als Beuteattrappe dient eine Insektennadel (No. 00), die an einem Kraftmessgerät (FORT25, WPI Inc., USA) befestigt wird. Da die Tiere ausschließlich auf sich bewegende Beuteobjekte reagieren, wurde das Kraftmessgerät an einem beweglichen Mikromanipulator befestigt. Bei Bewegung des Mikromanipulators „schießt" der Käfer auf den Stecknadelkopf, so dass der Sensor des Kraftmessers ausgelenkt und die entstehenden Kräfte aufgezeichnet (MP100 WSW, BIOPAC Systems Inc., USA) werden. Durch diesen neu entwickelten Versuchsansatz, war es erstmals möglich, den genauen zeitlichen Kraftverlauf während des Fangschlages bei Vertretern der Gattung *Stenus* darzustellen (Abb.5).

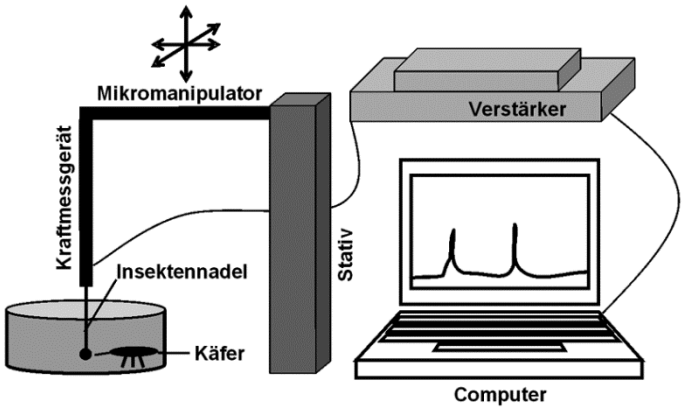

Abb.4: Versuchsaufbau zur Bestimmung der beim Fangschlag erzeugten Druck- und Zugkräfte. Verändert nach Publikation I.

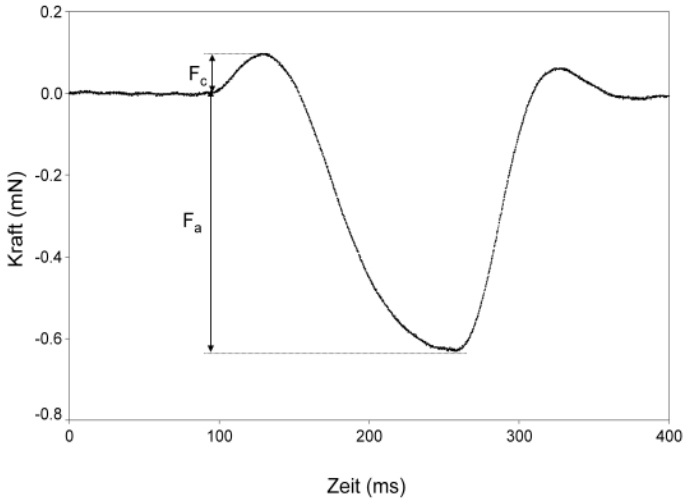

Abb.5: Zeitlicher Verlauf der während des Fangaktes auftretenden Kräfte. F_c kennzeichnet die maximale Druckkraft, F_a die maximale Zugkraft während dieses Fangschlages.

Die während des Klebfanges entstehenden Druck- (beim Auftreffen der Klebpolster auf die Beuteattrappe) sowie Adhäsionskräfte (beim Rückzug der Klebpolster von der Attrappe) wurden bei 14 Vertretern der Gattung *Stenus* bestimmt, wobei jeweils 15-20 Fangversuche pro Individuum aufgezeichnet und jeweils nur die Maximalwerte statistisch ausgewertet wurden (Publikation III). Die

morphometrischen Daten der Haftpolster wurden anschließend am Rasterelektronenmikroskop (REM) bestimmt. Dieser Versuchsaufbau diente auch zur Bestimmung der Haftleistung der Klebzunge zweier *Stenus*-Arten (*S. bimaculatus* und *S. juno*) auf standardisierten Oberflächen mit unterschiedlicher Rauheit (Publikation II).

2.1.2 Zusammenhang zwischen der Morphologie der Haftpolster, der resultierenden Haftkraft und des Beutefangerfolges (Publikation III)

2.1.2.1 Morphologie der Haftpolster

Bei den 14 untersuchten *Stenus*-Arten entspricht die Morphologie der Haftpolster dem Grundtyp, d.h. die ventrale Klebpolsterfläche weist eine etwa elliptische Form auf und ist auf ihrer Oberfläche mit zahlreichen, terminal verzweigten Hafthaaren ausgestattet (Betz 1996). Die Ergebnisse der vorliegenden Arbeit bestätigen frühere Untersuchungen von Betz (1996), der zeigte, dass die Morphologie der Haftpolster bei *Stenus* große interspezifische Unterscheide zeigt (vor allem in der Haftpolsterfläche, der Anzahl der Hafthaare und der Anzahl deren terminaler Verzweigungen).

Die morphologischen Analysen zeigen, dass die Körpergröße der untersuchten *Stenus*-Arten mit den verschiedenen morphologischen Parametern der Haftpolster korreliert ist. Dementsprechend besitzen größere *Stenus*-Arten auch längere Fanglabien, größere Haftpolster mit einer größeren Anzahl an Hafthaaren und Haftkontakten (entspricht der Anzahl an Hafthaaren pro Klebpolster multipliziert mit der Anzahl an Verzweigungen pro Hafthaar). Die Größe der Haftpolster korreliert positiv mit der Anzahl an Hafthaaren und Haftkontakten, wohingegen die Dichte der Hafthaare eine negative Korrelation mit der Klebpolsterfläche zeigt.

Die PGLS-Analyse (*phylogenetic general least squares*) zeigte, dass die Haftpolsterfläche positiv allometrisch mit der Pronotumlänge steigt (r = 0.724, p = 0.003, Steigung b = 2.46; 95% Konfidenzintervall: 1.13, 3.79; Abb.7A). Allerdings ist dieser Unterschied nicht signifikant von dem bei Isometrie zu erwartendem Wert von 2 (Unterschied zur Steigung von 2: t = 0.69, p > 0.05; Unterschied zur Steigung von 3: t = -0.79, p > 0.05). Im Vergleich zur Körpergröße besitzen die Bewohner offener Uferflächen *S. biguttatus*, *S. fossulatus*, *S. guttula* und *S. comma* sehr kleine Haftpolster (Abb.7A: offene Quadrate). Führt man die PGLS-Analyse ohne diese Arten durch, zeigen die restlichen Arten eine hoch signifikante Korrelation zwischen der Pronotumlänge und der Haftpolsterfläche (r = 0.95, p < 0.001) und einen Allometriekoeffizienten (b = 2.93; 95%-Konfidenzintervall: 2.28, 3.57), der sich signifikant von dem bei Isometrie zu erwartendem Wert von 2 unterscheidet (Unterschied zur Steigung von 2: t = 2.82, p < 0.05).

2.1.2.2 Interspezifischer Vergleich der Druck- und Adhäsionskräfte

Die Kraftmessungen zeigten starke interspezifische Unterschiede, sowohl in den Druck- als auch den Adhäsionskräften (Abb.6).

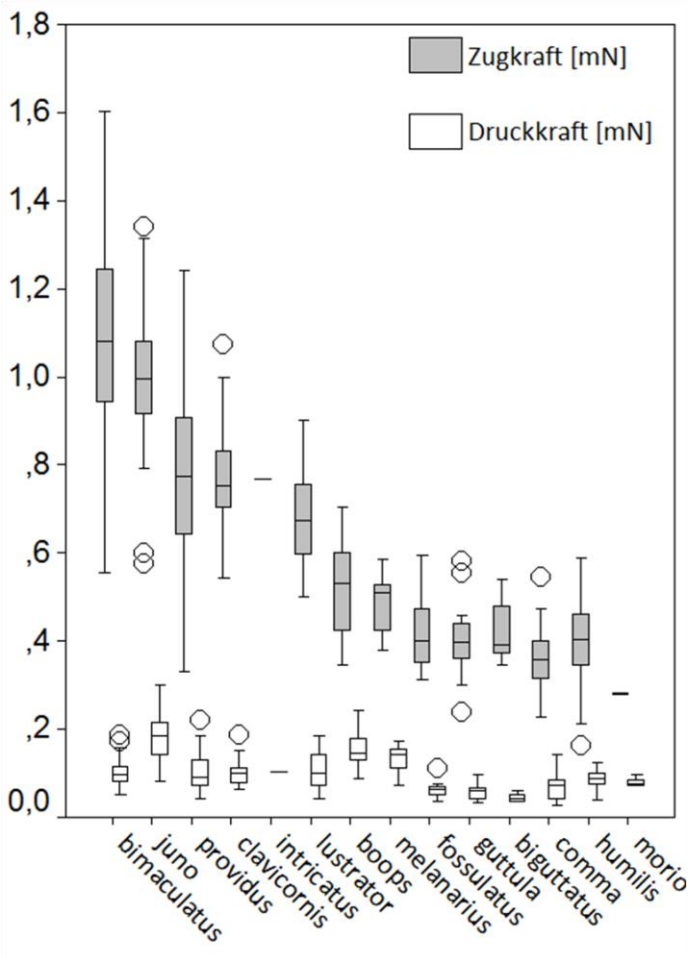

Abb.6: Interspezifischer Vergleich der beim Klebfang auftretenden Adhäsions- und Druckkräfte. Die 14 untersuchten *Stenus*-Arten unterscheiden sich vor allem in den erzeugten Zug-(Adhäsions-)kräften. Basierend auf Daten aus Publikationen I und III.

Um mit den Klebpolstern eine hohe Kleb- (Zug)kraft zu erwirken, sollte der Anpressdruck in Verbindung mit der Wirkung des Haftsekretes möglichst hohe Werte erreichen. Ein entsprechender Anpressdruck wird dadurch erreicht, dass die vom Labium zu überbrückende Entfernung zum Beutetier nur etwa halb so groß ist wie die Länge des vorgestreckten Labiums (Betz 1996, 1998a). Neben der Einhaltung einer gewissen Fangdistanz wird dieses zusätzlich dadurch erreicht, dass die Tiere während des mit dem Labium durchgeführten Angriffs einen Vorstoß mit dem gesamten Körper unternehmen, um auf diese Weise dem Beutetier möglichst nahe zu kommen. Gewöhnlich werden dadurch etwas 10-30% der Fangdistanz überwunden, während die verbleibende Strecke durch das vorgestreckte Labium überbrückt wird (Betz 1996, 1998a). Dies führt dazu, dass die Haftpolster mit einem gewissen Anpressdruck auf dem Beutetier auftreffen, wodurch ihre Haftung an der Beute erst ermöglicht wird (durchschnittliche Druckkräfte zwischen 0.05 mN bei *S. biguttatus* und 0.18 mN bei *S. juno*; Publikation III). Diese Aussagen werden durch die Kraftmessungen bestätigt, da ein

signifikanter Zusammenhang zwischen Druck- und Adhäsionskraft besteht (r = 0.60, p = 0.023; Abb.7B), d.h. je größer die Kraft, mit der die Klebpolster auf ein Beuteobjekt auftreffen, desto größer ist auch die resultierende Adhäsionskraft. Dieses Ergebnis weist auf einen druckempfindlichen Haftmechanismus bei *Stenus* hin. Den Einfluss höherer Druckkräfte auf die Haftperformanz kann man sehr gut bei einem Vergleich der Arten *S. juno* und *S. bimaculatus* sehen: im Vergleich zu *S. bimaculatus* generiert *S. juno* eine ungefähr doppelt so große Druckkraft (0.10 *vs.* 0.18 mN) und erreicht dadurch nahezu dieselbe Haftwirkung (1.08 vs. 1.00 mN), obwohl *S. bimaculatus* eine ca. 30% größere Haftpolsterfläche besitzt (Publikation I, II). Der Vorteil höherer Druckkräfte liegt darin, dass sie (1) zu einer Reduktion der Schichtdicke des Haftsekretes in der Kontaktzone führen (Bowden & Tabor 1986) und (2) das Haftsekret in Oberflächenunregelmäßigkeiten des Beutetiers drücken und dadurch die effektive Kontaktfläche zwischen Beutetier und Haftorgan vergrößern (Habenicht 2009; vgl. Publikation II).

Interessanterweise zeigen die Regressionsanalysen, dass die Druckkräfte größenunabhängig sind (Abb.7D) und größere *Stenus*-Arten somit auch keine höheren Druckkräfte erzeugen. Die Bewohner freier Uferflächen *S. biguttatus, S. fossulatus, S. guttula* und *S. comma* erzeugen die geringsten Druckkräfte (0.05-0.07 mN; Abb.7D: offene Quadrate), während kleinere Arten, wie z. B. *S. melanarius, S. boops, S. morio* und *S. humilis*, wesentlich höhere Druckkräfte entwickeln (0.08-0.16 mN). Die interspezifischen Unterschiede in den erzeugten Druckkräften sind vermutlich auf unterschiedliche Fangdistanzen während des Fangschlages zurückzuführen (Betz 1996, 1998a; Publikation I, II). Vermutlich führen geringere Fangdistanzen zu einer Verbesserung der Effektivität des Fangschlages, indem sie den Anpressdruck der Klebpolster erhöhen. Allerdings muss diese Vermutung noch durch weitergehende Experimente verifiziert werden.

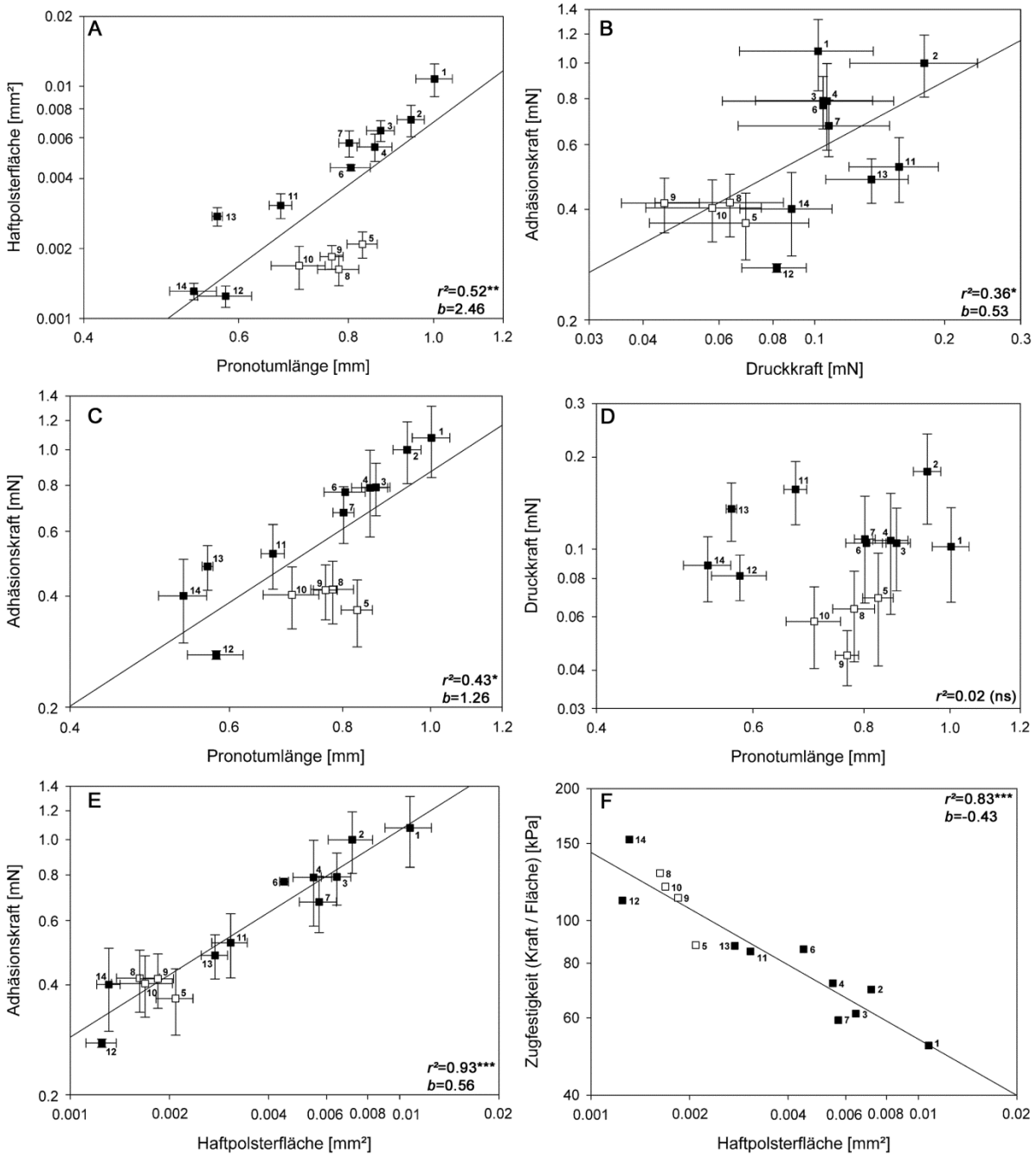

Abb.7: Abhängigkeiten zwischen der Pronotumlänge (als Maß für die Körperlänge bei *Stenus*) und den morphologischen und Performanzparametern des Fangapparates bei *Stenus*. Regressionsgeraden wurden durch *PGLS*-Analysen berechnet. Gefüllte Kästchen kennzeichnen Arten, die feuchten, bodennahen Pflanzendetritus besiedeln; offene Kästchen kennzeichnen Arten, die offene, schlammige oder sandige Stellen etwa an Gewässerufern besiedeln ("Oberflächenläufer"). Artkürzel: 1, *Stenus bimaculatus*; 2, *S. juno*; 3, *S. clavicornis*; 4, *S. providus*; 5, *S. comma*; 6, *S. intricatus*; 7, *S. lustrator*; 8, *S. fossulatus*; 9, *S. biguttatus*; 10, *S. guttula*; 11, *S. boops*; 12, *S. morio*; 13, *S. melanarius*; 14, *S. humilis*. Verändert nach Publikation III.

Mit Werten zwischen 0.28 mN bei *S. morio* und 1.08 mN bei *S. bimaculatus* sind die Adhäsionskräfte um fast eine fast Zehnerpotenz höher als die Druckkräfte (Abb.7B). Die Adhäsionskräfte verhalten sich negativ allometrisch zur Pronotumlänge (Steigung b = 1.26; r = 0.66, p = 0.011; 95% KI: 0.44, 2.09; Abb.7C). Allerdings unterscheidet sich dieser Wert nicht signifikant von dem bei Isometrie zu erwartenden Wert von 2 (Unterschied zur Steigung von 2: t = 1.74, p > 0.05). Arten, die infolge besonders geringer Haftfähigkeiten von der normalen Allometriebeziehung abweichen, sind die Bewohner freier Uferflächen *S. biguttatus*, *S. fossulatus*, *S. guttula* und *S. comma* (Abb.7C: offene Quadrate). Entfernt man diese Arten aus der Regressionsanalyse, zeigen die verbleibenden Arten eine hoch signifikante Korrelation zwischen der Adhäsionskraft und der Pronotumlänge (r = 0.940, p < 0.001, d.f. = 9) und eine Steigung von 1.67 (95% CI: 1.25, 2.10; Unterschied zur Steigung von 2: t = 1.52, p > 0.05).

Laut Betz (1996) ist für eine Verbesserung des Fangerfolges bei *Stenus* gegenüber großen (und damit relativ schweren) Beutetieren vor allem die Verteilung einer hohen Zahl von Hafthaaren und Haftpunkten auf einer möglichst großen Haftpolsterfläche entscheidend. Dies ist auf den Umstand zurückzuführen, dass Oberflächenstrukturen der Beute (z. B. Schuppen, Setae, Wachsausscheidungen), die die Haftung ganzer Haftpolsterbereiche beeinträchtigen könnten, bei großen Haftpolstern weniger ins Gewicht fallen als bei kleinen (Bauer & Pfeiffer 1991; Betz 1996). Klebpolster hingegen, die eine Erhöhung der Zahl der Haftpunkte im Wesentlichen durch eine Vergrößerung der Hafthaardichte oder der Verzweigungen pro Hafthaar erreichen, ohne dabei zugleich die Haftpolsterfläche zu erhöhen, sollten gegenüber großen Collembolen einen geringeren Selektionsvorteil besitzen (Betz 1994). Die Ergebnisse der Haftkraftmessungen unterstützen diese Aussagen, da sie zeigen, dass eine Vergrößerung der Haftpolsterfläche (r = 0.96, p < 0.001) bzw. eine (damit einhergehende) Erhöhung der Zahl der Hafthaare (r = 0.97, p < 0.001) und Haftkontakte (r = 0.86, p < 0.001) zu einer Verbesserung der Haftperformanz (Adhäsionskraft) der Haftpolster führen, während die Anzahl an Hafthaarverzweigungen (r = 0.468, p = 0.092) sowie die Dichte der Hafthaare (r = -0.391, p = 0.167) und Haftkontakte (r = 0.097, p = 0.741) keinen Einfluss auf die Hafteigenschaften haben.

Bei den untersuchten Arten verhält sich die Adhäsionskraft negativ allometrisch zu Pronotumlänge (Steigung: 1.26; Abb.7C) und Körpergewicht (Steigung: 0.43), wohingegen sich die Haftpolsterfläche positiv allometrisch zu Pronotumlänge (Steigung: 2.46; Abb.7A) und Körpergewicht (Steigung: 0.83) verhält. Dementsprechend verhält sich auch die Adhäsionskraft negativ allometrisch zur Haftpolsterfläche (Steigung: 0.56; Abb.7E). Somit scheint der Gewinn an Adhäsionskraft durch eine extreme Vergrößerung der Haftpolsterfläche begrenzt zu sein. So resultiert z. B. eine Verzehnfachung der Haftpolsterfläche (von ca. 0.001 mm² bei *S. morio* zu 0.01 mm² bei *S. bimaculatus*) nur in einer Vervierfachung der Adhäsionskraft (von 0.28 mN bei *S. morio* zu 1.08 mN bei *S. bimaculatus*).

Interessanterweise zeigen die erhobenen morphologischen Daten von 230 *Stenus*-Arten, dass die Haftpolstergröße von *S. bimaculatus* ein oberes Limit des ellipsoiden Haftpolstertyps (häufigster Haftpolstertyp) erreicht hat, da diese Art die größten Haftpolster aller untersuchten Arten besitzt (Koerner & Betz, unpubl. Daten). Eine unbeschränkte Vergrößerung der Klebpolster ist aufgrund räumlicher Zwänge wahrscheinlich auch nicht möglich, weil diese dann in räumlicher Konkurrenz mit den Mandibeln sowie den Galeae und Laciniae der ersten Maxillen stehen würden. Außerdem wären für sehr große Haftpolster eine effektivere Stabilisierung vor mechanischer Beschädigung sowie eine wesentlich größere Sekretmenge und eine entsprechende Vermehrung der Zahl der Sekretkanäle erforderlich. Eine zu hohe Zahl von Sekretkanälen im Inneren des Labiums (bzw. Drüsenzellen im Kopf) würde zu räumlichen Konkurrenzsituationen mit anderen Geweben führen oder könnte gar zu einer Beeinträchtigung des Fangmechanismus führen (Betz 1996).

Allerdings haben die Haftpolster in einigen Artengruppen innerhalb der Untergattungen *Hemistenus* und *Hypostenus* eine deutliche Vergrößerung ihrer Oberfläche erfahren, was zum Teil mit erheblichen morphologischen Abweichungen von der als ursprünglich anzusehenden ellipsoiden Form einhergeht und entgehen dadurch wohl den vorher erwähnten räumlichen Zwängen. So besitzen einige *Hypostenus*-Arten (z. B. *S. latifrons*, *S. fulvicornis*, *S. persicus* (Abb.8b, c)) longitudinal stark verlängerte Paraglossen (longiformer Typ; Betz 1996, 2006). Einige mittel- bzw. südamerikanischen *Hemistenus*-Arten (z. B. *S. emily*, *S. electriger*, *S. alpaca* (Abb.8e)) besitzen auch verlängerte Paraglossen, allerdings mit langen tentakelförmigen Hafthaaren, die zur Klebpolstermitte hin immer länger werden (actiniformer Typ; Betz 2006; Puthz 2005, 2015b). Einige orientalische Arten der Untergattung *Hemistenus* (z. B. *S. luteolunatus*, *S. stigmaticus* (Abb.8d)) haben spitzkegelige Haftpolster (koniformer Typ; Betz 1996; Puthz 1998) oder Haftpolster mit extrem langen, springbrunnenartig angeordneten Hafthaaren (sileniformer Typ, z. B. bei *S. pilicornis*, *S. nepalensis* (Abb.8f); Puthz 2012). Allerdings liegen über den Beutefang dieser Arten bislang keine Beobachtungen vor.

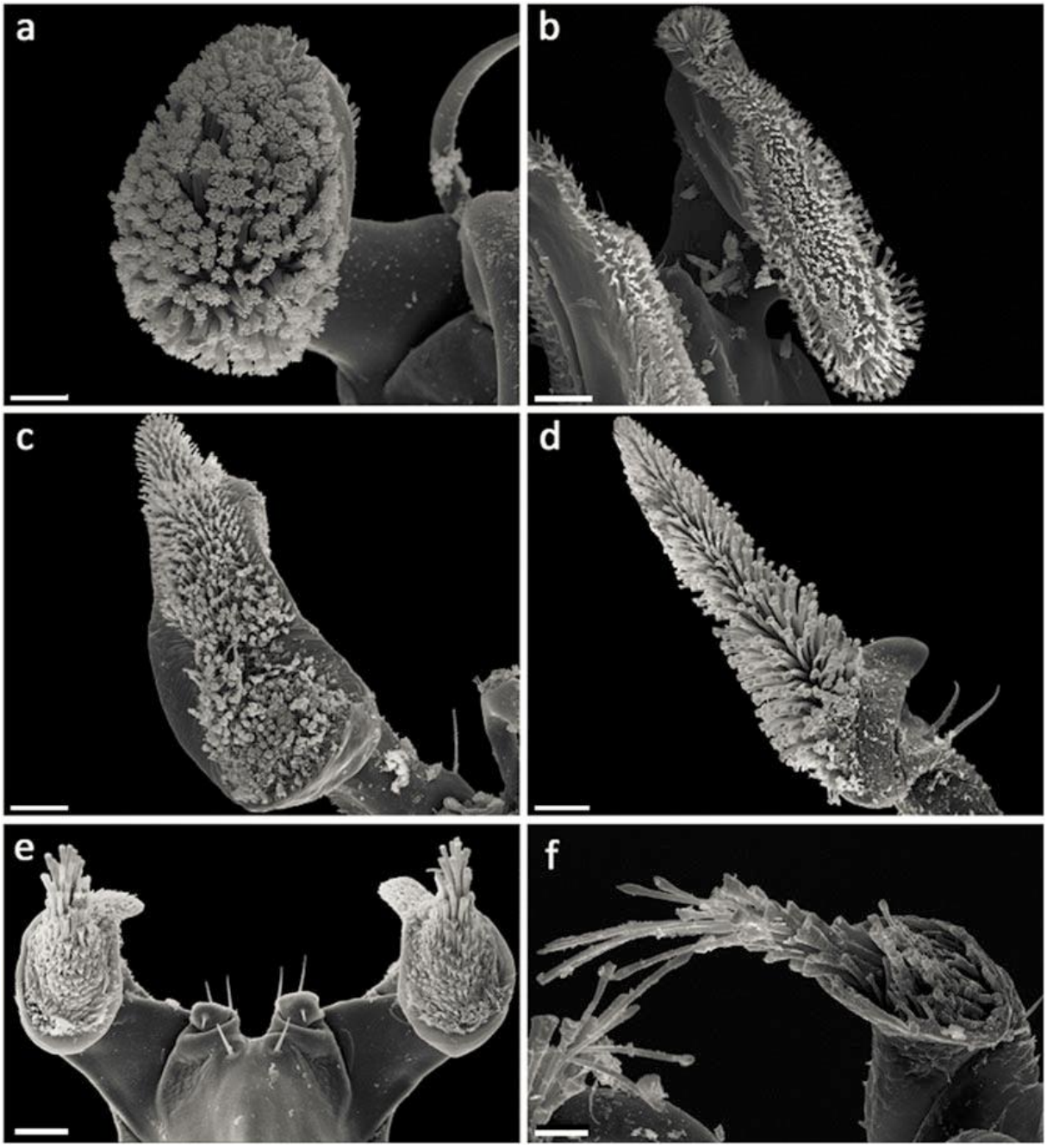

Abb.8: Haftpolstertypen bei *Stenus* spp. a) ellipsoid (*S. biguttatus*). Maßstabsbalken = 10 µm. (b, c) longiform (*S. fulvicornis, S. persicus*). Maßstabsbalken = 20 µm. (d) koniform (*S. stigmaticus*). Maßstabsbalken = 20 µm. (e) actiniform (*S. alpaca*). Maßstabsbalken = 20 µm. (f) sileniform (*S. nepalensis*), Maßstabsbalken = 10 µm. Aus Betz et al. 2018. Mit freundlicher Genehmigung des Springer-Verlags, Heidelberg.

2.1.2.3 Vergleich mit anderen biologischen Haftsystemen

Ändert sich die Größe eines Körpers, so ändert sich auch dessen Verhältnis zwischen Oberfläche und Volumen. Bei einer Vergrößerung des Körpers wächst die Oberfläche langsamer als das Volumen, denn die Oberfläche wächst nur quadratisch, das Volumen dagegen kubisch. Wenn also die Größe

eines Tieres zunimmt, nimmt dessen Körperoberfläche im Verhältnis zum Volumen ab. Dementsprechend haben sehr kleine Tiere eine ausgedehnte Körperoberfläche bei sehr geringem Volumen und sehr große Tiere hauptsächlich Volumen mit geringer Oberfläche. Das stellt größere kletternde Tiere vor ein Problem: wenn sie größer und schwerer sind, wird ihre Körperoberfläche im Verhältnis zum Körpervolumen kleiner und somit steht ihnen vergleichsweise weniger Körperoberfläche für ihr Haftsystem zur Verfügung. Um diese gewichtsbezogene Adhäsionsabnahme zu kompensieren, können große Tiere überproportional große Haftpolster oder Anpassungen entwickeln, die die Haftperformanz pro Flächeneinheit erhöhen (z. B. durch Erhöhung der Viskosität des Adhäsionssekretes). Labonte und Federle (2015) zeigten, dass kletternde Tiere (Eidechsen, Baumfrösche, Insekten) den vorhergesagten Adhäsionsverlust nicht durch positive Allometrie der Haftpolstergröße kompensieren – die meisten Daten zeigten, dass sich die Haftpolstergröße isometrisch oder sogar negativ allometrisch zur Körpergröße verhält. Allerdings scheinen kletternde Tiere das ungünstigere Oberflächen-Volumen-Verhältnis durch eine Verbesserung des Wirkungsgrades (der Haftfähigkeit pro Flächeneinheit) zu kompensieren, d.h. die Haftkräfte verhalten sich positiv allometrisch zur Haftpolsterfläche (Labonte & Federle 2015).

Im Gegensatz dazu verhält sich die Haftpolstergröße des Beutefangapparates der Gattung *Stenus* positiv allometrisch zur Körpergröße, d.h. die Haftpolsterfläche wächst mit der Körpermasse$^{0.83}$ (0.66 bei Isometrie) und mit der Pronotumlänge$^{2.46}$ (2 bei Isometrie) (Abb. 7A). Dementsprechend kompensieren größere *Stenus*-Arten das ungünstigere Oberflächen-Volumen-Verhältnis durch die Ausbildung überproportional größerer Haftpolster. Im Gegensatz zu kletternden Tieren, bei denen die Haftkraft schneller wächst als die Haftpolstergröße (d.h. die Hafteffizienz steigt mit zunehmender Körpergröße), verhalten sich die Adhäsionskräfte beim *Stenus*-Fangapparat negativ allometrisch zur Körpergröße, d.h. die Hafteffizienz sinkt mit zunehmender Körper- und Haftpolstergröße (Skalierungskoeffizienten < 2 für Pronotumlänge (*Stenus*: 1.26), < 0.66 für Körpermasse (*Stenus*: 0.43), < 1 für Haftpolsterfläche (*Stenus*: 0.56)).

Zusammenfassend kann man sagen, dass sich die Haftpolsterfläche bei *Stenus* positiv allometrisch und die Adhäsionskraft negativ zur Körpergröße verhält; somit entwickeln größere *Stenus*-Arten überproportional größere Haftpolster, die deren verringerte Hafteffizienz ausgleichen. Folglich verringerte sich auch die Zugfestigkeit (Haftkraft pro Haftposterfläche) mit zunehmender Haftpolsterfläche (b = -0.43, 95% Konfidenzintervall: -0.52, -0.34; Abb.7F), sodass *Stenus*-Arten mit kleineren Haftpolstern zwar geringere absolute Adhäsionskräfte erzeugen, aber insgesamt höhere Zugfestigkeiten erreichen und somit adhäsiv effizientere Haftpolster besitzen. Die berechneten Werte für die Zugfestigkeit lagen dabei zwischen 51.9 kPa bei *S. bimaculatus* und 153.2 kPa bei *S. humilis* (Abb.7F). Die Gründe für die verringerte Hafteffizienz größerer Haftpolster sind noch unklar. Ähnlich wie bei den Tarsen von Schwebfliegen (Syrphidae) könnte deren verringerte Hafteffizienz damit

zusammenhängen, dass es bei größeren Haftpolstern wahrscheinlicher ist, dass nicht die gesamte Haftpolsteroberfläche mit der Beuteoberfläche in Berührung kommt (Gorb et al. 2001). Laut Betz und Kölsch (2004) muss sich das Haftsekret bei *Stenus* von einer sehr verengten Zone am äußeren Rand der Haftpolster über den gesamten Bereich der Hafthaare verteilen. Man kann daher annehmen, dass sich das Haftsekret wesentlich leichter über eine kleinere Fläche ausbreitet als über eine größere. Somit könnte die verminderte Hafteffizienz größerer Haftpolster auch aus einer ungleichen Verteilung des Haftsekretes auf der Haftpolsteroberfläche resultieren. Andererseits zeigt die negative Korrelation von Zugfestigkeit und Haftpolsterfläche, dass das Haftsekret, welches während des Fangschlages über die Fläche des Haftpolsters verteilt wird, einen sehr großen Beitrag zur Haftfähigkeit des Fangapparates leistet.

2.1.2.4 Beutefang

Die während des Fangschlages auftretenden Kräfte können in Bezug mit bereits vorhandenen Daten über den Fangerfolg bei verschiedenen Beutegrößen gesetzt werden. Bei diesen Fangversuchen wurden die *Stenus*-Arten mit verschiedenen Größen- (bzw. Gewichts-)klassen der Collembolenart *Heteromurus nitidus* konfrontiert und die Anwendungshäufigkeiten beider Fangtechniken (Labium/Mandibel) sowie der Fangerfolg analysiert. Im Verhaltensexperiment erweisen sich die Haftpolster des Fangapparates von *Stenus* als sehr effektive Haftorgane, mit denen die Tiere hohe Fangerfolge erzielen. Dabei werden die Beutetiere unmittelbar im Moment der Berührung an die Haftpolster festgeklebt, wobei der Fangerfolg umso höher ist, je größer die Haftpolster sind und je mehr Hafthaare und Haftkontakte auf ihrer Oberfläche untergebracht werden können (Betz 1996, 1998a; Publikation III).

Die phylogenetisch vergleichenden Analysen zeigten, dass eine höhere Adhäsionskraft der Klebpolster zu einem höheren Fangerfolg gegenüber Collembolen der Art *Heteromurus nitidus* führt. Dieser Effekt war beim Fang größerer Collembolen wesentlich stärker ausgeprägt ($r = 0.95$, $p < 0.001$; Abb.9) als beim Fang kleiner Collembolen ($r = 0.49$, $p = 0.09$; Abb.9).

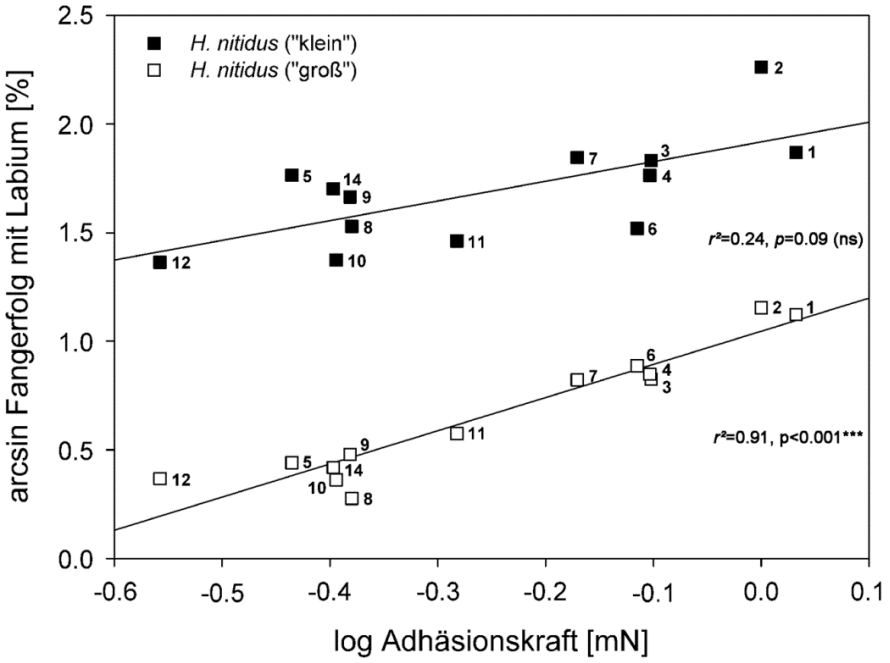

Abb.9: Abhängigkeit des Fangerfolges gegenüber großen und kleinen Collembolen der Art *Heteromurus nitidus* von der Adhäsionskraft [mN]. Regressionslinien wurden durch *PGLS*-Analysen berechnet. Artkürzel siehe Abb.7. Verändert nach Publikation III.

2.1.2.5 Ökomorphologie - Zusammenhang zwischen Morphologie, Beutefangverhalten und Leistungsfähigkeit des Fangapparates

Bei der ökomorphologischen Forschung steht die Frage im Vordergrund, welche Bedeutung ein bestimmter Form-Funktionskomplex für die Ökologie eines Organismus (insbesondere dessen Ressourcennutzung) hat. Zentraler Bestandteil dieses Ansatzes ist dabei die Integration von (1) funktioneller Morphologie, (2) Messung der Leistungskapazität des untersuchten Form-Funktionskomplexes sowie (3) der mit seiner Hilfe erreichten ökologischen Ressourcennutzung in der natürlichen Umwelt (z. B. Wainwright 1991; Reilly & Wainwright 1994; Betz 2006). Mit Hilfe multivariater Statistik (Hauptkomponenten- und Diskriminanzanalyse) wird dabei versucht, Korrelationen zwischen Morphologie und Ökologie (Ressourcennutzung) zu finden (z. B. Leisler & Winkler 1991). Beide Ebenen (Morphologie und Ökologie) werden dabei durch das Verhalten und die Leistungsfähigkeit der morphologischen Strukturen verbunden. Durch die verschiedenen multivariaten Methoden ist es möglich, Rückschlüsse auf die Struktur und Organisation verschiedener Lebensgemeinschaften oder Verwandtschaftsgruppen zu ziehen. Anhand der Verteilung der Arten im morphologischen Raum kann man deren morphologisch-ökologische Beziehungen beurteilen. Des Weiteren können auch phylogenetische Aspekte einbezogen werden und Auskunft über die Evolution einzelner morphologischer Merkmale gegeben werden.

Aufbauend auf diesem ökomorphologischen Forschungskonzept wurde ein Zusammenhang zwischen der Morphologie und der Leistungsfähigkeit des Fangapparates sowie dem Beutefangverhalten der Gattung *Stenus* hergestellt. Dazu wurde die Anordnung der Arten in einem Merkmalsraum getrennt für die morphologischen Variablen sowie die Variablen aus dem Bereich Verhalten/Performanz des Fangapparates mit Hilfe phylogenetischer Hauptkomponentenanalysen (PCA) untersucht. Zur Klärung der Frage nach den Beziehungen zwischen Morphologie einerseits und Verhalten/Performanz andererseits wurden abschließend die extrahierten Hauptkomponenten beider Bereiche auf signifikante Korrelationen überprüft.

Tab.1: Ergebnisse der phylogenetischen Hauptkomponentenanalysen von 13 *Stenus*-Arten hinsichtlich der Variablen aus den Bereichen Morphologie (PCA I) und Verhalten/Performanz (PCA II) basierend auf dem phylogenetischen Baum in Abb.3 in Publikation III. Fett markiert sind Faktorladungen > 0.6 und < -0.6.

	PC1	PC2	PC3
PCA I (Morphologie)			
Anteil erklärter Varianz %	62.23%	19.23%	12.12%
Parameter			
Klebpolsterfläche	**-0.928**	-0.087	0.131
Labiumlänge	**-0.923**	-0.200	-0.189
Anzahl Hafthaare pro Klebpolster	**-0.918**	0.147	0.044
Anzahl Haftkontakte pro Klebpolster	**-0.911**	0.378	0.070
Pronotumlänge	**-0.811**	-0.456	-0.299
Körpermasse	**-0.757**	-0.523	-0.368
Anzahl Hafthaarverzweigungen	**-0.705**	**0.619**	0.159
Dichte Hafthaare = Anzahl Hafthaare / 400µm²	**0.670**	0.066	**-0.695**
Dichte Haftkontakte = Anzahl Haftkontakte / 400µm²	-0.198	**0.806**	-0.547
PCA II (Verhalten/Performanz)			
Anteil erklärter Varianz %	56.29%	23.76%	8.68%
Parameter			
Fangerfolg mit Labium - große Collembolen	**-0.960**	0.117	-0.064
Adhäsionskraft	**-0.938**	0.094	-0.012
Zugfestigkeit (Adhäsionskraft/Klebpolsterfläche)	**0.867**	-0.190	-0.066
Druckkraft	**-0.805**	-0.136	0.447
Fangerfolg mit Labium - kleine Collembolen	**-0.747**	0.184	-0.530
Anwendungshäufigkeit mit Labium - große Collembolen	-0.424	**-0.845**	0.152
Anwendungshäufigkeit mit Labium - kleine Collembolen	-0.039	**-0.915**	-0.309

Die phylogenetische Hauptkomponentenanalyse der morphologischen Variablen zeigt, dass durch die ersten 3 Hauptkomponenten (PC) bereits 94% der morphologischen Gesamtvariation erklärt werden kann (Tab.1, Abb.10). Die erste Hauptkomponente (62% der Gesamtvariation) korreliert dabei negativ mit den Größenparametern (Pronotumlänge, Körpermasse) sowie morphologischen Parametern des Fangapparates (Haftpolsterfläche, Labiumlänge, Anzahl Hafthaare und Hafthaarverzweigungen, etc.). Dabei zeigt sich, dass besonders überdurchschnittliche Ausprägungen dieser Merkmale bei den untersuchten Arten *S. bimaculatus*, *S. juno*, *S. clavicornis* und *S. providus* auftreten. Hingegen zeigen Arten, wie z. B. *S. humilis*, *S. morio*, *S. comma* und *S. biguttatus* geringere Ausprägungen dieser Merkmale.

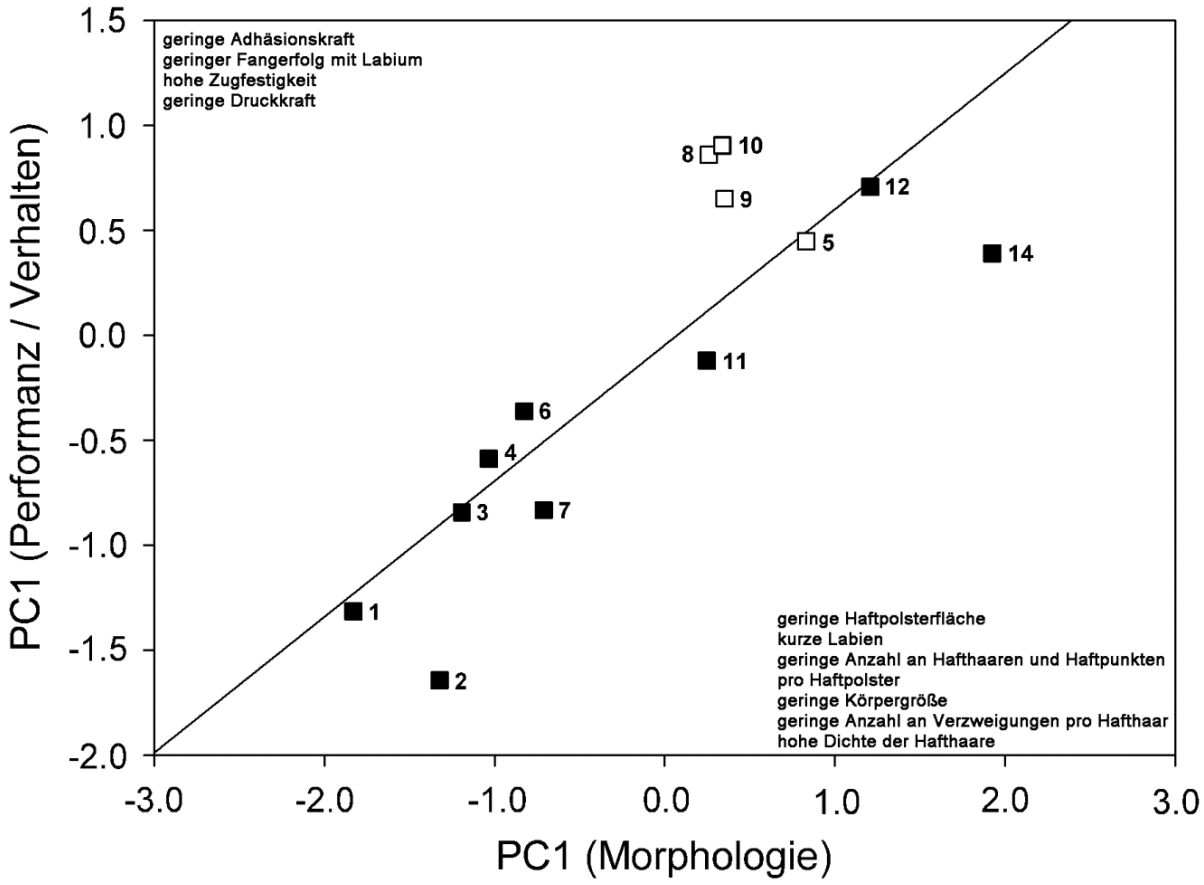

Abb.10: Beziehungen zwischen der Morphologie der Haftpolster und dem Beutefangverhalten bzw. der Performanz des Fangapparates bei 13 *Stenus*-Arten. Gegeneinander aufgetragen sind Hauptkomponente 1 aus dem Bereich und Verhalten/Performanz basierend auf einer phylogenetischen Hauptkomponentenanalyse (r = 0.758, p = 0.003). Gefüllte Kästchen kennzeichnen Arten, die feuchten, bodennahen Pflanzendetritus besiedeln; offene Kästchen kennzeichnen Arten, die offene, schlammige oder sandige Stellen etwa an Gewässerufern besiedeln ("Oberflächenläufer"). Artkürzel siehe Abb.7. Verändert nach Publikation III.

Wendet man die phylogenetische Hauptkomponentenanalyse auf die Merkmale aus dem Bereich Verhalten/Performanz an, lassen sich insgesamt 3 Hauptkomponenten extrahieren, welche zusammen 89% der Gesamtvariation der Arten erklären (Tab.1). Hauptkomponente 1 (56% der Gesamtvarianz) trennt dabei Arten mit hohen Adhäsions- und Druckkräften, geringen Zugfestigkeiten und hohem Fangerfolg (z. B. *S. juno, S. bimaculatus, S. clavicornis, S. lustrator*; Abb.10) von Arten mit geringen Adhäsions- und Druckkräften, hohen Zugfestigkeiten und geringem Fangerfolg (z. B. *S. guttula, S. fossulatus, S. morio, S. biguttatus*, *S.comma* and *S. humilis*; Abb. 10).

Mit den Faktorwerten jeder Art aus den phylogenetischen Hauptkomponentenanalysen kann deren Verteilung im Raum dargestellt werden. In Abbildung 10 sind jeweils die Faktorenwerte für Hauptkomponente 1 aus dem Bereich Morphologie und Verhalten/Performanz gegeneinander aufgetragen – beide Hauptkomponenten zeigen einen signifikanten Zusammenhang (r = 0.76, p = 0.003; Abb.10). Diese Abbildung zeigt die Positionierung der untersuchten *Stenus*-Arten im morphologischen/etho-ökologischen Raum und fasst somit die wichtigsten Ergebnisse der vorliegenden Arbeit zusammen.

Dementsprechend finden sich an einem Ende des Spektrums (niedrige Werte für beide Achsen) große *Stenus*-Arten, die lange Fanglabien sowie große Haftpolster mit einer großen Anzahl an Hafthaaren und -kontakten besitzen und dadurch hohe Adhäsionskräfte und hohe Fangerfolge, vor allem gegenüber großen Collembolen, erzielen. Am anderen Ende des Spektrums (hohe Werte für beide Achsen) finden sich kleine Arten, die kleine, einfach gebaute Haftpolster (d.h. mit einer geringen Anzahl an Hafthaaren und -kontakten) besitzen und dadurch nur geringe Adhäsionskräfte entwickeln. Gegenüber kleinen Collembolen erreichen diese Arten noch hohe Fangerfolgsraten von 40-60%, gegenüber großen Collembolen verringert sich deren Fangerfolg allerdings drastisch (3-5% Fangerfolg). Somit scheint dieser Beutetyp keine adäquate Beute für diese Arten darzustellen und die Haftperformanz des Labiums scheint bei diesen Arten bereits an die Grenze seiner Leistungsfähigkeit zu stoßen, da sich große und damit schwerere Beutetiere sehr leicht wieder von den Klebpolstern ablösen können. Diese Annahme wird auch dadurch bestätigt, dass kleinere *Stenus*-Arten (z. B. *S. humilis, S. boops*) nicht in der Lage sind, große Collembolen in den Bereich der Mandibeln zu ziehen (Koerner & Betz, pers. Beob.).

Bei den meisten der untersuchten *Stenus*-Arten handelt es sich um wenig agile Lebensformen, die im bodennahen Pflanzendetritus jagen (siehe Arten, die mit pl de gekennzeichnet sind) und aufgrund ihrer physiologisch bedingten geringeren Agilität und Reaktivität viel stärker vom Einsatz des Labiums beim Beutefang abhängen (vgl. Tab.4 in Publikation III). Der adaptive Wert des Fanglabiums liegt insbesondere für diese Arten darin, dass es ihnen trotz ihrer begrenzten Reaktivität den schnellen und überraschenden Zugriff selbst schwer zu fangender fluchtfähiger Beute ermöglicht (Betz 1996, 1998a,

b). Der Performanz-Vorteil des labialen Fangmechanismus gegenüber den Mandibeln liegt hierbei in seiner höheren Reichweite und Geschwindigkeit sowie der Möglichkeit der Fixierung der Beute im Moment der Berührung.

Im Gegensatz zu diesen wenig agilen Arten ergaben die Experimente, dass die Bewohner offener Uferflächen (*S. comma*, *S. fossulatus*, *S. guttula* und *S. biguttatus*) in geringerem Maße auf den labialen Fangapparat angewiesen sind (vgl. Tab.4 in Publikation III). Diese Arten besitzen weit vorstehende Augen mit einer großen Anzahl an Ommatidien, sehr lange Beine und Mandibeln und sind gekennzeichnet durch eine hohe Agilität, Reaktionsfähigkeit und Laufgeschwindigkeit (Bauer & Pfeiffer 1991; Betz 1996, 1998a, b, 1999, 2006). Außerdem zeichnen sich diese Arten durch einen Wechsel der Fangtechnik in Abhängigkeit von der Beutegröße aus. Während kleine Collembolen bevorzugt mit dem Labium erbeutet werden (von 66% bei *S. comma* bis zu 85% bei *S. biguttatus*), ergreifen diese Arten große Collembolen überwiegend mit den Mandibeln (*S. guttula*, *S. comma*, *S. fossulatus* zu 64-78%; *S. biguttatus* zu 50%). Dies korrespondiert mit dem entsprechenden Fangerfolg beider Fangtechniken: während das Labium gegenüber kleinen Collembolen der erfolgreichere Fangmechanismus ist, werden große Collembolen erfolgreicher mit den Mandibeln erbeutet. Mit zunehmender Beutegröße nimmt auch der Fangerfolg mit dem Labium ab. Beim Fang mit dem Labium haben diese Arten gegenüber kleinen Collembolen noch relativ große Erfolgsraten von 40-60%. Dieser Wert sinkt beim Fang großer Collembolen auf 2-6% (vgl. Abb.9). Dementsprechend scheint auch bei diesen Arten der Klebfangmechanismus an die Grenze seiner Leistungsfähigkeit zu stoßen. Dieser Nachteil wird allerdings durch eine verbesserte Mandibelfangtechnik und -morphologie kompensiert. Durch die relativ langen Mandibeln sowie durch ihre hohe Agilität und Wendigkeit (aufgrund der langen Beine sowie der verbesserten Augenmorphologie) sind sie in der Lage, selbst bei großen Collembolen hohe Fangerfolge mit den Mandibeln zu erreichen (20-40%) (Betz 1996, 1998a, 2006). Die vorliegenden Ergebnisse weisen möglicherweise auf eine mögliche sekundäre Reduktion des Fangapparates dieser Arten hin, da diese (1) in Relation zu ihrer Körpergröße sehr kleine, einfach strukturierte Haftpolster ausweisen (Abb.7A: offene Quadrate) und (2) sehr geringe Druckkräfte während des Fangschlages generieren (Abb.7B: offene Quadrate). Möglicherweise hat die Verbesserung der Mandibelfangtechnik bei Bewohnern offener Bodenbiotope zu einer Reduktion des labialen Fangapparates geführt, welche die verminderte Leistungsfähigkeit der Haftpolster vor allem beim Fang größerer Beutetiere kompensiert. Interessanterweise zeigen die phylogenetischen Untersuchungen (Publikation V), dass sich agile, reaktionsfähige Lebensformen mindestens zweimal unabhängig voneinander innerhalb der Gattung *Stenus* entwickelt haben, da die Artenpaare *S. fossulatus* / *S. guttula* (gehörend zur *guttula*-Artengruppe; Puthz 2008) und *S. comma* / *S. biguttatus* (gehörend zur *comma*-Artengruppe; Puthz 2008) keine sehr enge Verwandtschaftsbeziehung haben (Abb.18-22). Die vorliegende Phylogenie unterstützt außerdem unsere Hypothese einer sekundären

Reduktion des Klebfangapparates, da diese Arten innerhalb von Artengruppen mit komplexeren Fanglabien clustern.

Interessanterweise scheint eine Sekundärreduktion des Fangapparates auch bei Vertretern der *S. canaliculatus*-Gruppe aufzutreten, die stark verkürzte Fanglabien mit stark reduzierten Haftpolstern aufweisen (Betz 1996, 1998a, b, 2006; Publikation V). Hierfür spricht neben anatomischen Details (Betz 1996) auch die Beobachtung bei *S. canaliculatus* und *S. nitens* (gehörend zur *canaliculatus*-Artengruppe; Puthz, 2008), dass das Labium weder beim Beutefang noch in einem anderen Zusammenhang eine biologische Rolle spielt. Die Tiere erbeuten Collembolen ausschließlich mit den Mandibeln, wobei sie sehr hohe Fangerfolge erzielen. Die Spezialisierung auf den Fang mit den Mandibeln ist vielleicht sogar die Ursache für die Reduktion der Fangapparate dieser Arten, weil diese durch den Wechsel der Fangtechnik keiner stabilisierenden Selektion mehr unterlagen (Betz 1994). Somit war bei *Stenus* eine Spezialisierung auf größere Beute offenbar auf zwei entgegengesetzten Wegen möglich: einerseits durch eine Vergrößerung der Haftpolster (z. B. bei *S. bimaculatus*, *S. juno*, *S. clavicornis*), andererseits durch eine Verbesserung der Mandibelmorphologie und –fangtechnik (z. B. *S. comma*, *S. biguttatus*, *S. fossulatus*, *S. guttula*, *S. canaliculatus*-Artengruppe) bei gleichzeitiger Rückbildung des Fangapparates.

2.1.3 Einfluss der Oberflächenrauheit und -energie auf die resultierende Haftkraft (Publikation II)

Stenus-Arten sind polyphage Räuber, die eine Vielzahl an Invertebraten erbeuten, z. B. Oligochaeten, kleine Spinnen, Milben, Blattläuse, Collembolen, Fliegen (Betz 1998b; Heethoff et al. 2011). Die hohe Diversität potenzieller Beutetiere bringt es dabei mit sich, dass die Haftpolster an Beuteobjekten mit sehr unterschiedlichen Oberflächenstrukturen und physikochemischen Eigenschaften anhaften können müssen. Untersuchungen an tarsalen Haftorganen von Insekten haben gezeigt, dass sowohl die Oberflächenrauheit als auch die Oberflächenenergie die Haftfähigkeit beeinflussen (Gorb 2001; Bullock & Federle 2010; Gorb & Gorb 2009; Lüken et al. 2009). Die Oberflächenrauheit kann durch eine Verringerung der verfügbaren Kontaktfläche zwischen zwei Oberflächen zu einer verminderten Adhäsionskraft führen (Fuller und Tabor 1975). So haben Kraftmessungen an haarigen (d.h. mit mikroskopisch kleinen, biegsamen Hafthaaren) tarsalen Haftorganen von Käfern und Fliegen gezeigt, dass bei einem Unebenheitsdurchmesser im Bereich von 0.05 bis 1.0 µm ein Minimum an erzeugten Haftkräften auftritt (Gorb 2001; Peressadko & Gorb 2004; Voigt et al. 2008b; Bullock & Federle 2010). Diese „kritische Oberflächenrauheit“ resultiert aus einer reduzierten Kontaktfläche zwischen

den Oberflächenunregelmäßigkeiten und den terminalen Elementen (Spatulae) der Haftorgane (Peressadko & Gorb 2004).

Laut Holdgate (1955) bestehen außerdem starke interspezifische Unterschiede in den Benetzungseigenschaften der Insektencuticula. Aufgrund des Vorhandenseins von Wachsen auf der Epicuticula möglicher Beutetiere von *Stenus* ist deren Körperoberfläche im Allgemeinen hydrophob (Holdgate 1955; Wagner et al. 1996; Voigt et al. 2008a). Sogar unterschiedliche Oberflächenbereiche eines Individuums können große Unterschiede in den Benetzungseigenschaften aufweisen (Holdgate 1955; Noble-Nesbitt 1963) - diese Unterschiede korrelieren mit der Variationen der Oberflächenstrukturen. Zusätzliche Strukturen auf der Körperoberfläche, wie Papillen, Dornen, Schuppen oder Haaren, führen zu noch höheren Kontaktwinkeln und dadurch zu einer stark hydrophoben oder sogar super-hydrophoben Cuticula (Holdgate 1955; Noble-Nesbitt 1963; Wagner et al. 1996). Solche Oberflächenstrukturen können sich leicht ablösen und dadurch zusätzlich zur Verringerung der Haftwirkung beitragen (Bauer & Pfeiffer 1991).

Demnach besitzt die Körperoberfläche potentieller Beutetiere eine Vielzahl von Eigenschaften, sowohl in Bezug auf Struktur und Chemismus, sodass der Fangapparat der Gattung *Stenus* an eine Vielzahl an Oberflächen angepasst sein sollte. Vermutlich wirken die drei funktionellen Elemente der Haftpolster (das Haftsekret, die terminal verzweigten Hafthaare und das Netzwerk aus endocuticulären Fasern innerhalb des Haftpolsters) synergistisch zusammen, und stellen damit eine möglichst große Kontaktfläche mit der Beute her. Darüber hinaus könnte die biphasische Zusammensetzung des Haftsekretes (Kölsch 2000; Publikation I) eine gute Benetzbarkeit der Körperoberflächen möglicher Beutetiere gewährleisten. Diese Vermutungen wurden experimentell getestet, indem die Haftperformanz des Fangapparates zweier *Stenus*-Arten (*S. bimaculatus* und *S. juno*) auf Substraten verschiedener Oberflächenrauheiten und -energien gemessen wurde.

Zur Bestimmung der Haftperformanz des Fangapparates auf Oberflächen mit unterschiedlicher Rauheit wurden die Käfer auf sechs verschiedenen Substraten mit unterschiedlichen Rauheitsstufen getestet: Epoxidharzabdrücke von Polierpapieren (Buehlers Fibrmet Discss, Buehler, Lake Bluff, IL, USA) der Partikelgrößen 0, 0.3 µm, 1 µm, 3 µm, 9 µm und 12 µm (zur Präparationsmethode der Epoxidharzabdrücke siehe Scherge & Gorb 2001). Die Epoxidharzabdrücke wurden auf einen Insektennadelkopf geklebt und die Kraftmessungen wie in Abschnitt 2.1.1 beschrieben durchgeführt.

Die Ergebnisse dieser Kraftmessungen zeigten beim *Stenus*-Fangapparat keine signifikanten Unterschiede auf den getesteten Oberflächen unterschiedlicher Rauheit (Abb.11). Im Gegensatz dazu zeigten Zentrifugalexperimente des tarsalen Haftsystems auf denselben Oberflächen signifikante Unterschiede zwischen den verschiedenen Oberflächenrauigkeiten (Abb.12) mit einem Minimum an erzeugten Haftkräften bei einem Unebenheitsdurchmesser im Bereich von 0.3 bis 1.0 µm. Mehrere Studien an tarsalen Haftorganen von Insekten haben denselben Einfluss der Oberflächenrauheit auf die

Haft(Reibungs)kräfte gezeigt (Gorb 2001; Peressadko & Gorb 2004; Voigt et al. 2008b; Al Bitar et al. 2010; Gorb & Gorb 2009; Bullock & Federle 2010; Gorb et al. 2010). Demnach waren die Reibungskräfte sowohl auf glatten als auch sehr rauen Oberflächen (mit Partikelgrößen >3µm) groß, während im Rauheitsbereich von 0.05-1 µm minimale Kräfte auftraten („kritische Rauheit“). Dieser Effekt resultiert vermutlich aus einem reduzierten Kontakt zwischen den kleinen Oberflächenunebenheiten und den terminalen Elementen der tarsalen Hafthaare (Spatulae). Im Gegensatz zu den tarsalen Haftsystemen weisen natürliche Haftsysteme, bei denen ein echter Klebstoff an der Haftung beteiligt ist, eine Erhöhung der Haftkraft mit zunehmender Rauheit auf (z. B. Seepocken, Napfschnecken, Stachelhäuter; Yule & Walker 1984, 1987; Grenon & Walker 1981; Santos et al. 2005).

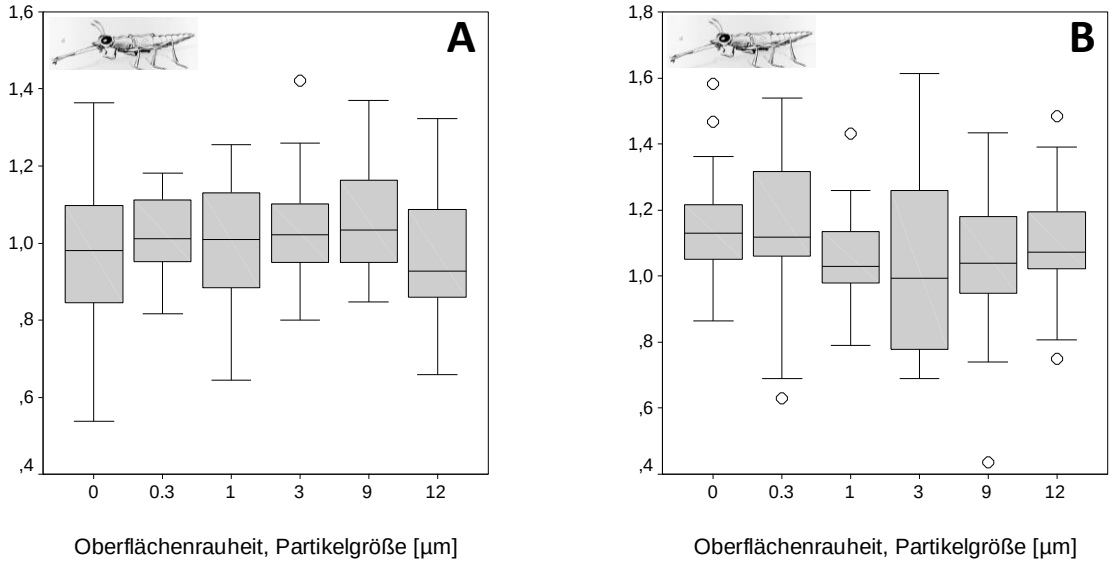

Abb.11: Haftfähigkeit (Adhäsionskraft) der Klebpolster von (**A**) *S. bimaculatus* und (**B**) *S. juno* auf Kunstharzoberflächen mit unterschiedlichen Rauheit (Durchmesser der Oberflächenunebenheiten 0 (glatt), 0.3, 1.0, 3.0, 9.0 und 12 µm). Die Haftleistung der Klebpolster auf den untersuchten Oberflächen unterscheidet sich bei beiden Arten nicht signifikant (Kruskal–Wallis-Test; *S. juno*: $p > 0.05$, $\chi^2 = 6.94$, $df = 5$, *S. bimaculatus*: $p > 0.05$, $\chi^2 = 7.90$, $df = 5$). Verändert nach Publikation II.

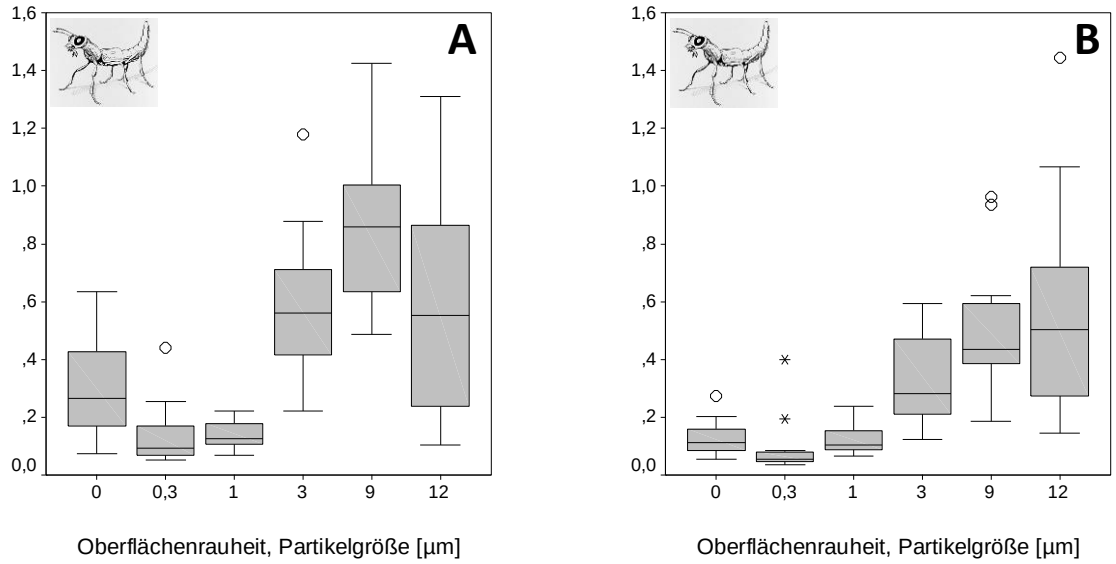

Abb.12: Tarsale Haftkraft (Reibungskraft) von *S. bimaculatus* (**A**) und *S. juno* (**B**) im Zentrifugalexperiment auf Kunstharzoberflächen mit unterschiedlichen Rauheit (Durchmesser der Oberflächenunebenheiten 0 (glatt), 0.3, 1.0, 3.0, 9.0 und 12 µm). n = 18 (*S. bimaculatus*), n = 12 (*S. juno*). Die Haftkräfte wurden mit der Zentrifugaleinrichtung BIOSPIN-01 (Tetra GmbH, Ilmenau, Deutschland) ermittelt. Die Käfer wurden dabei horizontal auf die mit den Kunstharzoberflächen bestückte Zentrifugentrommel gesetzt und kontinuierlich innerhalb von 20 Sekunden bis maximal 3000 Umdrehungen pro Minute beschleunigt. Glitt das Tier von der Trommel, wurden seine Position (Trommelradius) und Endgeschwindigkeit (Umdrehungen pro Minute) automatisch festgehalten und mit der gerätespezifischen Software PC Fly auf dem Monitor dargestellt. Aus diesen Daten wurde zusammen mit dem ermittelten Körpergewicht nach der Methode von Gorb et al. (2001) die maximale Haftkraft [mN] errechnet. Unpublizierte Daten.

Diese Beobachtung weist darauf hin, dass es sich bei dem Haftsekret des *Stenus*-Labiums um einen echten Klebstoff handelt, da auch diese eine gute Haftperformanz auf allen Oberflächen erreichen. Die Bedeutung rauer Oberflächen für die Haftkraft liegt vor allem in der Vergrößerung der Kontaktfläche zwischen Klebstofffilm und Substrat und damit in der Steigerung der spezifischen Adhäsionskräfte (Kendall 2001; Drechsler & Federle 2006; Federle 2006; Persson 2007; Gorb 2008). Dieses Prinzip scheint auch beim *Stenus*-Fangapparat eine wesentliche Rolle zu spielen: REM-Aufnahmen der Sekretabdrücke auf den getesteten Oberflächen zeigen, dass das Haftsekret die Unregelmäßigkeiten der Oberfläche benetzt und so die Kontaktfläche zum Substrat erhöht. Die große Sekretmenge auf den Haftpolstern bei *Stenus* scheint demnach eine Anpassung an die unterschiedlichen Oberflächenstrukturen der potentiellen Beute zu sein. Eine wichtige Funktion beim Adhäsionsvorgang hat dabei auch die Druckkraft, die beim Hervorschnellen des Labiums und beim Angriffsvorstoß des Käfers entsteht (Betz 1996, 1998a; Kölsch 2000). Ein höherer Anpressdruck ist auf glatten Oberflächen vorteilhaft, da er zu einer Reduktion der Schichtdicke des Sekretes in der Kontaktzone

führt (Bowden & Tabor 1986; Habenicht 2009). Auf rauen Oberflächen bewirken höhere Druckkräfte eine Vergrößerung der wirksamen Kontaktfläche zwischen Substrat und Haftorgan, da das Haftsekret effektiver in die Oberflächenunebenheiten gedrückt wird (Habenicht 2009).

Während viele haarige tarsale Haftsysteme spatelförmige Haftelemente aufweisen (z. B. Stork 1980; Walker 1993; Varenberg et al. 2010), sind die Spitzen der Verzweigungen beim *Stenus*-Fangapparat sphärisch geformt, mit Durchmessern zwischen 0.17 und 0.24 µm (Publikation I). Je kleiner diese Haftelemente sind, desto größer ist das Spektrum an Oberflächen, die sie kompensieren können. Bei *Stenus* sind diese terminalen Haftelemente kleiner als die Durchmesser der getesteten Oberflächenrauheiten, wodurch sie einen engen Kontakt mit diesen Oberflächentexturen herstellen können. Im Gegensatz dazu liegen die Durchmesser der Spatulae bei behaarten tarsalen Haftorganen im Bereich von 1 bis 10 µm (Peattie & Full 2007) und korrespondieren damit mit den Partikelgrößen der getesteten Unebenheiten. Die kritische Rauheit bei Insektentarsen entsteht dadurch, dass die Flexibilität der terminalen Elemente (Spatulae) nicht ausreicht, um vollen Kontakt zur Oberflächenrauheit herzustellen (Peressadko & Gorb 2004). Zusammenfassend lässt sich sagen, dass die Haftung des Fangapparates von *Stenus* an unterschiedlichen Oberflächenrauheiten durch folgende Parameter gewährleistet wird: (1) die geringe Größe der Verzweigungen der Hafthaare, (2) das Haftsekret, das in die Kontaktzone abgegeben wird und (3) die Flexibilität und Elastizität des Polstergewebes, der Hafthaare und deren Verzweigungen (Betz 1996; Kölsch & Betz 1998; Publikation I).

Zur Bestimmung der Abhängigkeit der Haftperformanz des Fangapparates von der Oberflächenenergie wurden zwei unterschiedliche Glasoberflächen verwendet. Die hydrophile bzw. hydrophobe Glasoberfläche weist Kontaktwinkel mit Wasser von 68° (Oberflächenenergie 59 mN/m) bzw. 122° (Oberflächenenergie 12 mN/m) auf. Diese Oberflächen wurden am Insektennadelkopf angebracht und die Kraftmessungen wie oben beschrieben durchgeführt (siehe Abschnitt 2.1.1).

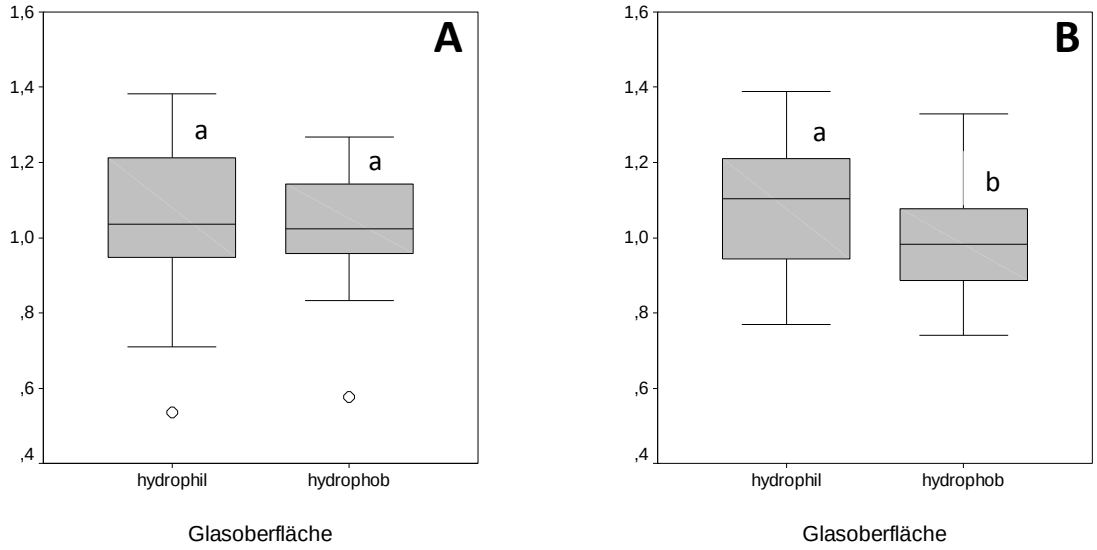

Abb.13: Haftfähigkeit der Klebpolster von *S. bimaculatus* (**A**) und *S. juno* (**B**) auf Oberflächen mit unterschiedlichen Oberflächenenergien (hydrophil: Oberflächenenergie 59 mN m^{-1}; hydrophob: Oberflächenenergie 12 mN m^{-1}). Die Haftleistung der Klebpolster auf den Oberflächen unterscheidet sich nur bei *S. juno* signifikant (Mann–Whitney U-Test; *S. juno*: $p < 0.05$, $Z = -2.07$, *S. bimaculatus*: $p > 0.05$, $Z = -0.49$). Verändert nach Publikation II.

Die Ergebnisse dieser Messungen zeigten nur geringfügige Unterschiede auf der hydrophilen (hohe Oberflächenenergie) bzw. hydrophoben (geringe Oberflächenenergie) Glasoberfläche (Abb.13). Bei beiden untersuchten Arten wurde die höhere Haftkraft auf der hydrophilen Oberfläche gemessen - die Haftkraft war auf der hydrophoben Oberfläche bei *S. bimaculatus* um 1.81% und bei *S. juno* um 9.03% reduziert. Allerdings waren diese Unterschiede nur bei *S. juno* signifikant ($p < 0.05$). Ähnliche Ergebnisse zeigten auch Insektentarsen, bei denen eine erhöhte Hydrophobizität (geringe Oberflächenenergie) ebenfalls zu einer verringerten Haftung führten (Al Bitar et al. 2009; Gorb & Gorb 2009; Gorb et al. 2010; Lüken et al. 2009).

Diese Ergebnisse unterstützen die Daten zur chemischen Zusammensetzung des Haftsekretes bei *Stenus*. Frühere Untersuchungen haben gezeigt, dass es sich beim *Stenus*-Haftsekret um ein disperses System handelt, bei dem Lipidtröpfchen in einer mächtigeren proteinhaltigen wässrigen Fraktion emulgiert vorliegen (Kölsch 2000; Betz & Kölsch 2004). Histochemische Analysen haben diese Ergebnisse bestätigt und zeigten positive Reaktionen auf Kohlenhydrate (Mucopolysaccharide), Proteine und Lipide (Betz et al. 2009). Der Vorteil solcher Emulsionen liegt vermutlich in den verbesserten Benetzungseigenschaften gegenüber Substraten mit hydrophilen als auch hydrophoben Eigenschaften (Kölsch 2000; Gorb 2001; Vötsch et al. 2002; Al Bitar et al. 2009; Betz 2010). Dementsprechend ist die Haftleistung des Beutefangapparates bei *Stenus* auf Oberflächen mit geringer

Oberflächenenergie (hydrophob) zwar vermindert, kann jedoch infolge der Zusammensetzung des Haftsekretes aus hydrophilen und hydrophoben Komponenten kompensiert werden.

2.1.4 Funktionelle Grundprinzipien des *Stenus*-Haftsystems (Publikation I)

Die Klebpolster der Kurzflügelkäfergattung *Stenus* bestehen aus drei Funktionselementen, die synergistisch während des Beutefangprozesses zusammenwirken. Das in Abbildung 14 in der unteren rasterelektronenmikroskopischen Aufnahme dargestellte Netzwerk aus weichen endokutikularen Fasern stabilisiert das Polsterinnere und verleiht der gesamten Struktur Flexibilität und Elastizität (Betz 1996; Kölsch & Betz 1998), sodass sich die Haftpolster an die spezielle Form und Oberflächenunregelmäßigkeiten des Beutetieres anpassen kann. Die Flexibilität und Elastizität des gesamten Systems wird durch den Einbau des elastischen Proteins Resilin gewährleistet (vgl. Abb. 8C, D in Publikation I). Das „*Rubber*-Protein“ Resilin sorgt dafür, dass der Fangapparat, trotz hoher mechanischer Beanspruchung, keine Abnutzung und Materialermüdung aufweist – eine ähnliche Funktion hat das Resilin im Insektenflügel (Haas et al. 2000a, b).

Das dichte Netz aus endocutikularen Fasern unterstützt hierbei mechanisch die eigentliche Kleboberfläche, die in zahlreiche Hafthaare strukturiert ist (Abb.2B). Die Hafthaare sind in einem hexagonalen Muster angeordnet. Jedes Hafthaar ist am terminalen Ende je nach Art mehrfach verzweigt. Im Vergleich zu unverzweigten Haaren ermöglichen derartige endständige Verzweigungsstrukturen generell eine höhere Packungsdichte der kleineren, endständigen Äste. Die Gesamtzahl der adhäsiven Kontakte bei *Stenus*-Käfern beläuft sich so auf mehrere Tausend pro Klebpolster (Bauer & Pfeiffer 1991; Betz 1996; Publikation III). Darüber hinaus verhindert die endständige Verzweigung ein Verkleben benachbarter Hafthaare und erhöht die Toleranz gegenüber rauen Oberflächen (Jagota & Bennison 2002). Elektronenmikroskopische und kryo-rasterelektronenmikroskopische Aufnahmen haben gezeigt, dass diese haarähnlichen Auswüchse tief in das klebrige Sekret eintauchen (Abb.15 C, D), sodass nur die Spitzen der Verzweigungen herausstehen (Kölsch 2000; Publikation I).

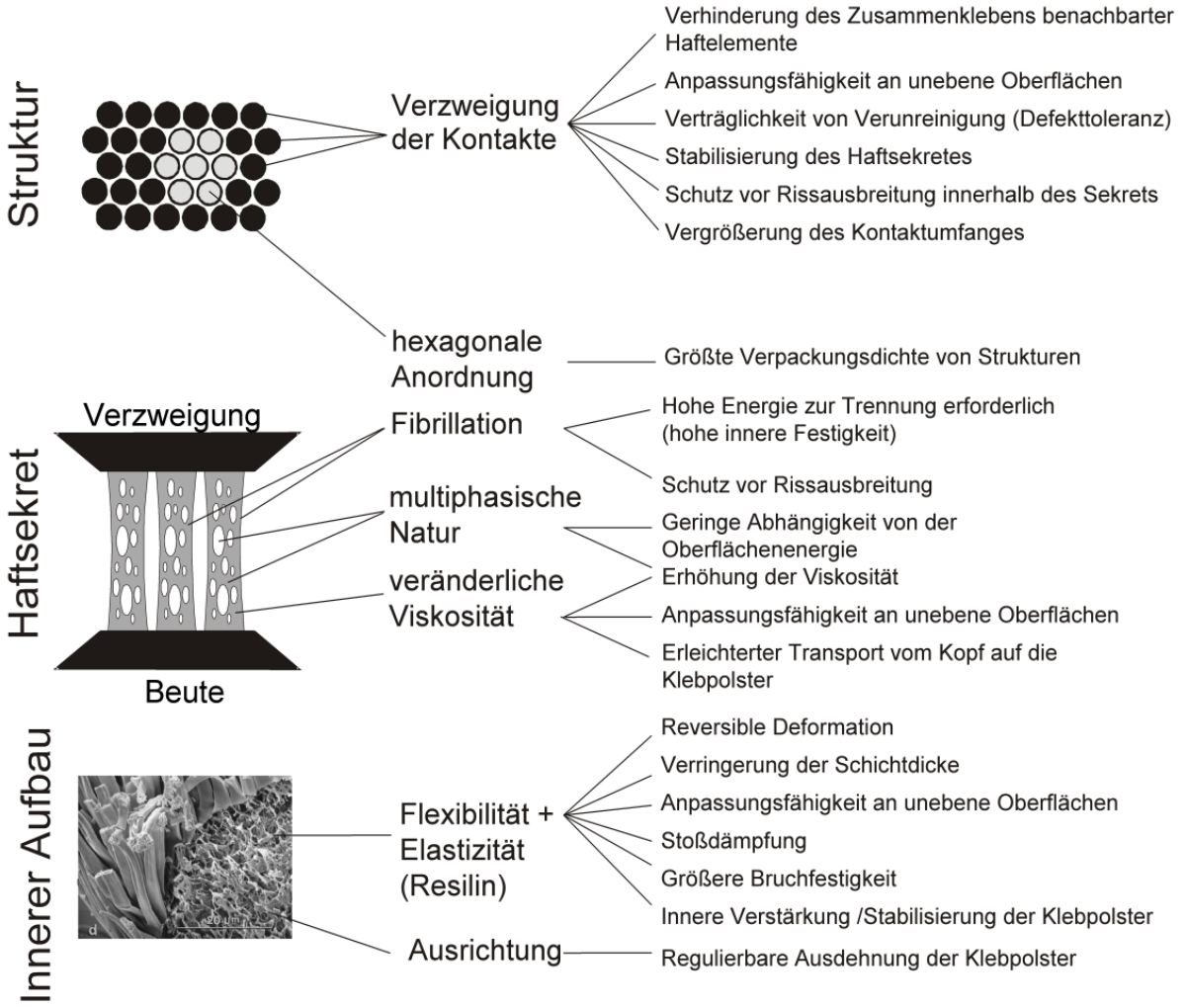

Abb.14: Zusammenfassung der Funktionsprinzipien des Beutefangapparates der Gattung *Stenus*. Verändert nach Publikation I.

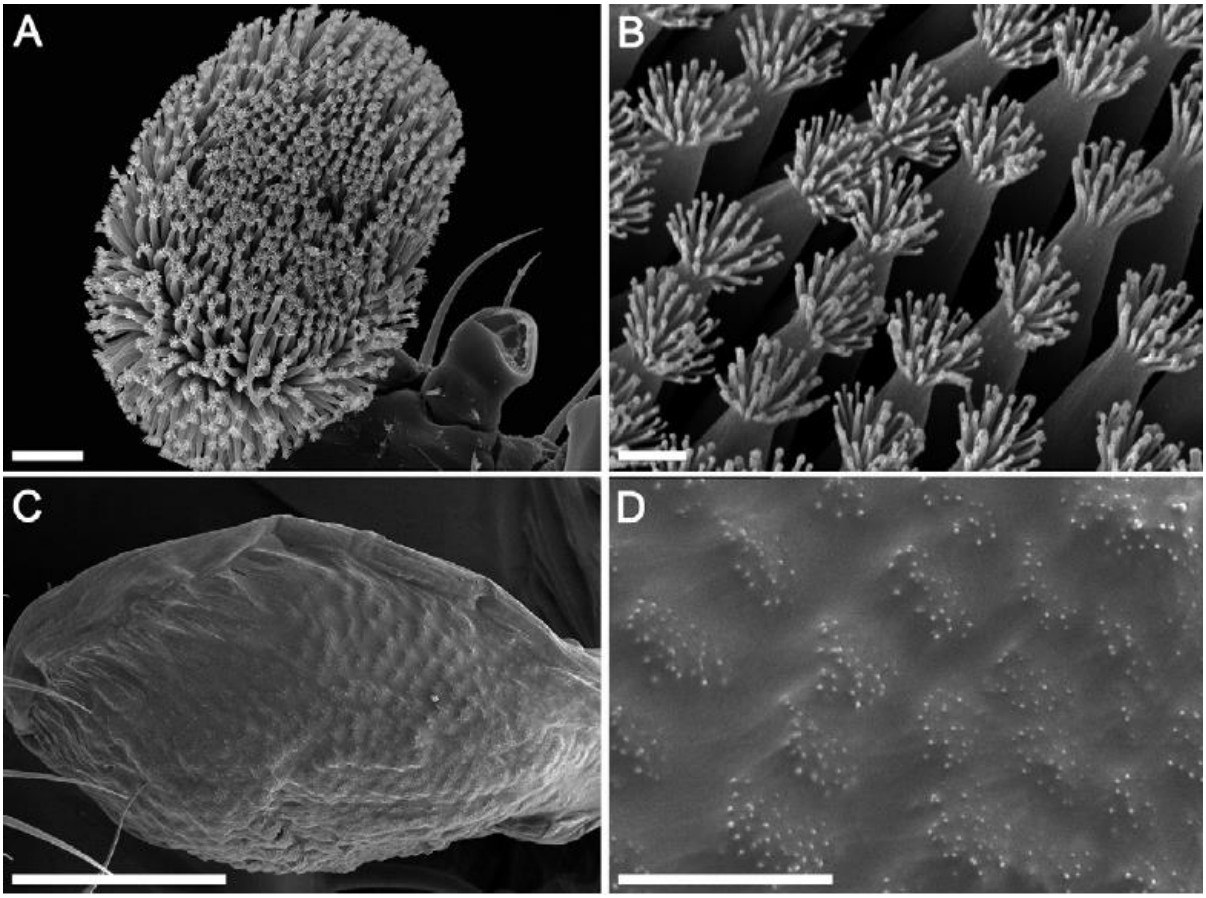

Abb.15: Aufnahmen der Haftpolster von *S. juno*. (A-B) REM-Aufnahmen, (C-D) Kryo-REM-Aufnahmen. (A) Ventralansicht (Maßstab = 20 µm). (B) Hafthaare mit terminalen Verzweigungen (Maßstab = 2 µm). (C) Während des Beutefanges sind die Hafthaare vollständig mit dem Klebsekret benetzt. (Maßstab = 30 µm). (D) Lediglich die terminalen Verzweigungen der Hafthaare ragen aus dem Klebsekret heraus (Maßstab = 2µm). Aus Publikation I. Mit freundlicher Genehmigung von Elsevier.

Generell hat der Einsatz adhäsiver Sekrete in natürlichen Haftsystemen mehrere Vorteile. Diese bestehen zum einen in der Möglichkeit der Verbindung von Materialien mit unterschiedlichen physikalischen und chemischen Eigenschaften, der verbesserten Spannungsverteilung an der Kontaktzone sowie der Vergrößerung der aktuellen Kontaktfläche durch Einebnen leichter Unregelmäßigkeiten an der Oberfläche (vgl. Kapitel 2.1.3).

Das Haftsekret wird über laterale Öffnungen am äußeren Rand der Klebpolster ausgeleitet (Kölsch & Betz 1998; Abb.2C). Von hier aus muss es über die gesamte Klebpolsteroberfläche verteilt werden, ohne die darunter liegenden, seitlichen Flankenbereiche zu verunreinigen, welche mit der Beute nicht direkt in Kontakt kommen. Diese kontrolliert gerichtete Verteilung wird wahrscheinlich durch starke Kapillarkräfte bewirkt, die von dem Lückenraum zwischen den Schäften und den endständigen Zweigen der Hafthaare ausgehen. Laut Kölsch (2000) besteht das Sekret aus zwei nicht mischbaren Phasen. So legen Ultrastrukturbilder nahe, dass fettähnliche Tröpfchen emulgiert in einer größeren

wässrigen proteinösen Fraktion vorliegen. In zusätzlichen histochemischen Tests konnten wasserlösliche Zucker, Proteine und Lipide nachgewiesen werden, sodass es sich bei dem Sekret um ein komplexes Gemisch aus mehr als nur einer chemischen Phase handelt (Betz et al. 2009). Wie für das Tarsalsekret von Heuschrecken (Vötsch et al. 2002) vermutet, könnte eine solche Emulsion für die effektive Verteilung des Sekrets über verschiedene Oberflächentypen (hydrophil und lipophil) von Vorteil sein (vgl. Kapitel 2.1.3). Darüber hinaus könnten am Außenrand des Klebpolsters koaleszierende Lipidtröpfchen die darunter liegende wässrige Proteinphase vor dem Austrocknen schützen. Auf diese Weise würden die Klebpolster permanent feucht und damit einsatzbereit gehalten. Die große Sekretmenge sowie die hohe gemessene Zugkraft lassen vermuten, dass der Adhäsionsmechanismus neben Kapillarkräften auf den viskosen Eigenschaften des Sekrets basiert (Stefan-Adhäsion). Die vermutete hohe Viskosität konnte durch Hochgeschwindigkeits-Videoaufnahmen belegt werden, auf denen das Zurückziehen der Klebpolster von einer Oberfläche zu sehen ist: wie bei kommerziell verfügbaren Haftklebstoffen, dehnt sich das Sekret dabei aus und gliedert sich in lange parallele Fasern auf, bevor es am Schluss an der Kontaktzone mit dem Substrat abreißt (Abb.16). Diese Beobachtung unterstreicht die hohe Bedeutung kohäsiver Kräfte, welche dem Sekret eine hohe innere Festigkeit verleihen, sodass die Verbindung nicht innerhalb des Sekretes bricht. Darüber hinaus hat das beobachtete Zerfasern des Klebstoffs den Vorteil, dass es eine höhere Energie zur Trennung der Oberflächen erfordert (Creton 2002).

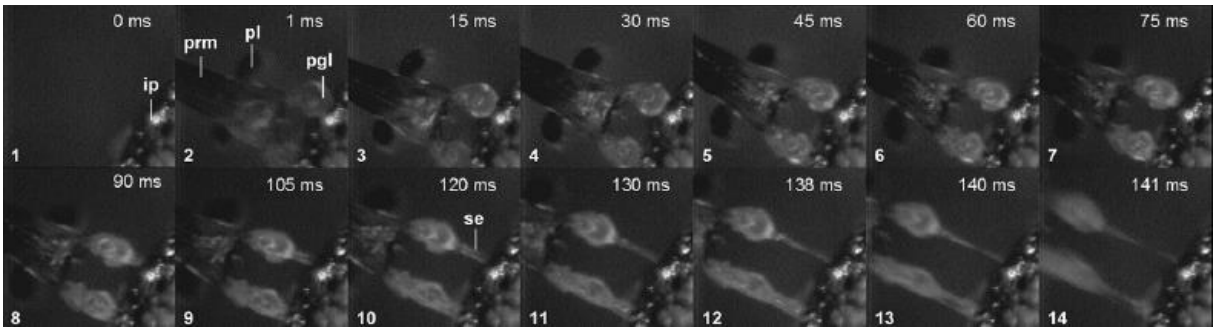

Abb.16: Hochgeschwindigkeitsaufnahmen der auf eine Beuteattrappe auftreffenden Klebpolster. Beim Rückzug der Klebpolster werden die extreme Viskosität des Klebsekrets sowie die starke Verformung der Klebpolster erkennbar. Aus Publikation I. Mit freundlicher Genehmigung von Elsevier.

2.1.5 Die Haftpolster der Gattung *Stenus* als Träger von Bakterien (Publikation IV)

In transmissionselektronenmikroskopischen Untersuchungen wurden im Klebsekret von *S. juno* und *S. bimaculatus* Bakterien in relativ hohen Dichten festgestellt (Abb.17; Kölsch 2010).

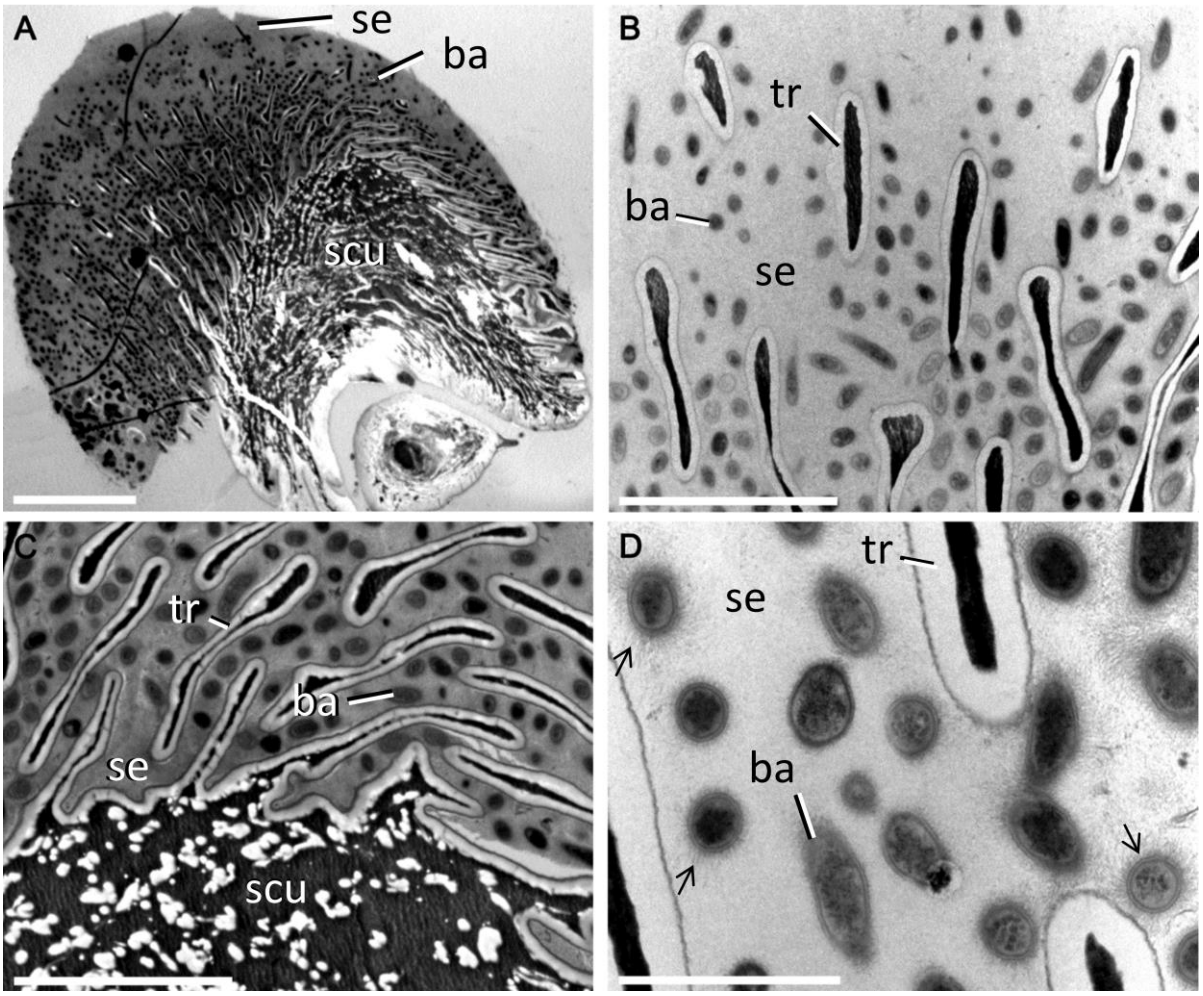

Abb.17: Transmissionselektronenmikroskopische Aufnahmen eines Transversalschnittes durch ein Klebpolster von *S. bimaculatus*, welches die Bakterien innerhalb des Haftsekretes zeigt. (A) Gesamtes Haftpolster. (B-D) Detailansichten der Bakterien im Haftsekret. Die Pfeile weisen auf Zellanhänge (Fimbrien) der Bakterien hin. Maßstab: (A) 10 µm, (B) 2.5 µm, (C) 2 µm, (D) 1 µm. Abkürzungen: ba Bakterien, se Haftsekret, scu Netzwerk aus endocuticulären Fasern innerhalb des Haftpolsters, tr Hafttrichom (= Hafthaar). Aus Publikation IV. Mit freundlicher Genehmigung der E. Schweizerbart'schen Verlagsbuchhandlung, Stuttgart.

Diese Bakterien wurden über die Sequenzierung des ribosomalen 16S rRNA-Gens identifiziert. Die Analyse ergab eine vielfältige Bakterienzusammensetzung mit 8 identifizierten bakteriellen Gensequenzen bei *S. bimaculatus* und 5 identifizierten Gensequenzen bei *S. juno*. Die meisten dieser Bakterien konnten den Gruppen der Actinomycetales (*Arthrobacter*, *Microbacterium*, *Rhodococcus*)

und Pseudomonadales (*Acinetobacter*, *Pseudomonas*) zugeordnet werden (Tab.2). Die Bakteriendiversität innerhalb des Haftsekretes ist wahrscheinlich sogar noch größer, da nur Arten identifiziert werden konnten, die *in vitro* auf Agarplatten kultiviert werden konnten.

In histochemischen Tests konnten wasserlösliche Zucker, Proteine und Lipide im Haftsekret nachgewiesen werden (Betz et al. 2009). Da die Bakterien auch im Haftsekret von frisch gesammelten Individuen nachgewiesen werden konnten, kann man schließen, dass die Bakterien auch im Freiland im *Stenus*-Haftsekret vorkommen und als Kommensalen möglicherweise die verschiedenen Komponenten des Haftsekretes als Nahrungsquelle nutzen. Inwieweit sich das Vorkommen der Bakterien auf die chemische Zusammensetzung und Struktur des Haftsekretes auswirkt und dadurch die Haftperformanz beeinflusst, erfordert allerdings weitergehende Untersuchungen.

Tab.2: Bakterien im Haftsekret von *S. juno* and *S. bimaculatus*, die auf Agarplatten kultiviert werden konnten (Identifizierung der Bakterienstämme durch höchste Sequenzähnlichkeit in GenBank). Identische Symbole kennzeichnen Bakterienarten, die zusammen im Haftsekret gefunden wurden.

Stenus-Art	Bakterienordnung	Identifizierte Bakteriengattung bzw. –art / GenBank-Eintragsnummer	Gemeinsames Vorkommen im Haftsekret
S. bimaculatus	Actinomycetales	*Microbacterium arabinogalactanolyticum* strain B15 KM210235.1	+
		Rhodococcus sp. KAR52 KR055013.1	+
	Enterobacteriales	*Pantoea agglomerans* FJ614257.1	
	Flavobacteriales	*Chryseobacterium jejuense* dbi/AB682422.1	+
	Pseudomonadales	*Acinetobacter* sp. SFX14 KP717090	+
		Acinetobacter Artichoke A3 KM587007.1	+
		Acinetobacter berenziniae KM062029.1	+
		Pseudomonas oryzihabitans IHB B 13621 KP762549.1	+
S. juno	Actinomycetales	*Arthrobacter* sp. BS2 KR063182.1	
		Arthrobacter nikotianae BS 12 KR063192.1	
	Flavobacteriales	*Chryseobacterium* sp. HJ-85 JQ511867.1	#
	Lactobacillales	*Enterococcus haemoperoxidus* NBRC 100709 1136936.1	#
	Pseudomonadales	*Acinetobacter iwoffii* ex19 KF317889.1	#

2.2 Molekulare Phylogenie der Kurzflügelkäfergattungen *Stenus* Latreille, 1797 und *Dianous* Leach, 1819 (Coleoptera, Staphylinidae, Steninae)

Publikation V: Loss of the sticky harpoon - COI sequences indicate paraphyly of *Stenus* with respect to *Dianous* (Staphylinidae, Steninae). Lars Koerner, Michael Laumann, Oliver Betz & Michael Heethoff (2013). Zoologischer Anzeiger, 252:337–347.

Zur Klärung der phylogenetischen Verwandtschaftverhältnisse innerhalb der Gattung *Stenus* und zwischen den Gattungen *Stenus* und *Dianous*, wurde ein ungefähr 826-pb langes Fragment des Cytochrom Oxidase I (COI)-Gens mit dem Primer-Paar C1-J-2183 (alias Jerry, CAACATTTATTTGATTTTTTGG) und TL2-N-3014 (alias Pat, TCCATTGCACTAATCTGCCATATTA) (Simon et al. 1994) amplifiziert. Das COI-Gen wird als taxonomischer Standard-Barcode sowohl für die Artidentifikation als auch für biogeographische Analysen herangezogen (Folmer et al. 1994; Hebert et al. 2003; Ribera et al. 2003, 2004; Pons et al. 2006; Hunt et al. 2007; Heethoff et al. 2011). Einerseits sind die universellen Primer der COI sehr robust, andererseits besitzt dieser Genabschnitt eine weitaus größere Anzahl phylogenetischer Signale als jedes andere mitochondriale Gen (Hebert et al. 2003). Die phylogenetischen Verwandtschaftsbeziehungen wurden mit verschiedenen Berechnungsalgorithmen analysiert (*Maximum Parsimony* (MP), *Maximum Likelihood* (ML), *Neighbour Joining* (NJ), Bayesianische Analyse (BA)).

Es wurden 12 Arten der *Dianous*-Gruppe II, 30 Arten der Gattung *Stenus* sowie 2 Außengruppenvertreter (*Euconnus* sp., Scydmaeninae; *Euaesthetus ruficapillus*, Euaesthetinae; Tabelle 3) in die Stammbaumrekonstruktion einbezogen. Vertreter der *Dianous*-Gruppe I wurden in einer weiteren Arbeit in Kooperation mit dem Lehrstuhl Tierökologie II der Universität Bayreuth untersucht (Lang et al. 2015; Abb.22).

Tab.3: Für die phylogenetischen Analysen verwendete *Stenus*-, *Dianous*-, *Euaesthetus*- und *Euconnus*-Arten.

Genus	Subgenus	Art	Fundort
Stenus	*Stenus* s.str.	*bimaculatus* Gyllenhal, 1810	Germany, Schleswig-Holstein, Kiel
			Germany, Schleswig-Holstein, Friedrichsruh
		juno (Paykull, 1789)	Germany, Schleswig-Holstein, Kiel
			Canada, Alberta
		lustrator Erichson, 1839	Germany, Bavaria, Bayreuth area
			Germany, Baden-Württemberg, Tübingen
		clavicornis (Scopoli, 1763)	Germany, Baden-Württemberg, Tübingen
			Germany, Schleswig-Holstein, Kiel
		providus Erichson, 1839	Germany, Baden-Württemberg, Tübingen
			Germany, Baden-Württemberg, Tübingen
		comma Leconte, 1863	Germany, Baden-Württemberg, Tübingen
			Canada, Alberta
			China
		biguttatus (Linnaeus, 1758)	Germany, Schleswig-Holstein, Strande
			Germany, Schleswig-Holstein, Strande
		insignatus Puthz, 1981	China, Hainan Prov., Qiongzhong County, Limu shan
			China, Hainan Prov., Qiongzhong County, Limu shan
		tenuipes Sharp, 1874	China, Shanghai City
			China, Shanghai City
		guttula Müller, 1831	Germany, Schleswig-Holstein, Strande
			Germany, Baden-Württemberg, Tübingen
		fossulatus Erichson, 1840	Germany, Schleswig-Holstein, Strande
			Germany, Schleswig-Holstein, Strande
		boops Ljungh, 1804	Germany, Baden-Württemberg, Tübingen
			Germany, Baden-Württemberg, Tübingen
		melanarius Stephens, 1883	China, Shanghai City
			China, Shanghai City
		canaliculatus Gyllenhal, 1827	Germany, Baden-Württemberg, Tübingen
			Germany, Baden-Württemberg, Tübingen
		nitens Stephens, 1833	Germany, Baden-Württemberg, Tübingen
		humilis Erichson, 1839	Germany, Baden-Württemberg, Tübingen
			Germany, Baden-Württemberg, Tübingen
		proclinatus L. Benick, 1922	China, Shanghai City
	Tesnus	*pilosiventris* Bernhauer, 1915	China, Guizhou Prov., Tongren City, Mayanghe N. R.
	Hypostenus	*similis* (Herbst, 1784)	Germany, Bavaria, Limmersdorfer Forst
			United Kingdom
		cicindeloides (Schaller, 1783)	Germany, Schleswig-Holstein, Flintbek
			China, Hainan Prov.
		solutus Erichson, 1840	Germany, Schleswig-Holstein, Strande
			Germany, Schleswig-Holstein, Strande
		tarsalis Ljungh, 1804	Germany, Schleswig-Holstein, Flintbek
			Germany, Bavaria, Limmersdorfer Forst
	Metatesnus	*bifoveolatus* Gyllenhal, 1827	Germany, Schleswig-Holstein, Kiel
			Germany, Schleswig-Holstein, Kiel
		nitidiusculus Stephens, 1833	Germany, Niedersachsen, Langwedel
			Germany, Baden-Württemberg, Tübingen
		pubescens Stephens, 1833	Germany, Baden-Württemberg, Tübingen
	Hemistenus	*impressus* Germar, 1824	Germany, Schleswig-Holstein, Kiel
		rugipennis Sharp, 1874	China, Zhejiang
		coronatus L. Benick, 1928	China, Beijing
		paradecens Tang & Li, 2005	China, Anhui
		tenuimargo Cameron, 1913	China, Yunnan Prov., Jinghong City, Nabanhe N. R.

Genus	Subgenus	Art	Fundort
Dianous	group II	*coerulescens* (Gyllenhal, 1810)	Germany, Bavaria, Röslau, Eger Falls United Kingdom
		srivichaii Rougemont, 1981	China, Yunnan Prov., Jinghong City, Nabanhe N. R.
		alternans Zheng, 1993	China, Yunnan Prov., Jinghong City, Nabanhe N. R.
		punctiventris Champion, 1919	China, Yunnan Prov., Jinghong City, Nabanhe N. R.
		obliquenotatus Champion, 1921	China, Yunnan Prov., Jinghong City, Nabanhe N. R.
		elegantulus Zheng, 1993	China, Guizhou Prov., Tongren City, Mayanghe N. R.
		pseudacutus Puthz, 2009	China, Yunnan Prov., Jinghong City, Nabanhe N. R.
		ocellifer Puthz, 2000	China, Yunnan Prov., Jinghong City, Nabanhe N. R.
		verticosus Eppelsheim, 1895	China, Yunnan Prov., Jinghong City, Nabanhe N. R.
		vietnamensis Puthz, 1980	China, Yunnan Prov., Jinghong City, Nabanhe N. R.
		andrewesi Cameron, 1914	China, Yunnan Prov., Jinghong City, Nabanhe N. R.
		banghaasi Bernhauer, 1916	China, Guizhou Prov., Tongren City, Mayanghe N. R.
Außengruppen			
Euaesthetus (Euaesthetinae)		*ruficapillus*	
Euconnus (Scydmaeninae)		sp.	

Die phylogenetischen Analysen zeigten interessanterweise, dass die untersuchten *Dianous*-Arten der *Dianous*-Gruppe II eine monophyletische Gruppe innerhalb der Gattung *Stenus* bilden, wobei Arten der Untergattung *Stenus* s. str. (*S. ater*-, *clavicornis*-, *humilis*- und *guttula*-Gruppe) dabei eine Nachbarposition zu *Dianous* einnehmen (Abb.18-21). Neuere phylogenetische Analysen der Gensequenzabschnitte COI, 16S rRNA und Histon H3 bestätigen dieses wichtige Ergebnis (Lang et al. 2015; Abb.22). Lang et al. (2015) konnten zeigen, dass die untersuchten *Dianous*-Arten aus den *Dianous*-Gruppen I und II ein konsistentes Cluster bilden, wobei die Art *D. fengtingae* aus der *Dianous*-Gruppe I eine Nachbarposition zu den Arten *D. coerulescens*, *D. fellowesi* und *D. vietnamensis* der Gruppe II einnimmt (Abb.22). Chemische Analysen des Pygidialdrüsensekretes der *Dianous*-Arten *D. coerulescens*, *D. obliquenotatus*, *D. karen* (zur *Dianous*-Gruppe II gehörend), sowie *D. betzi* (zur *Dianous*-Gruppe I gehörend) zeigen, dass diese die gleichen Piperidinalkaloidverbindungen wie *Stenus* besitzen (Stenusin und Norstenusin) und deshalb chemotaxonomisch zur Piperidin-Gruppe innerhalb der Gattung *Stenus* gehören (Abb.22 rot markierte Arten; Lang et al. 2015).

Der Klebfangapparat wurde bisher als prominenteste Autapomorphie der Gattung *Stenus* angesehen, die als wesentliches Abgrenzungsmerkmal für die Monophylie dieser Gattung gegenüber der Schwestergattung *Dianous* galt. Im Vergleich zu *Stenus* zeigt das Labium der Gattung *Dianous* allerdings den gleichen Grundbauplan (Abb.3), nur in verkürzter Form, wobei die Paraglossen bei *Dianous* nicht zu Haftpolstern differenziert sind (Weinreich 1968; Puthz 1981). Wie schon erwähnt, wurde bisher davon ausgegangen, dass das morphologisch einfach gebaute, verkürzte Labium von *Dianous* den plesiomorphen, und das vorschnellbare Fanglabium mit den modifizierten Paraglossen von *Stenus* den apomorphen Zustand darstellen würde. Aus Konsequenz der phylogenetischen Untersuchungen ist allerdings eine sekundäre Reduktion des ehemals komplexeren Fangapparates bei *Dianous* wahrscheinlich. Interessanterweise haben auch einige Vertreter der *Stenus canaliculatus*-

Gruppe stark verkürzte Fanglabien mit reduzierten Klebpolstern (vgl. Kapitel 2.1.2.5). Auch die Fanglabien dieser Formen stellen vermutlich Rudimente des ehemals komplexeren labialen Fangapparates dar (Betz 2006). Hierfür spricht neben anatomischen Details (Betz 1996) auch deren phylogenetische Position in den Stammbäumen sowie die Beobachtung, dass das Labium bei den Arten *S. canaliculatus* und *S. nitens* weder beim Beutefang noch in einem anderen Zusammenhang eine biologische Rolle spielt (Betz 1996; Koerner pers. Beob.).

Wie bereits in der Einleitung erwähnt, ist die traditionelle Untergattungs-Einteilung bei *Stenus* nur eine Determinationshilfe bis eine Neueinteilung nach phylogenetischen Gesichtspunkten erfolgen kann. Die herkömmliche Untergattungseinteilung bei *Stenus* basiert vor allem auf der unterschiedlichen Tarsusmorphologie sowie des Vorhandenseins einer Abdominalrandung (Paratergite). Diese Merkmale stehen allerdings im funktionellen Zusammenhang mit der Besiedlung unterschiedlicher Habitate und wurden in phylogenetisch verschiedenen Gruppen mehrfach unabhängig voneinander ausgebildet (Puthz 1971). Diese Merkmale sind sogar innerhalb einer monophyletischen Gruppe unterschiedlich ausgebildet, was fälschlicherweise dazu führte, solche Abstammungsgemeinschaften verschiedenen Subgenera zuzuordnen (Puthz 1971). Die Ergebnisse der vorliegenden Arbeit unterstützen die traditionelle Untergattungseinteilung nicht, da die Subgenera *Stenus* s. str., *Hypostenus* und *Metatesnus* als para- oder polyphyletische Gruppen auftreten. Aufgrund der beschriebenen Probleme, die das traditionelle Untergattungs-Konzept aufwirft, führte Puthz (2001, 2008), basierend auf einer Reihe morphologischer Charakteristika, wie z. B. der Struktur des Aedeagus und der Spermatheken, eine große Zahl an monophyletischen Gruppen ein. Einige dieser monophyletischen Gruppen werden durch die vorliegende Arbeit unterstützt, z. B. die *S. guttula*-, *S. humilis*- und *S. boops*-Gruppe (Abb.18-21).

Da die konstruierten Stammbäume viele konsistente Topologien aufweisen, scheint die ausgewählte COI-Gensequenz gut für die Auflösung der phylogenetischen Verwandtschaftsbeziehungen der Steninae geeignet zu sein. Allerdings ist die basale Auflösung leider unbefriedigend. Die ML- und BA-Analysen zeigen die Subgenera *Hypostenus* und *Metatesnus* als basale Linie der Steninae, die MP- und NJ-Analysen allerdings Vertreter der *S. comma*-Gruppe (NJ: *S. biguttatus*, MP: *S. comma*). Ähnlich der Staphyliniden-Gattung *Aleochara*, könnte die fehlende basale Auflösung der *Stenus*-Arten eine Phase sehr schneller Evolution mit vielen Aufspaltungsereignissen innerhalb eines sehr kurzen Zeitraumes kennzeichnen (Maus et al. 2001; Maddison 1989), möglicherweise durch die Entstehung einer Schlüsselinnovation wie dem labialen Fangapparat. Weitergehende molekulare Untersuchungen mit einer größeren Artenzahl sowie anderen, mehr konservierten Genen, könnten zu einer besseren basalen Auflösung beitragen und dadurch ein genaueres Bild über die Verwandtschaftsbeziehungen sowohl innerhalb der Gattung *Stenus*, als auch zwischen den „Schwestergattungen“ *Stenus* und *Dianous* geben.

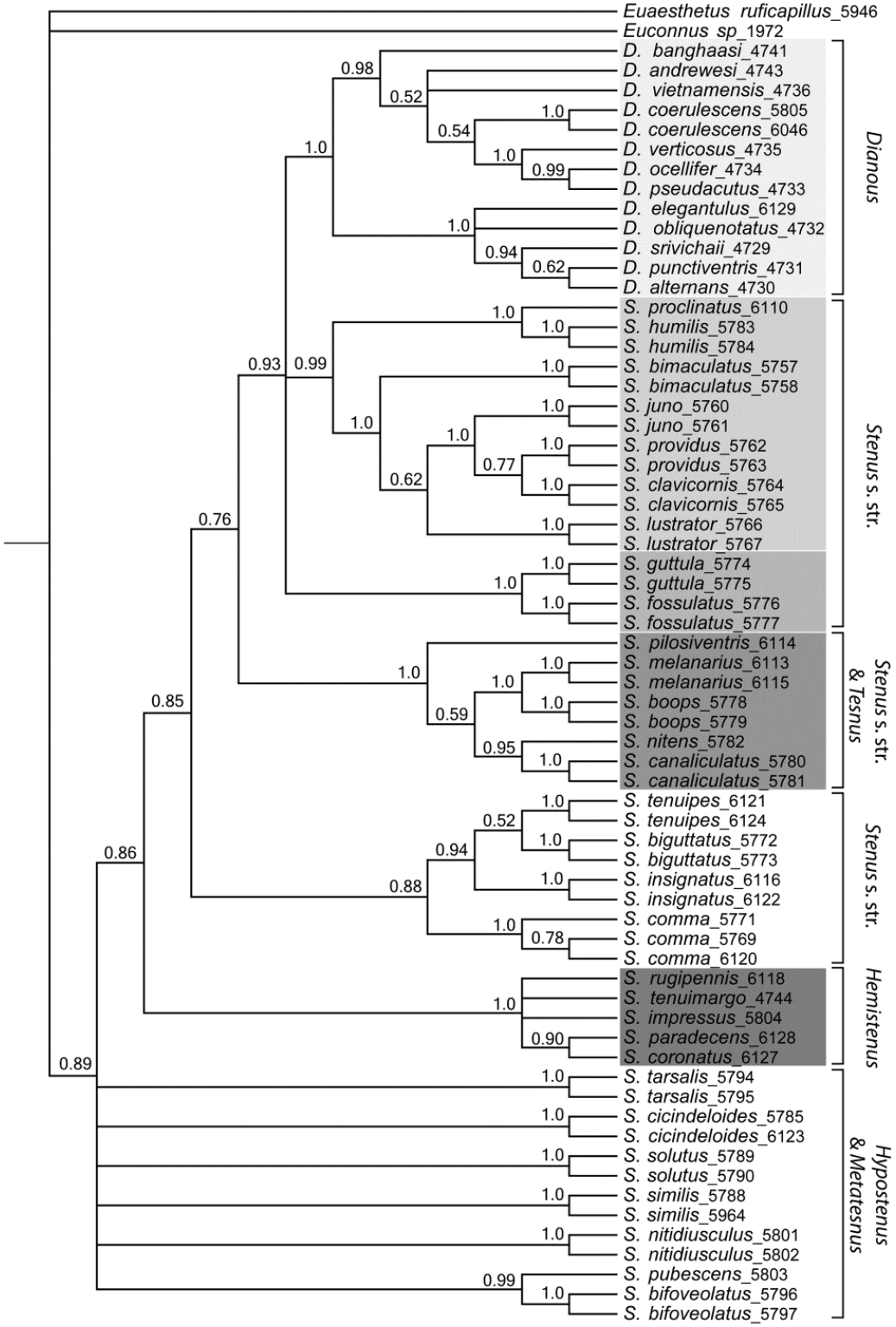

Abb.18: BA-Stammbaum auf der Maximum-a-posteriori-Methode basierend (Ronquist & Huelsenbeck, 2003); die Zahlen an den Verzweigungen bzw. Ästen des Baumes stellen Bayesische Posteriorwahrscheinlich-keiten (BPP) ≥ 0.50 dar. Konsistente Baumtopologien, die in allen phylogenetischen Analysen auftreten, sind grau markiert. Aus Publikation V. Mit freundlicher Genehmigung von Elsevier.

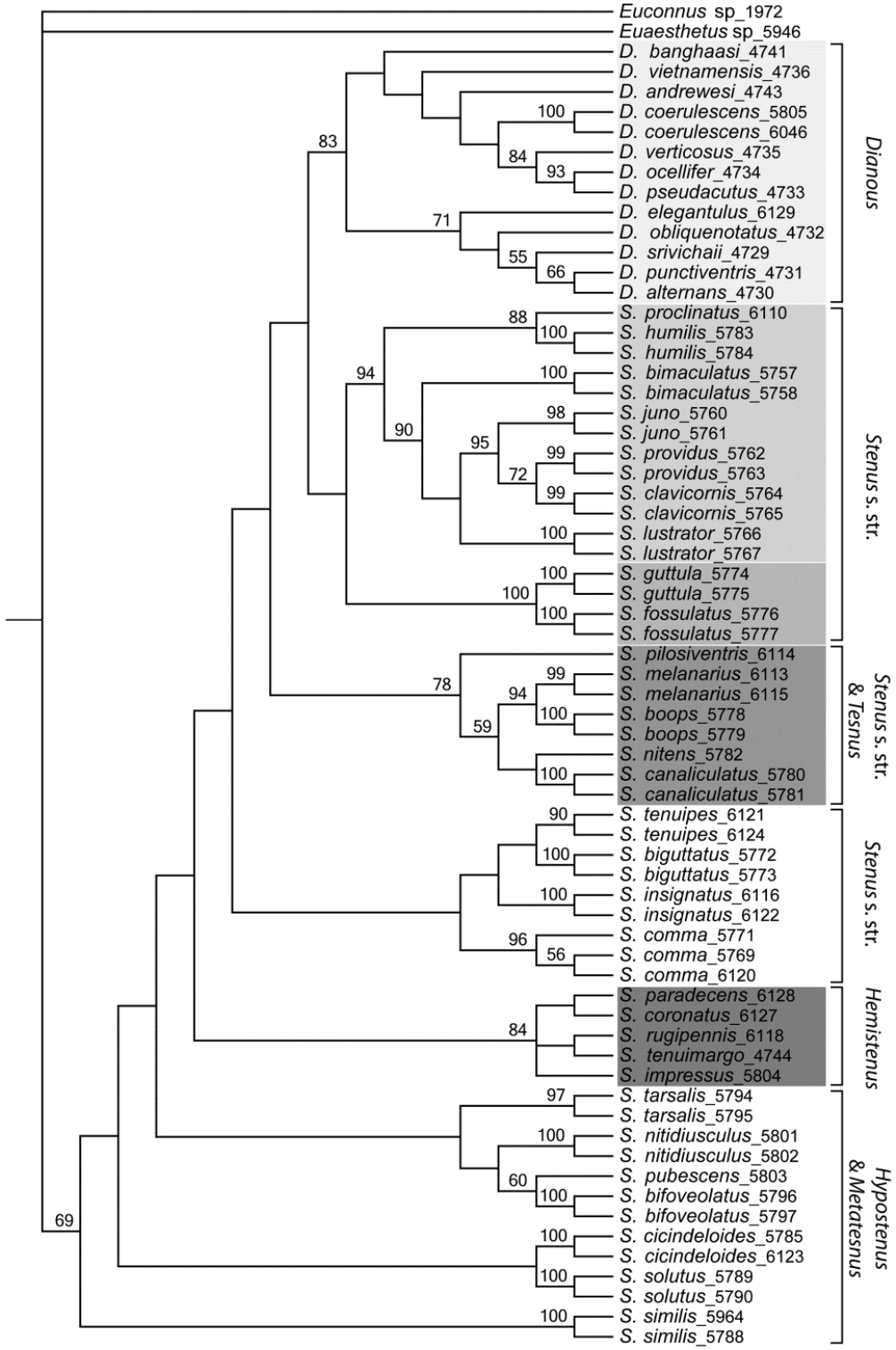

Abb.19: Phylogenetische Beziehungen nach *Maximum Likelihood*-Analyse. Gezeigt ist der beste gefundene Baum aus der ML-Analyse. Die zugehörigen bootstrap-Werte (≥ 50) aus 100 bootstrap-Replikaten sind an den Verzweigungen angegeben. Konsistente Baumtopologien, die in allen phylogenetischen Analysen auftreten, sind grau markiert. Aus Publikation V. Mit freundlicher Genehmigung von Elsevier.

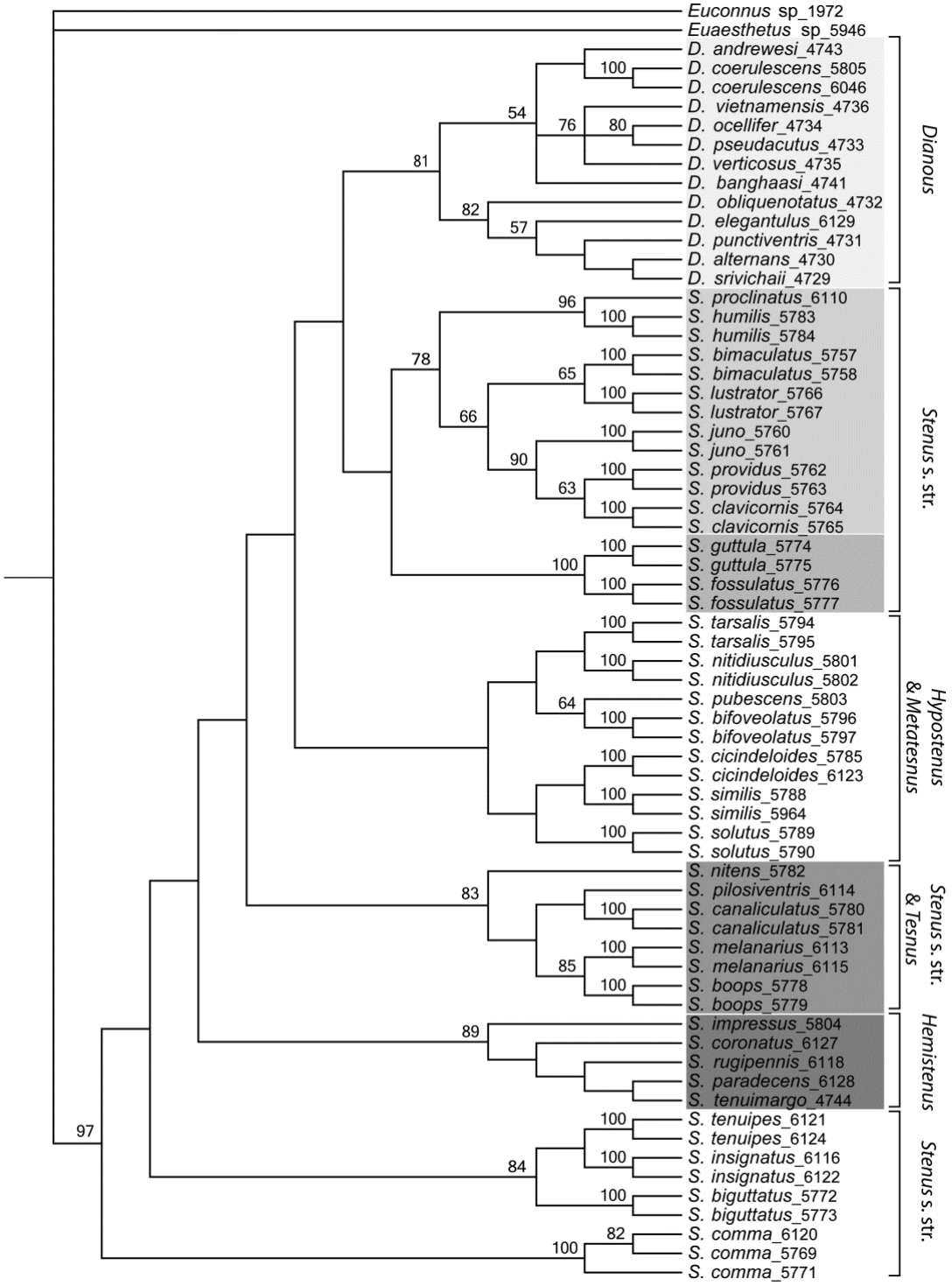

Abb.20: Phylogenetische Beziehungen nach *Maximum Parsimony*-Analyse. Die Topologie ist aus einem Konsensus der 3 most parsimonious trees hervorgegangen. Die zugehörigen bootstrap-Werte (≥ 50) aus 100 bootstrap-Replikaten sind an den Verzweigungen angegeben. Konsistente Baumtopologien, die in allen phylogenetischen Analysen auftreten, sind grau markiert. Aus Publikation V. Mit freundlicher Genehmigung von Elsevier.

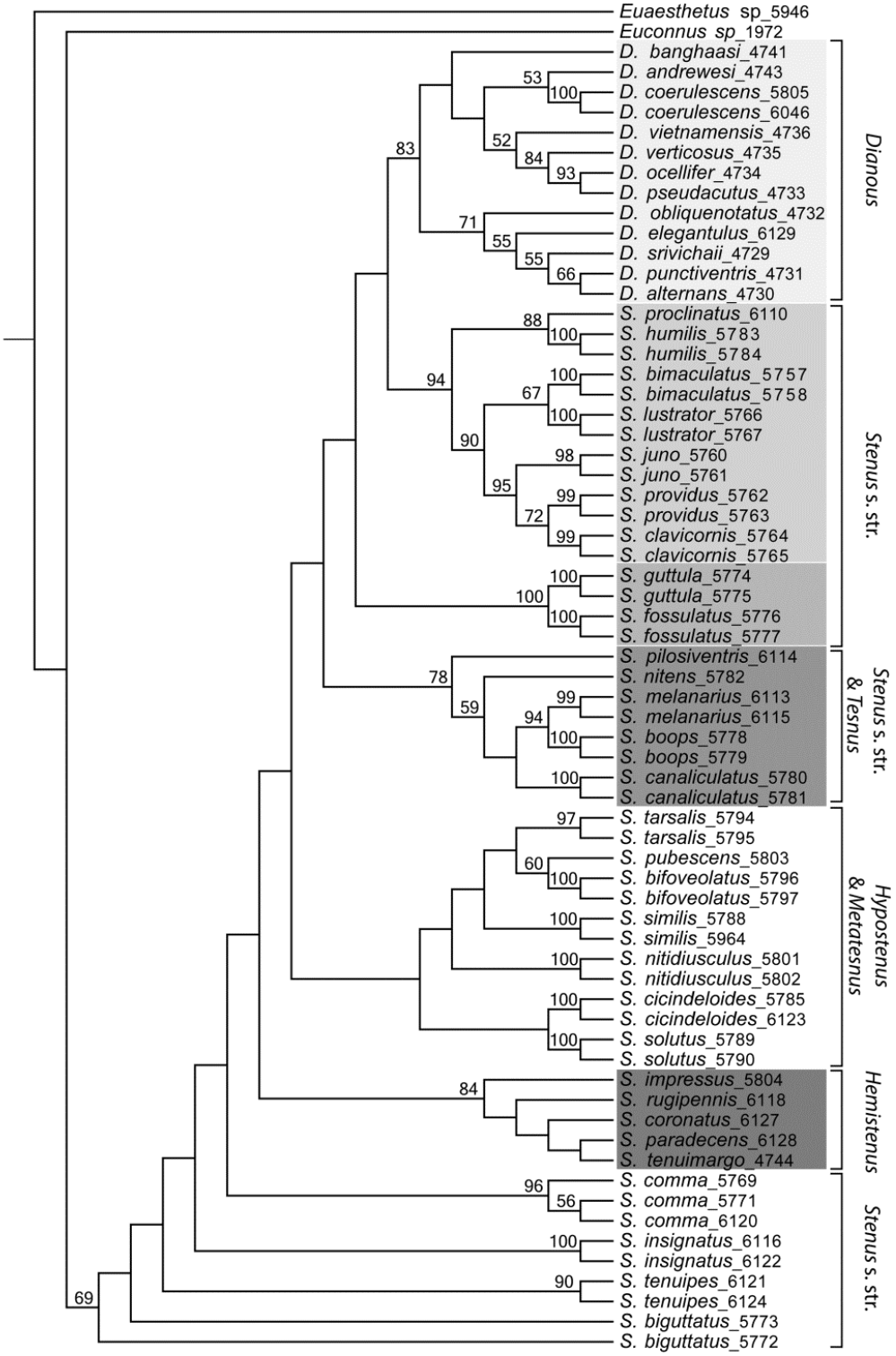

Abb.21: Phylogenetische Beziehungen nach Neighbour Joining-Analyse basierend auf ML-Distanzen. Die zugehörigen bootstrap-Werte (≥ 50) aus 100 bootstrap-Replikaten sind an den Verzweigungen angegeben. Konsistente Baumtopologien, die in allen phylogenetischen Analysen auftreten, sind grau markiert. Aus Publikation V. Mit freundlicher Genehmigung von Elsevier.

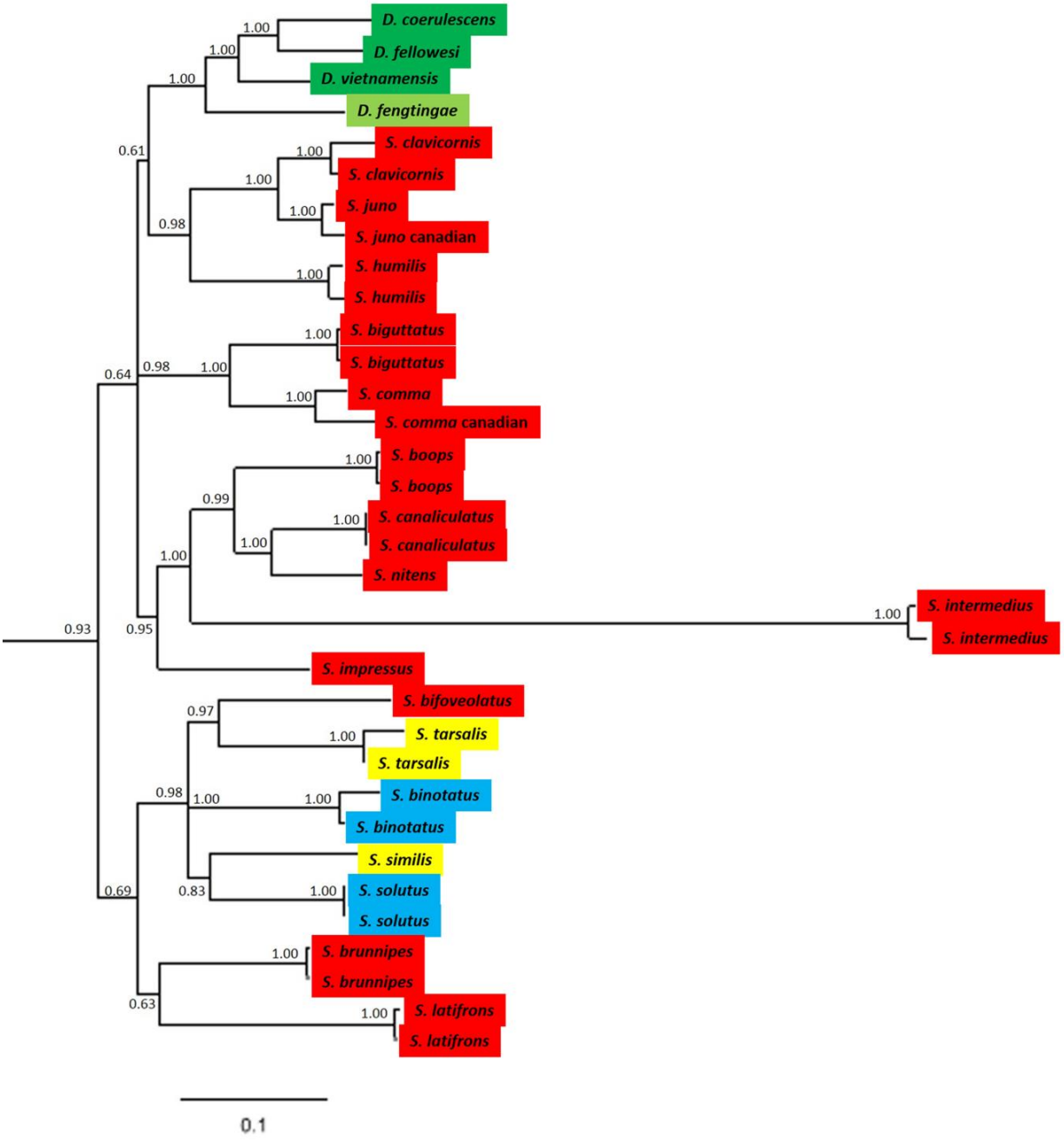

Abb.22: BA-Stammbaum auf der Maximum-a-posteriori-Methode basierend (aus Lang et al. 2015); die Zahlen an den Verzweigungen bzw. Ästen des Baumes stellen Bayesische Posteriorwahrscheinlichkeiten (BPP) ≥ 0.50 dar. Mitglieder der chemotaxonomischen Gruppen bei *Stenus* sind farbig markiert (nach Schierling et al. 2013); rot: Piperidin-Gruppe, gelb: Pyridin-Gruppe, blau: Epoxypiperidein-Gruppe; Mitglieder der *Dianous*-Komplexe I und II sind grün markiert; die Wurzel des Baumes bestehend aus *E. ruficapillus* ist nicht abgebildet. Aus Lang et al. 2015. Mit freundlicher Genehmigung des Springer Verlags, Basel.

Al Bitar, L., Voigt, D., Zebitz, C.P., Gorb, S.N. (2009). Tarsal morphology and attachment ability of the codling moth *Cydia pomonella* L. (Lepidoptera, Tortricidae) to smooth surfaces. Journal of Insect Physiology 55: 1029–1038.

Al Bitar, L., Voigt, D., Zebitz, C.P.W., Gorb, S.N. (2010). Attachment ability of the codling moth *Cydia pomonella* L. to rough substrates. Journal of Insect Physiology 56: 1966–1972.

Arzt, E., Gorb, S., Spolenak, R. (2003). From micro to nano contacts in biological attachment devices. Proceedings of the National Academy of Science 100(19): 10603–10606.

Attygalle, A. B., Aneshansley, D. J., Meinwald, J., Eisner, T. (2000). Defense by foot adhesion in a chrysomelid beetle (*Hemisphaerota cyanea*): characterization of the adhesive oil. Zoology 103: 1–6.

Bauer, T., Pfeiffer, M. (1991). 'Shooting' springtails with a sticky rod: the flexible hunting behaviour of *Stenus comma* (Coleoptera; Staphylinidae) and the counter-strategies of its prey. Animal Behaviour 41: 819–828.

Betz, O. (1994). Der Fangapparat bei *Stenus* spp. (Coleoptera, Staphylinidae): Bau, Funktion, Evolution. Inauguraldissertation, Universität Bayreuth.

Betz, O. (1996). Function and evolution of the adhesion-capture apparatus of *Stenus* species (Coleoptera, Staphylinidae). Zoomorphology 116: 15–34.

Betz, O. (1998a). Comparative studies on the predatory behaviour of *Stenus* spp. (Coleoptera: Staphylinidae): the significance of its specialized labial apparatus. Journal of Zoology London 244: 527–544.

Betz, O. (1998b). Life forms and hunting behaviour of some central European *Stenus* species (Coleoptera, Staphylinidae). Applied Soil Ecology 9: 69–74.

Betz, O. (1999). A behavioural inventory of adult *Stenus* species (Coleoptera: Staphylinidae). Journal of Natural History 33: 1691–1712.

Betz, O. (2006). Der Anpassungswert morphologischer Strukturen: Integration von Form, Funktion und Ökologie am Beispiel der Kurzflügelkäfer-Gattung *Stenus* (Coleoptera, Staphylinidae). Entomologie heute 18: 3–26.

Betz, O. (2010). Adhesive exocrine glands in insects: morphology, ultrastructure, and adhesive secretion. Biological adhesive systems. From nature to technical and medical application. (eds J. von Byern & I. Grunwald), Springer, Berlin, p 111–152.

Betz, O., Kölsch, G. (2004). The role of adhesion in prey-capture and predator defence in arthropods. Arthropod Structure & Development 33: 3–30.

Betz O., Koerner L., Dettner, K. (2018). The Biology of Steninae. In: Betz O., Irmler U., Klimaszewski J. (eds.). Biology of Rove Beetles (Staphylinidae). Springer, Cham. p 229-283.

Betz, O., Koerner, L., Gorb, S.N. (2009). Learning from nature: An insect's tongue as the model for two-phase viscous adhesives. Adhesion Adhesives & Sealants 3: 32-35.

Beutel, R.G., Gorb, S.N. (2001). Ultrastructure of attachment specializations of hexapods (Arthropoda): evolutionary patterns inferred from a revised ordinal phylogeny. Journal of Zoological Systematics and Evolutionary Research 39: 177–207.

Bowden, F.P., Tabor, D. (1986). The Friction and Lubrication of Solids. Oxford University Press, Oxford.

Bullock, J.M.R., Federle, W. (2010). The effect of surface roughness on claw and adhesive hair performance in the dock beetle *Gastrophysa viridula*. Insect Science 18: 298–304.

Clarke, D.J., Grebennikov, V.V. (2009). Monophyly of Euaesthetinae (Coleoptera: Staphylinidae): phylogenetic evidence from adults and larvae, review of austral genera, and new larval descriptions. Systematic Entomology 34: 346–397.

Creton, C. (2003). Pressure-sensitive adhesives: an introductory course. MRS Bulletin 28(6): 434–439.

Dewitz, H. (1883). Ueber die Fortbewegung der Thiere an senkrechten glatten Flächen vermittelst eines Secretes. Pflügers Archiv ges. Physiol. 33: 440–481.

Dixon, A.F.G., Croghan, P.C., Gowing, R.P. (1990). The mechanism by which aphids adhere to smooth surfaces. J. Exp. Biol. 152: 243–253

Drechsler, P., Federle, W. (2006). Biomechanics of smooth adhesive pads in insects: influence of tarsal secretion on attachment performance. J. Comp. Physiol. A 192: 1213–1222.

Federle, W. (2006). Why are so many adhesive pads hairy? J. Exp. Biol. 209: 2611–2621.

Federle, W., Rohrseitz, K., Hölldobler, B. (2000). Attachment forces of ants measured with a centrifuge: better "wax-runners" have a poorer attachment to a smooth surface. J. Exp. Biol. 203: 505–512.

Federle, W., Riehle, M., Curtis, A.S.G., Full, R.J. (2002). An integrative study of insect adhesion: mechanics and wet adhesion of pretarsal pads in ants. Integrative and Comparative Biology 42: 1100–1106.

Folmer, O., Black, M., Hoeh, W., Lutz, R., Vrijenhoek, R. (1994). DNA primers for amplification of mitochondrial cytochrome c oxidase subunit I from diverse metazoan invertebrates. Molecular Marine Biology and Biotechnology 3: 294–297.

Fuller, K.N.G., Tabor, D. (1975). The effect of surface roughness on the adhesion of elastic solids. Proceedings of the Royal Society London A 345: 327–342.

Gorb, E.V., Hosoda, N., Miksch, C., Gorb, S.N. (2010). Slippery pores: anti-adhesive effect of nanoporous substrates on the beetle attachment system. Journal of the Royal Society Interface 7: 1571–1579.

Gorb, S.N. (2001). Attachment Devices of Insect Cuticle. Kluwer Academic Publishers, Dordrecht.

Gorb, S.N. (2008). Biological attachment devices: exploring nature's diversity for biomimetic. Philosophical Transactions of the Royal Society A. 366: 1557–1574.

Gorb, S., Gorb, E., Kastner, V. (2001). Scale effects on the attachment pads and friction forces in syrphid flies (Diptera, Syrphidae). J. Exp. Biol. 204: 1421–1431.

Gorb, S.N., Gorb, E.V. (2009). Effects of surface topography and chemistry of *Rumex obtusifolius* leaves on the attachment of the beetle *Gastrophysa viridula*. Entomologia Experimentalis et Applicata 130: 222–228.

Grebennikov, V.V., Newton, A.F. (2009). Good-bye Scymaenidae, or why the antlike stone beetles should become megadiverse Staphylinidae sensu latissimo (Coleoptera). European Journal of Entomology 106: 275–301.

Grenon, J.F., Walker, G. (1981). The tenacity of the limpet, *Patella vulgata* L An experimental approach. Journal of Experimental Marine Biology and Ecology 54: 277–308.

Haas, F., Gorb, S.N., Wootton, R.J., 2000a. Elastic joints in dermapteran hind wings: materials and wing folding. Arthr. Str. Dev. 29: 137–146.

Haas, F., Gorb, S.N., Blickhan, R. (2000b). The function of resilin in beetle wings. Proc. R. Soc. Lond. B 267: 1375–1381.

Habenicht, G. (2009). Kleben: Grundlagen, Technologien, Anwendung, 6th edn. Springer, Berlin.

Hansen, M. (1997). Phylogeny and classification of the staphyliniform beetle families (Coleoptera). Biologiske Skrifter 48: 1–339.

Hebert, P.D.N., Cywinska, A., Ball, S.L., deWaard, J.R. (2003). Biological identifications through DNA barcodes. Proceedings of the Royal Society of London Series B 270: 313–321.

Heethoff, M., Koerner, L., Norton, R.A., Raspotnig, G. (2011). Tasty but protected - first evidence of chemical defense in oribatid mites. Journal of Chemical Ecology 37: 1037–1043.

Heethoff, M., Laumann, M., Weigmann, G., Raspotnig, G. (2011). Integrative taxonomy: Combining morphological, molecular and chemical data for species delineation in the parthenogenetic *Trhypochthonius tectorum* complex (Acari, Oribatida, Trhypochthoniidae). Frontiers in Zoology, 8: 2.

Herrel A., Rowe N.P., Speck T. (eds.) (2005). Ecology and biomechanics: A mechanical approach to the ecology of animals and plants. CRC Press.

Holdgate, M. (1955). The wetting of insect cuticles by water. J. Exp. Biol. 32: 591–617.

Hunt, T., Bergsten, J., Levkanicova, Z., Papadopoulou, A., John, O.S., Wild, R., Hammond, P.M., Ahrens, D., Balke, M., Caterino, M.S., Gómez-Zurita, J., Ribera, I., Barraclough, T.G., Bocakova, M., Bocak, L., Vogler, A.P. (2007). A comprehensive phylogeny of beetles reveals the evolutionary origins of a superradiation. Science 318: 1913–1916.

Israelachvili, J.N. (1991). Intermolecular and surface forces. Academic Press, London.

Jagota, A., Bennison, S.J. (2002). Mechanics of adhesion through a fibrillar microstructure. Integrative and Comparative Biology 42: 1140–1145.

Jiao, Y., Gorb, S., Scherge, M. (2000). Adhesion measured on the attachment pads of *Tettigonia viridissima* (Orthoptera, Insecta). J. Exp. Biol. 203: 1887–1895.

Kendall, K. (2001). Molecular Adhesion and Its Applications. Kluwer Academic Publishers, New York.

Kendall, M.D. (1970). The anatomy of the tarsi of *Schistocerca gregaria* Forskal. Z. Zellforsch. 109: 112–137.

Kölsch, G. (2000). The ultrastructure of glands and the production and function of the secretion in the adhesive capture apparatus of *Stenus* species (Coleoptera: Staphylinidae). Canadian Journal of Zoology 78: 465–475.

Kölsch, G., Betz, O. (1998). Ultrastructure and function of the adhesion-capture apparatus of *Stenus* species (Coleoptera, Staphylinidae). Zoomorphology 118: 263–272.

Labonte, D., Federle, W. (2015). Scaling and biomechanics of surface attachment in climbing animals. Philosophical Transactions of the Royal Society of London. Series B: Biological Sciences 370(1661): 20140027.

Lang, C., Koerner, L., Betz, O., Puthz, V., Dettner, K. (2015). Phylogenetic relationships and chemical evolution of the genera *Stenus* and *Dianous* (Coleoptera: Staphylinidae). Chemoecology 25: 11–24.

Lauder G.V. (2003), The intellectual challenge of biomechnics and evolution. In: Bels, V.L., Gasc, J.-P., Casinos, A. (eds). Vertebrate Biomechanics and Evolution. Oxford: BIOS Scientific Publishers. p 319–325

Lees, A.D., Hardie J. (1988). The organs of adhesion in the aphid *Megoura viciae*. J. Exp. Biol. 136: 209–228.

Leisler, B., Winkler, H. (1991). Ergebnisse und Konzepte ökomorphologischer Untersuchungen an Vögeln. J. Orn. 132: 373–425.

Leschen, R.A.B., Newton, A.F. (2003). Larval description, adult feeding behavior, and phylogenetic placement of *Megalopinus* (Coleoptera: Staphylinidae). Coleopterists Bulletin 57: 469–493.

Lüken, D., Voigt, D., Gorb, S.N., Zebitz, C.P.W. (2009). Tarsal morphology and attachment ability of the sweet potato weevil *Cylas puncticollis* Boh. to smooth surfaces with different physico-chemical properties. Mitteilungen der Deutschen Gesellschaft für Allgemeine und Angewandte Entomologie 17: 109–113.

Maddison, W.P. (1989). Reconstructing character evolution on polytomous cladograms. Cladistics – The International Journal of the Willi Hennig Society 5: 365–377.

Maus, C., Peschke, K., Dobler, S. (2001). Phylogeny of the genus *Aleochara* inferred from mitochondrial cytochrome oxidase sequences (Coleoptera: Staphylinidae), Mol. Phylogenet. Evol. 18(2): 202–216.

Noble-Nesbitt, J. (1963). Transpiration in *Podura aquatica* L. and the wetting properties of its cuticle. J. Exp. Biol. 40: 681–700.

Peattie, M., Full, R.J. (2007). Phylogenetic analysis of the scaling of wet and dry biological fibrillar adhesives. Proceedings of the National Academy of Sciences Online (US) 104: 18595–18600.

Peressadko, A., Gorb, S.N. (2004). Surface profile and friction force generated by insects. In: Boblan, I., Bannasch, R. (eds.). Fortschritt-Berichte VDI, vol. 249. VDI Verlag, Düsseldorf, p 257–263.

Persson, B.N.J. (2007). Biological adhesion for locomotion on rough surfaces: basic principles and a theorist's view. MRS Bull. 32: 486–490.

Pfeiffer, M. (1989). Augenbau und Beutefang bei *Stenus comma*, Leconte, 1863 und *Dianous coerulescens*, Leach, 1891. Diploma Thesis. University of Tübingen, Tübingen, Germany.

Pons, J., Barraclough, T.G., Gomez-Zurita, J., Cardoso, A., Duran, D.P., Hazell, S., Kamoun, S., Sumlin, W.D., Vogler, A.P. (2006). Sequence-based species delimitation for the DNA taxonomy of undescribed insects. Systematic Biology 55: 595–609.

Puthz, V. (1971). Revision der afrikanischen Steninenfauna und Allgemeines über die Gattung *Stenus* Latreille (Coleoptera Staphylinidae) (56. Beitrag zur Kenntnis der Steninen). Ann. R. Mus. Afr. Centr. Serie 8(187): 1–376.

Puthz, V. (1981). Was ist *Dianous* Leach, 1819, was ist *Stenus* Latreille, 1796? Oder: Die Aporie des Stenologen und ihre taxonomischen Konsequenzen (Coleoptera, Staphylinidae). Entomol. Abh. Mus. Tierk. Dresden 44: 87–132.

Puthz, V. (1998). Die Gattung *Stenus* Latreille in Vietnam (Coleoptera, Staphylinidae). Rev. Suisse Zool. 105: 383–394.

Puthz, V. (2000). The genus *Dianous* Leach in China (Coleoptera: Staphylinidae) 261. Contribution to the knowledge of Steninae. Revue Suisse de Zoologie 107: 419–559.

Puthz, V. (2001). Beiträge zur Kenntnis der Steninen CCLXIX Zur Ordnung in der Gattung *Stenus* Latreille, 1796 (Staphylinidae, Coleoptera). Philippia 10: 31–41.

Puthz, V. (2005). Neue und alte neotropische *Stenus* (Hemistenus-) Arten (Coleoptera: Staphylinidae). Mitteilungen Int. Entomol. Vereins Suppl. XI: 1–60.

Puthz, V. (2008). *Stenus* LATREILLE und die segenreiche Himmelstochter (Coleoptera Staphylinidae). Linzer biologische Beiträge 40: 137–230.

Puthz, V. (2012). On the *Stenus* LATREILLE 1797 from Taiwan with non-spotted elytra (Coleoptera, Staphylinidae) (327th Contribution to the Knowledge of Steninae). Linzer biologische Beiträge 44(2): 1431–1475.

Puthz, V. (2015a). Übersicht über die Arten der Gattung *Dianous* LEACH group I (Coleoptera, Staphylinidae) 345. Beitrag zur Kenntnis der Steninen. Linzer biologische Beiträge 47(2): 1747–1783.

Puthz, V. (2015b). Neotropische *Stenus*-Arten mit seitlich gerandetem Abdomen und gelappten Tarsen (Coleoptera, Staphylinidae) 344. Beitrag zur Kenntnis der Steninen. Linzer biologische Beiträge 47(2): 1601–1727.

Reilly, S.M., Wainwright, P.C. (1994). Conclusion: Ecological morphology and the power of integration. In: Wainwright, P.C., Reilly, S.M. (eds) Ecological morphology. University of Chicago Press, Chicago, p 339–354.

Ribera, I., Bilton, D.T., Vogler, A.P. (2003). Mitochondrial DNA phylogeography and population history of *Meladema* diving beetles on the Atlantic Islands and in the Mediterranean basin (Coleoptera, Dytiscidae). Molecular Ecology 12: 153–167.

Ribera, I., Nilsson, A.N., Vogler, A.P. (2004). Phylogeny and historical biogeography of Agabinae diving beetles (Coleoptera) inferred from mitochondrial DNA sequences. Molecular Phylogenetics and Evolution 30: 545–562.

Ronquist, F., Huelsenbeck, J.P. (2003). MrBayes 3: Bayesian phylogenetic inference under mixed models. Bioinformatics 19: 1572–1574.

Santos, R., Gorb, S.N., Jamar, V., Flammang, P. (2005). Adhesion of echinoderm tube feet to rough surfaces. J. Exp. Biol. 208: 2555–2567.

Scherge, M., Gorb, S.N. (2001). Biological macro- and nanotribology. Nature's solutions. Springer, Berlin, Heidelberg.

Schierling, A., Seifert, K., Sinterhauf, S., Rieß, J.B., Rupprecht, J.C., Dettner, K. (2013). The multifunctional pygidial gland secretion of the Steninae (Coleoptera: Staphylinidae): ecological significance and evolution. Chemoecology 23: 45–57.

Schmitz, G. (1943). Le labium et les structures bucco-pharyngiennes du genre *Stenus* LATREILLE. Cellule 49: 291–334.

Shi, K., Zhou, H.Z. (2009). A new *Dianous* species (Coleoptera, Staphylinidae Steninae) from China, with a key to Chinese species of the *coerulescens* complex. Deutsche Entomologische Zeitschrift 56: 289–294.

Shi, K., Zhou, H.-Z. (2011). Taxonomy of the genus *Dianous* (Coleoptera: Staphylinidae: Steninae) in China and zoogeographic patterns of its distribution. Insect Science 18: 363–378.

Simon, C., Frati, F., Beckenbach, A., Crespi, B., Liu, H., Flook, P. (1994). Evolution, weighting, and phylogenetic utility of mitochondrial gene sequences and a compilation of conserved polymerase chain reaction primers. Annals of the Entomological Society of America 87: 651–701.

Stork, N.E. (1980). Experimental analysis of *Chrysolina polita* (Chrysomelidae: Coleoptera) on a variety of surfaces. J. Exp. Biol. 88: 91–107.

Tang, L., Li, L.-Z., Cao, G.-H. (2011). On Chinese species of *Dianous* group I (Coleoptera, Staphylinidae Steninae). ZooKeys 111: 67–85.

Thayer, M.K. (2005). Staphylinidae. In: Beutel, R.G., Leschen, R.A.B. (eds.), Handbook of Zoology, Coleoptera, vol. 1. De Gruyter, Berlin, p 296–344.

Varenberg, M., Pugno, N., Gorb, S.N. (2010). Spatulate structures in biological fibrillar adhesion. Soft Matter 6: 3269–3272.

Vötsch, W., Nicholson, G., Müller, R., Stierhof, Y.-D., Gorb, S., Schwarz, U. (2002). Chemical composition of the attachment pad secretion of the locust *Locusta migratoria*. Insect Biochemisty and Molecular Biology 32: 1605–1613.

Voigt, D., Peisker, H., Gorb, S.N. (2008a). Visualization of epicuticular grease on the covering wings on the Colorado Potato Beetle: a scanning probe approach. In: Bhushan, B., Fuchs, H. (eds.), Applied Scanning Probe Methods XIII. Springer, Heidelberg, p 1–16.

Voigt, D., Schuppert, J.M., Dattinger, S., Gorb, S.N. (2008b). Sexual dimorphism in the attachment ability of the Colorado potato beetle *Leptinotarsa decemlineata* (Coleoptera: Chrysomelidae) to rough substrates. Journal of Insect Physiology 54: 765–776.

Wagner, T., Neinhuis, C., Barthlott, W. (1996). Wettability and contaminability of insect wings as a function of their surface sculptures. Acta Zoologica 77: 213–225.

Wainwright, P.C. (1991). Ecomorphology: Experimental functional anatomy for ecological problems. American Zoologist 31: 680–693.

Walker, G. (1993). Adhesion to smooth surfaces by insects – a review. Int. J. Adhes. 13: 3–7.

Weinreich, E. (1968). Über den Klebfangapparat der Imagines von *Stenus* LATR. (Coleopt., Staphylinidae) mit einem Beitrag zur Kenntnis der Jugendstadien dieser Gattung. Zeitschrift für Morphologie und Ökologie der Tiere 62: 162–210.

Yule, A.B., Walker, G. (1984). The temporary adhesion of barnacle cyprids: effects of some differing surface characteristics. Journal of the Marine Biological Association of the United Kingdom 64: 429–439.

Yule, A.B., Walker, G. (1987). Adhesion in barnacles. In: Southward, A.J. (ed.), Crustacean Issues, Biology of Barnacles. Balkema, Rotterdam, p 389–402.

Was lange währt, wird endlich gut!

An dieser Stelle möchte ich meinen besonderen Dank nachstehenden Personen entgegenbringen, ohne deren Ideen, Mithilfe und konstruktive Kritik die Anfertigung dieser Promotionsschrift niemals zustande gekommen wäre.

Mein Dank gilt zunächst Prof. Dr. Oliver Betz für die Betreuung dieser Arbeit, der freundlichen Hilfe und der mannigfachen Ideengebung, die mir einen kritischen Zugang zu dieser Thematik eröffnete.

Besonders danken möchte ich meiner Familie: meiner Frau Christiane, meiner Tochter Amalia sowie meinen Eltern Wolfram und Ingrid, für ihre Unterstützung und ihr Verständnis bei der Anfertigung dieser Doktorarbeit.

Bedanken möchte ich mich ebenfalls bei nachstehenden, ehemaligen Mitgliedern der AG Betz für die schöne (Leidens)Zeit, die intensiven Gespräche und Diskussionen, die gemeinsamen Abende innerhalb und außerhalb der Uni: Michael Heethoff, Daniela Weide, Christian Schmitt, Julius Braun, Michael Laumann, Christoph Allgaier und Paavo Bergmann.

Des Weiteren möchte ich mich bei Karl-Heinz Helmer, Monika Meinert und Julia Straube für die stundenlange, ermüdende Arbeit am Rasterelektronenmikroskop bedanken.

Mein außerordentlicher Dank gilt Volker Puthz für die wissenschaftliche Beratung, die Überlassung und Bestimmung der *Stenus*- und *Dianous*-Arten sowie die Beschreibung des *Stenus koerneri*.

Ein besonderer Dank gilt unseren Kooperationspartnern Stanislav Gorb (Universität Kiel), Konrad Dettner, Inka Lusebrink und Carolin Lang (Universität Bayreuth), Klaus Peschke und Thomas Schmitt (Universität Freiburg) sowie Volkmar Braun (Max-Planck-Institut für Entwicklungsbiologie, Tübingen).

Ich danke Herrn PD Dr. Michael Heethoff für die hilfsbereite und wissenschaftliche Betreuung als Zweitgutachter sowie Dr. Nils Anthes und Prof. Dr. Heinz-R. Köhler für die Funktion als Prüfer im Prüfungskomitee.

Ferner danke ich der DFG, dem BMBF sowie der Landesgraduiertenförderung Baden-Württemberg für die Finanzierung meines Projektes.

Persönliche Daten

Name	Koerner
Vorname	Lars
Geburtsdatum	06.12.1977
Geburtsort	Berlin
Familienstand	Verheiratet
Staatsangehörigkeit	Deutsch

(wissenschaftlich-) berufliche Tätigkeiten

ab Juli 2012	Publishing Editor im Springer-Verlag, Heidelberg (Programmplanung Zoologie)
Oktober 2008 bis Juli 2012	Wissenschaftlicher und technischer Angestellter, Institut für Evolution und Ökologie der Eberhard-Karls-Universität Tübingen Angestellter im Rahmen des DFG-Projektes
April 2007 bis September 2008	Stipendiat der Landesgraduiertenförderung des Landes Baden-Württemberg
Januar 2004 bis September 2004	studentische Hilfskraft, Christian-Albrechts-Universität Kiel

Studium

seit 2006	Dissertation an der Eberhard-Karls-Universität Tübingen: Ökomorphologische Diversität und Funktion des Klebfangapparates mitteleuropäischer *Stenus*-Arten (Coleoptera, Staphylinidae)

2005 bis 2006	Diplomarbeit am Lehrstuhl für Ökologie der Christian-Albrechts-Universität Kiel: Morphologische und ökologische Diversität bei *Stenus*-Arten (Coleoptera, Staphylinidae)
1999 bis 2005	Diplombiologiestudium (Christian-Albrechts-Universität Kiel) Hauptfach: Zoologie; Nebenfächer: Ökologie, Geologie
1998 bis 1999	Studium der Pharmazie an der Christian-Albrechts-Universität Kiel

Publikationen

2018	Betz O., **Koerner L.**, Dettner, K. The Biology of Steninae. In: Betz O., Irmler U., Klimaszewski J. (eds) Biology of Rove Beetles (Staphylinidae). Springer, Cham. p 229-283.
2017	**Koerner L**, Garamszegi LZ, Heethoff M, Betz O. Divergent morphologies of adhesive predatory mouthparts of *Stenus* species (Coleoptera, Staphylinidae) explain differences in adhesive performance and resulting prey-capture success. *Zoological Journal of the Linnean Society*, 181: 500-518.
2016	**Koerner L**, Braun V, Betz O. The labial adhesive pads of rove beetles of the genus *Stenus* (Coleoptera: Staphylinidae) as carriers of bacteria. *Entomologia Generalis* 36: 33-41.
2015	Lang C, **Koerner L**, Betz O, Puthz V, Dettner K. Phylogenetic relationships and chemical evolution of the genera *Stenus* and *Dianous* (Coleoptera: Staphylinidae). *Chemoecology* 251: 11-24.
2013	**Koerner L**, Laumann M, Betz O, Heethoff M. Loss of the sticky harpoon—COI sequences indicate paraphyly of *Stenus* with respect to *Dianous* (Staphylinidae, Steninae). *Zoologischer Anzeiger* 252:337-347.

2012	**Koerner L**, Gorb SN, Betz O. Adhesion of the stick-capture apparatus of the rove beetles *Stenus* spp. (Coleoptera, Staphylinidae) to different surfaces. *Journal of Insect Physiology* 58: 155-163. **Koerner L**, Gorb SN, Betz O. Adhesive performance and functional morphology of the stick-capture apparatus of the rove beetles *Stenus* spp. (Coleoptera, Staphylinidae). *Zoology* 115: 117-127.
2011	Heethoff M, **Koerner L**, Norton, RA, Raspotnig G. Tasty but protected - first proof of chemical defence in oribatid mites. *Journal of Chemical Ecology* 37: 1037-1043
2009	Betz O, **Koerner L**, Gorb S. An insect's tongue as the model for two-phase viscous adhesives? *Adhesion Adhesives & Sealants* 3: 32-35. Schmitt C, Rack A, **Koerner L**, Dieterich A, Zabler S, Betz O. High-speed X-ray cineradiography for imaging the mouthpart kinematics of living insects. *ANKA Highlights* 25-26.
2008	Betz O, Rack A, Schmitt C, Ershov A, Dieterich A, **Koerner L**, Haas D, Baumbach T. High-speed X-ray cineradiography for analyzing complex kinematics in living insects. *Synchrotron Radiation News* 21: 34-38. Betz O, **Koerner L**, Gorb S. Insektenzunge als Vorbild für biphasisch viskose Klebstoffe? *Adhäsion* 6: 38-41.
2007	Heethoff M, **Koerner L**. Small but powerful - The oribatid mite *Archegozetes longisetosus* Aoki (Acari, Oribatida) produces disproportionate high forces. *Journal of Experimental Biology* 210: 3036-3042.

Publikation I

Functional morphology and adhesive performance of the stick-capture apparatus of the rove beetles *Stenus* spp. (Coleoptera, Staphylinidae)

Lars Koerner, Stanislav N Gorb, Oliver Betz

Zoology 115 (2012): 117–127

Zoology 115 (2012) 117–127

Contents lists available at SciVerse ScienceDirect

Zoology

journal homepage: www.elsevier.de/zool

Functional morphology and adhesive performance of the stick-capture apparatus of the rove beetles *Stenus* spp. (Coleoptera, Staphylinidae)

Lars Koerner[a,*], Stanislav N. Gorb[b], Oliver Betz[a]

[a] *Department of Evolutionary Biology of Invertebrates, Institute for Evolution and Ecology, University of Tübingen, Auf der Morgenstelle 28E, D-72076 Tübingen, Germany*
[b] *Department of Functional Morphology and Biomechanics, Zoological Institute, University of Kiel, Am Botanischen Garten 1-9, D-24098 Kiel, Germany*

ARTICLE INFO

Article history:
Received 21 July 2011
Received in revised form
15 September 2011
Accepted 18 September 2011

Keywords:
Adhesion
Force measurement
Predation
Prey-capture apparatus
Sticky pads

ABSTRACT

The adhesive prey-capture apparatus of the representatives of the rove beetle genus *Stenus* (Coleoptera, Staphylinidae) is an outstanding example of biological adhesive systems. This unique prey-capture device is used for catching elusive prey by combining (i) hierarchically structured adhesive outgrowths, (ii) an adhesive secretion, and (iii) a network of cuticular fibres within the pad. The outgrowths arise from a pad-like cuticle and are completely immersed within the secretion. To date, the forces generated during the predatory strike of these beetles have only been estimated theoretically. In the present study, we used force transducers to measure both the compressive and adhesive forces during the predatory strike of two *Stenus* species. The experiments revealed that the compressive forces are low, ranging from 0.10 mN (*Stenus bimaculatus*) to 0.18 mN (*Stenus juno*), whereas the corresponding adhesive forces attain up to 1.0 mN in *S. juno* and 1.08 mN in *S. bimaculatus*. The tenacity or adhesive strength (adhesive force per apparent unit area) amounts to 51.9 kPa (*S. bimaculatus*) and 69.7 kPa (*S. juno*). *S. juno* beetles possess significantly smaller pad surface areas than *S. bimaculatus* but seem to compensate for this disadvantage by generating higher compressive forces. Consequently, *S. juno* beetles reach almost identical adhesive properties and an equal prey-capture success in attacks on larger prey. The possible functions of the various parts of the adhesive system during the adhesive prey-capture process are discussed in detail.

1. Introduction

So far, most studies on animal adhesive organs have focused on the adhesive pads of legs in the context of locomotion. Adhesive structures of mouthparts used in prey capture have been less extensively studied (reviewed in Betz and Kölsch, 2004). An outstanding adhesive prey-capture apparatus is formed by the labium of rove beetles of the genus *Stenus* Latreille, 1797 (e.g., Weinreich, 1968) (Fig. 1). This system belongs to the hairy, branched and wet (with adhesive fluid) type.

The genus *Stenus* comprises more than 2500 species worldwide and is therefore one of the most diverse beetle genera (Puthz, 2010). Their elongated labium can be protruded towards the potential prey extremely rapidly (within 1–3 ms) by haemolymph pressure (Bauer and Pfeiffer, 1991). The paraglossae at the distal end of the rod-like prementum are modified into sticky pads (Figs. 1 and 2A), whose surface is differentiated into terminally branched outgrowths (Fig. 2B). As soon as the prey adheres to these sticky pads, the labium is instantly retracted and the beetle can seize the prey with its mandibles. The structure and function of this adhesion-capture apparatus have been described in several previous publications (e.g., Schmitz, 1943; Weinreich, 1968; Betz, 1996, 1998; Kölsch and Betz, 1998; Kölsch, 2000; Betz et al., 2009). Most *Stenus* species make use of their mandibles as an alternative prey-capture technique (Bauer and Pfeiffer, 1991; Betz, 1996, 1998).

The sticky pads maintain their adhesive function via an adhesive secretion that is produced in specialised glands within the head capsule (Schmitz, 1943; Weinreich, 1968) and secreted onto the pad surface (Fig. 2C and D). The secretion has been assumed to consist of at least two immiscible phases: proteinaceous and lipoid (Kölsch, 2000). The biphasic nature of the secretion might be advantageous for effective spreading over substrates with various surface energies.

The prey-capture apparatus of *Stenus* spp. functions like a catapult (see supplementary video mmc1 in Appendix A), i.e., the elastic elements of the labium are preloaded indirectly via increased haemolymph pressure prior to the strike and are finally released to hit the prey suddenly with high impact pressure (Kölsch and Betz, 1998; Betz, 1998, 1999, 2006). The antagonists of this system are represented by large retractor muscles of the mouth angles (Weinreich, 1968). When the labium is retracted, adhesive forces develop perpendicularly with respect to the prey surface (Betz, 2006). In contrast to tarsal attachment devices, in which van der Waals and capillary forces are considered to be the major

* Corresponding author.
E-mail address: larskoerner3@hotmail.com (L. Koerner).

0944-2006/$ – see front matter © 2012 Elsevier GmbH. All rights reserved.
doi:10.1016/j.zool.2011.09.006

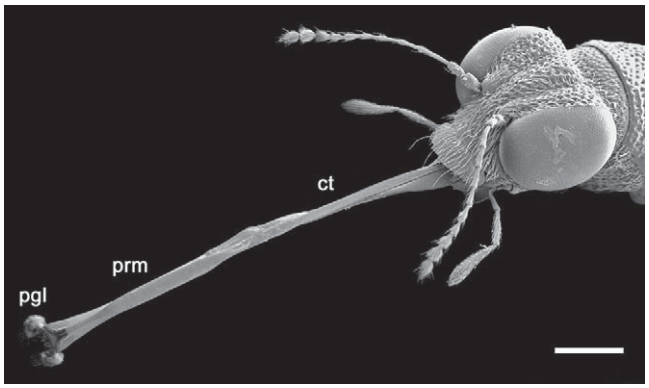

Fig. 1. The adhesion-capture apparatus of *Stenus bimaculatus*. Scanning electron microscopic image of the head with the protruded labium. Scale bar = 0.5 mm. Abbreviations: ct = connecting tube, pgl = paraglossa, prm = prementum.

adhesive mechanisms (e.g., Stork, 1980; Alexander, 1992; Autumn et al., 2002; Langer et al., 2004; Huber et al., 2005), viscous forces (Stefan adhesion) are assumed to be the major adhesive mechanism of the *Stenus* labium (Kölsch, 2000; Betz and Kölsch, 2004). According to Betz (1996), the sticky pads of the labium have been modified in various ways from a general type during the course of evolution. These changes mainly involve (i) the area of the sticky pads, (ii) the number of outgrowths on the pads, and (iii) the degree of branching of single outgrowths. These morphological parameters greatly influence prey-capture success, which is presumably based on differences in the adhesive performance (Betz, 1996, 1998).

To date, the attractive forces that act during the predatory strike of the *Stenus* labium have only been indirectly estimated (Kölsch, 2000). According to these calculations, the strongest expected viscosity-based adhesive force in the species *Stenus comma* LeConte amounts to 66.4 μN. However, direct measurements of adhesive forces are lacking in the literature. The present study presents *in vivo* force measurements carried out during the predatory strike of two species of the genus *Stenus*.

The following questions have been addressed in our study. (i) What functional principles underlie the adhesive prey-capturing mechanism of *Stenus*? (ii) How does the morphology of the labial adhesive pads influence adhesion? (iii) Is there a correlation between the generated compressive (impact) force and the adhesive force? The forces measured in the present study are compared with forces previously obtained from other adhesive systems of insects, such as tarsal attachment devices.

2. Materials and methods

2.1. Animals

Studies were carried out with adult *Stenus juno* Paykull 1800 and *Stenus bimaculatus* Gyllenhal 1810. Both these species were collected from the reed zone of a small pond near Tuebingen, southern Germany (48°31′30.74″N, 9°00′46.53″E). They were kept in the laboratory in plastic boxes lined with moist gypsum plaster mixed with activated charcoal to prevent contamination with microorganisms and to ensure a constant high humidity. Beetles were fed with living collembolans ad libitum.

2.2. Force measurements on living beetles

Before the experiments were performed, the beetles were starved for 5–7 days. The experimental set-up for determining the compressive and adhesive forces generated during the beetles' predatory strike is shown in Fig. 3. The spherical head of an insect pin (No. 00; Morpho, Austria) with a diameter of 1.0 mm was used as a dummy prey. It was connected to a force sensor (FORT25; WPI

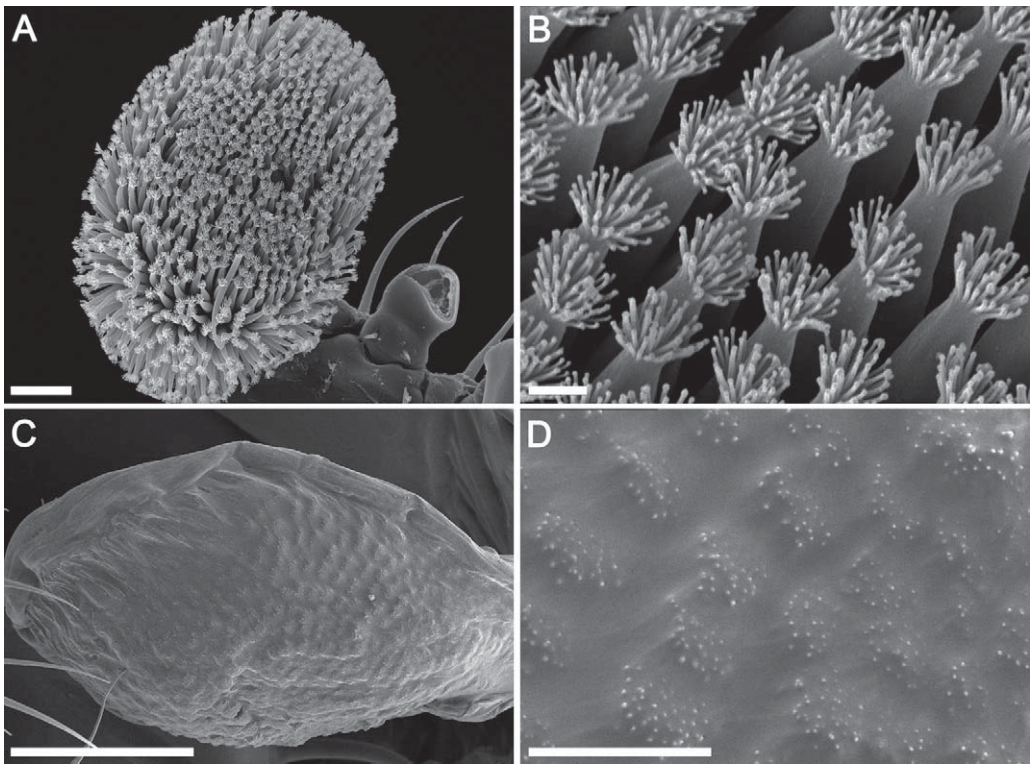

Fig. 2. Images of the paraglossae, which are modified into sticky pads, in *Stenus juno*. (A–B) SEM images, (C–D) cryo-SEM images. (A) Ventral aspect of a sticky pad. Scale bar = 20 μm. (B) Adhesive outgrowths with terminal ramifications. Scale bar = 2 μm. (C) During prey capture, the adhesive outgrowths are deeply immersed within the adhesive secretion. Scale bar = 30 μm. (D) Adhesive secretion with protruding terminal ramifications of the adhesive outgrowths. Scale bar = 2 μm.

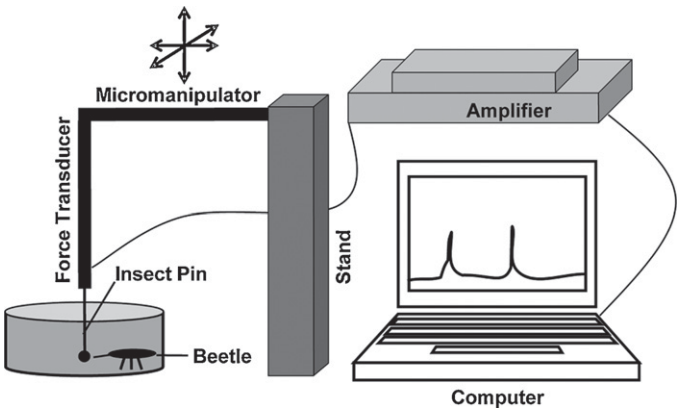

Fig. 3. Experimental set-up for force measurements during dummy prey-capture. The beetle is located in a circular arena. The head of an insect pin is used as dummy prey. The pin is fixed to a force transducer that is connected to a micromanipulator, which is movable in various directions to attract the attention of the beetle. When the beetle strikes the insect pin, the resulting forces are amplified and recorded.

Inc., Sarasota, FL, USA) that was calibrated prior to the experiments by means of a 20 mN weight. Since the adhesive and compressive forces generated during the predatory strike develop perpendicular to the surface, we used a single-axis force sensor for our measurements. Because the beetles only react to moving objects, the force sensor with the attached insect pin was mounted on a micromanipulator that was moved back and forth to attract the beetles' attention. The force sensor was attached to an amplifier (BIOPAC Systems Inc., Goleta, CA, USA) and a computer-based data-acquisition and processing system (MP100 WSW, BIOPAC Systems Inc., USA). The strike of the beetle at the dummy caused force sensor deflection that was digitally recorded and later processed. After each individual test, the insect pin was cleaned with ethanol (70%) and distilled water. The experiments were performed with 27 individuals of each species, with 15–25 strikes per individual beetle. The maximum compressive and adhesive forces of each beetle were obtained by means of the software AcqKnowledge 3.8.2 (BIOPAC Systems Inc., USA) and used for statistical evaluation. Prior to the experiments, the beetles were weighed individually by using an analytical balance (GR-202-EC Dual Range; A&D Instruments Ltd., Abingdon, UK).

The free surface energy of the insect pin and its dispersive and polar components were measured by using a video-based optical contact angle-measuring device (OCAH 200; Dataphysics Instruments GmbH, Filderstadt, Germany). The free surface energy was calculated by using a series of liquids (water, diiodomethane, ethylene glycol). The contact angles of the liquids on the insect pin were evaluated by the sessile drop method (droplet volume: 1 μl) and ellipse-fitting. The surface energy and its components were determined according to the Owens–Wendt–Kaelble method (Owens and Wendt, 1969). The contact angle of water of the head of the insect pin was $84.03 \pm 1.7^\circ$ ($n = 4$) and its surface energy was 30.77 ± 1.4 mN/m (dispersive component: 26.9 ± 1.3 mN/m; polar component 3.8 ± 0.4 mN/m).

2.3. High-speed video recordings

Representative predatory strikes on the insect pin were recorded at 2000 frames s^{-1} with a high-speed camera (Kodak Motion Corder Analyzer PS-110; Eastman Kodak Company, Rochester, NY, USA) mounted on a binocular microscope (Leica MZ6; Leica Microsystems, Wetzlar, Germany).

2.4. Microscopy techniques

For scanning electron microscopy (SEM), beetle heads with the labia extended were cleaned with H_2O_2, dehydrated in an ethanol series, critical-point dried (Polaron E3000; Quorum Technologies, East Grinstead, UK), fixed to stubs with silver paint, sputter-coated with gold–palladium (SCD 030; Balzers Instruments, Balzers, Liechtenstein) and observed in a stereoscan 250 MK2 SEM (Cambridge Instruments, Cambridge, UK). The following morphological parameters of the sticky pads were measured with tpsDig 1.40 (Rohlf, 2004): (1) surface area of the sticky pads, (2) number of adhesive outgrowths per sticky pad, (3) length, (4) diameter and (5) cross-sectional area of the shaft of a single outgrowth, (6) number of terminal ramifications per adhesive outgrowth and (7) length, (8) diameter and (9) cross-sectional area of a single ramification. The length, diameter, and cross-sectional area (calculated from the diameter) of the outgrowths and ramifications as well as the number of ramifications were measured at the centre of the sticky pad (for a given specimen, the mean of five measurements of each variable was calculated). The aspect ratios of the outgrowths and ramifications were calculated by dividing their lengths by their diameters. The newly obtained data of the surface area of the sticky pads, the number of adhesive outgrowths per sticky pad, the number of terminal ramifications per adhesive outgrowth and the number of terminal ramifications per sticky pad were merged with the data obtained by Betz (1996).

For cryo-SEM, the heads with the extended labia were glued to holders with Tissue-Tek OCT compound (Sakura Finetek Europe B.V., Zoeterwoude, The Netherlands) or were mechanically gripped in a small vice on holders. The specimens were frozen in liquid nitrogen and transferred to a cryo-stage of the preparation chamber at $-140\,^\circ$C (Gatan ALTO 2500 cryo-preparation system; Gatan Inc., Abingdon, UK). Frozen samples were sublimated at a temperature of $-90\,^\circ$C for 3 min, sputter-coated with gold–palladium (thickness 6 nm) and studied in a cryo-SEM Hitachi S-4800 (Hitachi Corp., Tokyo, Japan) at an accelerating voltage of 3 kV and $-120\,^\circ$C. This allowed us, for the first time, to visualise labium structures with the adhesive secretion located on their surfaces at high resolution.

To visualise secretion prints left on the dummy prey, the head of the insect pin was coated with gold–palladium and examined by conventional SEM (Cambridge Stereoscan 250 MK2; Cambridge Instruments, Cambridge, UK) as described above.

Additionally, the thickness profile of the cured secretion prints left on the surface of clean cover glasses (Nr. 0; Hecht, Sondheim, Germany) was analysed by using a scanning white light interferometer (Zygo NewView 5000; Zygo Corp., Middlefield, CT, USA).

2.5. Bright-field light microscopy and fluorescent microscopy

To visualise resilin-bearing parts of the prey-capture apparatus, the labia of freshly killed beetles were cut off, mounted on cover-slips in a water-soluble medium (Moviol; Hoechst, Frankfurt, Germany) and observed by fluorescence microscopy (Zeiss Axioplan; Carl Zeiss Inc., Oberkochen, Germany) under bright-field illumination or one of three wavelength bands: green (excitation 512–546 nm, emission 600–640 nm), red (excitation 710–775 nm, emission 810–890 nm) or ultraviolet (excitation 340–380 nm, emission 425 nm). Images taken in the fluorescence mode were superimposed in order to show the autofluorescence of the cuticular structures (Gorb, 1999, 2004; Niederegger and Gorb, 2003; Perez Goodwyn et al., 2006). Insect cuticle has strong autofluorescence at wavelengths from blue-green to deep-red, whereas resilin has autofluorescence at a narrow band of wavelengths around 400 nm (Andersen and Weis-Fogh, 1964) and therefore appears blue in fluorescence images.

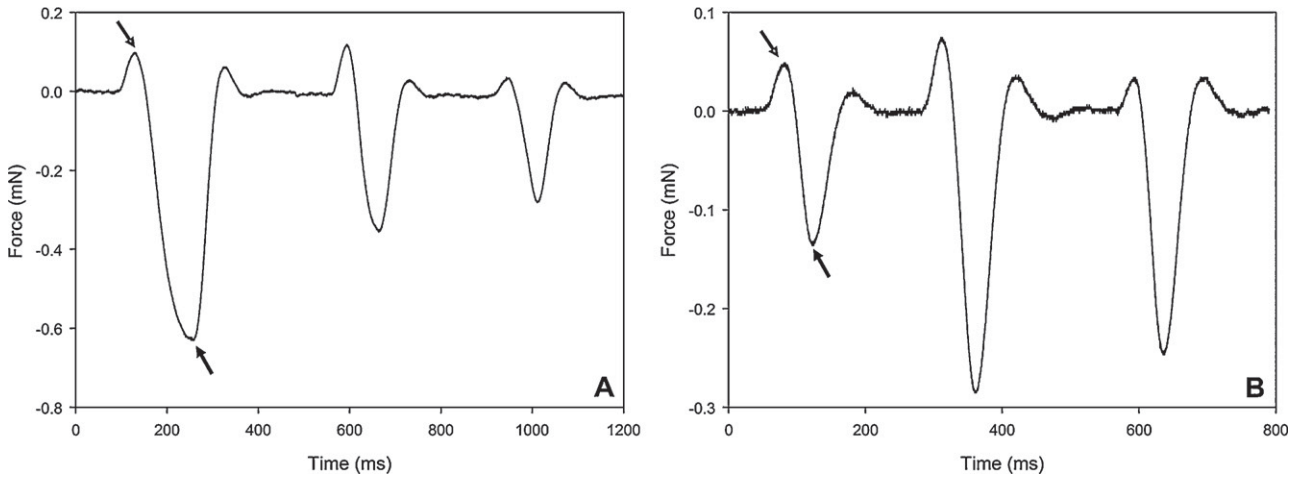

Fig. 4. Representative force–time curves of three consecutive strikes of (A) *S. juno* and (B) *S. bimaculatus* on the dummy prey. Upon prey capture, the labium transfers a definite impact force (compressive force) to the dummy prey, as indicated by the first arrows. The second arrows indicate the maximum adhesive force that arises during the retraction of the labium. Note that the compressive forces are much lower than the resulting adhesive forces.

2.6. Prey-capture experiments

To obtain a higher sample size, additional prey-capture experiments were conducted on *Heteromurus nitidus* Templeton 1835 springtails of various sizes according to Betz (1996, 1998). Similar to his experiments, 10–15 attacks per specimen were evaluated. The newly obtained data were added to the data of *S. bimaculatus* and *S. juno* obtained by Betz (1996, 1998) and statistically analysed. The fresh weights ranged from 8.4 ± 5.6 μg in "small" springtails to 62.3 ± 25 μg in "large" springtails (data from Betz, 1996, 1998).

2.7. Statistical analyses

Statistical analyses were performed with SPSS 11.0 (SPSS Inc., Chicago, IL, USA). Data were tested for normality by using the Shapiro–Wilk test. If the data followed the normal distribution, Student's *t*-test was used for further analysis. Otherwise, the Mann–Whitney *U*-test was employed.

3. Results

3.1. Force measurements

Both the impact (compressive) forces of the labium hitting the dummy prey and the resulting adhesive forces were directly measured in the investigated *Stenus* beetles. Examples of typical force–time curves are shown in Fig. 4A and B. Upon prey-capture strike, the labium transmits a compressive force F_c to the prey. The mean compressive forces amounted to 0.102 mN for *S. bimaculatus* and 0.179 mN for *S. juno* (Table 1, Fig. 5). These differences were significant (*t*-test, $t = -5.90$, df = 52, $p < 0.001$). During the retraction of the sticky pads from the contacted surface, an adhesive force F_a could be measured (Fig. 4). The average adhesive forces did not differ statistically between *S. bimaculatus* (1.1 mN, $N = 27$) and *S. juno* (1.0 mN, $N = 27$) (Table 1, Figs. 4 and 5; *t*-test, $t = 1.32$, 34 df = 52, $p > 0.05$).

Our measurements showed that in both species investigated the compressive force was significantly lower than the resulting adhesive force (Fig. 5; paired *t*-test, *S. bimaculatus*: $t = -22.44$, df = 26, $p < 0.001$; *S. juno*: $t = -22.48$, df = 26, $p < 0.001$). The maximum F_a/F_c ratio was significantly higher in *S. bimaculatus* (11.41 ± 3.6; $N = 27$) than in *S. juno* (6.21 ± 2.5; $N = 27$) (*t*-test, $t = 6.18$, df = 52, $p < 0.001$).

The mean tenacities (average adhesive forces divided by the mean surface areas of the sticky pads) amounted to 51.89 kPa in *S. bimaculatus* and 69.65 kPa in *S. juno* (Table 1). Within each species, no or only weak relationships seemed to be present between the compressive and the resulting adhesive force. In both species, both variables positively correlated in only 3 out of the 27 individuals tested.

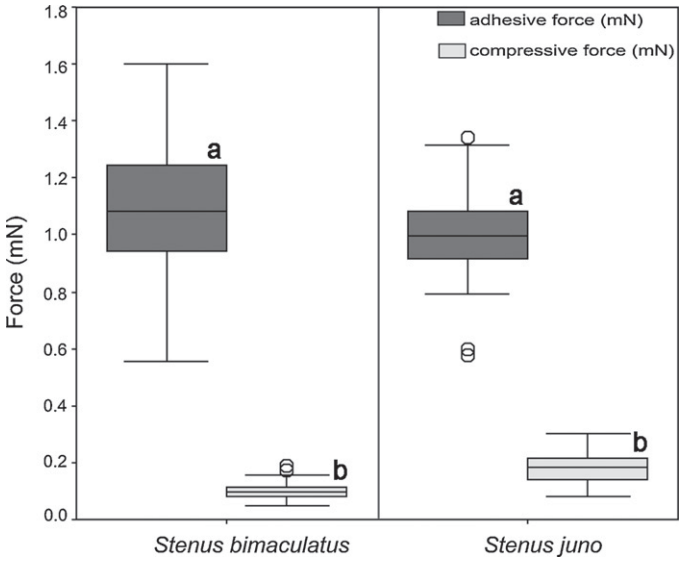

Fig. 5. Maximum adhesive (dark grey boxes) and compressive forces (light grey boxes) in *S. bimaculatus* and *S. juno*. Plot shows medians (centre lines), interquartile ranges (boxes), maximum and minimum values (whiskers), and outliers (circles). The outliers are cases with values between 1.5 and 3 box-lengths from the 75th percentile or 25th percentile. Different letters indicate statistical differences between the compressive and adhesive forces of each species (paired *t*-test). $n = 27$.

3.2. Morphology of the sticky pads

The ventral part of each paraglossa is modified into a sticky pad that is covered with a large number of brush-like adhesive outgrowths that are terminally differentiated into numerous ramifications (Fig. 2A and B). Strong interspecific differences exist in the morphology of the sticky pads of *Stenus* beetles, especially with respect to their surface area, the number of adhesive outgrowths and the number of adhesive contacts (Betz, 1996).

The morphological characters of the sticky pads of the two investigated species are summarised in Table 2. The two species differ

Table 1
Body mass, compressive, and adhesive forces obtained during the predatory strike on the dummy prey by *S. bimaculatus* and *S. juno*. Values are presented as means ± standard deviations. Force/weight ratios are given in parentheses. $N = 27$. p = significance level of tests for differences of the means between both species (t-test).

	S. bimaculatus	p	*S. juno*
Body mass [mg]	5.052 ± 0.35	***	3.526 ± 0.37
Compressive force [mN]	0.102 ± 0.04 (2.07)	***	0.179 ± 0.06 (5.25)
Adhesive force [mN]	1.077 ± 0.24 (21.91)	n.s.	1.000 ± 0.19 (29.13)
Ratio adhesive/compressive force	11.408 ± 3.57	***	6.213 ± 2.53
Tenacity [kPa]	51.89	–	69.65

n.s., $p > 0.05$.
*** $p < 0.001$.

Table 2
Morphological parameters of the sticky pads in *S. bimaculatus* and *S. juno*. Values are presented as means ± standard deviations (SD). The number of individuals used (N) is indicated for all parameters. p = significance level of tests indicating differences of the means between both species (t-test).

Morphological parameter	*S. bimaculatus*				*S. juno*		
	N	Mean	SD	p	N	Mean	SD
Surface area of the sticky pad [μm^2]	20	10,755.13	1728.1	***	19	7176.94	1108.4
Adhesive outgrowths per sticky pad	14	586.21	51.0	n.s.	14	590.64	83.0
Adhesive outgrowths per μm^2	14	0.054	0.01	***	14	0.083	0.02
Length of outgrowth [μm]	9	24.98	2.4	***	6	20.30	0.8
Diameter of outgrowth [μm]	9	2.51	0.1	*	6	2.71	0.2
Cross-sectional area of shaft of outgrowth [μm^2]	9	4.99	0.3	*	6	5.84	0.8
Aspect ratio of outgrowth	9	10.03	0.9	***	6	7.57	0.6
Terminal ramifications per outgrowth	9	28.91	1.7	n.s.	8	25.23	6.8
Terminal ramifications per sticky pad	13	17,910.64	3030.4	n.s.	9	16401.15	3700.0
Terminal ramifications per surface area of 1 μm^2	13	1.64	0.3	***	9	2.34	0.5
Length of terminal ramification [μm]	9	1.62	0.1	*	6	1.45	0.1
Diameter of single terminal ramification [μm]	9	0.237	0.04	***	6	0.171	0.02
Cross-sectional area of terminal ramification [μm^2]	9	0.049	0.03	*	6	0.024	0.01
Aspect ratio of terminal ramification	9	7.16	0.7	*	6	8.63	1.4

n.s., $p > 0.05$.
* $p < 0.05$.
*** $p < 0.001$.

significantly in the area of their sticky pads (t-test; $t = -8.74$, df = 46, $p < 0.001$), whereas the number of adhesive outgrowths and adhesive contacts per sticky pad and the number of ramifications per adhesive outgrowth do not differ significantly. In relation to the shaft of the adhesive outgrowth, the terminal ramifications are extremely short (ratio shaft/terminal ramifications: *S. bimaculatus*, 15.38; *S. juno*, 13.96) and have a much smaller cross-sectional area (ratio cross-sectional area of the shaft/cross-sectional area of its terminal ramifications: *S. bimaculatus*, 101.84; *S. juno*, 243.33). Both investigated species possess outgrowths and ramifications with high aspect ratios. The average aspect ratio of the outgrowths for *S. bimaculatus* was 10.03 ($N = 9$) and for *S. juno* 7.57 ($N = 6$), whereas the aspect ratio of the ramifications for *S. bimaculatus* was 7.16 ($N = 9$) and for *S. juno* 8.63 ($N = 6$) (Table 2). The outgrowths are arranged at a right or slightly oblique angle ($\leq 90^\circ$) relative to the surface of the sticky pad (Fig. 2A). In both species the tips of the ramifications are spherically shaped.

3.3. Adhesive secretion

During prey capture, the outgrowths are deeply immersed in the adhesive secretion (Fig. 2C), with only the tips of their terminal ramifications slightly protruding (Fig. 2D). Both the high-speed video recordings (Fig. 6; see also supplementary video no. 2 in Appendix A) and the secretion prints (Fig. 7) show that an exceptionally large amount of secretion is involved in the prey-capture process. Furthermore, these images suggest that the secretion is highly viscous (Figs. 6, frames 10–14 and 7B), since it stretches and splits into long fibres (fibrillation) before it finally tears off at the contact zone with the substratum. According to our high-speed video recordings (see supplementary video mmc2 in Appendix A), the sticky pads, while being retracted from the head of the insect pin, are stretched longwise first (Fig. 6, frames 5–9; indicative of their low E-modulus), followed by the stretching of the secretion (Fig. 6, frames 9–14).

White-light interferometry revealed a minimum secretion layer thickness of the prints left on the glass surface of about 30–150 nm. The actual value might even be lower, since it was estimated from secretion prints after retraction of the sticky pads from the glass surface.

3.4. Resilin occurrence

Fluorescence microscopy revealed the presence of resilin in the material of the entire sticky pads; high concentrations of resilin are also present within the mobile joints (e.g., of the labial palpus) (Fig. 8C and D).

3.5. Prey-capture experiments

The prey-capture experiments revealed a higher prey-capture success in *S. juno* for small springtails (Table 3: Mann–Whitney U-test; $Z = -3.49$; $p < 0.001$), whereas no difference between the two species was detected for large springtails (Table 3). In both of these species, the prey-capture success in attacks on small springtails was significantly higher than that on large springtails (*S. bimaculatus*: Mann–Whitney U-test, $Z = -5.71$, $p < 0.001$; *S. juno*: Mann–Whitney U-test, $Z = -6.61$, $p < 0.001$).

3.6. Mechanism of adhesion

In order to determine the physical mechanism of adhesion involved in the prey capture of *Stenus* beetles we calculated the theoretical adhesive forces and compared them with the measured

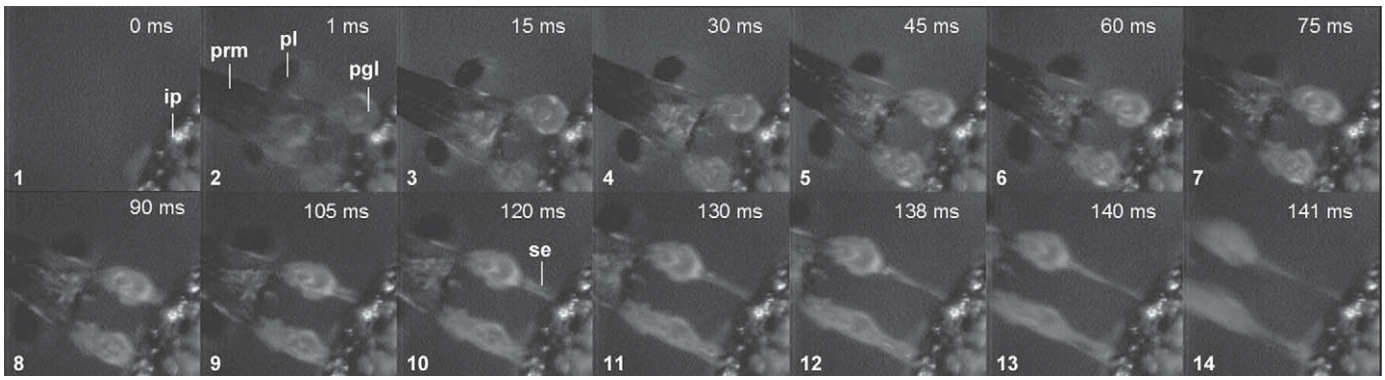

Fig. 6. High-speed video images of the strike on the head of an insect pin in *S. bimaculatus*. The insect pin is situated on the right side, whereas both sticky pads approach from the left. The actual strike lasts only 1 ms (frames 1–2). The time line of the depicted sequence is indicated in milliseconds in the upper right corner of each frame. The adhesive secretion is viscous, as can be seen in frames 9–14, in which it is stretched out into long fibres. The sticky pads are extremely flexible (frames 5–13) and stretch in length just before the secretion stretches. Scale bar = 50 μm. Abbreviations: ip = insect pin, pl = palpus labialis, pgl = paraglossa, prm = prementum, se = secretion.

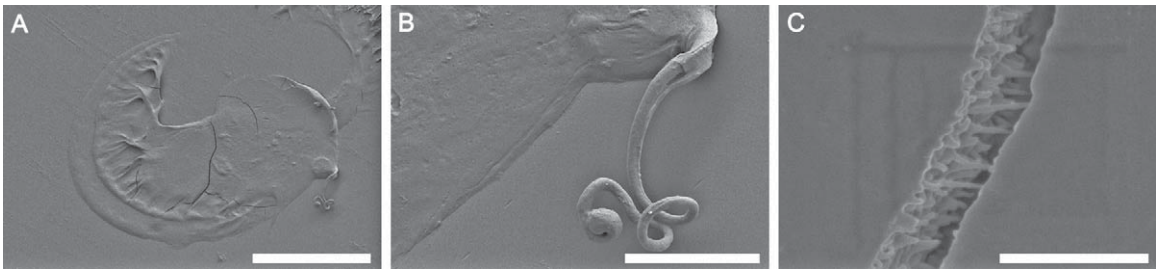

Fig. 7. SEM images of the secretion left on the dummy prey by *S. juno*. (A) Whole secretion print. Scale bar = 50 μm. (B) During retraction of the sticky pads, the secretion stretches into long fibres until it breaks. The depicted fibre is indicative of the high viscosity of the secretion. Scale bar = 10 μm. (C) Example of the fibrillar structures inside the secretion. Scale bar = 1 μm.

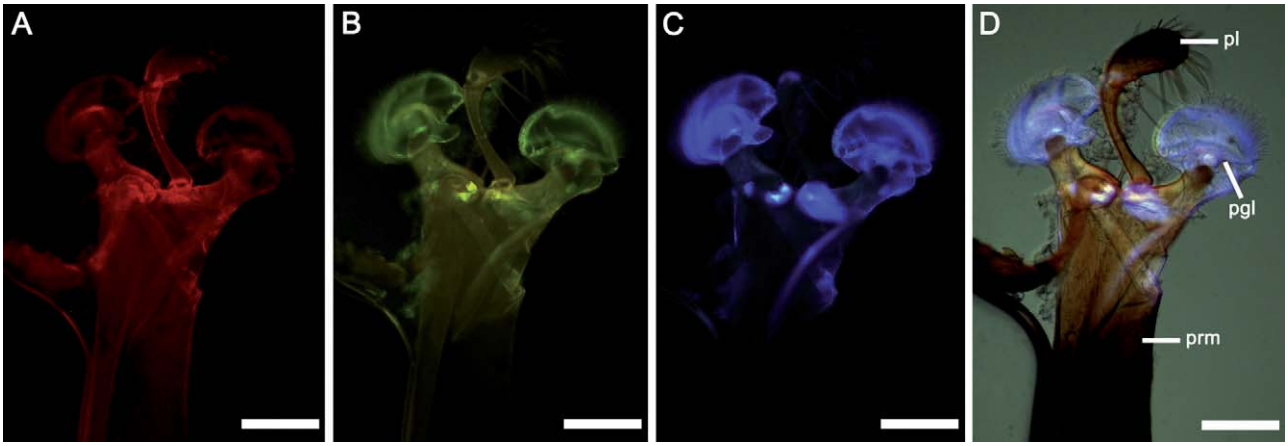

Fig. 8. Light micrographs of the labium of *S. bimaculatus*. View in (A) the green band (excitation 512–546 nm, emission 600–640 nm), (B) the red band (excitation 710–775 nm, emission 810–890 nm), and (C) the UV band (excitation 340–380 nm, emission 420 nm). (D) All three images taken at various wavelengths (A–C) superimposed. Resilin exhibits auto-fluorescence in an extremely narrow wavelength band (ca. 400 nm) so that it can only be seen in the UV band (C and D). Scale bars = 85 μm. Abbreviations: pl = palpus labialis, pgl = paraglossa, prm = prementum.

Table 3
Percentage of successful attacks conducted with the labium by *S. bimaculatus* and *S. juno* on small and large springtails (*Heteromurus nitidus*). Values are presented as means ± standard deviations. *p* = significance level of tests for differences between both species (Mann–Whitney *U*-test), *n* = number of individuals tested (according to Betz, 1996, 1998).

Successful attacks conducted with the labium [%]	*S. bimaculatus*	*p*	*S. juno*
Small springtails	64.72 ± 23.1 (*n* = 43)	***	81.87 ± 16.6 (*n* = 43)
Large springtails	28.36 ± 22.5 (*n* = 42)	n.s.	29.78 ± 27.9 (*n* = 39)

n.s., $p > 0.05$.
*** $p < 0.001$.

ones. The theoretically determined adhesive force attributable to Stefan adhesion was calculated with the formula (Bowden and Tabor, 1950; Kölsch, 2000):

$$F_{\text{Viscosity}} = \frac{3\pi\eta R^4}{4td^2} \quad (1)$$

and amounted to 0.98×10^{-3} N in *S. juno* and 2.21×10^{-3} N in *S. bimaculatus*. The following values were used for these calculations: (1) the radius (R) of the sticky pad (estimated from the pad area): 4.78×10^{-5} m (*S. juno*) and 5.85×10^{-5} m (*S. bimaculatus*), (2) the thickness of the secretion layer (d): 5×10^{-8} m as measured by white-light interferometry, (3) the time required for the separation of the surfaces to infinity (t): 0.1 s (Fig. 6), and (4) the viscosity of the adhesive (η): 0.01 N s m^{-2} (similar to that of vegetable oils; Kölsch, 2000).

The force of adhesion attributable to surface tension can be calculated as:

$$F_{\text{surface tension}} = 4\pi R\gamma\cos\theta, \quad (2)$$

where R is the radius of the sticky pad, γ is the surface tension of the fluid, and θ is the contact angle of the fluid (McFarlane and Tabor, 1950; Israelachvili, 1991; Kölsch, 2000). Apart from the radius of the sticky pads (see above), the following values were inserted into the calculation: (1) the surface tension of the secretion: 72 mJ m^2 (Kölsch, 2000) and (2) the contact angle of the fluid to the surface: 30° (estimated from white-light interferometry and SEM images). According to this calculation, the forces attributable to the surface tension of the secretion amounted to 7.49×10^{-5} N in *S. juno* and 9.17×10^{-5} N in *S. bimaculatus*.

4. Discussion

Complementing our study on the adhesive performance toward various surfaces (Koerner et al., 2012), the present study follows a more general approach, combining morphological analyses and force experiments in order to determine the forces that occur during the course of the prey-capture process in two species of the genus *Stenus*. These experiments helped to enhance our understanding of the underlying functional principles of this adhesive prey-capture mechanism (Fig. 9).

4.1. External morphology

The external structures of the labial sticky pads of *Stenus* beetles must have been subject to strong selective forces during their evolution (Betz, 1996). In *Stenus* species whose labial sticky pads have larger surface areas (e.g., *S. bimaculatus*, *S. juno*, *S. latifrons*), a higher number of adhesive outgrowths and adhesive contacts has experimentally been shown to lead to improved adhesion and thus to increased prey-capture success (Betz, 1996, 1998).

Adhesion between an adhesive pad and a substrate can be increased by splitting up the contact zone into many subcontacts, especially on uneven substrates (Varenberg et al., 2006, 2010). This principle can be seen in *Stenus* species, where the labial sticky pads show a hierarchical structure comprising the surface of the sticky pads with numerous adhesive outgrowths and their extremely fine terminal ramifications (Fig. 2; Table 2). The functional advantage of a hierarchically organised structure lies in the break-up of the adhesive surface into a large number of independent elements that compensate for possible surface irregularities of the prey (Betz and Kölsch, 2004). Contact splitting also ensures defect tolerance since the failure of a single element or a few elements does not impact the adhesion of the ensemble significantly (Spolenak et al., 2005b). In *Stenus* species, the subdivision of the contacts leads to enhanced adhesion, although in the present case of a "flooded regime" (Bhushan, 2003; Mate, 2008), in which the adhesive contacts are deeply immersed within the secretion (cf. Fig. 2C and D), the actual number of single contacts should be less important than the perimeter of the entire sticky pad.

A spherically shaped contact provides good adhesion, if the radius of the contact is reduced to scales below 100 nm (Spolenak et al., 2005b). Therefore, the spherically shaped tips of the ramifications in *Stenus* species (cf. Fig. 2B), with radii from 80 to 120 nm (as approximated from the diameter), might not only result in intimate contact with small-scale surface irregularities, but also ensure adhesion, although a large amount of viscous secretion is still needed. Additionally, the high aspect ratio of both the outgrowths and the ramifications in *Stenus* species (Table 2) makes these structures more compliant and therefore improves their adaptability to the uneven profile of the prey surface, comparable to the tarsal adhesive setae of insects (Kölsch and Betz, 1998; Peressadko and Gorb, 2004; Chan et al., 2007; Voigt et al., 2008).

In tarsal adhesive pads, a branched morphology of the setae is additionally advantageous, because the condensation between neighbouring setae is reduced as a result of the stronger stiffness of same-level neighbouring branches as compared to the adhesive strength of contacting spatula (Jagota and Benninson, 2002; Spolenak et al., 2005a; Federle, 2006). *Stenus juno* beetles have a significantly higher density of adhesive outgrowths than *S. bimaculatus* beetles (Table 2), which makes such structures potentially more susceptible to condensation (Jagota and Benninson, 2002; Spolenak et al., 2005a; Federle, 2006). However, *S. juno* beetles seem to have evolved various morphological adaptations to avoid this problem. First, these beetles have shorter, but wider and thus presumably stiffer, adhesive outgrowths than *S. bimaculatus*. Additionally, *S. juno* beetles possess an equally large number of shorter and more densely packed ramifications (Table 2). Embedding of the outgrowths within the adhesive secretion in both species (Fig. 2D) provides further protection against condensation because of the absence of capillarity and reduced van der Waals interactions (Israelachvili, 1991).

4.2. Adhesive performance

Our *in vivo* force measurements revealed much lower values for the compressive force than for the resulting adhesive force (Table 1). Thus, in *Stenus* beetles the ratio of the adhesive force and the applied (compressive) force is much higher (6.21 in *S. juno* and 11.41 in *S. bimaculatus*) than in tarsal adhesive systems (Table 1, Fig. 5); e.g., in the cricket *Tettigonia viridissima* L. (Ensifera, Tettigoniidae), the value of this ratio lies between 1.6 and 3.5 (as calculated from Fig. 6B in Jiao et al., 2000). Accordingly, the adhesive system of *Stenus* beetles achieves much higher adhesive forces with lower applied forces. One might speculate that this is advantageous, since the adhesive secretion of *Stenus* beetles might behave in a non-Newtonian manner (cf. Gorb, 2001; Federle et al., 2002; Vötsch et al., 2002; Drechsler and Federle, 2006; Dirks et al., 2009) and such behaviour in interaction with a relatively low compressive force would improve its flow into surface irregularities. In contrast, higher compressive forces would cause the secretion to behave more solid-like, resulting in pushing away the prey (see supplementary video mmc3 in Appendix A)

Adhesion is affected by the area of contact, which is a function of the normal load, surface roughness and mechanical properties of both contacting materials (Bhushan, 2003). During the predatory strike of the beetles, a substantial impact (compressive) force is attained, because the distance to the prey that must be bridged by the labium only amounts to half the length of the labium (Betz, 1996, 1998). Additionally, the beetles often perform forward lunges during the strike (Betz, 1996, 1998). The resulting increased compressive force (Table 1) should help to further enhance adhesion

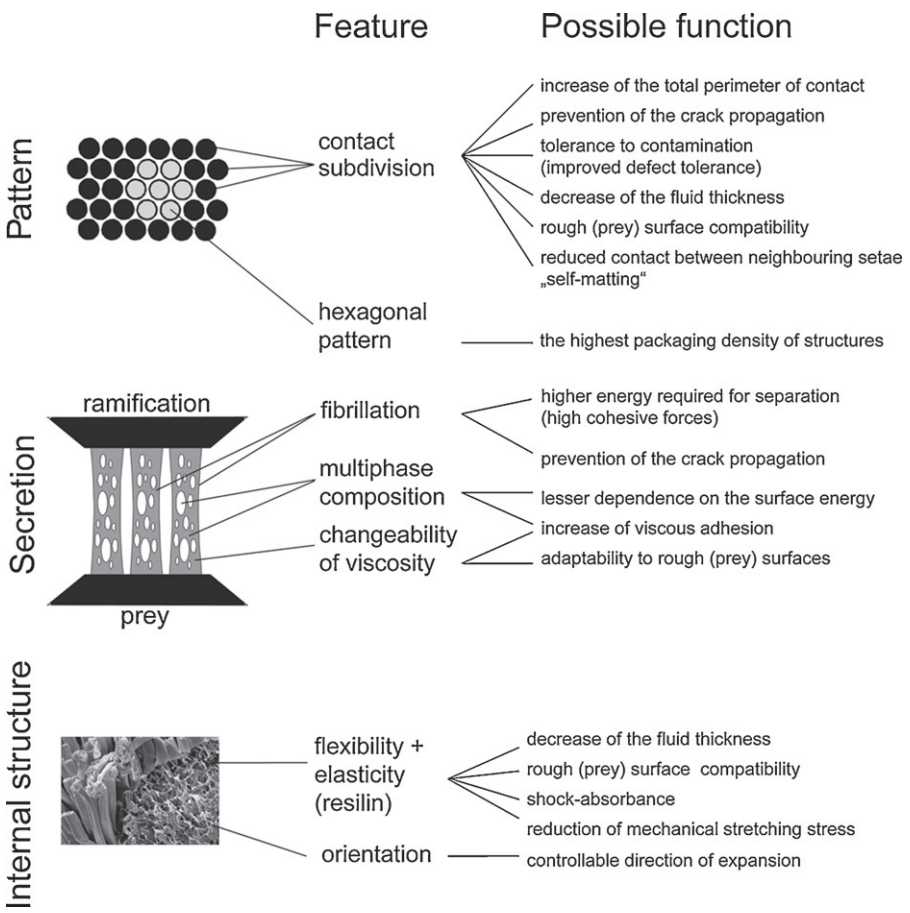

Fig. 9. Summary of the observed structural principles (regarding pattern, secretion and internal structure) and the possibly resulting functional features in the sticky pads of *Stenus* beetles.

by reducing the thickness of the secretion layer (Bowden and Tabor, 1986) and by pressing both the adhesive contacts and the secretion into the irregularities of the prey surface. In tarsal adhesive systems, the adhesion force has been shown to increase with increasing applied normal force and to remain constant when the applied force exceeds a certain value (Jiao et al., 2000; Scherge and Gorb, 2001). Betz (1996) assumed that the push (compressive force) that contacts the prey should be as large as possible in order to achieve considerable adhesive forces. Accordingly, compressive and adhesive forces might be expected to be positively correlated. In contrast to this assumption, in most investigated individuals of both species no such correlation has been observed. However, since the intraspecific variation of the compressive force is very low (Table 1), a relationship between the compressive and the adhesive forces is difficult to detect within a species. Only a broader interspecific comparsion might reveal a relation between both of these forces.

A possible insight into the influence of the compressive force on the adhesive performance may be gained from a comparison of the two *Stenus* species. The investigated *S. juno* beetles have significantly smaller pad areas than *S. bimaculatus* (Table 2) but seem to compensate for this disadvantage by generating higher compressive forces, so that the beetles of both species achieve almost identical adhesive properties (Table 1). Interestingly, whereas the prey-capture success of both species is equal for large springtails (Table 3), *S. juno* beetles with their smaller sticky pads attain even higher prey-capture success rates when catching springtails of small body size (Table 3; Betz, 1998). Variations of the attack distance may account for this enhanced compressive force in *S. juno*. Betz (1996, 1998) points out that the difference between the "critical attack distance" and the length of the forward body lunge performed by the beetles during the strike is equivalent to the attack distance to the prey that must be bridged by the labium. Since the *Stenus* labium is approximately twice as long as the remaining distances to be bridged, it is able to transfer a significant compressive force to the prey (Betz, 1996). Hence, the ability to vary this critical attack distance might be a powerful technique to adjust the strength of the catapult mechanism to the demands. Indeed, towards small springtails, *S. juno* beetles attain significantly smaller attack distances than *S. bimaculatus* (Betz, 1998). Alternatively, one may speculate whether the beetles are capable of adjusting the amount of the haemolymph pressure that is used for the catapult-like protrusion of the labium.

The tenacity (adhesive strength) generated by insect locomotory organs, measured perpendicularly to the contact surface, lies between 2 kPa (*T. viridissima*; Jiao et al., 2000) and 80 kPa (*H. cyanea*; Attygalle et al., 2000). The tenacities of the adhesive systems investigated in the present study (*S. bimaculatus*: 50 kPa; *S. juno*: 70 kPa) correspond well to this range. Higher lateral tenacity (shear strength) has been found in the locomotory organs of insects when measured parallel to the contact surface so that friction forces become more strongly involved (e.g., *Calliphora vomitoria* L., Diptera, Calliphoridae: 280 kPa; Walker, 1993).

4.3. Mechanism of adhesion

Previous investigations (Kölsch and Betz, 1998; Kölsch, 2000; Betz and Kölsch, 2004) have proposed the mode of adhesion in the labial sticky pads of *Stenus* beetles to be in accordance with the principle of Stefan adhesion, in which the viscosity of the secretion

plays the major role. Adhesion based on the formation of covalent bonds or on a type of glue that has to dry was ruled out, because of the high speed of the predatory strike (Kölsch, 2000). Also, the presence of an adhesive secretion makes dry adhesion attributable to van der Waals forces unlikely (Kölsch, 2000; Betz and Kölsch, 2004).

Kölsch (2000) calculated the strongest adhesive force attributable to Stefan adhesion to be 6.64×10^{-5} N in the species *S. comma*. Our results reveal that the measured adhesive forces are more than two orders of magnitude above these calculations (*S. juno*: 1.0×10^{-3} N; *S. bimaculatus*: 1.1×10^{-3} N). These measurements agree well with our theoretically determined adhesive force attributable to Stefan adhesion, which amounts to 0.98×10^{-3} N in *S. juno* and 2.21×10^{-3} N in *S. bimaculatus*. The theoretically calculated adhesive forces attributable to the surface tension of the secretion (see above) amounted to 7.49×10^{-5} N in *S. juno* and 9.17×10^{-5} N in *S. bimaculatus*. Therefore, adhesion is unlikely to be exclusively attributable to the surface tension. Moreover, the large amount of secretion involved (cf. Kölsch, 2000) argues against this mechanism playing a major role. These estimations make it plausible that Stefan adhesion is the major mechanism involved in the investigated adhesive system.

According to formula (1), Stefan adhesion is influenced by various parameters; thus there are different ways of optimizing the efficiency of the prey-capture apparatus (Betz, 1996; Kölsch, 2000). In order to improve the adhesive performance, the effective contact area should be high, whereas the thickness of the secretion layer (distance to the prey) should be low. The final thickness at the moment of contact with the prey presumably depends on the impact force during the predatory strike of the beetle. Thus, the significantly higher compressive forces generated by *S. juno* as compared to *S. bimaculatus* should reduce the thickness of the secretion layer in the contact area. This might be responsible for the observed enhanced adhesion in this species. Additionally, a highly viscous secretion is advantageous for adhesion. Kölsch (2000) estimated the viscosity of the secretion to lie between the viscosities of water ($0.001\ \mathrm{N\,s\,m^{-2}}$) and plant oils ($0.01\ \mathrm{N\,s\,m^{-2}}$). Indeed, our calculations reveal viscosities of $0.005\ \mathrm{N\,s\,m^{-2}}$ for *S. bimaculatus* and $0.01\ \mathrm{N\,s\,m^{-2}}$ for *S. juno* (calculated according to formula (1)), although the multiphasic chemical composition might further complicate these conditions by changing viscosity depending on the shear rate of the fluid (e.g., Dirks et al., 2009). Finally, the adhesive force resulting from Stefan adhesion can be increased by rapid retraction of the labium after prey capture (Kölsch, 2000; Betz and Kölsch, 2004) in order to bring the prey into the range of the mandibles.

4.4. Safety factor

Prey animals have developed diverse strategies to evade the hunting strategies of their predators (see review by Betz and Kölsch, 2004). For instance, springtails possess a powerful mechanism to escape from the adhesive surface of the predator (e.g., Christian, 1979). According to Kölsch (2000), the tractive force required (F_{requ}) for pulling the prey towards the predator is 0.0203 μN for small (body mass 8.4 μg) and 0.159 μN for large (body mass 62.3 μg) collembolans. According to our force measurements, *S. juno* and *S. bimaculatus* beetles generate adhesive forces (F_{a}) of ca. 1.0×10^{3} μN, corresponding to 6289 times (large springtails) and 49261 times (small springtails) the required forces. These safety factors ($SF = F_{\mathrm{a}}/F_{\mathrm{requ}}$) seem to be so large that the prey-capture success particularly towards large springtails should theoretically be much higher than that observed. However, these springtails are able to escape from the adhesive surface of the predator by releasing their powerful escape jump. In this way, they achieve maximum accelerations of $1000\ \mathrm{m\,s^{-2}}$ (Christian, 1979). Consequently, small and large collembolans produce forces (F_{Coll}) of 8.4×10^{-6} N and 6.23×10^{-5} N, respectively (as calculated by using the formula force = mass × acceleration). According to these calculations, the investigated *Stenus* species achieve safety factors ($SF = F_{\mathrm{a}}/F_{\mathrm{Coll}}$) of about 16 (large springtails) to 120 (small springtails). Therefore, the adhesive forces generated by *Stenus* beetles are theoretically sufficient to withstand a possible escape jump of a collembolan. However, a further reduction of the real safety factors is likely, because the prey items possess a variety of surface structures (setae, scales, waxy layers) that might easily get detached from their body surfaces when the beetle tries to retract the prey-capture device (Bauer and Pfeiffer, 1991; Betz and Kölsch, 2004). Additionally, these structures might contaminate the sticky pads, thus reducing the contact area between the labial prey-capture apparatus and the springtail surface in future prey-capture events.

4.5. Presence and function of resilin

According to Betz (1996) the adhesive outgrowths of *Stenus* beetles are strongly elastic. SEM photographs taken after the strike reveal no bending of the setae, although the sticky cushions are significantly compressed. This functional feature is due to the sticky pads being composed of a flexible, highly elastic cuticle containing resilin, an elastic protein (cf. Fig. 8). Resilin enables reversible deformation with extremely high resilience and provides low stiffness, high strain and efficient elastic energy storage (low elastic modulus) (Weis-Fogh, 1960; Andersen and Weis-Fogh, 1964; Gosline et al., 2002).

In the labial adhesive system of *Stenus* species, similar to insect tarsal adhesive systems (Niederegger and Gorb, 2003; Perez Goodwyn et al., 2006), resilin presumably makes the sticky pads flexible, resilient and, therefore, adaptable to the shape and surface irregularities of the prey. Since the labium is used for prey capture several hundred times during the beetle's life, resilin also makes the pads resistant to material fatigue, similar to the function of resilin in insect wing folds (Haas et al., 2000a,b). These possible material attributes are supported by our high-speed video recordings, which show that sticky pads and their outgrowths are able to deform extensively in both directions (i.e., compression and tension) and to regain their initial shape (Fig. 6, frames 7–13). In addition, the material of the sticky pads consists of a reticulum of endocuticular fibres, which further contribute to their flexibility and mechanical stability (Betz, 1996; Kölsch and Betz, 1998; Betz and Kölsch, 2004). Compression of the reticulum provides further adjustment to the outer shape of the prey (Kölsch and Betz, 1998).

4.6. Adhesive secretion

Possible functions of the adhesive secretion are summarised in Fig. 9 (see Betz, 2010 for a general review of the chemical and functional properties of insect adhesive secretion). The secretion released into the contact zone between the sticky pad and the potential prey (as is the case in the tarsi of many insects) is essential for the functioning of this adhesive system. However, the amount of secretion in *Stenus* beetles is considerably higher than in insect tarsi (Figs. 2C and 6; Kölsch, 2000). The main function of the adhesive secretion in the investigated prey-capture apparatus seems to be to increase the actual contact with rough prey surfaces. The compensation for surface roughness is generally considered to be of major importance in wet adhesive systems (Kendall, 2001; Drechsler and Federle, 2006; Persson, 2007; Gorb, 2008). In *Stenus* beetles, the secretion also has to compensate for diverse surface structures that have the potential to reduce prey-capture success (Bauer and Pfeiffer, 1991; Betz and Kölsch, 2004).

Furthermore, we can assume that the viscosity of the secretion rapidly changes during the prey-capture process. It is highly liquid when it is transported from special glands (described in Kölsch, 2000) within the head capsule to the sticky pads. Direct observations of the secretion suggest that it becomes more viscous upon contact with the (prey) surface (Fig. 7 B). The factors responsible for this increase in viscosity are unclear. One assumption is that the adhesive components are dissolved in a low-viscosity liquid that facilitates the transport of the secretion towards the sticky pads. Upon contact with the air, the solvent will evaporate, resulting in the observed increase in viscosity. Since the predatory system of *Stenus* beetles works at high speed, however, such a process is unlikely (Kölsch, 2000).

Another explanation might be that the biphasic adhesive secretion of *Stenus* beetles behaves in a non-Newtonian manner, showing shear-thickening depending on the shear rate of the fluid during the retraction of the labium (see above). A possible advantage of such emulsion-like colloids consisting of both hydrophilic and hydrophobic compounds would be their effective spreading over surfaces of various surface energies (Kölsch, 2000; Gorb, 2001; Vötsch et al., 2002).

The high viscosity of the secretion has been confirmed by our high-speed video recordings of the sticky pads during retraction from a surface (see supplementary video mmc2 in Appendix A). Similar to the behaviour of pressure-sensitive adhesives (e.g., Creton, 2003), the secretion stretches and splits into long fibres before it finally tears off at the contact zone with the substratum (Fig. 6, frames 9–14). This is indicative of the high viscosity of the adhesive imparting a high cohesive strength. Other possible advantages discussed in the context of adhesive fibrillation are the prevention of crack propagation (Ghatak et al., 2004; Chung and Chaudhury, 2005) and the fact that larger amounts of energy are required for the separation of multiple filaments due to higher energy dissipation (Creton, 2003).

5. Conclusions

The investigated adhesive system combines typical functional features of both wet and dry adhesive systems (Fig. 9). The existence of hierarchically structured sticky pads and the high density and small dimensions of the ramifications are comparable with the dry adhesive systems of geckos, anoles, and spiders. However, in the system of *Stenus* species, an adhesive secretion is present, which makes this system similar to the wet adhesive systems of insects, although in contrast to these systems, the adhesive outgrowths of *Stenus* mouthparts are deeply immersed within the secretion and only the tips of their terminal ramifications protrude.

Our *in vivo* force measurements revealed much lower values for the compressive force than for the resulting adhesive force. Although both investigated species differ significantly in their pad morphology (e.g., the pad area and the density of adhesive outgrowths and ramifications), they develop almost identical adhesive forces during predation. A possible explanation for this fact is the generation of higher compressive forces in *S. juno*, the species with a smaller pad area.

Force measurements and high-speed video recordings support the view that viscous forces (Stefan adhesion) are the major adhesive principle involved in the investigated adhesive system. Our measurements agree well with the theoretically estimated adhesive force attributable to Stefan adhesion.

The sticky pads have been modified in various ways during the course of *Stenus* evolution (Betz, 1996, 1998; Puthz, 1998, 2005). Thus, we can conclude that the pad morphology influences adhesion and directly affects prey-capture success. To test the role of the various pad morphologies and impact forces on adhesive performance, a broader range of *Stenus* species should be tested.

Acknowledgments

We would like to thank Karl-Heinz Hellmer for taking the SEM micrographs. We are grateful to Dr. Michael Heethoff, Dr. Dagmar Voigt, Christoph Allgaier, Christian Schmitt and Andreas Dieterich for their editorial help and assistance with photo-processing. Our thanks are also extended to Cornelia Miksch for technical help with the experimental set-up. This study was partly financed by a research grant from the Bundesministerium für Bildung und Forschung (Bionics Competition, BNK2-052) to O.B. and S.N.G. and from the German Science Foundation (DFG project GO 995/10-1) to S.N.G. Dr. Theresa Jones corrected the English.

Appendix A. Supplementary data

Supplementary data associated with this article can be found, in the online version, at doi:10.1016/j.zool.2011.09.006.

References

Alexander, R.M., 1992. Exploring Biomechanics: Animals in Motion. Scientific American Library, New York.
Andersen, S.O., Weis-Fogh, T., 1964. Resilin. A rubberlike protein in arthropod cuticle. Adv. Insect Physiol. 2, 1–65.
Attygalle, A.B., Aneshansley, D.J., Meinwald, J., Eisner, T., 2000. Defense by foot adhesion in a chrysomelid beetle (*Hemisphaerota cyanea*): characterization of the adhesive oil. Zoology 103, 1–6.
Autumn, K., Sitti, M., Liang, Y.A., Peattie, A.M., Hansen, W.R., Sponberg, S., Kenny, T.W., Fearing, R., Israelachvili, J.N., Full, R.J., 2002. Evidence for van der Waals adhesion in gecko setae. Proc. Natl. Acad. Sci. U.S.A. 99, 12252–12256.
Bauer, T., Pfeiffer, M., 1991. 'Shooting' springtails with a sticky rod: the flexible hunting behaviour of *Stenus comma* (Coleoptera, Staphylinidae) and the counter-strategies of its prey. Anim. Behav. 41, 819–828.
Betz, O., 1996. Function and evolution of the adhesion-capture apparatus of *Stenus* species (Coleoptera, Staphylinidae). Zoomorphology 116, 15–34.
Betz, O., 1998. Comparative studies on the predatory behaviour of *Stenus* spp. (Coleoptera: Staphylinidae): the significance of its specialized labial apparatus. J. Zool. Lond. 244, 527–544.
Betz, O., 1999. A behavioural inventory of adult *Stenus* species (Coleoptera: Staphylinidae). J. Nat. Hist. 33, 1691–1712.
Betz, O., 2006. Der Anpassungswert morphologischer Strukturen: Integration von Form, Funktion und Ökologie am Beispiel der Kurzflügelkäfer-Gattung *Stenus* (Coleoptera, Staphylinidae). Entomol. heute 18, 3–26.
Betz, O., 2010. Adhesive exocrine glands in insects: morphology, ultrastructure, and adhesive secretion. In: Byern, J., Grunwald, I. (Eds.), Biological Adhesive Systems. From Nature to Technical and Medical Application. Springer, Berlin, pp. 111–152.
Betz, O., Kölsch, G., 2004. The role of adhesion in prey capture and predator defence in arthropods. Arthr. Str. Dev. 33, 3–30.
Betz, O., Koerner, L., Gorb, S.N., 2009. An insect's tongue as the model for two-phase viscous adhesives? Adhesion 3, 32–35.
Bhushan, B., 2003. Adhesion and stiction: mechanisms, measurement techniques, and methods for reduction. J. Vac. Sci. Technol. B 21, 2262–2296.
Bowden, F.P., Tabor, D., 1950. The Friction and Lubrication of Solids. Oxford University Press, Oxford (reprint 1986).
Chan, E.P., Greiner, C., Arzt, E., Crosby, A.J., 2007. Designing model systems for enhanced adhesion. MRS Bull. 32, 496–503.
Christian, E., 1979. Der Sprung der Collembolen. Zool. Jb. Physiol. 83, 457–490.
Chung, J.Y., Chaudhury, M.K., 2005. Roles of discontinuities in bio-inspired adhesive pads. J. R. Soc. Interface 2, 55–61.
Creton, C., 2003. Pressure-sensitive adhesives: an introductory course. MRS Bull. 28, 434–439.
Dirks, J.-H., Clemente, C.J., Federle, W., 2009. Insect tricks: two-phasic foot pad secretion prevents slipping. J. R. Soc. Interface 7, 587–593.
Drechsler, P., Federle, W., 2006. Biomechanics of smooth adhesive pads in insects: influence of tarsal secretion on attachment performance. J. Comp. Physiol. A 192, 1213–1222.
Federle, W., 2006. Why are so many adhesive pads hairy? J. Exp. Biol. 209, 2611–2621.
Federle, W., Riehle, M., Curtis, A.S.G., Full, R.J., 2002. An integrative study of insect adhesion: mechanics and wet adhesion of pretarsal pads in ants. Integr. Comp. Biol. 42, 1100–1106.
Ghatak, A., Mahadevan, L., Chung, J.Y., Chaudhury, M.K., Shenoy, V., 2004. Peeling from a biomimetically patterned thin elastic film. Proc. R. Soc. Lond. A 460, 2725–2735.

Gorb, S.N., 1999. Serial elastic elements in the damselfly wing: mobile vein joints contain resilin. Naturwissenschaften 86, 552–555.
Gorb, S.N., 2001. Attachment Devices of Insect Cuticle. Kluwer Academic Publishers, Dordrecht.
Gorb, S.N., 2004. The jumping mechanism of cicada *Cercopis vulnerata* (Auchenorrhyncha, Cercopidae): skeleton–muscle organisation, frictional surfaces, and inverse-kinematic model of leg movements. Arthr. Str. Dev. 33, 201–220.
Gorb, S.N., 2008. Smooth attachment devices in insects. In: Casas, J., Simpson, S.J. (Eds.), Advances in Insect Physiology, vol. 34: Insect Mechanics and Control. Elsevier, London.
Gosline, J.M., Lillie, M., Carrington, E., Guerette, P., Ortlepp, C., Savage, K., 2002. Elastic proteins: biological roles and mechanical properties. Phil. Trans. R. Soc. B 357, 121–132.
Haas, F., Gorb, S.N., Wootton, R.J., 2000a. Elastic joints in dermapteran hind wings: materials and wing folding. Arthr. Str. Dev. 29, 137–146.
Haas, F., Gorb, S.N., Blickhan, R., 2000b. The function of resilin in beetle wings. Proc. R. Soc. Lond. B 267, 1375–1381.
Huber, G., Mantz, H., Spolenak, R., Mecke, K., Jacobs, K., Gorb, S.N., Arzt, E., 2005. Evidence for capillarity contributions to gecko adhesion from single spatula nanomechanical measurements. Proc. Natl. Acad. Sci. U.S.A. 102, 16293–16296.
Israelachvili, J.N., 1991. Intermolecular and Surface Forces. Academic Press, London.
Jagota, A., Benninson, S.J., 2002. Mechanics of adhesion through a fibrillar microstructure. Integr. Comp. Biol. 42, 1140–1145.
Jiao, Y., Gorb, S.N., Scherge, M., 2000. Adhesion measured on the attachment pads of *Tettigonia viridissima* (Orthoptera, Insecta). J. Exp. Biol. 203, 1887–1895.
Kendall, K., 2001. Molecular Adhesion and Its Applications. Kluwer Academic Publishers, New York.
Koerner, L., Gorb, S.N., Betz, O., 2012. Adhesive performance of the stick-capture apparatus of rove beetles of the genus *Stenus* (Coleoptera, Staphylinidae) toward various surfaces. J. Insect Physiol. 58, 155–163.
Kölsch, G., 2000. The ultrastructure of glands and the production and function of the secretion in the adhesive capture apparatus of *Stenus* species (Coleoptera: Staphylinidae). Can. J. Zool. 78, 465–475.
Kölsch, G., Betz, O., 1998. Ultrastructure and function of the adhesion-capture apparatus of *Stenus* species (Coleoptera: Staphylinidae). Zoomorphology 118, 263–272.
Langer, M.G., Ruppersberg, J.P., Gorb, S.N., 2004. Adhesion forces measured at the level of a terminal plate of the fly's seta. Proc. R. Soc. Lond. B 271, 2209–2215.
Mate, C.M., 2008. Tribology on the Small Scale: A Bottom up Approach to Friction, Lubrication, and Wear. Oxford University Press, Oxford.
McFarlane, J.S., Tabor, D., 1950. Adhesion of solids and the effect of surface films. Proc. R. Soc. Lond. A 202, 224–243.
Niederegger, S., Gorb, S.N., 2003. Tarsal movements in flies during leg attachment and detachment on a smooth substrate. J. Insect Physiol. 49, 611–620.
Owens, D.K., Wendt, R.C., 1969. Estimation of the surface free energy of polymers. J. Appl. Polym. Sci. 13, 1741–1747.
Peressadko, A., Gorb, S.N., 2004. Surface profile and friction force generated by insects. In: Boblan, I., Bannasch, R. (Eds.), Fortschritt-Berichte VDI, vol. 249. VDI Verlag, Düsseldorf, pp. 257–263.
Perez Goodwyn, P., Peressadko, A., Schwarz, H., Kastner, V., Gorb, S.N., 2006. Material structure, stiffness, and adhesion: why attachment pads of the grasshopper (*Tettigonia viridissima*) adhere more strongly than those of the locust (*Locusta migratoria*) (Insecta: Orthoptera). J. Comp. Physiol. A 192, 1233–1243.
Persson, B.N.J., 2007. Biological adhesion for locomotion on rough surfaces: basic principles and a theorist's view. MRS Bull. 32, 486–490.
Puthz, V., 1998. Die Gattung *Stenus* Latreille in Vietnam (Coleoptera, Staphylinidae). Rev. Suisse Zool. 105, 383–394.
Puthz, V., 2005. Neue und alte neotropische *Stenus* (*Hemistenus*-) Arten (Coleoptera: Staphylinidae). Mitteilungen Int. Entomol. Vereins Suppl. XI, 1–60.
Puthz, V., 2010. *Stenus* Latreille, 1797 aus dem Baltischen Bernstein nebst Bemerkungen über andere fossile *Stenus*-Arten (Coleoptera, Staphylinidae). Ent. Bl. 106, 265–287.
Rohlf, F.J., 2004. tpsDig, Version 2.0. Department of Ecology and Evolution, State University of New York at Stony Brook.
Scherge, M., Gorb, S.N., 2001. Biological Micro- and Nanotribology. Springer, Berlin.
Schmitz, G., 1943. Le labium et les structures bucco-pharyngiennes du genre *Stenus* Latreille. Cellule 49, 291–334.
Spolenak, R., Gorb, S.N., Arzt, E., 2005a. Adhesion design maps for bioinspired attachment systems. Acta Biomater. 1, 5–13.
Spolenak, R., Gorb, S.N., Gao, H., Arzt, E., 2005b. Effect of contact shape on the scaling of biological attachments. Proc. R. Soc. Lond. A 461, 305–319.
Stork, N.E., 1980. Experimental analysis of adhesion of *Chrysolina polita* (Chrysomelidae: Coleoptera) on a variety of surfaces. J. Exp. Biol. 88, 91–107.
Varenberg, M., Peressadko, A., Gorb, S.N., Arzt, E., 2006. Effect of real contact geometry on adhesion. Appl. Phys. Lett. 89, 121905.
Varenberg, M., Pugno, N., Gorb, S.N., 2010. Spatulate structures in biological fibrillar adhesion. Soft Matter 6, 3269–3272.
Voigt, D., Schuppert, J.M., Dattinger, S., Gorb, S.N., 2008. Sexual dimorphism in the attachment ability of the Colorado potato beetle *Leptinotarsa decemlineata* (Coleoptera: Chrysomelidae) to rough substrates. J. Insect Physiol. 54, 765–776.
Vötsch, W., Nicholson, G., Müller, R., Stierhof, Y.-D., Gorb, S.N., Schwarz, U., 2002. Chemical composition of the attachment pad secretion of the locust *Locusta migratoria*. Insect Biochem. Mol. Biol. 32, 1605–1613.
Walker, G., 1993. Adhesion to smooth surfaces by insects – a review. Int. J. Adhes. 13, 3–7.
Weinreich, E., 1968. Über den Klebfangapparat der Imagines von *Stenus* Latr. (Coleopt., Staphylinidae) mit einem Beitrag zur Kenntnis der Jugendstadien dieser Gattung. Z. Morph. Ökol. Tiere 62, 162–210.
Weis-Fogh, T., 1960. A rubber-like protein in insect cuticle. J. Exp. Biol. 37, 887–907.

Publikation II

Adhesive performance of the stick-capture apparatus of rove beetles of the genus *Stenus* (Coleoptera, Staphylinidae) toward various surfaces

Lars Koerner, Stanislav N Gorb, Oliver Betz

Journal of Insect Physiology 58 (2012): 155–163

Journal of Insect Physiology 58 (2012) 155–163

Contents lists available at SciVerse ScienceDirect

Journal of Insect Physiology

journal homepage: www.elsevier.com/locate/jinsphys

Adhesive performance of the stick-capture apparatus of rove beetles of the genus *Stenus* (Coleoptera, Staphylinidae) toward various surfaces

Lars Koerner [a,*], Stanislav N. Gorb [b], Oliver Betz [a]

[a] Department of Evolutionary Biology of Invertebrates, Institute for Evolution and Ecology, University Tübingen, Auf der Morgenstelle 28E, 72076 Tübingen, Germany
[b] Department of Functional Morphology and Biomechanics, Zoological Institute, Christian-Albrechts-Universität zu Kiel, Am Botanischen Garten 2-9, 24098 Kiel, Germany

ARTICLE INFO

Article history:
Received 30 September 2011
Received in revised form 31 October 2011
Accepted 2 November 2011
Available online 18 November 2011

Keywords:
Adhesion
Attachment
Predation
Prey-capture
Surface roughness
Free surface energy
Force measurement
Ecomorphology

ABSTRACT

Rove beetles of the genus *Stenus* possess a unique adhesive prey-capture apparatus that enables them to catch elusive prey such as springtails over a distance of several millimeters. The prey-capture device combines the hierarchically organized morphology of dry adhesive systems with the properties of wet ones, since an adhesive secretion is released into the contact zone. We hypothesize that this combination enables *Stenus* species successfully to capture prey possessing a wide range of surface structures and chemistries. We have investigated the influence of both surface energy and roughness of the substrate on the adhesive performance of the prey-capture apparatus in two *Stenus* species. Force transducers have been used to measure both the compressive and adhesive forces generated during the predatory strike of the beetles on (1) epoxy resin surfaces with defined roughness values (smooth *versus* rough with asperity diameters ranging from 0.3 to 12 μm) and (2) hydrophobic *versus* hydrophilic glass surfaces. Our experiments show that neither the surface roughness nor the surface energy significantly influences the attachment ability of the prey-capture apparatus. Thus, in contrast to the performance of locomotory adhesive systems in geckos, beetles, and flies, no critical surface roughness exists that might impede adhesion of the prey-capture apparatus of *Stenus* beetles. The prey-capture apparatus of *Stenus* beetles is therefore well adapted to adhere to the various unpredictable surfaces with diverse roughness and surface energy occurring in a wide range of potential prey.

1. Introduction

A unique example of an adhesive prey-capture device is formed by the elongated labium of rove beetles of the genus *Stenus* Latreille, 1796 (Coleoptera, Staphylinidae). This prey-capture apparatus can be protruded within a few milliseconds toward a potential prey. Once the prey adheres to the sticky pads (i.e., the modified paraglossae) at the distal end of the prementum (Fig. 1A and C), the labium is instantly withdrawn, and the beetle can seize its prey with the mandibles. The surface of these sticky pads is subdivided into numerous, terminally branched outgrowths (Fig. 1B and D). During prey-capture these outgrowths are completely covered by an adhesive secretion that is produced in special glands within the head capsule (Schmitz, 1943; Weinreich, 1968; Kölsch, 2000; Koerner et al., in press). Thus, the adhesive pads of the prey-capture apparatus of *Stenus* beetles form a hairy, hierarchically structured, wet adhesive system. Both the morphology and function of this remarkable prey-capture apparatus have been described in previous publications (Schmitz, 1943; Weinreich, 1968; Betz, 1996, 1998; Kölsch and Betz, 1998; Kölsch, 2000; Koerner et al., in press).

Stenus beetles are polyphagous predators that feed on a variety of prey from diverse invertebrate taxa (e.g., oligochaetes, small spiders, mites, aphids, springtails, larvae of Cicadinae, flies, and hymenopterans) (Betz, 1998). Therefore, their prey-capture apparatus encounters a wide range of natural substrates with a variety of physico-chemical properties and surface topographies differing in dimensions by several orders of magnitude.

The attachment ability of adhesive organs of insects is strongly influenced by both the roughness and the free surface energy of the surfaces to which the insects attach (Gorb, 2001; Betz, 2002; Peressadko and Gorb, 2004; Voigt et al., 2008b; Bullock and Federle, 2010; Gorb and Gorb, 2009; Lüken et al., 2009). Surface roughness can result in the reduction of the adhesion by diminishing the available contact area for the attachment between the two surfaces (Fuller and Tabor, 1975). Force measurements on the "hairy" tarsi of beetles (Gorb, 2001; Peressadko and Gorb, 2004; Voigt et al., 2008b; Bullock and Federle, 2010) and flies (Peressadko and Gorb, 2004) on defined epoxy resin surfaces have demonstrated the influence of surface roughness on the attachment forces. Accordingly, a minimum of generated forces has been found on substrates with asperity sizes ranging from 0.05 to 1.0 μm. This effect has been explained as a result of the reduction of the available contact area between the surface irregularities and the

* Corresponding author.
E-mail address: larskoerner3@hotmail.com (L. Koerner).

0022-1910/$ - see front matter © 2011 Elsevier Ltd. All rights reserved.
doi:10.1016/j.jinsphys.2011.11.001

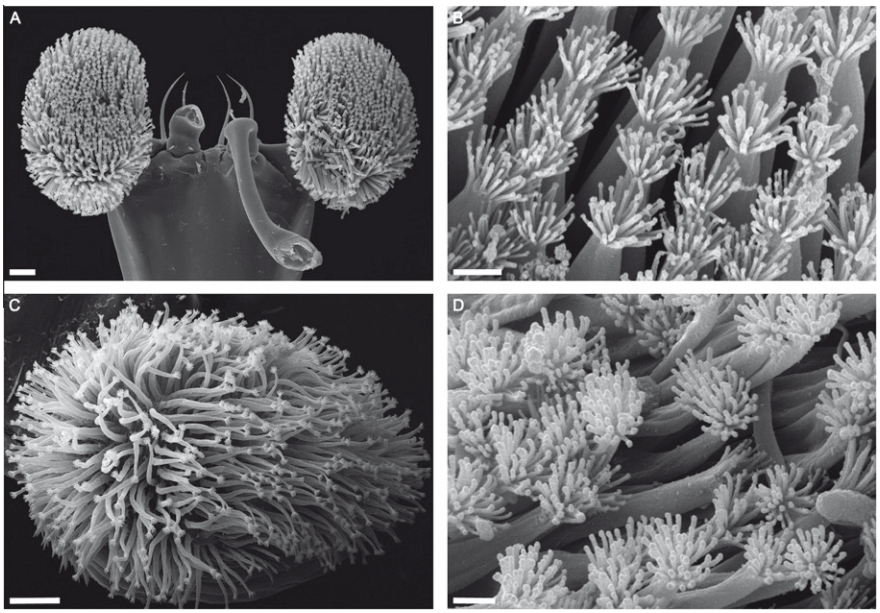

Fig. 1. SEM images of the ventral adhesive surface of the paraglossae, which are modified into adhesive pads, of *S. juno* (A and B) and *S. bimaculatus* (C and D). (A) Ventral view of the apex of the prementum with adhesive pads. Scale bar = 20 μm. (B and D) Adhesive outgrowths with terminal ramifications. Scale bar = 2 μm. (C) Ventral view of single adhesive pad. Scale bar = 20 μm.

terminal elements of the adhesive setae (Peressadko and Gorb, 2004). Above and below this critical surface roughness, attachment forces increase, presumably because the adhesive setae are able to build up an intimate contact with the surface. Additionally, on coarse rough surfaces, claws can additionally interlock with the surface asperities and generate high attachment forces (Dai et al., 2002; Betz, 2002; Heethoff and Koerner, 2007; Voigt et al., 2008b; Al Bitar et al., 2010; Bullock and Federle, 2010).

Furthermore, attachment is strongly influenced by the physicochemical properties of the substrate (e.g., Gorb and Gorb, 2009; Lüken et al., 2009). According to Holdgate (1955), the contact angles of water on insect surfaces show a wide range of variation, which is caused by surface roughness. Because of the presence of waxes on the epicuticle, the body surface of many potential prey items of *Stenus* beetles is generally hydrophobic, with contact angles of water between 90 and 100° (Holdgate, 1955; Wagner et al., 1996; Voigt et al., 2008a). The additional presence of surface structures on the body surface, such as papillae, pits, spines, and setae (Fig. 2), result in even higher contact angles, therefore making the cuticle strongly hydrophobic or even super-hydrophobic (Holdgate, 1955; Noble-Nesbitt, 1963; Wagner et al., 1996). Such surface structures might further reduce the adhesion force because of a combined effect of surface energy and geometry, thus reducing the prey-capture success (Bauer and Pfeiffer, 1991; Opell, 1994; Opell and Schwend, 2007). Accordingly, the prey-capture apparatus of *Stenus* beetles must be adapted to the surfaces of a variety of prey differing in both their surface energy and topography. In *Stenus* beetles, the adhesive secretion seems to consist of at least two immiscible phases: a proteinaceous and a lipid phase (Kölsch, 2000; reviewed in Betz, 2010). Such a biphasic composition has been assumed to be advantageous for the effective wetting of substrates with different surface energies (Kölsch, 2000; Gorb, 2001; Vötsch et al., 2002; Betz et al., 2009; Al Bitar et al., 2009; Koerner et al., in press).

Recently, we have presented the first *in vivo* force measurements of the adhesion prey-capture apparatus in two *Stenus* species toward a dummy prey (Koerner et al., in press). These measurements have revealed significantly higher compressive forces for *Stenus juno* (0.2 mN) than for *Stenus bimaculatus* (0.1 mN). When the labium is retracted from the dummy prey, pull-off (adhesive) forces develop perpendicularly with respect to the prey surface (Betz, 2006). The maximum measured adhesive forces amount to 1.1 mN (*S. bimaculatus*) and 1.0 mN (*S. juno*). The dummy prey used in these experiments is an insect pin with a relatively smooth surface having a water contact angle of 84°.

Since the body surface of the potential prey items of *Stenus* possess a variety of properties in terms of both roughness and

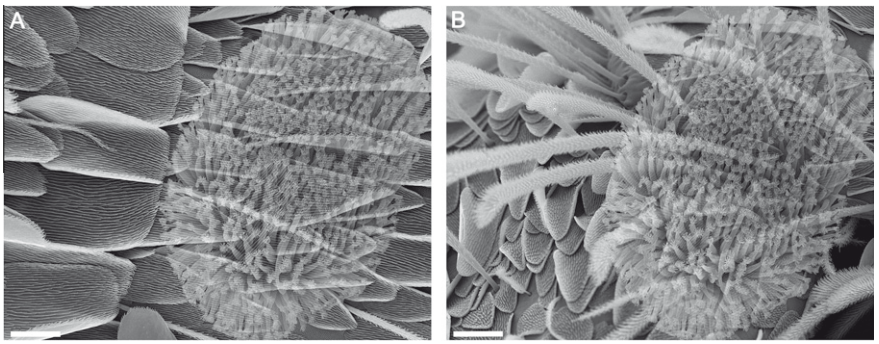

Fig. 2. SEM micrographs of the body surface of an individual of *Heteromurus nitidus* Templeton (Collembola, Entomobryidae) showing (A) the thoracic region and (B) the head region. The superimposed silhouette of the adhesive pad of *S. juno* illustrates the pad size relative to the surface texture of the springtail. Scale bars, 20 μm.

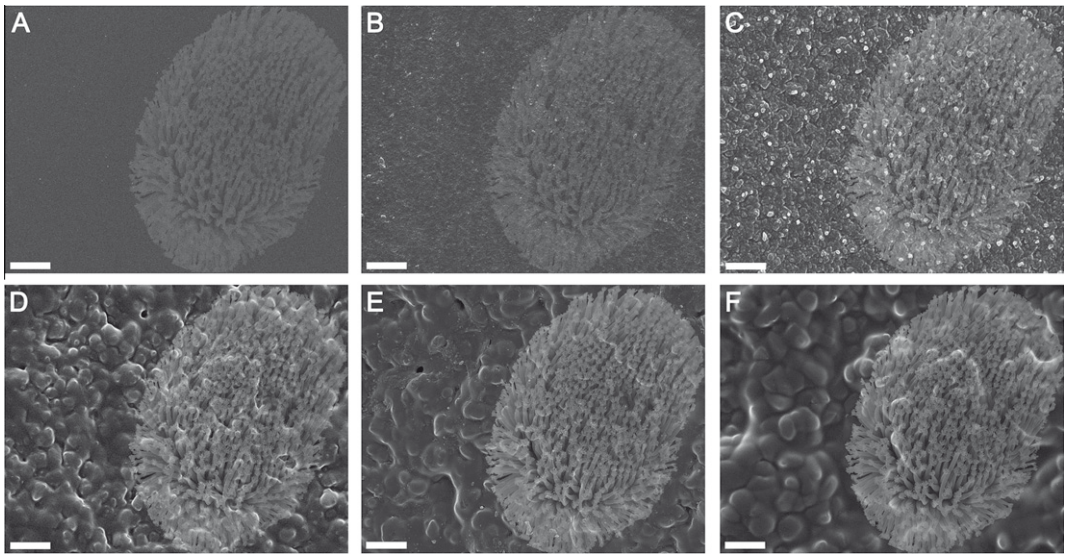

Fig. 3. SEM micrographs of the substrata used in the experiments: (A) smooth surface, (B) 0.3 μm asperity diameter, (C) 1.0 μm asperity diameter, (D) 3.0 μm asperity diameter, (E) 9.0 μm asperity diameter, (F) 12.0 μm asperity diameter. The superimposed silhouette of the adhesive pad of *S. juno* (Fig. 1A) illustrates the pad size relative to surface texture. Scale bars, 20 μm.

chemistry, we have addressed the questions as to whether and in what manner the roughness and surface energy influence the attachment forces generated during the predatory strike of these beetles. We assume that the three main functional elements of the adhesive pads (the adhesive secretion, the setose, terminally branched outgrowths, and the network of endocuticular fibers within the pads) act synergistically, thus, providing sufficient contact with prey surfaces. Furthermore, we consider the biphasic composition of the adhesive secretion (Kölsch, 2000; Koerner et al., in press) as an adaptation to catching a wide range of prey items differing in the wettability of their body surface. Accordingly, we hypothesize that the adhesive performance of the prey-capture apparatus of *Stenus* beetles is successful on a variety of surfaces. We have experimentally tested this hypothesis by analyzing the adhesive forces generated during the predatory strike of two *Stenus* species on (1) epoxy resin surfaces of various roughness (Fig. 3), and (2) glass surfaces differing in their wettability.

2. Materials and methods

2.1. Beetles

Force measurements were conducted with *S. juno* Paykull 1800 and *S. bimaculatus* Gyllenhal 1810 that have already been tested in our previous publication (Koerner et al., in press). Adult beetles were collected from a reed zone of a small pond near Tübingen, southern Germany (48° 31′ 30.74″ N 9° 00′ 46.53 ″E). They were kept in the laboratory in plastic boxes lined with moist plaster of Paris mixed with activated charcoal to receive a constant humidity and to prevent the growth of microorganisms. Beetles were fed with living collembolans (*Folsomia* sp.) *ad libitum*.

2.2. Force measurements on living beetles

Prior to the experiments, the beetles had been starved for 5–7 days. Force measurements were conducted in an arena that was lined with plaster to receive a constant high humidity at an air temperature of 19.76 ± 0.78 °C. The adhesive forces were measured on both a hydrophilic and a silanized hydrophobic glass coverslip and on epoxy resin substrates (Fig. 3). The latter were Spurr resin replicas of both a smooth glass surface and polishing papers of different roughness (Buehlers FibrMet Discs, Buehler, Lake Bluff, Ill., USA) with nominal sizes (diameters) of substrate asperities of 0.3, 1, 3, 9, and 12 μm (for the replica preparation method, see Scherge and Gorb, 2001; Gorb, 2007). These different levels of surface roughness correspond to those of natural substrates (e.g., Scherge and Gorb, 2001; Scholz et al., 2010). The RMS values (the root mean square average of the roughness profile ordinates) of the substrates were analyzed with a scanning white light interferometer (Zygo NewView 5000; Zygo Corporation, Middlefield, Conn., USA): RMS_0 (smooth) = 36.2 ± 4.1 nm; $RMS_{0.3}$ = 90.0 ± 2.7 nm; RMS_1 = 238.4 ± 6.0 nm; RMS_3 = 1156.7 ± 133.1 nm; RMS_9 = 2453.7 ± 87.2 nm; RMS_{12} = 3060.3 ± 207.7 nm (for additional surface roughness parameter, see Peressadko and Gorb, 2004). The substrates were identical with those used in previous studies by Peressadko and Gorb (2004), Huber et al. (2007), Voigt et al. (2008b), and Al Bitar et al. (2010).

The free surface energy of glass and their dispersive and polar components were measured by using a video-based optical contact angle-measuring device and software SCA 20 (OCAH 200, Dataphysics Instruments, Filderstadt, Germany). The free surface energies were calculated according to the Owens–Wendt-Kaelble method (Owens and Wendt, 1969) based on the contact angles of a series of liquids (*Aqua Millipore* water, diiodomethane, ethylene glycol) obtained by the sessile drop method and ellipse-fitting (droplet volume 1 μl). On hydrophilic glass, the contact angle of *Aqua Millipore* water was 68.3 ± 1.2° (mean ± SD, n = 3) and the surface energy 59 mN m^{-1} (dispersive component 18.0 mN m^{-1}, polar component 41.0 mN m^{-1}). On hydrophobic glass, the contact angle of *Aqua Millipore* water was 121.6 ± 1.1° (n = 3) and the surface energy was 12 mN m^{-1} (dispersive component 9.0 mN m^{-1}, polar component 3.0 mN m^{-1}).

To determine the forces generated during the predatory strike of the beetles, small pieces (diameter ca. 2 mm) of these planar substrates were firmly glued to the head of an insect pin, and the experimental setup as described in Koerner et al. (in press) was used. Accordingly, the insect pin was connected to a force sensor (FORT25, WPI, USA). The force sensor with the attached insect pin was mounted on a micromanipulator that was permanently moved up- and downwards to attract the attention of the beetles. The sensor was combined with an amplifier (BIOPAC Systems,

USA), a computer-based data-acquisition and processing system (MP100 WSW, BIOPAC Systems, USA), and the software AcqKnowledge 3.8.2 (BIOPAC Systems, USA). While the beetle was "shooting" at the test substrate, the force sensor was deflected, and force–time curves were recorded. After each individual test, the substrates were consecutively cleaned with ethanol (70%) and distilled water. Most beetles "shot" once or twice on the dummy prey and did not react afterwards anymore. Thus, beetles were taken out of the arena and the measurements were repeated 10 min later. This procedure was repeated until the beetle attacked the dummy prey at least 15 times.

We tried to test the same individuals on all surfaces. This was not always possible, because (1) some individuals died between the experiments and (2) a lot of individuals showed a learning effect and did not react on the dummy prey anymore. Therefore, the experiments were conducted with various numbers of individuals (between 21 and 34 individuals) per species (Table 1), and 15–25 attacks (shots) per beetle were recorded for each substrate. Only the maximum adhesive forces of each individual were used for further statistical analyses. Since neither the adhesive force nor the compressive force is correlated with body mass, a possible size effect can be ruled out (see Section 3.4).

2.3. Microscopy techniques

For imaging by scanning electron microscopy (SEM), beetle heads with extended labia were cleaned with H_2O_2, dehydrated in an ascending ethanol series, critical-point dried (Polaron E3000, Polaron Equipment, UK), fixed to stubs with silver paint, and sputter-coated with gold–palladium (Balzers SCD 030, Polaron Equipment, UK). Resin surfaces of different roughness, including such surfaces covered with air-dried secretion prints left after a strike, were attached to holders and sputter-coated with gold–palladium. The images (Fig. 4) show the remaining secretion prints of a single adhesive pad of *S. bimaculatus*. Additionally, prey items of the species *Heteromurus nitidus* Templeton (Collembola, Entomobryidae) were air-dried, glued to stubs with silver paint, and sputter-coated with gold–palladium. Observations were made by

Table 1
Maximum adhesive forces generated by *S. bimaculatus* and *S. juno* during the predatory strikes on smooth and rough surfaces (asperity sizes ranging from 0.3 to 12 μm). Values are presented as means and standard deviations. *N*, the number of tested individuals. *p* = significance level of tests for differences of the means of adhesive forces between the two species (Mann–Whitney *U*-test).

Surface	*S. bimaculatus*			*p*	*S. juno*		
	N	Body mass [mg]	Adhesive force [mN]		Adhesive force [mN]	Body mass [mg]	*N*
Epoxy smooth	32	5.04 ± 0.4	0.977 ± 0.21	**	1.154 ± 0.17	3.46 ± 0.2	24
Epoxy 0.3 μm	27	4.92 ± 0.4	1.022 ± 0.11	*	1.152 ± 0.25	3.42 ± 0.3	21
Epoxy 1.0 μm	31	5.10 ± 0.4	0.995 ± 0.17	n.s.	1.062 ± 0.14	3.63 ± 0.3	21
Epoxy 3.0 μm	31	5.13 ± 0.3	1.036 ± 0.14	n.s.	1.042 ± 0.27	3.59 ± 0.4	23
Epoxy 9.0 μm	30	5.10 ± 0.3	1.058 ± 0.14	n.s.	1.042 ± 0.22	3.56 ± 0.3	23
Epoxy 12.0 μm	30	5.14 ± 0.3	0.957 ± 0.17	**	1.095 ± 0.18	3.48 ± 0.4	31
Hydrophilic glass	32	5.05 ± 0.4	1.050 ± 0.21	n.s.	1.085 ± 0.18	3.51 ± 0.3	26
Hydrophobic glass	34	5.05 ± 0.4	1.031 ± 0.15	n.s.	0.987 ± 0.14	3.56 ± 0.2	25

Significance levels: n.s. = $p > 0.05$.
* $p < 0.05$.
** $p < 0.01$.

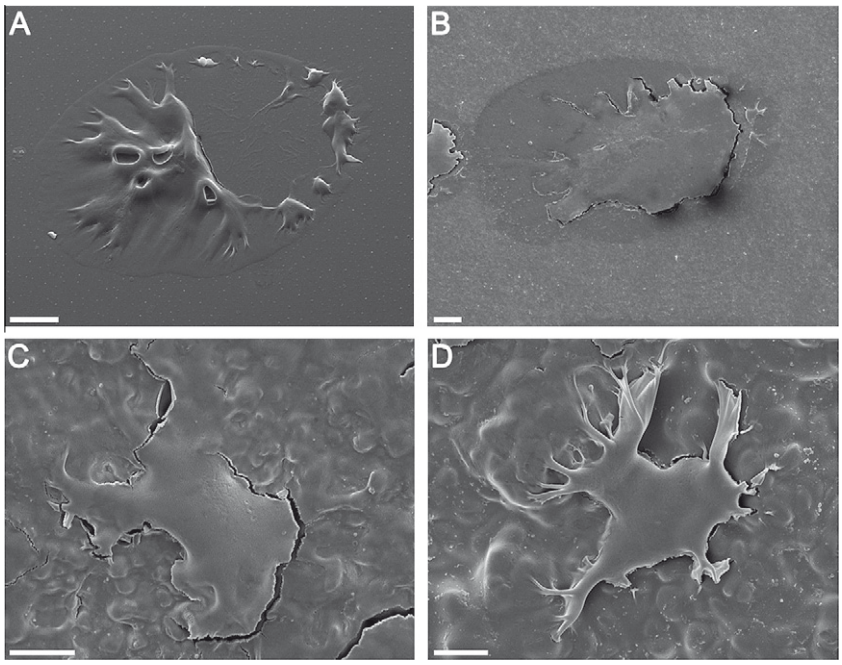

Fig. 4. SEM images of air-dried secretion prints left on the smooth surface (A) and on the surfaces with an asperity diameter of 0.3 μm (B), 3 μm (C), and 12 μm (D). Scale bar = 20 μm.

using a Cambridge Stereoscan 250 MK2 SEM (Cambridge Scientific Instruments, Cambridge, UK).

2.4. High-speed videorecordings

Some representative predatory strikes on dummy prey were recorded at 2000 frames s^{-1} with a high-speed camera (Kodak Motion Corder Analyzer PS-110 mounted on a binocular microscope Leica MZ6).

2.5. Statistical analyses

The data on the body mass and the experimental force data were not normally distributed (Shapiro–Wilks test). To compare force values generated on the various surfaces and body mass values, data sets were statistically analyzed with the nonparametric Kruskal–Wallis test. If significant differences were found, *a posteriori* pairwise comparisons were performed (Mann–Whitney *U*-test with subsequent Bonferroni correction). Differences between species in forces generated on single substrates were evaluated by using the Mann–Whitney *U*-test. Statistical processing of data was done using SPSS 11.0 software (SPSS, Chicago, USA).

3. Results

3.1. Adhesion on rough substrates

Adhesive forces generated during the predatory strike of both species on the substrates with different roughness values revealed no significant differences (Kruskal–Wallis test; *S. bimaculatus*: $p > 0.05$, $\chi^2 = 7.90$, df = 5; *S. juno*: $p > 0.05$, $\chi^2 = 6.94$, df = 5) (Fig. 5 and Table 1). Thus, in both species tested, the substrate roughness had no considerable effect on the adhesive force.

3.2. Adhesion on smooth hydrophilic and hydrophobic surfaces

In both the investigated species, a slightly stronger adhesion was found on the hydrophilic surface. However, these differences

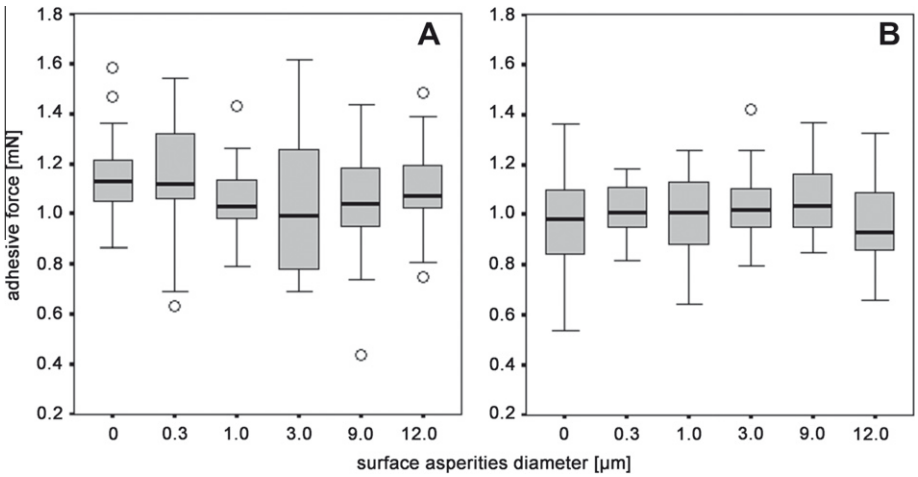

Fig. 5. Box plots showing maximum adhesive forces generated during the predatory strike on the epoxy resin surfaces having various roughness by (A) *S. juno* und (B) *S. bimaculatus*. Plot shows medians (center lines), interquartile ranges (boxes), maximum and minimum values (whiskers), and outliers (circles). The outliers are cases with the values between 1.5 and 3 box-lengths from the 75th or 25th percentile. Adhesive forces do not differ significantly in either species (Kruskal–Wallis test; *S. juno*: $p > 0.05$, $\chi^2 = 6.94$, df = 5, *S. bimaculatus*: $p > 0.05$, $\chi^2 = 7.90$, df = 5).

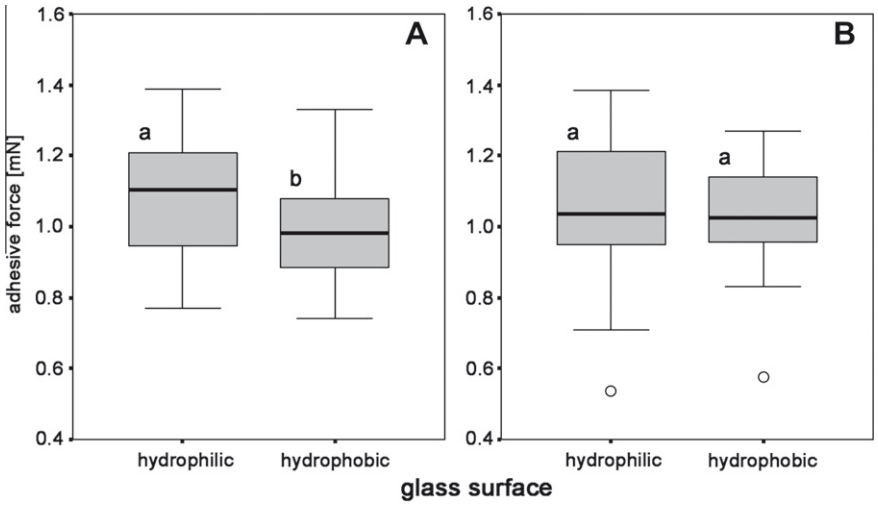

Fig. 6. Box plots showing maximum adhesive forces generated by *S. juno* (A) and *S. bimaculatus* (B) during the predatory strike on the hydrophilic (surface energy: 59 mN m^{-1}) and the hydrophobic (surface energy: 12 mN m^{-1}) glass surface. Plot shows medians (center lines), interquartile ranges (boxes), maximum and minimum values (whiskers), and outliers (circles). The outliers are cases with the values between 1.5 and 3 box-lengths from the 75th or 25th percentile. Significant differences with respect to surface energies for *S. juno* (Mann–Whitney *U*-test, $p < 0.05$, $Z = -2.07$), but none for *S. bimaculatus* (Mann–Whitney *U*-test, $p > 0.05$, $Z = -0.49$).

were only significant for *S. juno* (Mann–Whitney *U*-test, $p < 0.05$, $Z = -2.07$; Fig. 6A and Table 1). In *S. bimaculatus*, no significant differences were seen in the adhesive performance between the hydrophilic and hydrophobic surface (Mann–Whitney *U*-test, $p > 0.05$, $Z = -0.49$; Fig. 6B and Table 1). In contrast to the hydrophilic surface, the adhesion force on the hydrophobic surface was reduced by 1.81% in *S. bimaculatus* and by 9.03% in *S. juno*. In conclusion, these results suggest a minor effect of the hydrophobicity of the substrate on the adhesive performance.

3.3. Interspecific force comparisons

In contrast to *S. bimaculatus*, *S. juno* beetles achieved higher adhesive forces on most tested surfaces (except the hydrophobic surface and the surface with an asperity diameter of 9 μm). These differences were significant on the smooth surface ($p < 0.01$, $Z = -2.87$) and on the surfaces with asperity sizes of 0.3 μm ($p < 0.05$, $Z = -2.26$) and 12 μm ($p < 0.01$, $Z = -2.57$) (all Mann–Whitney *U*-tests; Table 1).

3.4. Influence of body mass on forces

The body masses of the individuals tested on each surface did not differ significantly (Kruskal–Wallis test; *S. bimaculatus*: $p > 0.05$, $\chi^2 = 9.77$, df = 7; *S. juno*: $p > 0.05$, $\chi^2 = 6.57$, df = 7). Neither the adhesive nor the compressive force was correlated with body masses of the individuals tested on each surface (Pearson correlations, all $p > 0.05$).

3.5. Scanning electron microscopy

The secretion prints left on the substrates (Fig. 4) and the results of our high-speed video recording (Movie 1 in electronic appendix) demonstrate the large amount of secretion involved in the prey-capture process. On all the tested surfaces, the surface irregularities are totally covered and wetted by the adhesive secretion (Fig. 4).

4. Discussion

The present study has experimentally evaluated the influence of both the surface topography and the surface chemistry on attachment forces generated during the predatory strike of beetles of two species of the genus *Stenus*. The adhesive performance has been measured toward six epoxy resin surfaces, which differ in roughness, and with regard to hydrophilic and hydrophobic smooth glass surfaces.

4.1. Adhesion on rough substrates

Surface roughness has previously been shown to influence the attachment (friction) forces of tarsal adhesive structures (e.g., Gorb, 2001; Peressadko and Gorb, 2004; Voigt et al., 2008b; Al Bitar et al., 2010; Gorb and Gorb, 2009; Bullock and Federle, 2010; Gorb et al., 2010). These studies have demonstrated strong friction forces on both smooth and rough surfaces with asperity sizes of >3.0 μm, whereas minimal adhesive forces occur on the substrates with asperity sizes between 0.05 and 1.0 μm. In contrast to tarsal adhesive systems of insects, commercial glues (Habenicht, 2009) and many natural glue-based adhesive systems (e.g., barnacles, limpets, echinoderms; Yule and Walker, 1984, 1987; Grenon and Walker, 1981; Santos et al., 2005) show an increase of adhesion forces with increasing roughness, attributable to an increase in the geometrical area of contact between the glue and the two surfaces.

In contrast to many previous experiments in which attachment forces have been measured under applied shear force (friction regime), in the present study, we have measured pull-off (adhesion regime), since the attachment forces of the retracting sticky labium are developed perpendicularly to the surface of the prey (cf., Movie 1 in electronic appendix). We have not revealed any considerable differences in the adhesive performance with respect to surface roughness (Table 1 and Fig. 5). Obviously, this adhesive system is not sensitive to critical surface roughness that might affect attachment performance. Such critical surface roughness has been reported from friction experiments with the tarsal hairy adhesive systems of leaf beetles (*Gastrophysa viridula* De Geer, *Leptinotarsa decemlineata* Say, Chrysomelidae; Gorb, 2001; Peressadko and Gorb, 2004; Voigt et al., 2008b; Bullock and Federle, 2010) and flies (*Musca domestica*, Muscidae; Peressadko and Gorb, 2004). Minimum friction forces are also known from the smooth tarsal adhesive pads of mirid bugs (*Dicyphus errans* Wolff, Miridae, Heteroptera; Voigt, 2005) and moths (*Cydia pomonella* L., Tortricidae, Lepidoptera; Al Bitar et al., 2010). Whereas many biological hairy adhesive systems involved in locomotion rely on spatulate structures (e.g., Stork, 1980; Walker, 1993; Varenberg et al., 2010), the tips of the adhesive ramifications in *Stenus* beetles (cf., Fig. 1B and D) are spherically shaped with tip diameters ranging between 0.17 and 0.24 μm (Koerner et al., in press). The smaller the terminal element of an adhesive structure, the wider the range of surface roughness length scales that it can compensate (Peressadko and Gorb, 2004; Huber et al., 2007; Voigt et al., 2008b; Bullock and Federle, 2010). Being smaller than the diameters of the tested surface asperities (Fig. 3), the terminal ramifications of the adhesive pad of *Stenus* beetles ensure intimate contact with all the tested substrate textures. In contrast, the spatular tips of hairy tarsal adhesive organs in insects possess considerably larger tip diameters, ranging from 1 to 10 μm (Peattie and Full, 2007) and therefore corresponding to the dimensions of the tested asperities. For these tarsal adhesive systems, the minimum of force is hypothesized to be attributable to a strongly reduced area of real contact between the surface irregularities and the characteristic dimensions and shape of the terminal elements of their setae (Peressadko and Gorb, 2004; Huber et al., 2007; Voigt et al., 2008b; Al Bitar et al., 2010). Thus, the flexibility of the terminal elements of tarsal insect setae is not sufficient to provide intimate contact between the setal tips and the surface profile at these critical length values (Peressadko and Gorb, 2004).

In addition to the small dimensions of the terminal elements, the adhesive secretion that is released into the contact zone between the adhesive pads of the *Stenus* prey-capture apparatus and the potential prey is an additional hierarchical level of organization that is essential to provide sufficient contact with the small surface irregularities of the prey. In contrast to insect tarsi, the amount of secretion used during prey-capture in *Stenus* beetles is significantly higher (Kölsch, 2000; Koerner et al., in press). Many studies suggest that the most important function of an adhesive secretion is to provide sufficient contact with rough surfaces (e.g., Kendall, 2001; Drechsler and Federle, 2006; Federle, 2006; Persson, 2007; Gorb, 2008). This principle also seems to be followed in the *Stenus* prey-capture apparatus, where the adhesion is also provided by a thick continuous secretion layer (Kölsch, 2000; Betz et al., 2009; Koerner et al., in press). SEM images of the air-dried secretion prints left on the substrates clearly demonstrate this feature (Fig. 4). On all the tested surfaces, the secretion is squeezed into the irregularities by the compressive force of the prey-capture apparatus and is able to fill the surface asperities, thus increasing the contact area with the substrate.

Using their labium, *Stenus* beetles attack prey without any *a priori* information about its surface properties, and consequently, the beetles are not able to adapt the amount of fluid to the surface

roughness. Surface roughness might prevent attachment if the height of the roughness is too large for surface minima to be completely filled with the adhesive secretion (Habenicht, 2009). Accordingly, with an increase in surface roughness, a larger amount of secretion is required to level out surface irregularities. Hence, the large amount of secretion always present on the adhesive pads seems to be an adaptation to enable good attachment to the variable surface roughness and structures of the potential prey of *Stenus*. The wetting of surface irregularities with the secretion depends on the relationship between the maximum distance between the highest peak and the lowest valley and the thickness of the fluid layer (Drechsler and Federle, 2006; Habenicht, 2009) and on the wetting properties of the fluid. The maximum thickness of the secretion layer on the adhesive pads of *Stenus* beetles corresponds to the length of their adhesive outgrowths, since these are completely embedded within the secretion. The length of the outgrowths of *S. bimaculatus* amounts to 25 μm, and those of *S. juno* to 20 μm (Koerner et al., in press), so that the surface asperities of this height should be compensated by the fluid film.

The final thickness of the secretion layer between the prey surface and the adhesive pad of the beetle depends on both the viscosity of the secretion and the impact pressure during the predatory strike. The impact pressure required for immediate contact with the prey surface is generated by the beetles, since they rapidly protrude their rod-like labium out of the body. A further enhancement in the development of the compressive force is achieved, because, during the strike, they hurl their entire body forward (Betz, 1996, 1998; Kölsch, 2000; Koerner et al., in press). According to our previous analysis, *S. juno* beetles compensate the smaller size of their sticky pads (mean single pad area: *S. juno* 0.007 mm^2; *S. bimaculatus* 0.01 mm^2) by generating significantly higher compressive forces (Koerner et al., in press). Consequently, these beetles develop nearly identical or even higher adhesive forces than *S. bimaculatus* beetles toward the tested smooth and rough surfaces (Table 1). One can conclude that, on smooth surfaces, higher compressive forces result in the reduction of the thickness of the secretion layer in the contact area (Bowden and Tabor, 1986; Habenicht, 2009), whereas on rough surfaces, higher impact forces additionally help to press the adhesive secretion into the surface contours and therefore increase the real area of contact (Habenicht, 2009). In addition to the generated compressive forces, the wetting of the tested surfaces is promoted by the relatively low viscosity of the adhesive secretion, which corresponds to the viscosity of plant oils (Kölsch, 2000; Koerner et al., in press), although the secretion might behave in a non-Newtonian manner showing viscosity changes with changing shear rate of the fluid (e.g., Dirks et al., 2010; Koerner et al., in press). Furthermore, extremely soft materials can compensate surface roughness, since these materials replicate the roughness profile of the opposing surface, thereby establishing intimate contact (Fuller and Tabor, 1975). Similar to the smooth tarsal adhesive pads of insects (Gorb et al., 2000; Jiao et al., 2000; Beutel and Gorb, 2001), the mechanical properties of the adhesive pads of *Stenus* beetles also contribute to the generation of strong adhesive forces because of the flexibility and elasticity of the pad material itself, as provided by the integration of the rubber-like protein resilin into the cuticle (Koerner et al., in press). Thus, the adhesive pads should have the capability of adapting closely to the surface profile of their prey items (Betz, 1996; Kölsch and Betz, 1998; Koerner et al., in press).

To sum up, the adhesive pads of *Stenus* beetles are able to conform to the surface roughness at various length scales, because of the following features: (1) the small dimensions and the flexibility of the terminal elements of their adhesive outgrowths, (2) the adhesive secretion, which is delivered into the contact zone, and which fills out the surface irregularities and (3) the mechanical properties of the pad tissue, adhesive outgrowths, and terminal ramifications.

One has to keep in mind that our tested surfaces are different from those found in nature. Natural surfaces, such as the prey of *Stenus* beetles (e.g., springtails), always possess diverse and sometimes elaborate surface irregularities and structures (e.g., setae, scales, spines, waxy, or greasy protuberances; Fig. 2) that might reduce the adhesion of the pads and affect prey-capture success (Bauer and Pfeiffer, 1991; Betz and Kölsch, 2004; Koerner et al., in press). Additionally, these surface structures might be detached from the body surface of the springtails and significantly impede the adhesive forces (Bauer and Pfeiffer, 1991).

4.2. Adhesion on smooth hydrophilic and hydrophobic glass surfaces

In addition to the surface roughness, the free surface energy (FSE) of the substrate affects the strength of adhesion between two contacting surfaces (Johnson et al., 1971; Kendall, 1971). Since *Stenus* beetles hunt on a great variety of prey animals (Betz, 1998), they encounter a wide range of prey differing in the physico-chemical properties of their surfaces. According to Holdgate (1955), strong inter-specific differences in the wetting properties of the cuticle surface are present in insects. Usually, the epicuticle of terrestrial insects is hydrophobic, because it is covered with a wax-like surface layer (Holdgate, 1955; Ghirardella and Radigan, 1974; Lockey, 1988).

The different surface structures of prey animals, such as spines, setae, acanthae, and microtrichia, further enhance their surface hydrophobicity (Holdgate, 1955; Wagner et al., 1996). Furthermore, large differences in the wetting properties of the various regions of the surface might exist, even within a single species (Holdgate, 1955; Noble-Nesbitt, 1963), and these differences are correlated with variations in surface structures and roughness. For instance, the cuticle of the water springtail *Podura aquatica* (Poduromorpha, Poduridae) exhibits both hydrophilic and hydrophobic areas (Noble-Nesbitt, 1963).

The smooth hydrophilic and hydrophobic glass surfaces chosen for our experiments have contact angles with water of 68 and 122°, respectively, which are comparable to those observed for aquatic and terrestrial insects (Holdgate, 1955). Our results show that the surface energy of a smooth glass surface does not considerably affect adhesion of the prey-capture apparatus of *Stenus* beetles. Both investigated species generate slightly stronger adhesion forces on a hydrophilic glass surface (high FSE) than on the silanized hydrophobic surface (low FSE), although these differences are only significant for *S. juno* (Fig. 6 and Table 1). Similar results have been obtained for insect tarsi, in which hydrophobicity (low FSE) leads to a decrease in the attachment forces (Gorb and Gorb, 2009; Al Bitar et al., 2009; Lüken et al., 2009; Gorb et al., 2010).

Our results are in agreement with the data in the literature with regard to the chemical composition of the adhesive secretion. Previous investigations have shown that the adhesive secretion of *Stenus* beetles consists of at least two immiscible phases, i.e., lipoid droplets are emulsified within a larger proteinaceous fraction (Kölsch, 2000). Histochemical analyses have confirmed these results, revealing positive reactions for carbohydrates (mucopolysaccharides), proteins, and lipids (Betz et al., 2009; Koerner et al., in press). Thus, the secretion of *Stenus* beetles seems to have similar chemical properties to the two-phasic (water-soluble and lipid-soluble) tarsal secretions found in other insects (Gorb, 2001; Federle et al., 2002; Vötsch et al., 2002; Dirks et al., 2010; reviewed in Betz 2010). The water-soluble component of such pad secretions mainly interacts with the polar parts of the surface molecules, whereas the lipid-soluble (oily) component interacts with the dispersive parts. Such two-phasic emulsions are considered to be

responsible for enhanced attachment to a variety of hydrophilic and hydrophobic surfaces (Kölsch, 2000; Gorb, 2001; Vötsch et al., 2002; Al Bitar et al., 2009; Betz, 2010). In the investigated *Stenus* beetles, such a multi-phasic adhesive might allow the beetle to handle a variety of potential prey surfaces.

5. Conclusions

Stenus species are polyphagous predators that consume a variety of prey species (Betz, 1998). Their prey-capture apparatus is adapted to a wide range of natural substrates with a variety of physico-chemical properties and surface topographies differing in dimensions by several orders of magnitude. Our results obtained by direct force measurements demonstrate that the attachment performance of the adhesive pads in the prey-capture apparatus of *Stenus* beetles is not affected by the surface roughness, since no critical surface roughness has been found such as that previously described for the tarsal adhesive organs of beetles and flies. The reason for this effect might be explained by (1) the small dimensions of the spherically shaped, terminal elements of their adhesive outgrowths and (2) the presence of a thick layer of adhesive secretion covering small substrate irregularities, thus increasing the real contact area with the non-smooth (prey) surface. Furthermore, the adhesive pads are able to attach to both hydrophobic and hydrophilic smooth surfaces. The latter effect might be explained by the multi-phasic composition of the adhesive secretion. Since, compared with the tarsal adhesive organs of insects, the reversibility of the adhesive bond probably does not represent a decisive constraint in the functioning of the investigated prey-capture apparatus, the major selective advantage in this system might arise from its ability to adapt to a variety of prey surfaces.

Acknowledgements

We wish to thank Karl-Heinz Hellmer (University of Tuebingen, Germany) for taking SEM micrographs and Dr. Michael Heethoff (University of Tuebingen, Germany), Dr. Dagmar Voigt (Dresden, Germany), and Christoph Allgaier (University of Tuebingen, Germany) for their valuable discussions, editorial help, and assistance with photo-processing. Thanks are due to Cornelia Miksch (Max Planck Institute for Intelligent Systems, Stuttgart, Germany) for technical help. Dr. Theresa Jones corrected the English. This study was partly financed by the German Ministry of Education and Research, BMBF (research grant, Bionics Competition, BNK2-052) to O.B. and S.N.G. and by the German Science Foundation, DFG to S.N.G. (project GO 995/10-1) and O.B. (project BE 2233/10-1).

Appendix A. Supplementary data

Supplementary data associated with this article can be found, in the online version, at doi:10.1016/j.jinsphys.2011.11.001.

References

Al Bitar, L., Voigt, D., Zebitz, C.P., Gorb, S.N., 2009. Tarsal morphology and attachment ability of the codling moth *Cydia pomonella* L. (Lepidoptera, Tortricidae) to smooth surfaces. Journal of Insect Physiology 55, 1029–1038.

Al Bitar, L., Voigt, D., Zebitz, C.P.W., Gorb, S.N., 2010. Attachment ability of the codling moth *Cydia pomonella* L. to rough substrates. Journal of Insect Physiology 56, 1966–1972.

Bauer, T., Pfeiffer, M., 1991. 'Shooting' springtails with a sticky rod: the flexible hunting behaviour of *Stenus comma* (Coleoptera; Staphylinidae) and the counter-strategies of its prey. Animal Behavior 41, 819–828.

Betz, O., 1996. Function and evolution of the adhesion-capture apparatus of *Stenus* species (Coleoptera, Staphylinidae). Zoomorphology 116, 15–34.

Betz, O., 1998. Comparative studies on the predatory behaviour of *Stenus* spp. (Coleoptera: Staphylinidae): the significance of its specialized labial apparatus. Journal of Zoology 244, 527–544.

Betz, O., 2002. Performance and adaptive value of tarsal morphology in rove beetles of the genus *Stenus* (Coleoptera, Staphylinidae). Journal of Experimental Biology 205, 1097–1113.

Betz, O., 2006. Ecomorphology: Integration of form, function, and ecology in the analysis of morphological structures. Mitteilungen der Deutschen Gesellschaft für Allgemeine und Angewandte Entomologie 15, 409–416.

Betz, O., 2010. Adhesive exocrine glands in insects: morphology, ultrastructure, and adhesive secretion. In: Byern, J., Grunwald, I. (Eds.), Biological adhesive systems. From Nature to Technical and Medical Application. Springer, pp. 111–152.

Betz, O., Kölsch, G., 2004. The role of adhesion in prey capture and predator defence in arthropods. Arthropod Structure and Development 33, 3–30.

Betz, O., Koerner, L., Gorb, S., 2009. An insect's tongue as the model for two-phase viscous adhesives? adhesion. Adhesives and Sealants 3, 32–35.

Beutel, R., Gorb, S.N., 2001. Ultrastructure of attachment specializations of hexapods (Arthropoda): evolutionary patterns inferred from a revised ordinal phylogeny. Journal of Zoological Systematics and Evolutionary Research 39, 177–207.

Bowden, F.P., Tabor, D., 1986. The Friction and Lubrication of Solids. Oxford University Press, Oxford.

Bullock, J.M.R., Federle, W., 2010. The effect of surface roughness on claw and adhesive hair performance in the dock beetle *Gastrophysa viridula*. Insect Science 18, 298–304.

Dai, Z., Gorb, S.N., Schwarz, U., 2002. Roughness-dependent friction force of the tarsal claw system in the beetle *Pachnoda marginata* (Coleoptera, Scarabeidae). Journal of Experimental Biology 205, 2479–2488.

Dirks, J.H., Clemente, C.J., Federle, W., 2010. Insect tricks: two-phasic foot pad secretion prevents slipping. Journal of the Royal Society Interface 7, 587–593.

Drechsler, P., Federle, W., 2006. Biomechanics of smooth adhesive pads in insects: influence of tarsal secretion on attachment performance. Journal of Comparative Physiology A 192, 1213–1222.

Federle, W., 2006. Why are so many adhesive pads hairy? Journal of Experimental Biology 209, 2611–2621.

Federle, W., Riehle, M., Curtis, A.S.G., Full, R.J., 2002. An integrative study of insect adhesion: mechanics and wet adhesion of pretarsal pads in ants. Integrative and Comparative Biology 42, 1100–1106.

Fuller, K.N.G., Tabor, D., 1975. The effect of surface roughness on the adhesion of elastic solids. Proceedings of the Royal Society London A 345, 327–342.

Ghirardella, H., Radigan, W., 1974. Collembolan cuticle: wax layer and antiwetting properties. Journal of Insect Physiology 20, 301–306.

Gorb, E.V., Hosoda, N., Miksch, C., Gorb, S.N., 2010. Slippery pores: anti-adhesive effect of nanoporous substrates on the beetle attachment system. Journal of the Royal Society Interface 7, 1571–1579.

Gorb, S.N., 2001. Attachment devices of insect cuticle. Kluwer Academic Publishers, Dordrecht, The Netherlands.

Gorb, S.N., 2007. Visualisation of native surfaces by two-step molding. Microscopy Today 15, 44–46.

Gorb, S.N., 2008. Smooth attachment devices in insects: functional morphology and biomechanics. In: Casa, J., Simpson, S.J. (Eds.), Advances in Insect Physiology. Insect Mechanics and Control, Vol. 34. Elsevier Ltd., London, pp. 81–116.

Gorb, S.N., Gorb, E.V., 2009. Effects of surface topography and chemistry of *Rumex obtusifolius* leaves on the attachment of the beetle *Gastrophysa viridula*. Entomologia Experimentalis et Applicata 130, 222–228.

Gorb, S.N., Jiao, Y., Scherge, M., 2000. Ultrastructural, architectural and mechanical properties of attachment pads in *Tettigonia viridissima* (Orthoptera, Tettigoniidae). Journal of Comparative Physiology A 186, 821–831.

Grenon, J.F., Walker, G., 1981. The tenacity of the limpet, *Patella vulgata* L An experimental approach. Journal of Experimental Marine Biology and Ecology 54, 277–308.

Habenicht, G., 2009. Kleben: Grundlagen, Technologien, Anwendung, sixth ed. Springer, Berlin.

Heethoff, M., Koerner, L., 2007. Small but powerful - the oribatid mite *Archegozetes longisetosus* Aoki (Acari, Oribatida) produces disproportionately high forces. Journal of Experimental Biology 210, 3036–3042.

Holdgate, M., 1955. The wetting of insect cuticles by water. Journal of Experimental Biology 32, 591–617.

Huber, G., Gorb, S.N., Hosoda, N., Spolenak, R., Arzt, E., 2007. Influence of surface roughness on gecko adhesion. Acta Biomaterialia 3, 607–610.

Jiao, Y., Gorb, S.N., Scherge, M., 2000. Adhesion measured on the attachment pads of *Tettigonia viridissima* (Orthoptera, Insecta). Journal of Experimental Biology 203, 1887–1895.

Johnson, K.L., Kendall, K., Roberts, A.D., 1971. Surface energy and the contact of elastic solids. Proceedings of the Royal Society London A 324, 301–313.

Kendall, K., 1971. The adhesion and surface energy of elastic bodies. Journal of Physics D: Applied Physics 4, 1186–1195.

Kendall, K., 2001. Molecular Adhesion and its Applications. Kluwer Academic Publishers, New York.

Kölsch, G., 2000. The ultrastructure of glands and the production and function of the secretion in the adhesive capture apparatus of *Stenus* species (Coleoptera: Staphylinidae). Canadian Journal of Zoology 78, 465–475.

Kölsch, G., Betz, O., 1998. Ultrastructure and function of the adhesion-capture apparatus of *Stenus* species (Coleoptera, Staphylinidae). Zoomorphology 118, 263–272.

Koerner, L., Gorb, S.N., Betz, O., in press. Adhesive performance and functional morphology of the stick-capture apparatus of the rove beetles *Stenus* spp. (Coleoptera, Staphylinidae). Zoology

Lockey, K.H., 1988. Lipids of the insect cuticle: origin, composition and function. Comparative Biochemistry and Physiology 89, 595–645.

Lüken, D., Voigt, D., Gorb, S.N., Zebitz, C.P.W., 2009. Tarsal morphology and attachment ability of the sweet potato weevil *Cylas puncticollis* Boh. to smooth surfaces with different physico-chemical properties. Mitteilungen der Deutschen Gesellschaft für Allgemeine und Angewandte Entomologie 17, 109–113.

Noble-Nesbitt, J., 1963. Transpiration in *Podura aquatica* L. and the wetting properties of its cuticle. Journal of Experimental Biology 40, 681–700.

Opell, B.D., 1994. The ability of spider cribellar prey capture thread to hold insects with different surface features. Functional Ecology 8, 145–150.

Opell, B.D., Schwend, H.S., 2007. The effect of insect surface features on the adhesion of viscous capture threads spun by orb-weaving spiders. Journal of Experimental Biology 210, 2352–2360.

Owens, D.K., Wendt, R.C., 1969. Estimation of the surface free energy of polymers. Journal of Applied Polymer Science 13, 1741–1747.

Peattie, M., Full, R.J., 2007. Phylogenetic analysis of the scaling of wet and dry biological fibrillar adhesives. Proceedings of the National Academy of Sciences Online (US) 104, 18595–18600.

Peressadko, A.G., Gorb, S.N., 2004. Surface profile and friction force generated by insects. In: Boblan, I., Bannasch, R. (Eds.), First International Conference Bionik 2004. VDI Verlag, Berlin, pp. 257–263.

Persson, B.N.J., 2007. Biological adhesion for locomotion on rough surfaces: basic principles and a theorist's view. MRS Bulletin 32, 486–490.

Santos, R., Gorb, S.N., Jamar, V., Flammang, P., 2005. Adhesion of echinoderm tube feet to rough surfaces. Journal of Experimental Biology 208, 2555–2567.

Scherge, M., Gorb, S.N., 2001. Biological Micro- and Nanotribology. Springer, Berlin.

Schmitz, G., 1943. Le labium et les structures bucco-pharyngiennes du genre *Stenus* LATREILLE. Cellule 49, 291–334.

Scholz, I., Bückins, M., Dolge, L., Erlinghagen, T., Weth, A., Hischen, F., Mayer, J., Hoffmann, S., Riederer, M., Riedel, M., Baumgartner, W., 2010. Slippery surfaces of pitcher plants: *Nepenthes* wax crystals minimize insect attachment via macroscopic surface roughness. Journal of Experimental Biology 213, 1115–1125.

Stork, N.E., 1980. A scanning electron microscope study of tarsal adhesive setae in the Coleoptera. Zoological Journal of the Linnean Society 68, 173–306.

Varenberg, M., Pugno, N.M., Gorb, S.N., 2010. Spatulate structures in biological fibrillar adhesion. Soft Matter 6, 3269–3272.

Vötsch, W., Nicholson, G., Müller, R., Stierhof, Y.-D., Gorb, S., Schwarz, U., 2002. Chemical composition of the attachment pad secretion of the locust *Locusta migratoria*. Insect Biochemistry and Molecular Biology 32, 1605–1613.

Voigt, D., 2005. Biologie und Ökologie der räuberischen Weichwanze Dicyphus errans Wolff (Heteroptera, Miridae, Bryocorinae). Technische Universität, Dresden, Germany, pp. 185, Dissertation.

Voigt, D., Peisker, H., Gorb, S.N., 2008a. Visualization of epicuticular grease on the covering wings on the Colorado Potato Beetle: a scanning probe approach. In: Bhushan, B., Fuchs, H. (Eds.), Applied Scanning Probe Methods XIII. Springer, Heidelberg, pp. 1–16.

Voigt, D., Schuppert, J.M., Dattinger, S., Gorb, S.N., 2008b. Sexual dimorphism in the attachment ability of the Colorado potato beetle *Leptinotarsa decemlineata* (Coleoptera: Chrysomelidae) to rough substrates. Journal of Insect Physiology 54, 765–776.

Wagner, T., Neinhuis, C., Barthlott, W., 1996. Wettability and contaminability of insect wings as a function of their surface sculptures. Acta Zoologica 77, 213–225.

Walker, G., 1993. Adhesion to smooth surfaces by insects – a review. International Journal of Adhesion and Adhesives 13, 3–7.

Weinreich, E., 1968. Über den Klebfangapparat der Imagines von *Stenus* LATR (Coleopt., Staphylinidae) mit einem Beitrag zur Kenntnis der Jugendstadien dieser Gattung. Zeitschrift für Morphologie und Ökologie der Tiere 62, 162–210.

Yule, A.B., Walker, G., 1984. The temporary adhesion of barnacle cyprids: effects of some differing surface characteristics. Journal of the Marine Biological Association of the United Kingdom 64, 429–439.

Yule, A.B., Walker, G., 1987. Adhesion in barnacles. In: Southward, A.J. (Ed.), Crustacean Issues, Biology of Barnacles. Balkema, Rotterdam, pp. 389–402.

Publikation III

Divergent morphologies of adhesive predatory mouthparts of *Stenus* species (Coleoptera, Staphylinidae) explain differences in adhesive performance and resulting prey-capture success

Lars Koerner, László Zsolt Garamszegi, Michael Heethoff, Oliver Betz

Zoological Journal of the Linnean Society 181 (2017): 500–518

Zoological Journal of the Linnean Society, 2017, **XX**, 1–19. With 6 figures.

Divergent morphologies of adhesive predatory mouthparts of *Stenus* species (Coleoptera: Staphylinidae) explain differences in adhesive performance and resulting prey-capture success

LARS KOERNER[1]*, LÁSZLÓ ZSOLT GARAMSZEGI[2], MICHAEL HEETHOFF[3] and OLIVER BETZ[1]

[1]*Department of Evolutionary Biology of Invertebrates, Institute for Evolution and Ecology, Universität Tübingen, Auf der Morgenstelle 28, D-72076 Tübingen, Germany*
[2]*Department of Evolutionary Ecology, Estación Biológica de Doñana-CSIC, c/ Americo Vespucio, s/n, 41092, Seville, Spain*
[3]*Ecological Networks, Technische Universität Darmstadt, Schnittspahnstraße 3, D-64287 Darmstadt, Germany*

Received 26 March 2016; revised 9 January 2017; accepted for publication 26 January 2017

Members of the genus *Stenus* (Coleoptera, Staphylinidae) possess a unique adhesive labial prey-capture apparatus as an adaptation to their predatory behaviour. In order to examine the relationships between the morphology of the prey-capture apparatus, its adhesive performance and the prey-capture success, we combined force measurements, morphological and behavioural investigations of representatives of 14 Central European species of this genus. The direct relationship between these traits was studied by using phylogenetic generalized least squares and a molecular phylogeny generated from mitochondrial cytochrome c oxidase I partial sequences. Force measurements revealed strong interspecific differences in the adhesive forces generated during the predatory attack; these differences entail significant differences in the prey-capture success. The interspecific differences in adhesive performance were functionally correlated with the pad morphology and divergences in the compressive forces generated during the predatory strike. Allometric analyses revealed that the pad area scaled with positive allometry with respect to body size, whereas the adhesive forces scaled with negative allometry with respect to body size, that is, the pads' efficiency decreased with body size. Our experimental approach demonstrates a direct functional relationship between the morphology of the prey-capture device of *Stenus* beetles and its performance in a natural behavioural context.

ADDITIONAL KEYWORDS: adhesion – adhesive force – allometry – ecomorphology – force measurement – functional morphology – performance – predation – scaling – tenacity.

INTRODUCTION

The genus *Stenus* Latreille, 1797 (Coleoptera, Staphylinidae) is one of the largest beetle genera, comprising more than 2800 species widely distributed throughout the world (Volker Puthz, pers. comm.). *Stenus* species are optically oriented predators that feed on a variety of prey from diverse invertebrates (e.g. Oligochaeta, small spiders, mites, aphids, springtails, nymphs of Cicadinae, flies, hymenopterans and small pyralid caterpillars) (Betz, 1998a; Ryvkin, 2012).

As an adaptation to their predatory behaviour, *Stenus* species have a unique elongated labium, which is one of the most specialized prey-capture structures among insects (Fig. 1; Weinreich, 1968; Puthz, 1981; Betz, 1996, 2006; Koerner, Gorb & Betz, 2012a, b). Dependent on the predatory behaviour of the beetle, this specialized labium can be protruded rapidly (within 1–3 ms) by haemolymph pressure towards the potential prey (Weinreich, 1968; Betz,

*Corresponding author. E-mail: LarsKoerner3@hotmail.com

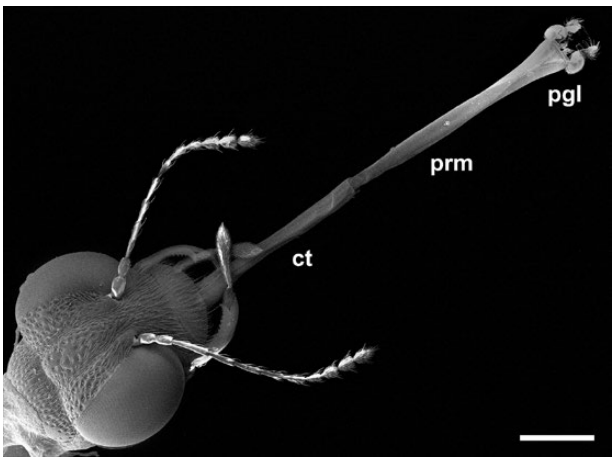

Figure 1. The adhesion-capture apparatus of *S. bimaculatus*. Scanning electron microscopic image of the head with the protruded labium. Scale bar = 0.5 mm. Abbreviations: pgl, paraglossae (modified into adhesive pads); prm, prementum; ct, connecting tube.

1996, 2006; Koerner *et al.*, 2012a, b). At the distal end of the labium are the paired paraglossae, which are modified into adhesive pads and whose surface is differentiated into numerous outgrowths (Fig. 2). Each outgrowth branches out terminally, which increases the total number of adhesive contacts. Once hit by the adhesive pads, the prey is fixed and, upon retraction of the labium, seized by the mandibles of the beetle (Weinreich, 1968; Bauer & Pfeiffer, 1991; Betz, 1996, 2006; Koerner *et al.*, 2012a, b). Alternatively, the beetles of most hitherto investigated species are able to catch their prey directly with the mandibles without using their specialized labium (Bauer & Pfeiffer, 1991; Betz, 1998a, b, 2006; Heethoff *et al.*, 2011).

Depending on the species, the adhesive pads differ in their surface area, their number of adhesive outgrowths and the degree of branching of a single adhesive outgrowth (Betz, 1996).

The number of both outgrowths and terminal branches is species-specific and may range from one to several thousands (Bauer & Pfeiffer, 1991; Betz, 1996). It has been determined experimentally that larger surface areas of the adhesive pads and more adhesive outgrowths and adhesive contacts lead to improved adhesion and consequently increased capture success (Betz, 1996, 1998a). In several species, such an improvement of the adhesive strength of the sticky cushions might have led to an enlargement of the feeding niche toward large and, at the same time, fast fleeing prey (Betz, 1998a).

Interestingly, at least two genera within the beetle family Staphylinidae have evolved a prey-capture apparatus analogous or even homologous to that of *Stenus*: the genus *Tyrannomastax* from Madagascar (Orousset, 1988) and an undescribed genus from Australia, which might actually belong to the Steninae (Leschen & Newton, 2003; Betz & Kölsch, 2004; Clarke & Grebennikov, 2009). However, detailed studies on the function of these structures are not yet available.

The adhesion of the pads of *Stenus* beetles is mediated by a secretion that is produced in glands within the head capsule and secreted onto the pad surface (Schmitz, 1943; Weinreich, 1968; Kölsch & Betz, 1998; Kölsch, 2000; Koerner *et al.*, 2012a, b). This secretion consists of at least two immiscible phases: a larger aqueous probably proteinaceous phase and a lipid phase (Kölsch, 2000; Betz, Koerner & Gorb, 2009; Betz, 2010). In contrast to the tarsal adhesive organs of insects, the adhesive outgrowths in *Stenus* are deeply immersed into the secretion and only their outermost branches protrude (Betz *et al.*, 2009; Koerner *et al.*, 2012a, b). Stefan adhesion based on the viscosity of the secretion was assumed to be the major adhesive mechanism in this prey-capture apparatus (Kölsch, 2000; Betz & Kölsch, 2004; Betz *et al.*, 2009; Koerner *et al.*, 2012b).

The prey-capture organ of *Stenus* functions as a catapult mechanism, that is, the labium is loaded by increasing haemolymph pressure prior to the strike and is suddenly released to hit the prey within milliseconds with a high compressive force (Kölsch & Betz, 1998; Koerner *et al.*, 2012a, b). During the retraction of the labium, the adhesive forces develop perpendicularly with respect to the surface (Betz, 2006; Koerner *et al.*, 2012a, b). The forces generated during the predatory strike have previously been measured in vivo in two *Stenus* species (Koerner *et al.*, 2012a, b). In the present contribution, we test a broader range of 14 *Stenus* species in order to examine the relationships between pad morphology, adhesive abilities and prey-capture success using conventional and phylogenetic comparative methods. We hypothesize that larger and more complex-structured adhesive pads (i.e. with larger numbers of adhesive outgrowths, adhesive contacts and ramifications) result in a better adhesive performance and therefore lead to enhanced prey-capture success. To test this assumption, we have followed an ecomorphological approach (e.g. Wainwright, 1991; Reilly & Wainwright, 1994; Betz, 2008) intended to relate interspecific morphological differences directly to performance traits in a natural behavioural context; such an approach is crucial to improve our understanding of the evolution of this highly specialized prey-capture device and its ecological relevance.

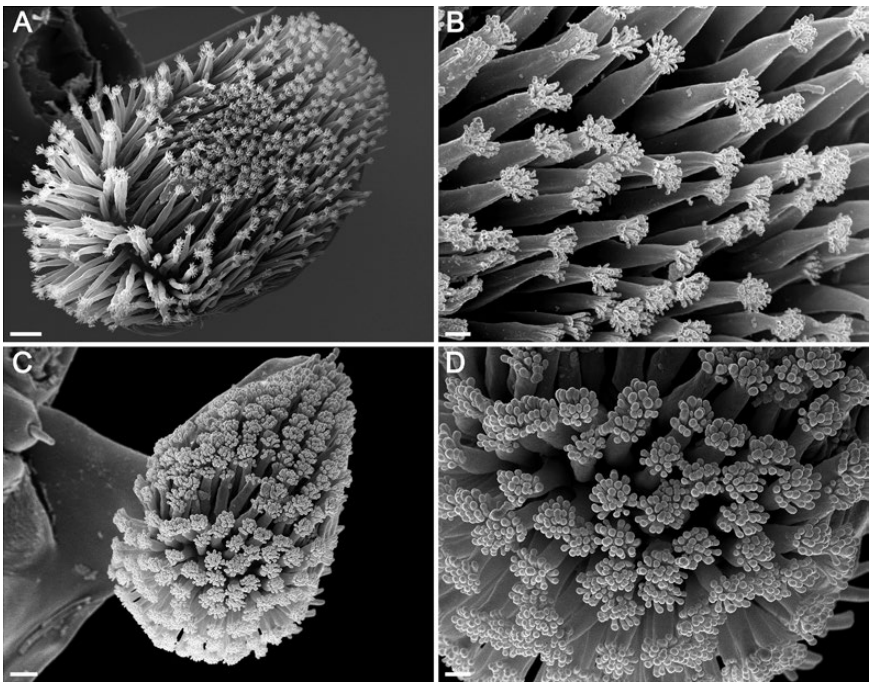

Figure 2. Ventral view of the adhesive pad (left) and the adhesive outgrowths (right) of (A, B) *Stenus clavicornis* and (C, D) *Stenus fossulatus*. Note that, during prey-capture, the outgrowths are deeply immersed into the adhesive secretion and only their outermost branches protrude (Koerner et al., 2012a, b). Scale bars: A = 10 µm, B and D = 2 µm, C = 5 µm.

Table 1. *Stenus* species investigated

Genus	Species	Collecting locality	GenBank accession no.
Ingroup			
Stenus	*bimaculatus* Gyllenhal, 1810	Germany, Schleswig-Holstein, Friedrichsruh	JQ085758
	juno (Paykull, 1789)	Germany, Schleswig-Holstein, Kiel	JQ085760
	intricatus Erichson, 1840	Spain, Andalucía, Cota de Doñana NP	JX828404
	lustrator Erichson, 1839	Germany, Baden-Württemberg, Tübingen	JQ085767
	clavicornis (Scopoli, 1763)	Germany, Baden-Württemberg, Tübingen	JQ085764
	providus Erichson, 1839	Germany, Baden-Württemberg, Tübingen	JQ085763
	comma Leconte, 1863	Germany, Baden-Württemberg, Tübingen	JQ085769
	biguttatus (Linnaeus, 1758)	Germany, Schleswig-Holstein, Strande	JQ085772
	guttula Müller, 1831	Germany, Baden-Württemberg, Tübingen	JQ085775
	fossulatus Erichson, 1840	Germany, Schleswig-Holstein, Strande	JQ085776
	boops Ljungh, 1804	Germany, Baden-Württemberg, Tübingen	JQ085778
	melanarius Stephens, 1883	Germany, Baden-Württemberg, Reusten	EU546115
	humilis Erichson, 1839	Germany, Baden-Württemberg, Tübingen	JQ085784
	morio Gravenhorst, 1806	Germany, Baden-Württemberg, Tübingen	JX828405
Outgroup			
Euaesthetus (Euaesthetinae)	*ruficapillus*	unknown	DQ155946

MATERIAL AND METHODS

BEETLES

The 14 species chosen for our investigations cover a representative size range of Central European *Stenus* species (Tables 1, 2). We intended to include species of the main Central European ecotypes (Betz, 1996, 1998b, 1999), that is, (1) inhabitants of moist humus or plant debris near the ground (pl de in Table 2), (2) 'surface runners' on bare ground (ba gr in Table 2) and

Table 2. Species means for morphological parameters and measured forces in the *Stenus* species investigated

Stenus species	Species label	Habitat	Pronotum length (mm)	Labium length (mm)	Body mass (mg)	Compressive force (mN)	Adhesive force (mN)	Tenacity (kPa)
S. bimaculatus	1	pl de	1.00 ± 0.05 (n = 10)	2.72 ± 0.14 (n = 10)	5.05 ± 0.4 (n = 27)	0.102 ± 0.04^{b,c,d} (n = 27)	1.077 ± 0.24^{a} (n = 27)	51.9
S. juno	2	pl de	0.94 ± 0.03 (n = 10)	2.17 ± 0.09 (n = 10)	3.53 ± 0.4 (n = 27)	0.179 ± 0.06^{a} (n = 27)	1.000 ± 0.19^{a} (n = 27)	69.7
S. clavicornis	3	pl de	0.87 ± 0.03 (n = 24)	2.06 ± 0.08 (n = 23)	2.77 ± 0.2 (n = 23)	0.105 ± 0.03^{b,c} (n = 23)	0.790 ± 0.13^{b} (n = 23)	61.3
S. providus	4	pl de	0.86 ± 0.04 (n = 10)	2.12 ± 0.02 (n = 10)	2.56 ± 0.3 (n = 25)	0.107 ± 0.05^{b,c} (n = 25)	0.788 ± 0.21^{b} (n = 25)	71.9
S. comma	5	ba gr	0.83 ± 0.03 (n = 10)	1.56 ± 0.08 (n = 10)	3.00 ± 0.3 (n = 21)	0.069 ± 0.03^{c,d,e} (n = 21)	0.367 ± 0.08^{d,e} (n = 21)	87.9
S. intricatus	6	pl de	0.81 ± 0.04 (n = 16)	1.90 ± 0.06 (n = 9)	2.60 (n = 1)	0.105 (n = 1)	0.767 (n = 1)	86.0
S. lustrator	7	pl de	0.80 ± 0.02 (n = 13)	2.17 ± 0.17 (n = 6)	2.15 ± 0.2 (n = 25)	0.108 ± 0.04^{b,c} (n = 25)	0.675 ± 0.12^{b,c} (n = 25)	59.3
S. fossulatus	8	ba gr	0.78 ± 0.04 (n = 10)	1.75 ± 0.11 (n = 10)	2.04 ± 0.2 (n = 20)	0.064 ± 0.02^{c,d,e} (n = 20)	0.417 ± 0.08^{d,e} (n = 20)	128.4
S. biguttatus	9	ba gr	0.77 ± 0.02 (n = 11)	1.71 ± 0.04 (n = 11)	1.84 ± 0.2 (n = 13)	0.045 ± 0.01^{e} (n = 13)	0.416 ± 0.07^{d,e} (n = 13)	112.7
S. guttula	10	ba gr	0.70 ± 0.05 (n = 21)	1.65 ± 0.08 (n = 11)	1.55 ± 0.1 (n = 21)	0.058 ± 0.02^{d,e} (n = 21)	0.403 ± 0.08^{d,e} (n = 21)	119.5
S. boops	11	pl de	0.67 ± 0.02 (n = 10)	1.42 ± 0.05 (n = 10)	1.17 ± 0.1 (n = 23)	0.157 ± 0.04^{a} (n = 23)	0.522 ± 0.10^{c,d} (n = 23)	85.1
S. morio	12	pl de	0.58 ± 0.04 (n = 10)	1.32 ± 0.07 (n = 10)	0.88 ± 0.1 (n = 4)	0.082 ± 0.01^{c,d,e} (n = 4)	0.277 ± 0.01^{e} (n = 4)	111.1
S. melanarius	13	pl de	0.57 ± 0.01 (n = 4)	1.25 ± 0.06 (n = 4)	0.87 ± 0.1 (n = 19)	0.135 ± 0.03^{a,b} (n = 19)	0.482 ± 0.07^{d} (n = 19)	87.6
S. humilis	14	pl de	0.53 ± 0.03 (n = 11)	1.22 ± 0.07 (n = 8)	0.85 ± 0.2 (n = 21)	0.088 ± 0.02^{c,d,e} (n = 21)	0.401 ± 0.10^{d,e} (n = 21)	153.2

Species are ordered according to the length of their pronotum. Given are arithmetic means ± SD. The tenacity was calculated by dividing the mean adhesive forces by the mean surface areas of both adhesive pads. Different letters in superscripts refer to statistically significant interspecific differences in the compressive and adhesive forces (Tukey's HSD test, $P_{Tukey} < 0.05$). n = number of individuals tested. Values of *S. juno* and *S. bimaculatus* taken from Koerner *et al.*, 2012b). Abbreviations: pl de, plant debris; ba gr, bare ground.

(3) plant climbers. However, since the plant climbers did not react to dummy prey, they were excluded from the experiments. Beetles were kept in plastic boxes on moist plaster of Paris mixed with activated charcoal and fed with living collembolans ad libitum.

Microscopic techniques

For imaging by scanning electron microscopy (SEM), the heads of the beetles with the extended labia were cleaned in H_2O_2 with a concentration of 5%, dehydrated in an ethanol series, critical-point dried (Polaron E3000, UK), fixed to stubs with silver paint, sputter-coated with gold-palladium (Balzers SCD 030, Germany) and observed in a Stereoscan (250 MK2, Cambridge Instruments, UK). The following morphological parameters of the adhesive pads were obtained: (1) the surface area, (2) the density (counted in the centre of the adhesive pads), (3) the total number of adhesive outgrowths, (4) the number of terminal ramifications per adhesive outgrowth (for a given specimen, the mean of five central outgrowths was determined), (5) the total number of adhesive contacts per adhesive pad (calculated as the total number of adhesive outgrowths per adhesive pad multiplied by the number of terminal ramifications per adhesive outgrowth) and (6) the density of adhesive contacts (calculated as the density of adhesive outgrowths multiplied by the mean number of terminal ramifications per adhesive outgrowth). In order to achieve larger sample sizes in some species, our measurements were complemented by data previously obtained by Betz (1996). Measurements of the adhesive pad area were made from the SEM images, using the 'ImageTools – Measure' option incorporated in the image analysis and morphometrics software tpsDig2 (Rohlf, 2004). Thus, we measured the 'projected' pad area that is the surface area of the adhesive pads specialized specifically

for generating adhesion (Labonte *et al.*, 2016). In fibrillar pads, only a fraction of this area might come into contact with the surface; thus, the 'real' contact area might be significantly smaller than the 'projected' contact area (Labonte *et al.*, 2016). However, our secretion prints (see fig. 4a, b in Koerner *et al.*, 2012a) revealed that the entire surface area of a pad can make contact with the prey contact surface, that is, the surface areas of the secretion prints are similar to the 'projected' surface areas of the adhesive pads measured from the SEM images.

In order to correlate the morphological parameters of the adhesive pads with indicators of body size, the length of the pronotum (the dorsal plate of an insect's prothorax) and the labium were measured with a micrometer by stereoscopic microscopy. Since the body length of staphylinids is too variable (staphylinids are able to stretch their abdomen or make it shorter), the pronotum length serves as an indicator of body size (Betz, 1996). Our morphological investigations on almost 200 *Stenus* species indicate that the length of the pronotum is a good proxy for body size (correlation between pronotum length and body length in *Stenus*: $r = 0.873$, $P < 0.001$, $n = 196$; L.K. & O.B., unpubl. data). However, we also present results with body mass as proxy for body size.

Force measurements on living beetles

Prior to the experiments, the beetles were individually weighed and starved for 5–7 days afterwards. Both the compressive and adhesive forces generated during the predatory strike were determined following the protocol of Koerner *et al.* (2012b). Accordingly, the forces generated during the predatory strike of *Stenus* beetles were measured with a force sensor (FORT25, WPI Inc., USA) to which the head of an insect pin (0.3 mm diameter) with a surface energy of 30.77 ± 1.4 mN m^{-1} (cf. Koerner *et al.*, 2012b) was connected as a dummy prey. While the beetle was 'shooting' onto the head of the insect pin, the forces were continuously recorded and amplified with a computer-based data-acquisition and processing system (MP100 WSW, BIOPAC Systems Inc., USA) and later analysed with the software AcqKnowledge 3.8.2 (BIOPAC Systems Inc., USA). Depending on the availability of the specimens in the field, the experiments were conducted with different numbers of individuals per species (Table 2), at which at least 15 attacks per individual were analysed. Only maximum compressive and adhesive forces of each beetle were considered for further statistical analysis. The tenacity was calculated by dividing the mean maximum adhesive forces (Table 2) by the mean 'projected' surface areas of the adhesive pads (Table 3).

Prey-capture experiments

The predatory behaviour towards springtails (*Heteromurus nitidus* Templeton, 1835) was analysed in standardized prey-capture experiments according to Betz (1996, 1998a). The prey-capture success and the rate of occurrence of attack with the labium towards small (fresh weight 8.4 ± 5.6 µg) and large (fresh weight 62.3 ± 25 µg) springtails were determined. The capture-success with the labium is defined as the percentage of attacks in which the beetle was able to pull the springtail into the range of the mandibles (attacks in which the prey was ingested). In some species, these experiments had previously been conducted by Betz (1996, 1998a), but in order to attain a larger sample size of individuals tested, additional prey-capture experiments were performed. The newly obtained data were added to the existing data obtained by Betz (1996, 1998a) and statistically analysed. Table 4 shows the grand mean (±SD) of the percentage values from each individual per species. For technical reasons, prey-capture experiments could not be conducted with individuals of the species *S. melanarius*, because all individuals of this species died after the force measurements and additional individuals were not available for prey-capture experiments.

Molecular phylogeny

In order to detect phylogenetic effects in our comparative data, phylogenetic distances were estimated using mitochondrial *COI* sequences taken from Koerner *et al.* (2013) or were sequenced for this study (*S. morio* and *S. intricatus*). Taxon information and GenBank accession numbers are given in Table 1.

Sequences were aligned manually without ambiguous positions. Phylogenetic analysis was based on maximum likelihood (ML) algorithms using PAUP* (Swofford, 1999). For ML in PAUP*, the best-fit model of sequence evolution was estimated using the BIC criterion with ModelTest (Posada & Crandall, 1998) and ModelTest Server (Posada, 2006). The best-fit model was GTR + G + I (I: 0.4413, G: 0.7973) with base frequencies: freqA = 0.3223, freqC = 0.1325, freqG = 0.1045, freqT = 0.4407 and substitution rates: R(a) = 0.2141, R(b) = 19.202, R(c) = 6.9777, R(d) = 5.1153, R(e) = 19.202 and R(f) = 1.0. ML analyses in PAUP* were performed with the starting tree obtained via neighbour joining. The TBR swapping was used for heuristic tree search.

Data analysis

All data are presented as species mean values ± SD. Phylogenetic methods have become indispensable in the analysis of interspecific data. This is because data

Table 3. Quantitative comparison of the morphology of the adhesive pads of the investigated *Stenus* species

Stenus species	Surface area of the adhesive pad (mm²)			Adhesive outgrowths per adhesive pad (no.)			Ramifications per outgrowth (no.)			Adhesive contacts per adhesive pad (no.)			Density of adhesive outgrowths (no./400 µm²)			Density of adhesive contacts (no./400 µm²)		
	$\bar{x}$	s	n	$\bar{x}$	s	n	$\bar{x}$	s	n	$\bar{x}$	s	n	$\bar{x}$	s	n	$\bar{x}$	s	n
*S. bimaculatus**	0.01076	0.0017	20	586.21	51.0	14	28.91	1.7	9	17910.64	3030.4	13	44.83	10.3	26	1287.44	303.60	17
*S. juno**	0.00718	0.0011	19	590.64	83.0	14	25.23	6.8	8	16401.15	3700.0	9	44.74	12.8	11	1313.44	732.10	8
*S. clavicornis**	0.00644	0.0007	21	510.29	23.8	17	27.85	8.6	16	14233.92	4388.5	16	33.13	10.9	18	934.12	539.51	16
S. lustrator	0.00569	0.0007	16	312.25	3.1	4	26.92	2.8	6	7868.26	345.7	4	31.28	5.0	5	815.65	112.86	5
*S. providus**	0.00548	0.0007	29	490.80	55.1	10	31.17	5.6	12	15626.68	3762.7	10	51.02	9.0	16	1464.69	411.49	9
S. intricatus	0.00446	0.0001	5	449.50	44.3	4	31.00	8.1	7	15610.53	4047.4	4	51.73	7.4	6	1776.03	417.32	5
*S. boops**	0.00307	0.0004	21	332.83	46.2	12	25.12	5.6	13	8681.90	2444.5	12	48.05	3.9	14	1124.76	319.91	8
S. melanarius	0.00275	0.0003	6	286.60	20.8	5	23.90	2.4	8	7128.70	945.1	5	39.23	5.5	6	961.46	140.13	6
*S. comma**	0.00209	0.0003	32	185.27	18.2	15	13.35	1.1	17	2502.91	246.5	14	58.91	8.0	15	806.57	134.85	14
*S. biguttatus**	0.00184	0.0002	20	232.62	28.2	13	22.42	1.5	12	5296.85	759.4	12	52.25	8.0	12	1151.23	173.04	11
*S. guttula**	0.00169	0.0004	22	220.30	29.5	10	27.35	6.2	11	6397.61	810.9	7	49.80	5.8	8	1491.20	476.18	7
*S. fossulatus**	0.00163	0.0002	31	226.11	25.7	9	24.73	2.5	9	5348.10	400.0	8	49.29	7.8	12	1168.58	204.89	8
S. humilis	0.00131	0.0001	13	193.33	15.4	3	13.64	1.1	4	2691.78	171.0	3	82.03	6.0	3	1149.58	174.81	3
*S. morio**	0.00125	0.0001	26	166.00	24.3	10	26.87	4.4	10	4459.45	1247.6	9	61.64	7.1	11	1672.45	403.07	10

Species are ordered according to the size of their adhesive pads. Abbreviations: $\bar{x}$ arithmetic mean, s standard deviation, n sample size. *Measurements pooled together with data obtained by Betz (1996).

Table 4. Percentage of attacks conducted with the labium and the resulting prey-capture success towards small and large springtails (*Heteromurus nitidus*) in the *Stenus* species investigated

Stenus species	Attacks conducted with labium (%)				Successful attacks conducted with labium (%)			
	Small springtails	*n*	Large springtails	*n*	Small springtails	*n*	Large springtails	*n*
*S. bimaculatus**	87.47 ± 17.9	42	68.56 ± 21.4	42	64.72 ± 23.1	43	28.36 ± 22.5	42
*S. juno**	77.33 ± 23.1	43	63.32 ± 30.4	41	81.87 ± 16.6	43	29.78 ± 27.9	39
S. clavicornis	84.22 ± 19.0	44	84.60 ± 17.6	66	62.90 ± 30.1	45	16.12 ± 19.0	63
*S. providus**	68.55 ± 26.3	28	55.46 ± 29.2	41	59.59 ± 26.3	26	16.97 ± 14.4	38
*S. comma**	65.65 ± 23.2	42	22.22 ± 20.6	42	59.61 ± 16.7	41	4.79 ± 10.4	34
S. intricatus	69.68 ± 18.1	3	62.37 ± 15.2	6	47.47 ± 47.1	3	18.44 ± 13.7	5
S. lustrator	95.86 ± 6.8	11	85.84 ± 15.0	15	63.60 ± 17.5	10	15.98 ± 26.4	14
*S. fossulatus**	80.04 ± 17.9	43	23.85 ± 19.0	42	47.92 ± 22.0	43	1.90 ± 7.9	35
*S. biguttatus**	85.11 ± 19.2	42	50.33 ± 21.5	40	54.68 ± 20.9	36	5.62 ± 10.2	42
S. guttula	81.89 ± 10.7	21	36.30 ± 18.7	21	40.25 ± 15.4	23	3.25 ± 9.0	21
*S. boops**	88.14 ± 14.8	42	74.56 ± 21.9	41	44.54 ± 24.1	42	8.04 ± 15.0	41
S. morio	81.67 ± 30.2	8	88.67 ± 17.6	5	39.71 ± 33.7	8	3.33 ± 7.5	5
S. humilis	95.90 ± 6.0	20	92.52 ± 10.0	20	56.54 ± 16.9	20	4.31 ± 5.6	20

Given are grand means ± SD. *n* = number of individuals tested. Values of *S. juno* and *S. bimaculatus* taken from Koerner *et al.* (2012b). *Measurements pooled together with data obtained by Betz (1996, 1998a).

for species are non-independent because phenotypic similarity can result from shared evolutionary history, that is, phylogenetic relatedness (Felsenstein, 1985; Harvey & Pagel, 1991). This non-independence can lead to inflated Type I error rates (Felsenstein, 1985) and inflated variance in the estimates of correlation and regression coefficients (Rohlf, 2006).

For phylogenetic analyses, the morphological parameters and the adhesive performance parameters were log-transformed or arcsine-transformed (percentage values). The phylogenetic analyses were performed using both gradual and speciational models of character evolution, with branch-lengths obtained from raw *COI* genetic distances for the gradual model (Fig. 3) or with branch lengths set to 1 for the speciational model of evolution (Garland *et al.*, 1993). Since the speciational model of evolution yielded the same results as the gradual model (Tables 5, 6), these results are not discussed further in the present study.

We used phylogenetic generalized least squares (PGLS) to analyse scaling relationships among the different parameters while accounting for non-independence in the data due to common descent (Symonds & Blomberg, 2014). Scaling coefficients were quantified by determining the slope of the log-log plots, and *t*-tests were used to compare these slopes to the slope of allometry.

We used PGLS because this method is an improvement over previous methods of incorporating phylogeny into statistical models, such as phylogenetic independent contrasts (PIC), because it provides information on how traits have evolved under the most appropriate evolutionary model (Freckleton, 2009). PGLS is a regression technique, where the residual error term incorporates the phylogeny of the species in the form of the variance–covariance matrix that would be expected based on the phylogenetic history of the taxa investigated (Rohlf, 2001; Paradis, 2006). The off-diagonal of this variance–covariance matrix can be adjusted to conform with different models of trait evolution assuming varying degrees of phylogenetic signal in the model residuals. For this transformation, we applied Pagel's model that modifies covariances between species by multiplying with a constant, λ, that can vary between 0 and 1. When residuals are phylogenetically uncorrelated, the phylogenetic scaling parameter is set to $\lambda = 0$, and the results are formally equivalent with the outcomes of the ordinary least square regression that uses species as data units without accounting for their phylogenetic relationship. When there is a strong phylogenetic signal within the data, $\lambda = 1$, the results correspond to what could be detected by using the approach based on phylogenetically independent contrasts (PIC) assuming Brownian motion model of evolution (Felsenstein, 1985). The value of the phylogenetic signal λ can be determined based on model fit; thus, we always adjusted this parameter to the value that provided the ML given the data and model at hand.

PGLS regressions were performed in R v.2.12 (R Development Core Team, 2011) using the package 'phylolm' (Ho & Ané, 2014).

Species means were taken for each variable and a phylogenetic principal components analysis (PCA) was performed on them to account for correlation structure of these variables while also taking into the account

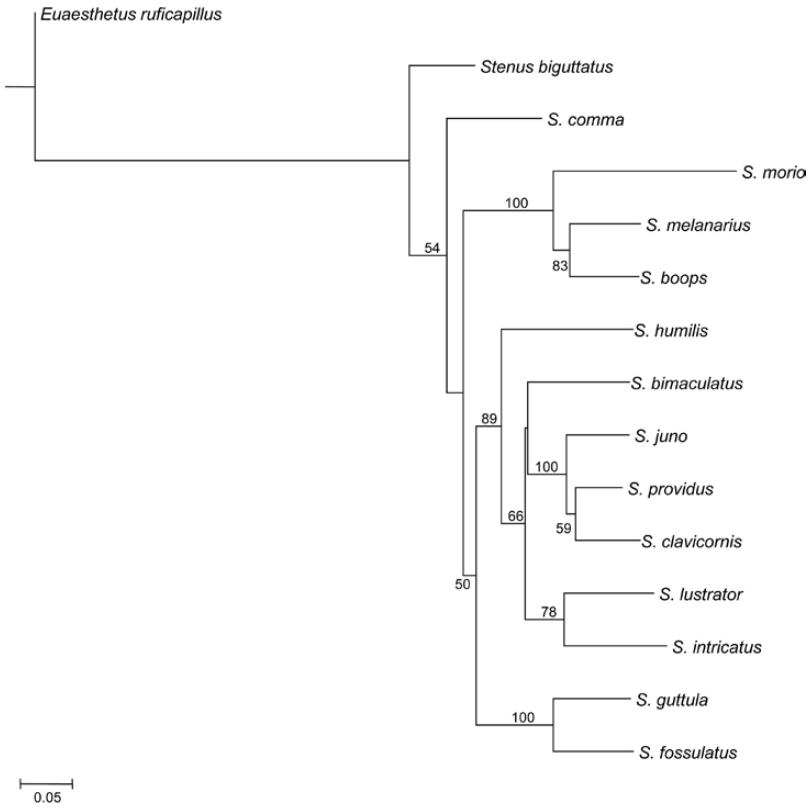

Figure 3. Phylogenetic tree for 14 *Stenus* species investigated based on mitochondrial cytochrome *c* oxidase I (*COI*) sequences resulting from the maximum-likelihood analysis (see Table 1 for species details). Bootstrap values >50% are indicated.

the phylogenetic history through the optimization of λ by using the package 'phytools' (Revell, 2012). We have extracted the first principal components from these analyses given that they explained a large proportion of variance in the data (see Table 7 for details). We performed these PCAs separately for the morphological variables and then for the ethological and performance variables and subsequently estimated the correlation between the corresponding two first axes by using PGLS.

RESULTS

PAD MORPHOLOGY

The adhesive pads of the 14 species investigated represent the general type, that is, the ventral surface has the shape of an ellipsoid and is slightly curved and the surface is covered with numerous, terminally branched adhesive outgrowths (Betz, 1996; Fig. 2). Our results confirmed previous investigations by Betz (1996) that show strong interspecific differences in the morphology of the adhesive pads in *Stenus* (Table 3). These differences primarily concerned the surface area, the number of adhesive outgrowths and the degree of branching of a single outgrowth. With regard to the correlation between the various pad parameters (Table 6), the size and complexity of the adhesive pads were related to the length of the labium (which corresponds to body size). Thus, larger species also possessed longer labia, larger adhesive pads with larger numbers of adhesive outgrowths and adhesive contacts (i.e. the number of adhesive outgrowths per adhesive pad multiplied by the number of terminal ramifications per adhesive outgrowth). The size of the adhesive pads was positively correlated with both the number of adhesive outgrowths and the number of adhesive contacts, whereas the density of the adhesive outgrowths showed a negative correlation with the adhesive surface area (Table 6).

The pad area increased with pronotum length (L_p) with an exponent of 2.46 (PGLS slope, 95% confidence interval (CI): 1.13, 3.79); Fig. 4A, Table 5), which was higher, although not significantly different from L_p^2 as expected through isometry (difference from slope of 2: $t = 0.686$, $P > 0.05$, d.f. = 12; difference from slope of 3: $t = -0.790$, $P > 0.05$, d.f. = 12). In relation to their body size, the 'surface runners' on bare ground, namely,

Table 5. Relationship between morphological and performance parameters using PGLS analyses (based on branch lengths from Fig. 3)

Parameters	Model	PGLS λ	Effect size ($r_{phylogenetic}$)	Parameter	Estimate ± SE	*t*	*P*
L_p vs. A	gradual	1.000	0.724	Intercept	–2.373 ± 0.118	–20.160	0.000
				slope	2.465 ± 0.677	3.639	0.003
					(1.137, 3.792)		
	speciational	1.000	0.747	Intercept	–2.452 ± 0.107	–22.906	0.000
				slope	2.280 ± 0.587	3.888	0.002
					(1.131, 3.430)		
M_b vs. A	gradual	1.000	0.704	Intercept	–2.906 ± 0.112	–25.879	0.000
				slope	0.833 ± 0.243	3.430	0.005
					(0.357, 1.309)		
	speciational	1.000	0.725	Intercept	–2.946 ± 0.105	–28.127	0.000
				slope	0.773 ± 0.212	3.648	0.003
					(0.358, 1.189)		
F_c vs. F_a	gradual	1.000	0.601	Intercept	0.290 ± 0.255	1.138	0.278
				slope	0.534 ± 0.205	2.606	0.023
					(0.132, 0.935)		
	speciational	1.000	0.474	Intercept	0.156 ± 0.302	0.514	0.616
				slope	0.437 ± 0.235	1.863	0.087
					(–0.023, 0.897)		
L_p vs. F_a	gradual	1.000	0.654	Intercept	–0.207 ± 0.073	–2.821	0.015
				slope	1.265 ± 0.422	2.997	0.011
					(0.437, 2.092)		
	speciational	1.000	0.661	Intercept	–0.265 ± 0.067	–3.976	0.002
				slope	1.115 ± 0.366	3.050	0.010
					(0.398, 1.831)		
M_b vs. F_a	gradual	1.000	0.636	Intercept	–0.480 ± 0.069	–6.935	0.000
				slope	0.428 ± 0.150	2.856	0.015
					(0.134, 0.721)		
	speciational	1.000	0.650	Intercept	–0.508 ± 0.064	–7.957	0.000
				slope	0.383 ± 0.129	2.963	0.012
					(0.130, 0.636)		
A vs. F_a	gradual	0.000	0.963	Intercept	1.153 ± 0.117	9.883	0.000
				slope	0.564 ± 0.046	12.340	0.000
					(0.475, 0.654)		
	speciational	0.668	0.924	Intercept	1.032 ± 0.171	6.037	0.000
				slope	0.524 ± 0.063	8.377	0.000
					(0.402, 0.647)		
A vs. T	gradual	1.000	–0.913	Intercept	0.871 ± 0.119	7.333	0.000
				slope	–0.428 ± 0.047	–9.200	0.000
					(–0.520, –0.337)		
	speciational	0.759	–0.907	Intercept	0.726 ± 0.175	4.154	0.001
				slope	–0.477 ± 0.064	–7.472	0.000
					(–0.602, –0.352)		
L_p vs. T	gradual	1.000	–0.685	Intercept	1.867 ± 0.063	29.627	0.000
				slope	–1.181 ± 0.363	–3.258	0.007
					(–1.892, –0.471)		
	speciational	0.914	–0.692	Intercept	1.884 ± 0.061	31.160	0.000
				slope	–1.149 ± 0.346	–3.325	0.006
					(–1.826, –0.472)		
M_b vs. T	gradual	1.000	–0.661	Intercept	2.121 ± 0.060	35.327	0.000
				slope	–0.397 ± 0.130	–3.055	0.010
					(–0.651, –0.142)		
	speciational	0.887	–0.666	Intercept	2.131 ± 0.057	37.211	0.000
				slope	–0.383 ± 0.124	–3.097	0.009
					(–0.625, –0.140)		

Shown are parameter estimates with standard errors (SE) and lower/upper 95% confidence interval of slope b (in brackets). Abbreviations: A, adhesive pad area; L_p, pronotum length; M_b, body mass; F_a, adhesive force; F_c, compressive force; T, tenacity.

Table 6. Correlations between morphological, performance and ethological parameters based on PGLS analyses

	PL	BM	LL	AF	CF	T	PA	AO	RO	AC	DO	DC	CS	CL	AS	AL
Pronotum length (PL)	1	**0.977**	**0.886**	**0.654**	0.137	**–0.685**	**0.724**	**0.623**	0.303	**0.540**	–0.407	–0.033	**0.619**	**0.691**	–0.430	–0.495
		0.000	**0.000**	**0.011**	0.639	**0.007**	**0.003**	**0.017**	0.292	**0.046**	0.148	0.911	**0.024**	**0.009**	0.143	0.086
		0.000	**1.000**	**1.000**	1.000	**1.000**	**1.000**	**1.000**	1.000	**1.000**	0.000	0.000	**0.000**	**0.964**	0.000	0.935
Body mass (BM)	**0.968**	1	**0.835**	**0.636**	0.125	**–0.661**	**0.704**	**0.584**	0.172	0.463	–0.230	–0.031	**0.631**	**0.692**	–0.457	–0.498
	0.000		**0.000**	**0.014**	0.671	**0.010**	**0.005**	**0.028**	0.558	0.095	0.429	0.916	**0.021**	**0.009**	0.117	0.083
	0.920		**1.000**	**1.000**	1.000	**1.000**	**1.000**	**1.000**	1.000	1.000	1.000	1.000	**0.000**	**1.000**	0.000	0.924
Labium length (LL)	**0.887**	**0.818**	1	**0.734**	0.089	**–0.744**	**0.806**	**0.668**	**0.543**	**0.665**	–0.529	0.131	**0.569**	**0.774**	0.103	–0.220
	0.000	**0.000**		**0.003**	0.762	**0.002**	**0.000**	**0.009**	**0.045**	**0.009**	0.052	0.655	**0.042**	**0.002**	0.737	0.471
	0.925	**1.000**		**1.000**	1.000	**1.000**	**1.000**	**1.000**	**1.000**	**1.000**	0.000	0.000	**0.000**	**0.503**	0.000	0.978
Adhesive force (AF)	**0.661**	**0.650**	**0.674**	1	**0.601**	**–0.703**	**0.963**	**0.965**	0.468	**0.855**	–0.391	0.097	0.487	**0.953**	0.038	0.025
	0.010	**0.012**	**0.008**		**0.023**	**0.005**	**0.000**	**0.000**	0.092	**0.000**	0.167	0.741	0.091	**0.000**	0.902	0.935
	1.000	**1.000**	**1.000**		**1.000**	**1.000**	**0.000**	**0.964**	1.000	**1.000**	1.000	1.000	1.000	**0.000**	1.000	1.000
Compressive force (CF)	0.073	0.055	0.047	0.474	1	–0.396	**0.537**	**0.570**	0.034	0.410	–0.193	–0.061	0.522	**0.626**	–0.015	0.494
	0.805	0.853	0.872	0.087		0.162	**0.047**	**0.033**	0.907	0.146	0.509	0.836	0.067	**0.022**	0.960	0.086
	1.000	1.000	1.000	1.000		1.000	**1.000**	**1.000**	1.000	1.000	1.000	1.000	1.000	**1.000**	0.000	0.000
Tenacity (T)	**–0.688**	**–0.659**	**–0.757**	**–0.639**	–0.280	1	**–0.913**	**–0.644**	–0.347	**–0.553**	**0.708**	0.186	**–0.575**	**–0.817**	0.117	–0.031
	0.007	**0.010**	**0.002**	**0.014**	0.333		**0.000**	**0.013**	0.225	**0.040**	**0.005**	0.524	**0.040**	**0.001**	0.702	0.921
	0.989	**0.983**	**1.000**	**0.957**	1.000		**1.000**	**1.000**	1.000	**1.000**	**0.000**	0.000	**0.000**	**0.000**	0.000	0.951
Pad area (PA)	**0.747**	**0.725**	**0.801**	**0.924**	0.406	**–0.903**	1	**0.938**	0.447	**0.773**	**–0.644**	–0.025	**0.635**	**0.938**	–0.055	0.016
	0.002	**0.003**	**0.001**	**0.000**	0.149	**0.000**		**0.000**	0.109	**0.001**	**0.013**	0.933	**0.020**	**0.000**	0.859	0.959
	1.000	**1.000**	**1.000**	**0.668**	1.000	**0.969**		**0.000**	1.000	**1.000**	**0.000**	0.000	**0.000**	**0.000**	0.000	0.945
Number of adhesive outgrowths (AO)	**0.617**	**0.592**	**0.612**	**0.961**	0.446	**–0.601**	**0.926**	1	**0.563**	**0.927**	–0.360	0.202	0.360	**0.923**	–0.153	–0.036
	0.019	**0.026**	**0.020**	**0.000**	0.110	**0.023**	**0.000**		**0.037**	**0.000**	0.206	0.489	0.227	**0.000**	0.617	0.907
	1.000	**1.000**	**0.938**	**0.762**	1.000	**0.813**	**0.000**		**1.000**	**1.000**	1.000	1.000	1.000	**0.000**	1.000	0.968
Ramifications per outgrowth (RO)	0.302	0.167	0.516	0.343	0.115	–0.285	0.352	0.477	1	**0.822**	**–0.606**	**0.567**	–0.189	0.371	–0.020	0.016
	0.295	0.569	0.059	0.229	0.696	0.323	0.217	0.085		**0.000**	**0.022**	**0.035**	0.535	0.213	0.948	0.957
	1.000	1.000	1.000	1.000	1.000	1.000	1.000	1.000		**1.000**	**0.000**	**0.000**	0.587	0.785	0.000	0.958
Number of adhesive contacts per pad (AC)	0.528	0.454	**0.618**	**0.781**	0.235	–0.469	**0.701**	**0.892**	**0.814**	1	–0.367	0.411	0.111	**0.834**	–0.197	–0.069
	0.052	0.103	**0.019**	**0.001**	0.418	0.091	**0.005**	**0.000**	**0.000**		0.197	0.144	0.718	**0.000**	0.520	0.822
	1.000	1.000	**0.944**	**1.000**	1.000	0.927	**0.882**	**1.000**	**0.979**		1.000	1.000	1.000	**0.000**	1.000	1.000
Density of adhesive outgrowths (DO)	–0.372	–0.277	**–0.532**	–0.384	–0.120	**0.674**	**–0.658**	–0.452	**–0.593**	**–0.554**	1	0.277	–0.316	–0.328	–0.130	–0.209
	0.190	0.337	**0.050**	0.175	0.682	**0.008**	**0.010**	0.105	**0.025**	**0.040**		0.338	0.292	0.274	0.671	0.494
	0.000	1.000	**0.000**	1.000	1.000	**0.000**	**0.000**	0.790	**0.000**	**0.561**		0.000	0.000	0.746	0.000	1.000
Density of adhesive contacts (DC)	–0.201	–0.102	0.061	0.034	–0.147	0.253	–0.054	0.152	**0.650**	0.423	0.199	1	–0.328	0.186	–0.162	–0.213
	0.492	0.728	0.835	0.909	0.615	0.383	0.855	0.604	**0.012**	0.132	0.495		0.275	0.543	0.598	0.485
	0.000	1.000	0.000	1.000	1.000	0.000	0.000	1.000	**0.000**	1.000	0.000		0.483	0.966	0.000	1.000
Capture success -small springtails (CS)	**0.630**	**0.657**	**0.555**	0.350	0.489	–0.549	**0.607**	0.174	–0.375	0.124	–0.189	–0.507	1	**0.681**	0.031	0.011
	0.021	**0.015**	**0.049**	0.241	0.090	0.052	**0.028**	0.569	0.206	0.686	0.536	0.077		**0.010**	0.919	0.973
	0.000	**0.000**	**0.000**	1.000	1.000	0.000	**0.000**	1.000	0.715	1.000	0.574	0.632		**1.000**	0.000	0.950
Capture success -large springtails (CL)	**0.659**	**0.658**	**0.710**	**0.940**	0.511	**–0.722**	**0.938**	**0.917**	0.303	**0.806**	–0.320	0.147	**0.569**	1	0.050	0.006
	0.014	**0.015**	**0.007**	**0.000**	0.074	**0.005**	**0.000**	**0.000**	0.315	**0.001**	0.287	0.631	**0.042**		0.871	0.985
	1.000	**1.000**	**0.726**	**0.000**	1.000	**0.517**	**0.000**	**0.000**	1.000	**0.000**	0.804	1.000	**0.741**		0.000	0.953
Attacks with labium -small springtails (AS)	–0.448	–0.507	–0.060	–0.089	–0.034	0.181	–0.026	–0.234	–0.201	–0.300	–0.126	–0.071	0.054	–0.015	1	**0.766**
	0.125	0.077	0.846	0.774	0.913	0.553	0.934	0.441	0.509	0.319	0.682	0.817	0.860	0.961		**0.002**
	0.000	0.000	0.000	1.000	0.000	0.000	0.000	1.000	0.000	1.000	0.000	0.000	0.000	0.000		**1.000**
Attacks with labium -large springtails (AL)	**–0.671**	**–0.679**	–0.398	0.293	0.483	–0.153	0.216	0.303	0.087	0.281	–0.061	0.333	0.059	0.171	**0.745**	1
	0.012	**0.011**	0.178	0.331	0.094	0.618	0.478	0.314	0.777	0.352	0.843	0.266	0.847	0.576	**0.003**	
	0.874	**0.866**	0.911	1.000	0.000	0.893	0.939	1.000	0.956	1.000	0.875	0.000	0.890	0.973	**1.000**	

Results on PGLS for gradual character evolution (based on branch lengths from Fig. 3) are given above the diagonal; results on PGLS for speciational character evolution (branch length set to 1) are given below the diagonal. Bold values indicate significant correlations. First values indicate correlation coefficient r, second values p-value, third values PGLS λ.

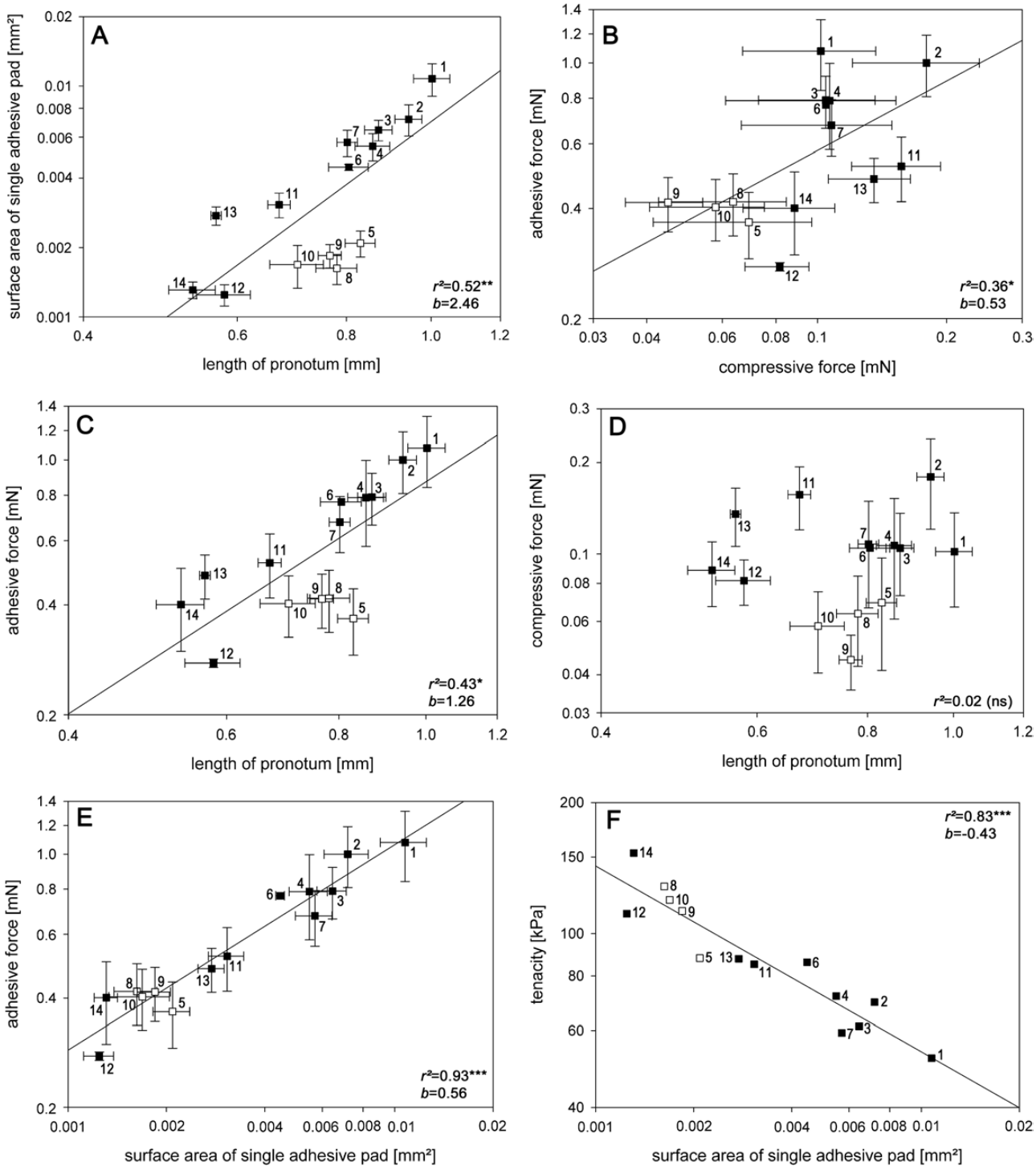

Figure 4. Relationships between length of pronotum (as a measure of body size), morphological and performance parameters of the prey-capture apparatus of *Stenus* beetles (log-log plots). Trend lines were computed using phylogenetic regression (PGLS) for gradual model of character evolution (see also Table 5). Filled squares represent inhabitants of moist humus or plant debris near the ground (pl de in Table 2), open squares represent 'surface runners' on bare ground (ba gr in Table 2). See Table 2 for species labels.

S. biguttatus, *S. fossulatus*, *S. guttula* and *S. comma*, possess only small adhesive pads and therefore do not fit well to the regression line (cf. open squares in Fig. 4A). Omitting these species from the analysis, the remaining species showed a stronger relationship between the adhesive pad area and the pronotum length ($r = 0.953$, $P < 0.001$, d.f. = 9, $\lambda = 0$) and a higher scaling exponent (2.929; 95% CI: 2.28, 3.57), which differed significantly from the increase expected through isometry (difference from slope of 2: $t = 2.82$, $P = 0.022$, d.f. = 8).

In agreement with the pronotum length allometry, the adhesive pad area scaled with body mass to the power of 0.83 (95% CI: 0.36, 1.31) (Table 5), which was higher, although not significantly different than the value of 2/3 expected for isometry (difference from slope of 2/3: $t = 0.711$, $P > 0.05$, d.f. = 12). Omitting the 'surface runners' from this analysis, the remaining species demonstrate a strong relationship between both parameters ($r = 0.938$, $P < 0.001$, d.f. = 9, $\lambda = 0$) and a higher scaling exponent (1.009; 95% CI: 0.75, 1.27) that is significantly different from the increase expected through isometry (difference from slope of 2/3: $t = 2.59$, $P < 0.05$, d.f. = 8).

Comparison of compressive and adhesive forces

Force sensors were used to measure both the impact (compressive) forces and the resulting adhesive forces *in vivo* with respect to the head of an insect pin. These experiments revealed strong interspecific differences in both the compressive and the adhesive forces (Table 2, Fig. 4B).

Compressive forces differed significantly among the species tested (one-way ANOVA: $F_{13,255} = 26.14$, $P < 0.001$). Mean absolute values of compressive forces ranged from 0.05 mN in *S. biguttatus* to 0.18 mN in *S. juno* (Table 2). The lowest absolute values were observed in the group of the middle-sized 'surface runners' on bare ground (*S. biguttatus*, *S. fossulatus*, *S. guttula* and *S. comma*; cf. open squares in Fig. 4B). In comparison with these species, the small-sized taxa *S. melanarius*, *S. boops*, *S. morio* and *S. humilis* developed higher compressive forces (Table 2). Phylogenetic regression analyses revealed that compressive forces were independent of the size of the beetles, that is, pronotum length and body mass (Fig. 4D, Table 6); thus, larger *Stenus* species did not generate higher compressive forces. An important result was the correlation between the compressive forces and adhesive forces (PGLS analysis: $r = 0.601$, $P = 0.023$; Fig. 4B), which indicated a pressure-sensitive adhesive mechanism. Adhesive forces were related to compressive forces to the power of 0.53 (95% CI: 0.13, 0.93) (Fig. 4B). This allometric exponent was significantly lower from a slope of 1 as expected through isometry (difference from slope of 1: $t = 2.279$, $P < 0.05$, d.f. = 12). Compressive forces were also positively related to the surface area of the adhesive pads and to the number of adhesive outgrowths (all $P < 0.05$; Table 6).

Adhesive forces differed significantly among species (one-way ANOVA: $F_{13,255} = = 68.38$, $P < 0.001$). The absolute values of the adhesive forces, which ranged from 0.28 in *S. morio* to 1.08 mN in *S. bimaculatus*, were nearly one order of magnitude higher than the compressive forces (Table 2). Adhesive forces scaled as pronotum length$^{1.26}$ (95% CI: 0.44, 2.09; Fig. 4C). This allometric exponent was lower than, but not significantly different from L_p^2 as predicted through isometry (difference from slope of 2: $t = 1.743$, $P > 0.05$, d.f. = 12). Measurements of the adhesive forces also revealed a scaling coefficient of 0.43 with body mass (95% CI: 0.13, 0.72), not significantly different from the prediction for area scaling (difference from slope of 2/3, $t = 1.597$, $P > 0.05$, d.f. = 12; Table 5).

In relation to body size, the 'surface runners' on bare ground had reduced adhesive abilities (cf. open squares in Fig. 4C). Excluding these species from the analysis, the remaining species showed a highly significant relationship between the adhesive force and the length of the pronotum ($r = 0.940$, $P < 0.001$, d.f. = 9) and a slope of 1.674 (95% CI: 1.25, 2.10), which was not significantly different from L_p^2 as predicted through isometry (difference from slope of 2: $t = 1.516$, $P > 0.05$, d.f. = 8).

Our force measurements revealed a highly significant relationship between the adhesive forces and the pad area ($r = 0.963$, $P < 0.001$, d.f. = 12; Fig. 4E). Thus, adhesive forces were related to the adhesive pad area to the power of 0.56 (95% CI: 0.47, 0.65). This slope was not significantly different from a value of 0.5 (difference from slope of 0.5: $t = 1.407$, $P > 0.05$, d.f. = 12) but significantly different from a value of 1 (difference from slope of 1: $t = 9.534$, $P < 0.001$, d.f. = 12).

Additionally, the adhesive force was positively correlated with the number of adhesive outgrowths and adhesive contacts (Table 6). Instead, the number of ramifications per adhesive outgrowth ($r = 0.468$, $P = 0.092$) and the density of the adhesive outgrowths ($r = -0.391$, $P = 0.167$) and adhesive contacts ($r = 0.097$, $P = 0.741$) were not related to the adhesive force (Table 6).

Tenacity (adhesive forces per unit contact area)

The mean tenacity, as calculated by dividing the mean adhesive force by the mean surface areas of both adhesive pads, amounted to between 51.9 kPa in *S. bimaculatus* and 153.2 kPa in *S. humilis* (Table 2).

The tenacity decreased with the surface area of the adhesive pad (PGLS slope –0.43, 95% CI: –0.52, –0.34; Fig. 4F, Table 5). Additionally, the tenacity showed negative correlations with the size parameters, that is, pronotum length and body mass (Table 6). Thus, although species with smaller adhesive pads (which usually corresponded to smaller body sizes) generated lower absolute values of the adhesive forces, they attained higher tenacities and therefore had more adhesively efficient pads.

Predation

In agreement with previous investigations (Betz, 1996, 1998a, b, 2006), most *Stenus* species (except *S. morio*) tended to decrease the percentage of labial attacks with increasing prey size (i.e. correspondingly, they increased the percentage of attacks with their mandibles) (Table 4). These differences in the frequency of usage of the labium towards small and large springtails were significant for *S. bimaculatus*, *S. comma*, *S. fossulatus*, *S. biguttatus* and *S. guttula* (Mann–Whitney *U* tests, all $P < 0.001$), *S. boops* (Mann–Whitney *U* test, $P < 0.01$) and *S. juno* (Mann–Whitney *U* test, $P < 0.05$). The 'surface runners' on bare ground, namely, *S. fossulatus*, *S. guttula*, *S. comma* and *S. biguttatus*, even changed the type of attack depending on prey size, since the percentage of attacks with the mandibles distinctly increased for large springtails (Table 4). The species *S. lustrator*, *S. providus*, *S. intricatus*, *S. clavicornis* and *S. morio* showed no significant differences in the frequency of usage of the labium towards small and large springtails (Mann–Whitney *U* tests, all $P > 0.05$). When using their labium, most species (except *S. intricatus*) attacked small springtails significantly more successfully than large ones (Mann–Whitney *U* tests, all $P < 0.001$; Fig. 5, Table 4).

The prey-capture success depends on the morphology of the adhesive pads. The PGLS analysis revealed a correlation between the prey-capture success and the surface area of the adhesive pads for both small ($r = 0.635$, $P = 0.020$) and large springtails ($r = 0.938$, $P < 0.001$) (Table 6). For large springtails, the prey-capture success was additionally related to the number of adhesive outgrowths ($r = 0.923$, $P < 0.001$) and the number of adhesive contacts ($r = 0.834$, $P < 0.001$).

The analysis revealed that the adhesive forces attained by the various pad morphologies influenced the prey-capture success towards large springtails ($r = 0.953$, $P < 0.001$; Fig. 5), while this relationship was significant only at a 0.1 significance level for small springtails ($r = 0.487$, $P = 0.091$; Fig. 5). Thus, higher adhesive forces lead to higher prey-capture success rates in *Stenus* beetles; this effect was more pronounced towards large-sized springtails.

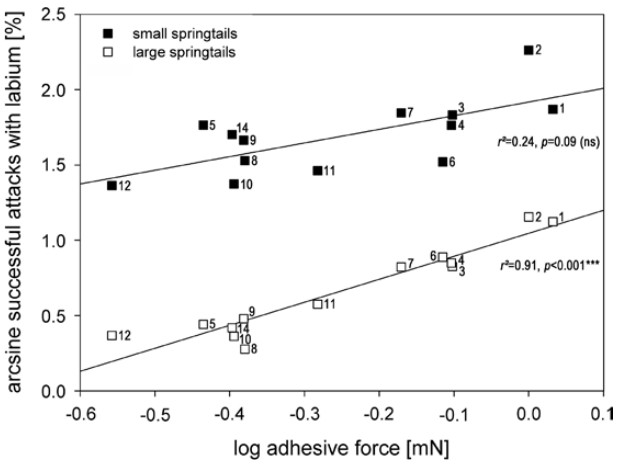

Figure 5. Relationship between the adhesive force and the prey-capture success with the labium towards small (filled squares) and large springtails (open squares). Trend lines were computed using phylogenetic regression (PGLS) for gradual model of character evolution. See Table 2 for species labels.

Relationships between morphology, predatory behaviour and adhesive performance

In order to determine the morphological space occupied by the *Stenus* species investigated, a phylogenetic PCA including all morphological parameters was performed (Table 7, Fig. 6). This analysis extracted three factors that accounted for 93.6% of the total variance (Table 7). The first factor that accounted to 62.2% of the variance contained several parameters of the prey-capture apparatus and parameters of size (pronotum length, body mass). This factor contrasted species with large complex-structured adhesive pads (i.e. with large numbers of adhesive outgrowths and adhesive contacts), large body size and long labia (such as *S. bimaculatus*, *S. juno*, *S. clavicornis*, *S. providus*) with species with small, simple-structured adhesive pads, short labia and smaller body size (such as *S. humilis*, *S. morio*, *S. comma*, *S. biguttatus*).

A second phylogenetic PCA was conducted with all ethological and performance traits (Table 7). This analysis revealed three factors that explained 88.7% of the total variation. The first factor accounted to 56.3% and contrasted species which generated high adhesive and compressive forces, low tenacities and achieved high prey-capture success rates, especially towards large springtails (i.e. *S. juno*, *S. bimaculatus*, *S. clavicornis*, *S. lustrator*), with species with low adhesive and compressive forces, high tenacities, and low prey-capture success rates, such as *S. guttula*, *S. fossulatus*, *S. morio*, *S. biguttatus*, *S. comma* and *S. humilis* (Table 7, Fig. 6).

The PGLS analysis revealed a high correlation between both the first morphological and the

Table 7. Loadings of phylogenetic principal component analyses of morphological (PCA I; PGLS λ = 0.000) and ethological and performance parameters (PCA II; PGLS λ = 0.000) for gradual evolution model (based on branch lengths from Fig. 3) (see also Fig. 6)

	PC1	PC2	PC3
PCA I (morphology)			
% Variance	62.23%	19.23%	12.12%
Variable			
Area of the adhesive pad	**–0.928**	–0.087	0.131
Labium length	**–0.923**	–0.200	–0.189
Adhesive outgrowths per pad	**–0.918**	0.147	0.044
Adhesive contacts per pad	**–0.911**	0.378	0.070
Pronotum length	**–0.811**	–0.456	–0.299
Body mass	**–0.757**	–0.523	–0.368
Ramifications per outgrowth	**–0.705**	**0.619**	0.159
Density of adhesive outgrowths	**0.670**	0.066	**–0.695**
Density of adhesive contacts	–0.198	**0.806**	–0.547
PCA II (behaviour/performance)			
% Variance	56.29%	23.76%	8.68%
Variable			
Successful attacks with labium – large springtails	**–0.960**	0.117	–0.064
Adhesive force	**–0.938**	0.094	–0.012
Tenacity	**0.867**	–0.190	–0.066
Compressive force	**–0.805**	–0.136	0.447
Successful attacks with labium – small springtails	**–0.747**	0.184	–0.530
Attacks with labium – large springtails	–0.424	**–0.845**	0.152
Attacks with labium – small springtails	–0.039	**–0.915**	–0.309

Bold values indicate eigenvector scores >0.6 and <–0.6.

first ethological/performance factor (r = 0.758, P = 0.003; Fig. 6).

DISCUSSION

In our previous studies concerning force measurements, we investigated the influence of the surface energy and surface roughness on the adhesive performance of the prey-capture apparatus in two similarly sized *Stenus* species (Koerner *et al.*, 2012a) and described the possible functional features of various parts of their adhesive system (Koerner *et al.*, 2012b). These investigations revealed that neither the surface energy nor the surface roughness had a considerable effect on adhesive performance (Koerner *et al.*, 2012a). The roughness independence can probably be attributed to different functional elements of their adhesive pads acting synergistically during the process of prey-capture (cf. fig. 9 in Koerner *et al.*, 2012b). In the present study, performance tests extended our mechanistic understanding with regard to the way that different pad morphologies are linked to differences in the adhesive performance, the predatory behaviour and the prey-capture success of various *Stenus* species. This knowledge is important to improve our

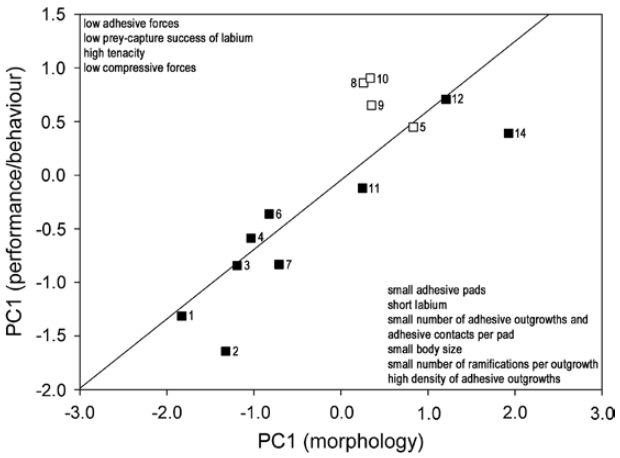

Figure 6. Relationship between morphology, performance, and behaviour in *Stenus* based on phylogenetic principal component analyses, using the gradual model of character evolution. See Table 7 for factor loadings. Trend line was computed using phylogenetic regression (PGLS) for gradual model of character evolution (PGLS λ = 0.830, r = 0.758, P = 0.003). Filled squares represent inhabitants of moist humus or plant debris near the ground (pl de in Table 2), open squares represent 'surface runners' on bare ground (ba gr in Table 2). See Table 2 for species labels.

comprehension of the evolution of their highly specialized labial prey-capture device.

Compressive force

In the *Stenus* prey-capture apparatus, a substantial compressive force is attained, because (1) the distance to the prey that must be bridged by the labium only amounts to half the length of the labium (Betz, 1996; Koerner *et al.*, 2012a, b) and (2) the species often perform forward lunges during the predatory strike (Betz, 1996, 1998a). Interestingly, compressive forces in *Stenus* are independent of the body size (Fig. 4D, Table 6). Thus, variations of the attack distance set by the beetles prior to the predatory strike are probably responsible for the interspecific differences in the compressive forces exerted by the labium (Betz, 1996, 1998a; Koerner *et al.*, 2012a, b), although this assumption has to be tested in further experiments. Since increased haemolymph pressure causes the protrusion of the labium (Kölsch & Betz, 1998), differences in the haemolymph pressure generated might also be responsible for variations in the compressive forces.

The effect of higher compressive forces on the adhesive performance can be seen by a comparison of *S. juno* and *S. bimaculatus*. *Stenus juno* specimens achieve nearly twice the compressive forces of *S. bimaculatus* and therefore attain almost the same adhesive properties, although the latter species has a 30% larger pad area (Koerner *et al.*, 2012a, b). Higher compressive forces might reduce the thickness of the secretion layer between the prey and the adhesive pad surface (cf. Bowden & Tabor, 1986) and squeeze the adhesive secretion into the surface irregularities of the prey, thus enhancing the effective contact area and therefore adhesion. Taken together, our experiments strongly suggest that the involved adhesive mechanism is pressure-sensitive, that is, that higher compressive forces result in better adhesive performances (Figs 4B, 6).

Another interesting aspect is the reduced compressive force established by species that hunt in sparsely vegetated habitats (*S. comma*, *S. biguttatus*, *S. fossulatus*, *S. guttula*). The physiological mechanism accounting for their low compressive forces is unknown but might be correlated with an assumed ongoing reduction of the prey-capture apparatus of these species, which have instead improved their mandibular prey-capture mechanism (see below).

Adhesive force

Betz (1996) has suggested that for an improvement of the performance of the adhesive pads in *Stenus* species, it might be advantageous to spread a large number of adhesive outgrowths and contacts over adhesive pads that should be as extensive as possible. Our analyses support this view, since we have shown that an enlargement of the adhesive pads, together with an increase in the number of its adhesive outgrowths and adhesive contacts, leads to an increase in adhesive performance (Figs 4E, 6, Table 6). In contrast, adhesive pads in which only the degree of branching of a single outgrowth or the density of the adhesive outgrowths and contacts is increased without a simultaneous increase in their pad area (e.g. in *S. morio*, *S. humilis*, *S. comma*, *S. guttula*) have a lower advantage regarding their adhesive performance (Table 6).

In *Stenus* beetles, adhesive forces scaled with pronotum length (slope: 1.26; Fig. 4C) and body mass (slope: 0.43; Table 5) at a lower rate, whereas the adhesive pad area scaled with pronotum length (slope: 2.46; Fig. 4A) and body mass (slope: 0.83; Table 5) at a higher rate than predicted from isometry. Consequently, the adhesive force increases with the pad area to a lower extent than predicted from isometry (slope: 0.56; Fig. 4E). Accordingly, the gain in terms of adhesion attained by an increase of the adhesive pad area seems to be limited, for example a ten-fold increase in the adhesive pad area (from *c*. 0.001 mm^2 in *S. morio* to 0.01 mm^2 in *S. bimaculatus*) only results in a nearly four-fold increase of the adhesive force (from 0.28 mN in *S. morio* to 1.08 mN in *S. bimaculatus*). Hence, the gain in the adhesive performance that is attainable by an increase in pad size seems to be limited. Indeed, the adhesive pads of the species *S. bimaculatus* seem to have reached an upper size limit of the ellipsoid-shaped type of adhesive pads that is the most common type among *Stenus* species, because this species has the largest pads out of 230 species measured (L.K. & O.B., unpubl. data). Similar constraints of the pad size are described from the adhesive tarsi of syrphid flies (Gorb, Gorb & Kastner, 2001). The authors explained this constraint with problems in the operation of a large attachment area so that a smaller number of setae would be able to make contact with the substratum. Further constraints in the pad size of *Stenus* beetles probably arise, since a much larger amount of adhesive secretion and a more effective stabilization and protection from mechanical damage would be required for larger adhesive pads. Furthermore, extremely large adhesive pads would cause spatial competition with other mouthparts, such as the maxillae and mandibles (Betz, 1996).

Comparison of scaling relationships with other biological adhesive structures

Due to their smaller surface-to-volume ratio, and because it becomes increasingly difficult to distribute load uniformly across large contact area, larger animals are expected to attach less well to surfaces

(Labonte & Federle, 2015). Thus, in order to compensate for this decrease of weight-specific adhesion, large animals could evolve overproportionally large pads, or adaptations that increase attachment efficiency (adhesion or friction per unit contact area). Labonte & Federle (2015) summarize the available data on scaling relationships between adhesive pad areas and the resulting attachment forces in different climbing animals. This survey revealed that neither lizards, tree frogs nor insects seem to compensate the predicted loss of adhesion by positive allometry of the size of their adhesive pads – most data for interspecific scaling revealed that the attachment pad area scales close to isometry or even with negative allometry. In terms of adhesive forces, the scaling coefficients of some climbing animals indicate an increase in pad efficiency with body size, that is, that attachment forces grow faster than pad area (scaling coefficients more than 2 for body length, more than 1 for pad area or more than 0.66 for body mass) to compensate for the weight-specific decrease of adhesion and is thus of high biological relevance (Labonte & Federle, 2015).

The adhesive pads of *Stenus* show a positive allometry with respect to body size, that is, pad area scaled with body mass $M_b^{0.83}$ and with pronotum length $L_p^{2.46}$ (Fig. 4A, Table 5). Thus, larger *Stenus* species have evolved overproportionally larger adhesive pads. However, in contrast to some climbing animals where adhesion grows faster than pad area, that is, the pads' efficiency increases with body size, the adhesive forces in *Stenus* beetles revealed negative allometry, that is, the pads' efficiency decreases with body size (scaling coefficients less than 2 for body length (*Stenus*: 1.26), less than 1 for pad area (*Stenus*: 0.56) or less than 0.66 for body mass (*Stenus*: 0.43)). Accordingly, our results indicate that the adhesive pad area tends to scale positively allometric, whereas adhesive force scales with negative allometry with respect to body size. Thus, larger *Stenus* species evolved overproportionally large adhesive pads that compensate for the decrease in attachment efficiency. According to our previous considerations, the tenacity (force per unit pad area) decreases with an increase of the area of the adhesive pads (Fig. 4F), resulting in smaller pads being adhesively more efficient than larger ones. The reasons underlying the decrease in pad efficiency in larger adhesive pads are still unclear. Similar to the suggestion of Gorb *et al.* (2001) regarding the tarsi of syrphid flies, this might be explainable by the fact that in larger adhesive pads there is a higher risk that not all the adhesive outgrowths come into contact with the surface. According to Betz & Kölsch (2004), the adhesive secretion of *Stenus* species has to spread all over the adhesive pads from a very restricted zone at the outer margin of the beetles' paraglossae. We assume that the secretion spreads more easily over a smaller surface than a larger one; thus, the lower adhesive efficiency of larger pads might also arise from an unequal distribution of the secretion on the adhesive pads. In addition, the negative scaling might mean that the action of the adhesive secretion alone plays a more important role than the size and morphological complexity of the adhesive pads, that is, the adhesive strength of the secretion probably overrides the adhesive impact of the pad size and the intercorrelated number of adhesive contacts. This would be an important functional feature, especially for species with smaller adhesive pads, since it enables them notwithstanding to achieve a relatively high adhesive performance. Hence, the evolution of the adhesive secretion in addition to the pad morphology might have largely improved the functional performance of the prey-capture apparatus in *Stenus* species, providing it with an additional gain of adhesive strength that makes them more independent from the pad size.

Ecomorphological considerations

In the speciose staphylinid genus *Stenus* (>2800 species worldwide), the highly specialized labial prey-capture apparatus has been considered a key innovation that has initiated the evolutionary success of this genus in various habitats (Betz, 2006). Previous studies have revealed that larger and structurally more complex-structured adhesive pads lead to enhanced prey-capture success (Betz, 1996). This conclusion is supported by our experiments and, with the integration of our performance measurements, the prey-capture success can be directly ascribed to the morphology of the adhesive pads. Accordingly, the adhesive forces mainly depend on the size and the structural complexity of the adhesive pads (i.e. the number of adhesive outgrowths and adhesive contacts) and on the compressive forces generated (Tables 6, 7). On the other hand, the negative scaling of the tenacity with the surface area (Fig. 4F) suggests that the adhesive secretion released onto the surface of the adhesive pads makes a large contribution to the total adhesive strength partly overriding the influence of the pure pad size.

One aim of ecomorphological research is to contribute to a mechanistic understanding of the often complex relationship between the morphology and the ecology of a taxon by including performance measurements of ecologically relevant functional systems (e.g. Wainwright, 1991; Reilly & Wainwright, 1994). Figure 6 illustrates the positioning of the species in the morphological and ethological/performance space and therefore summarizes the most important results of our study. Accordingly, at the one end of the spectrum (low scores for both axes) are large species that possess long labia and large adhesive pads with large numbers of adhesive outgrowths and adhesive contacts

that therefore develop high adhesive forces and attain a high prey-capture success, especially towards large springtails.

At the other end of the spectrum (high scores for both axes) are small species with small, simple adhesive pads (i.e. with low numbers of adhesive outgrowths and adhesive contacts), which therefore develop low adhesive forces. Since these species show only low capture success rates with their labium towards large springtails (3–5%), large elusive prey does not seem to be adequate prey for these species. This assumption is confirmed by the observation that small *Stenus* species (e.g. *S. humilis*, *S. boops*) are often not strong enough to pull large springtails into the range of the mandibles and thus the retraction of the labium might fail or last up to one minute (L.K. & O.B., pers. observ.). Instead, the relatively high prey-capture success rates for small springtails (40–60%) indicate that this is a more suitable prey size. Most *Stenus* species investigated are slow-moving and clumsy (cf. species indicated with pl de in Table 2), that is, they cannot pursue fast moving prey accurately and for a long period of time (Betz, 1998b) and mainly use their labial apparatus during prey-capture (Table 4). The biological advantage of the usage of their prey-capture apparatus is that it permits even those predator types of *Stenus*, whose agility and running speed is limited for physiological reasons, to catch prey in a rapid and surprising manner (Betz, 1996, 1998a, b).

In contrast to these less agile predator types, species that forage on bare ground in open habitats (*S. comma*, *S. fossulatus*, *S. guttula*, and *S. biguttatus*) show some interesting morphological and behavioural adaptations, that is, they possess widely protruding eyes with a large number of ommatidia and very long legs and are characterized by a high physiological agility and running speed that enables these species to follow the changes of direction of the unpredictably moving prey precisely and rapidly (Bauer & Pfeiffer, 1991; Betz, 1996, 1998a, b, 1999, 2006). Furthermore, they change the type of attack depending on prey size (i.e. small prey items are predominantly attacked with the labium, whereas large prey is mainly attacked with the mandibles; Table 4). The advantage of this shift in the prey-capture technique is an enhanced prey-capture success rate with the mandibles, which compensates the adhesive performance failure of their small labial adhesive pads towards large prey. For example, when catching large springtails with their labium, these species exhibit success rates of only 2–6 % (cf. open squares in Fig. 5, Table 4), whereas by means of their mandibles, this rate increases to 20–40% (Betz, 1996, 1998a, 2006). According to Betz (1998b), the selective value of the use of the mandibles in these species probably lies in an extension of the feeding niche, since this attack type enables these beetles to catch large prey that are fast moving and that are capable of rapid escape responses. Thus, these species depend to a lesser degree on their labial prey-capture apparatus (Table 4). Our results are also indicative of a process of possible secondary reduction of their labial prey-capture apparatus, since these species possess, in relation to their body size, extremely small and simple-structured adhesive pads (cf. open squares in Fig. 4A) and generate exceptionally low compressive forces (Fig. 4D). Taken together, both these features result in diminished adhesive abilities of the prey-capture apparatus (Fig. 4C). The improvement of the mandible attack mechanism in these specialists seems to compensate for the limitation of the adhesive strength of the labium towards larger prey. Interestingly, the phylogeny based on 30 *Stenus* species (Koerner *et al.*, 2013) indicates that the agile ecotype has evolved independently at least twice in this genus because the species pairs *S. fossulatus*/*S. guttula* (belonging to the '*guttula*' species group; Puthz, 2008, Koerner *et al.*, 2013) and *S. comma*/*S. biguttatus* (belonging to the '*comma*' species group; Puthz, 2008, Koerner *et al.*, 2013) seem to have no very close phylogenetic relationship, implying that the morphological and behavioural similarities between them result from convergence due to similar ecological demands. Since these species are nested within the genus *Stenus* and cluster within species groups possessing more complex labia, the phylogenetic information available also supports our hypothesis of a secondary reduction of their labial prey-capture apparatus. Interestingly, the secondary reduction (vestigialization) of the labial prey-capture apparatus seems to have also occurred in members of the *S. canaliculatus* group, which possess simplified labia that are largely shortened and have only minute paraglossae (Betz, 1996, 1998, 2006; Koerner *et al.*, 2013).

CONCLUSIONS

One central aim of morphological research in the context of ecological and evolutionary theory is to ascribe differences in resource utilization between organisms to differences in their performance as determined by their morphological and physiological capacities. Instead of retaining the mechanistic basis of ecological phenomena a 'black box' as implicit in many ecological studies, this way, ecologically relevant organismal functions such as prey-capture success towards different types of prey can be explained combining (1) functional morphological studies, (2) measurements of the maximum performance capacity and (3) analyses of actual niche realization. In the present contribution, we use a phylogenetically controlled comparative ecomorphological approach to investigate the functional

and ecological relevance of different morphologies of the predatory adhesive mouthparts of 14 representatives of the beetle genus *Stenus*. Our approach reveals how interspecific differences in the surface area of the adhesive pads (paraglossae) found at the labial tips lead to differences in the adhesive forces generated during the predatory attack and this way influences the prey-capture success towards springtails. This largely contributes to a mechanistic understanding of the ecomorphological radiation and niche evolution of this megadiverse beetle taxon.

ACKNOWLEDGEMENTS

We thank Karl-Heinz Hellmer and Monika Meinert for taking the scanning electron micrographs. This study was partly financed by the German Science Foundation (project PAK 478: BE 2233/10–1). LZG was supported by funds from The Ministry of Economy and Competitiveness (Spain) (CGL2015-70639-P) and The National Research, Development and Innovation Office (NKFIH, K-115970). Dr. Theresa Jones corrected the English. The authors declare no conflicts of interests.

REFERENCES

Bauer T, Pfeiffer M. 1991. 'Shooting' springtails with a sticky rod: the flexible hunting behaviour of *Stenus comma* (Coleoptera; Staphylinidae) and the counter-strategies of its prey. *Animal Behaviour* **41:** 819–828.

Betz O. 1996. Function and evolution of the adhesion-capture apparatus of *Stenus* species (Coleoptera, Staphylinidae). *Zoomorphology* **116:** 15–34.

Betz O. 1998a. Comparative studies on the predatory behaviour of *Stenus* spp. (Coleoptera: Staphylinidae): the significance of its specialized labial apparatus. *Journal of Zoology London* **244:** 527–544.

Betz O. 1998b. Life forms and hunting behaviour of some central European *Stenus* species (Coleoptera, Staphylinidae). *Applied Soil Ecology* **9:** 69–74.

Betz O. 1999. A behavioural inventory of adult *Stenus* species (Coleoptera: Staphylinidae). *Journal of Natural History* **33:** 1691–1712.

Betz O. 2006. Der Anpassungswert morphologischer Strukturen: Integration von Form, Funktion und Ökologie am Beispiel der Kurzflügelkäfer-Gattung *Stenus* (Coleoptera, Staphylinidae). *Entomologie heute* **18:** 3–26.

Betz O. 2008. Ökomorphologie: Die Analyse der Form und Funktion von Strukturen in ihrer Beziehung zur Umwelt. *Entomologia Generalis* **31:** 129–139.

Betz O. 2010. Adhesive exocrine glands in insects: morphology, ultrastructure, and adhesive secretion. In: von Byern J, Grunwald I, eds. *Biological adhesive systems. From nature to technical and medical application*. Berlin: Springer, 111–152.

Betz O, Kölsch G. 2004. The role of adhesion in prey-capture and predator defence in arthropods. *Arthropod Structure & Development* **33:** 3–30.

Betz O, Koerner L, Gorb S. 2009. An insect's tongue as the model for two-phase viscous adhesives? *Adhesion Adhesives & Sealants* **3:** 32–35.

Bowden FP, Tabor D. 1986. *The friction and lubrication of solids*. Oxford: Oxford University Press.

Clarke DJ, Grebennikov VV. 2009. Monophyly of Euaesthetinae (Coleoptera: Staphylinidae): phylogenetic evidence from adults and larvae, review of austral genera, and new larval descriptions. *Systematic Entomology* **34:** 346–397.

Felsenstein J. 1985. Phylogenies and the comparative method. *American Naturalist* **125:** 1–25.

Freckleton RP. 2009. The seven deadly sins of comparative analysis. *Journal of Evolutionary Biology* **22:** 1367–1375.

Garland T, Dickerman AW, Janis CM, Jones JA. 1993. Phylogenetic analysis of covariance by computer simulation. *Systematic Biology* **42:** 265–292.

Gorb S, Gorb E, Kastner V. 2001. Scale effects on the attachment pads and friction forces in syrphid flies (Diptera, Syrphidae). *Journal of Experimental Biology* **204:** 1421–1431.

Harvey PH, Pagel MD. 1991. *The comparative method in evolutionary biology*. Oxford: Oxford University Press.

Heethoff M, Koerner L, Norton RA, Raspotnig G. 2011. Tasty but protected – first evidence of chemical defense in oribatid mites. *Journal of Chemical Ecology* **37:** 1037–1043.

Ho LST, Ané C. 2014. A linear-time algorithm for Gaussian and non-Gaussian trait evolution models. *Systematic Biology* **63:** 397–408.

Koerner L, Gorb SN, Betz O. 2012a. Adhesive performance of the stick-capture apparatus of rove beetles of the genus *Stenus* (Coleoptera, Staphylinidae) toward various surfaces. *Journal of Insect Physiology* **58:** 155–163.

Koerner L, Gorb SN, Betz O. 2012b. Adhesive performance and functional morphology of the stick-capture apparatus of the rove beetles *Stenus* spp. (Coleoptera, Staphylinidae). *Zoology* **115:** 117–127.

Koerner L, Laumann M, Betz O, Heethoff M. 2013. Loss of the sticky harpoon – COI sequences indicate paraphyly of *Stenus* with respect to *Dianous* (Staphylinidae, Steninae). *Zoologischer Anzeiger* **252:** 337–347.

Kölsch G. 2000. The ultrastructure of glands and the production and function of the secretion in the adhesive capture apparatus of *Stenus* species (Coleoptera: Staphylinidae). *Canadian Journal of Zoology* **78:** 465–475.

Kölsch G, Betz O. 1998. Ultrastructure and function of the adhesion-capture apparatus of *Stenus* species (Coleoptera, Staphylinidae). *Zoomorphology* **118:** 263–272.

Labonte D, Clemente CJ, Dittrich A, Kuo C-Y, Crosby AJ, Irschick DJ, Federle W. 2016. Extreme positive allometry of animal adhesive pads and the size limits of adhesion-based climbing. *PNAS* **113:** 1297–1302.

Labonte D, Federle W. 2015. Scaling and biomechanics of surface attachment in climbing animals. Philosophical

Transactions of the Royal Society of London. *Series B: Biological Sciences* **370:** 20140027.

Leschen RAB, Newton AF. 2003. Larval description, adult feeding behavior, and phylogenetic placement of *Megalopinus* (Coleoptera: Staphylinidae). *Coleopterists Bulletin* **57:** 469–493.

Orousset J. 1988. *Faune de Madagascar 71. Insectes Coleopteres Staphylinidae Euaesthetinae.* Paris: Muséum National d'Histoire Naturelle.

Paradis E. 2006. *Analysis of phylogenetics and evolution with R.* New York: Springer.

Posada D. 2006. ModelTest Server: a web-based tool for the statistical selection of models of nucleotide substitution online. *Nucleic Acids Research* **34:** 700–703.

Posada D, Crandall KA. 1998. ModelTest: testing the model of DNA substitution. *Bioinformatics* **14:** 817–818.

Puthz V. 1981. Was ist *Dianous* Leach, 1819, was ist *Stenus* Latreille, 1796? Oder: Die Aporie des Stenologen und ihre taxonomischen Konsequenzen (Coleoptera, Staphylinidae). *Entomologische Abhandlungen Museum für Tierkunde Dresden* **44:** 87–132.

Puthz V. 2008. *Stenus* Latreille und die segensreiche Himmelstochter (Coleoptera Staphylinidae). *Linzer biologische Beiträge* **40:**137–230.

R Development Core Team. 2011. R: A language and environment for statistical computing. The R Foundation for Statistical Computing, Vienna, Austria. Available at: http://www.R-project.org/

Reilly SM, Wainwright PC. 1994. Conclusion: ecological morphology and the power of integration. In: Wainwright PC, Reilly SM, eds. *Ecological morphology.* Chicago: University of Chicago Press, 339–354.

Revell LJ. 2012. phytools: an R package for phylogenetic comparative biology (and other things). *Methods in Ecology and Evolution* **3:** 217–223.

Rohlf FJ. 2001. Comparative methods for the analysis of continuous variables: geometric interpretations. *Evolution* **55:** 2143–2160.

Rohlf FJ. 2004. *TPSDIG. Ver. 2.0.* Stony Brook, NY: Department of Ecology and Evolution, State University of New York, 24 p.

Rohlf FJ. 2006. A comment on phylogenetic correction. *Evolution* **60:** 1509–1515.

Ryvkin AB. 2012. New species and records of *Stenus* (*Nestus*) of the *canaliculatus* group, with the erection of a new species group (Insecta: Coleoptera: Staphylinidae: Steninae). *European Journal of Taxonomy* **13:** 1–62.

Schmitz G. 1943. Le labium et les structures bucco-pharyngiennes du genre *Stenus* LATREILLE. *Cellule* **49:** 291–334.

Swofford DL. 1999. PAUP*. *Phylogenetic Analysis Using Parsimony (*and Other 16 Methods). Version 4*. Sunderland: Sinauer Associates.

Symonds MRE, Blomberg SP. 2014. A primer on phylogenetic generalised least squares. In: Garamszegi LZ, ed. *Modern phylogenetic comparative methods and their application in evolutionary biology: concepts and practice*. Berlin Heidelberg: Springer, 105–130.

Wainwright PC. 1991. Ecomorphology: experimental functional anatomy for ecological problems. *American Zoologist* **31:** 680–693.

Weinreich E. 1968. Über den Klebfangapparat der Imagines von *Stenus* LATR. (Coleopt., Staphylinidae) mit einem Beitrag zur Kenntnis der Jugendstadien dieser Gattung. *Zeitschrift für Morphologie und Ökologie der Tiere* **62:** 162–210.

Publikation IV

The labial adhesive pads of rove beetles of the genus *Stenus* (Coleoptera: Staphylinidae) as carriers of bacteria

Lars Koerner, Volkmar Braun, Oliver Betz

Entomologia Generalis 36 (2016): 33–41

Entomologia Generalis, **Vol. 36 (2016), Issue 1,** 033–041 **Article**
Published in print July 2016

The labial adhesive pads of rove beetles of the genus *Stenus* (Coleoptera: Staphylinidae) as carriers of bacteria

Lars Koerner[1], Volkmar Braun[2] & Oliver Betz*[1]

[1]Institut für Evolution und Ökologie, Abteilung für Evolutionsbiologie der Invertebraten, Universität Tübingen, Auf der Morgenstelle 28E, D-72076 Tübingen, Germany
[2]Max Planck Institut für Entwicklungsbiologie, Spemannstrasse 35, D-72076 Tübingen, Germany, email: volkmar.braun@tuebingen.mpg.de

With 3 figures and 1 table

Abstract: The ground-dwelling staphylinid beetles *Stenus juno* (Paykull, 1789) and *S. bimaculatus* Gyllenhal, 1810, inhabit moist bacterial-rich habitats such as detritus or leaf litter. Transmission electron microscopy has revealed bacteria in high densities immersed in the adhesive secretion exuded by special head glands onto the labial pads that form part of the advanced sticky prey-capture apparatus of these beetles. Using 16S rRNA sequence analysis, we have identified 13 different bacterial sequences, mostly belonging to the Actinomycetales and Pseudomonadales.

Keywords: adhesion – bacteria-insect relationship – mouthparts – secretion

*Corresponding author: oliver.betz@uni-tuebingen.de

1. Introduction

With almost 2,600 species (Puthz 2010, 2013), the genus *Stenus* (Coleoptera, Staphylinidae) is one of the largest beetle genera worldwide. Whereas most representatives of this genus inhabit vegetation, others live in detritus, leaf litter, or mosses (e.g., Betz 1998a, 1999, 2002, Lusebrink, Dettner & Seifert 2008). *Stenus* species possess pygidial glands that release alkaloids that have an antimicrobial effect on entomopathogenic bacteria and fungi (Lusebrink, Dettner & Seifert 2008)

 www.schweizerbart.de
DOI: 10.1127/entomologia/2016/0308 0171-8177/16/0308 $ 2.25

that might be of special importance in the moist habitats that are inhabited by *Stenus* species. Accordingly, the alkaloids (stenusine and norstenusine) protect the beetles from infestation with microorganisms. Moreover, these secretions function in defense against predators by producing a high spreading pressure that acts on the surface of water and that rapidly propels the beetle over the water away from potential predators (e.g., Schildknecht et al. 1976, Enders et al. 1993). *Stenus* beetles are

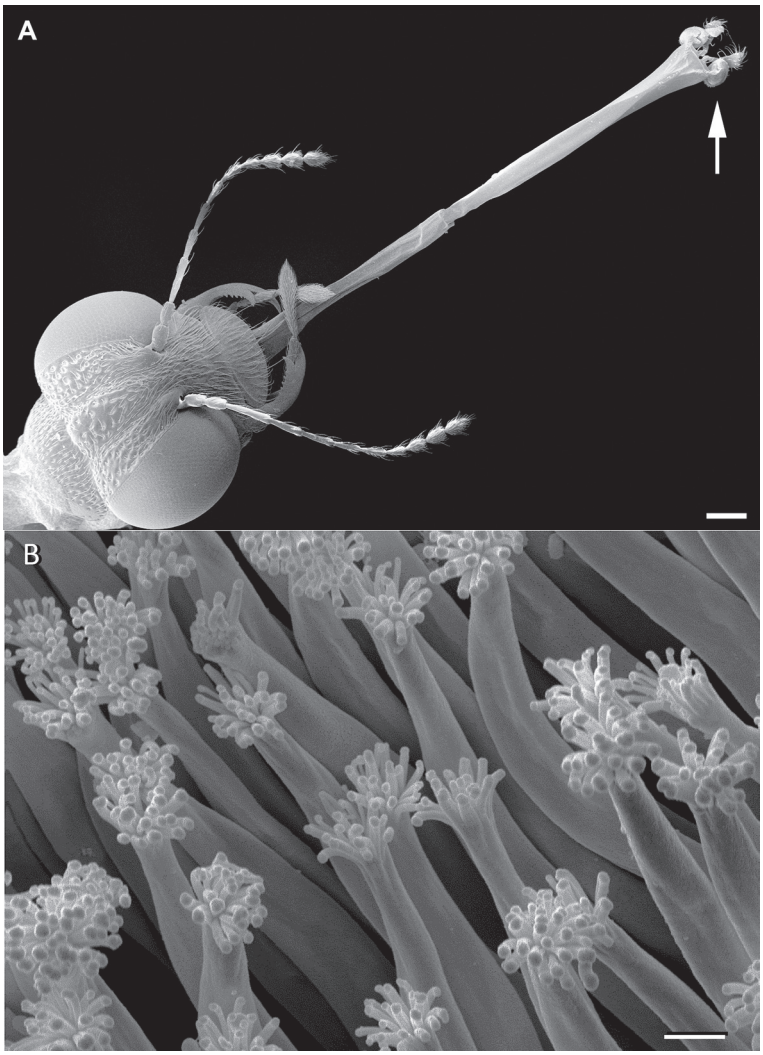

Fig. 1. SEM of a *Stenus bimaculatus* beetle. (A) Head with protruded labium, which, at its tip, bears two paraglossae (arrow) modified into adhesive pads. (B) Adhesive trichomes on the surface of the adhesive pads. During prey-capture, these trichomes are deeply immersed into the adhesive secretion in which the reported bacteria occur (cf. Fig. 3C–D in Koerner et al. 2012). Scale bars: (A) 200 µm, (B) 2 µm.

characterized by a unique prey-capture apparatus formed by the rod-shaped lower lip (labium) with two adhesive pads (the modified paraglossae) (e.g., Schmitz 1943, Weinreich 1968, Betz 1996, 1998b) whose surface is differentiated into numerous terminally branched outgrowths (Fig. 1). The adhesive pads obtain their adhesive function via an adhesive secretion that is produced in special glands within the head capsule and secreted onto their surface (Schmitz 1943, Weinreich 1968, Kölsch 2000, Betz, Koerner & Gorb 2009, Koerner, Gorb & Betz 2011, 2012). The aim of our study was (1) to detect microscopically bacteria within the adhesive secretion of the labial pads and (2) to identify these bacteria by using 16S rRNA sequence analysis. In this way, we intended to elucidate whether the *Stenus* sticky adhesive pads contained a bacterial community. This knowledge might contribute to our understanding of the possible function of the adhesive secretion that occurs on the labial adhesive prey-capture apparatus of these beetles and that is possibly modified by their bacterial fauna. It might also reveal the way that the antimicrobial alkaloids stenusine and norstenusine (Lusebrink, Dettner & Seifert 2008) produced by the pygidial glands of these beetles affect the final composition of the bacterial community on the outer cuticle of these beetles.

2. Materials and Methods

2.1. Transmission electron microscopy

Stenus bimaculatus Gyllenhal, 1810, and *Stenus juno* (Paykull, 1789) beetles were anesthetized with carbon dioxide, killed with diethyl ether, and kept in a vial on ice. The labia were fixed with glutaraldehyde (2.5% solution in 0.1 M cacodylate buffer, pH 7.4) and osmium tetroxide (1% solution in buffer), gradually dehydrated in isopropanol and propylene oxide, and embedded in Spurr's medium (Electron Microscopy Sciences). Serial ultrathin sections were stained with uranyl acetate and lead citrate (Robinson et al. 1985), mounted on single-slot grids on Formvar film, and viewed in a Siemens Elmiskop 101 (Siemens, Germany) or a Philips Tecnai 10 (FEI, The Netherlands) transmission electron microscope.

2.2. Isolation of bacteria from beetles and their identification

Adult beetles of *S. bimaculatus* and *S. juno* were collected from the reed zone of a small pond near Tübingen, Southern Germany (48° 31′ 30.74″ N 9° 00′ 46.53″ E) in January, June, and July 2010 and 2011 and kept in transparent plastic boxes (20 × 10 × 6 cm) on moist plaster of Paris mixed with 5% activated charcoal in order to prevent microbial infection. Smear preparations of the adhesive pads on LB (Luria broth) plates were obtained between 1–14 days after capture in the field. In order to analyze the bacteria within the secretion of the adhesive pads, two different methods were used: (1) beetles were anesthetized with carbon dioxide and pulled over the

surface of LB plates with their adhesive pads (4 *S. bimaculatus*, 2 *S. juno* beetles), or (2) beetles were anesthetized with diethylether, and their adhesive pads were cut off with scissors and placed directly onto LB plates made of nutrient agar (10 g nutrient broth, 5 g yeast extract, 5 g NaCl, 15 g agar-agar in 1 l H_2O) (1 *S. bimaculatus*, 2 *S. juno* beetles). The LB plates were incubated at room temperature for 7–10 days, and growing bacterial colonies were streaked onto LB in order to obtain single colonies. They were purified by re-streaking several times on LB agar. Morphological homogeneity was microscopically analyzed (Zeiss Axiophot, Sony 3CCD color video camera, Zeiss, Germany) (Fig. 2). DNA was extracted from single colonies by using the Aqua Pure genomic DNA kit of Bio-Rad (Hercules, CA, USA). Bacterial 16S rRNA genes were amplified by the polymerase chain reaction (PCR) in 20 µl reactions with the primers 27f (5′-AGAGTTTGATCMTGGCTCAG-3′) and 1492r (5′-TACGGYTACCTTGTTACGACTT-3′) (Lane 1991). Thermal cycling was as follows: 3 min at 95 °C followed by 35 cycles of 15 sec at 95 °C, 30 sec at 55 °C, 1.5 min at 72 °C, and a final step of 8 min at 72 °C. The reaction mixture contained 2 µl 10x PCR buffer, 2 µl 2 mM dNTPs, 1 µl 10 mM 27f primer, 1 µl 10 µM 1492r primer, one unit of Taq DNA polymerase, 12.8 µl H_2O, and 1 µl bacterial DNA. The PCR products were examined by agarose gel electrophoresis (Sambrook, Fritsch & Maniatis 1989), and the bands were excised. DNA was extracted from the bands by using the QIAquick gel extraction kit (Qiagen, Valencia, CA, USA). PCR products were added to the Big Dye terminator sequencing mix (Applied Biosiences, Foster City, CA, USA) and sequenced by using the primers initially used for amplification (see above). Gene sequences were aligned by using Seqman (DNA Star, Madison, WI, USA) and compared with the GenBank database sequences by using BLAST searches with 90% sequence similarity matches.

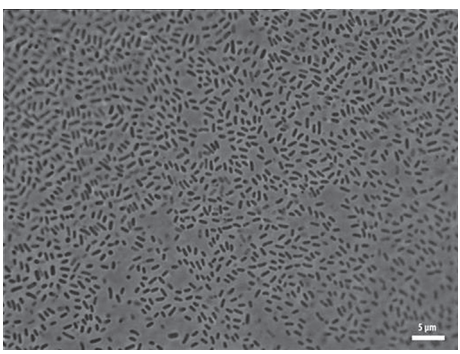

Fig. 2. Light micrograph of *Pseudomonas oryzihabitans* isolated and cultivated from the adhesive pad of *Stenus bimaculatus*. Scale bar: 5 µm.

3. Results

3.1. Transmission electron microscopy

In some regions of the adhesive secretion, our TEM analyses revealed high densities of bacteria whose diameters were ca. 0.3 µm (Fig. 3). They showed their highest densities at the base of the adhesive trichomes, whereas they thinned out towards the periphery of the adhesive pads (Fig. 3A). As shown in Fig. 3D, the bacteria contained dense material in addition to that accounted for by DNA and ribosomes. In some cells, the material was condensed into defined particles. Some bacteria were surrounded by long dense fimbriae that extended from the bacterial cells and served for adhesion of the bacteria to surfaces (arrows in Fig. 3D).

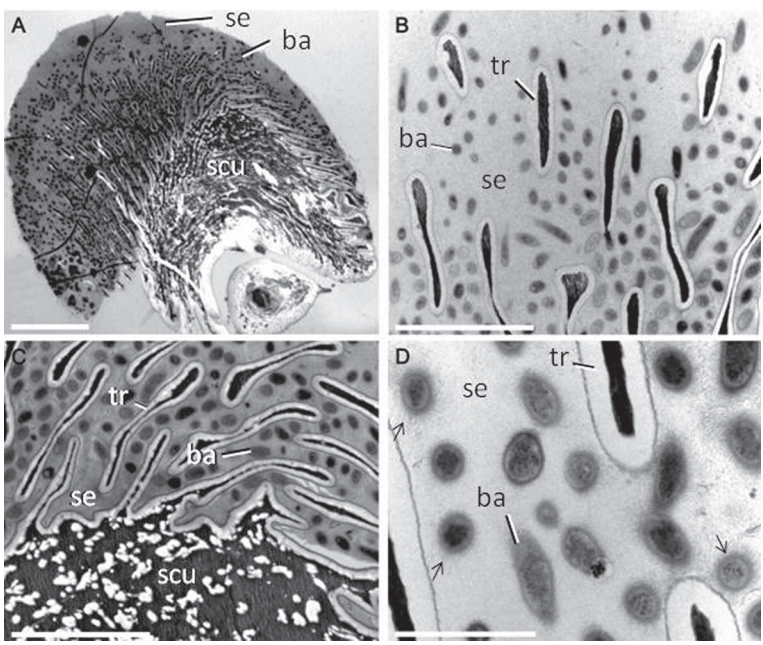

Fig. 3. TEMs of transverse sections through an adhesive pad of *Stenus bimaculatus* showing the bacteria within the adhesive secretion. (A) Overview of an entire adhesive pad. (B)–(D) Higher magnification views of (A) showing bacteria immersed in the adhesive secretion. The arrows indicate fibrous material (fimbriae) around the bacterial cells. Scale bars: (A) 10 µm, (B) 2.5 µm, (C) 2µm, (D) 1 µm. Abbreviations: ba bacteria, se secretion, scu sponge-like cuticle, tr adhesive trichomes (= adhesive "hairs").

Table 1. Bacteria that were isolated from the secretion of the adhesive pads of *S. juno* and *S. bimaculatus* and that could be cultivated on nutrient agar. The assignment of the established 16S rRNA sequences to bacterial strains was carried out according to their closest similarity to sequences reported in GenBank. Bacteria species that co-occurred in the same adhesive pad, are labeled with identical special signs in column four. The numbers in column four are indicative of the number of *Stenus* individuals, in which this bacterium was found.

Stenus species	Identified bacterial order	Identified bacterial genus / species GenBank accession numer	Co-occurrence / number of records	Ecological / physiological characteristics
bimaculatus	Actinomycetales	*Microbacterium arabinogalactanolyticum* strain B15 KM210235.1	+ / 1	aerobe; glycosidases; multiple metal resistant
		Rhodococcus sp. KAR52 KR055013.1	+ / 1	aerobe; heterotrophic soil bacterium; metabolizes many organic substances
	Enterobacteriales	*Pantoea agglomerans* FJ614257.1	1	aerobe; on plant materials; in the gut of other insects
	Flavobacteriales	*Chryseobacterium jejuense* dbi/AB682422.1	+ / 2	aerobe soil bacterium; yellow-pigmented
	Pseudomondales	*Acinetobacter* sp. SFX14 KP717090	+ / 2	aerobe soil bacterium
		Acinetobacter Artichoke A3 KM587007.1	+ / 1	
		Acinetobacter berenziniae KM062029.1	+ / 1	
		Pseudomonas oryzihabitans IHB B 136211 KP762549.1		saprotrophic soil bacterium; yellow-pigmented
juno	Actinomycetales	*Arthrobacter* sp. BS2 KR063192.1	1	soil bacterium; metabolizes many organic nutritional substances
		Arthrobacter nikotianae BS 12 KR063192.1	1	
	Flavobacteriales	*Chryseobacterium* sp. HJ-85 JQ511867.1	# / 1	mostly aerobe; associated with aquatic animals
	Lactobacillales	*Enterococcus haemoperoxidus* NBRC 100709 1136936.1	# / 1	aerobe; isolated from water
	Pseudomonadales	*Acinetobacter Iwoffii* ex19 KF317889.1	# / 1	

3.2. Molecular identification of the bacteria

Sequencing of the 16S ribosomal RNA gene revealed a diverse bacterial composition within the adhesive secretion (Table 1) with eight bacterial sequences being present in *S. bimaculatus* and five in *S. juno*. The majority of the bacteria belonged to the Actinomycetales (*Arthrobacter*, *Microbacterium*, *Rhodococcus*) and Pseudomonadales (*Acinetobacter*, *Pseudomonas*).

In two cases, in which the adhesive pads were cut off and directly placed on the LB plates, we established the co-occurrence of several bacterial species from different orders in the same adhesive pad (cf. column 4 in Table 1).

4. Discussion

In this study, we intended to determine (1) whether the adhesive secretion of the sticky pads (i.e., the modified paraglossae of the labium) of the beetles of the genus *Stenus* contained bacteria and (2) the extent of the diversity of the bacterial population. Betz, Koerner & Gorb (2009) applied histochemical tests to fresh adhesive pads and identified water-soluble sugars, proteins and lipids, thereby revealing that the secretion is a complex mix of more than one chemical phase. Our present analysis has demonstrated an additional component of the adhesive secretion, namely a diverse set of bacteria. Since beetles freshly collected in the field possess bacteria, we conclude that bacteria naturally occur within the adhesive secretion of *Stenus*, in which they might use the various components of the secretion as a commensalic food source. The 13 identified bacterial species demonstrate an extensive variety, although this diversity is probably even larger, since only those species have been identified that can be cultivated in vitro.

In the abdominal accessory genital glands of *Stenus comma*, de Marzo (1994) reported dense masses of rod-like bacteria with a possible symbiotic function. In contrast, in his ultrastructural work on *Stenus* spp. (including *S. comma*), Kölsch (2000) did not detect any intracellular bacteria within the internal head glands that produce and transport the secretion towards the surface of the sticky pads. Hence, the bacteria that we have found in the adhesive secretion probably do not stem from the interior of the *Stenus* beetles and also do not move from the sticky adhesive pads into the gland tissue.

The effect of the detected infestation of the adhesive secretion on the beetles requires further investigations. Further microbiological characterization of the established bacteria might elucidate the way that they possibly influence the chemical composition of the secretion itself, as this might have an influence on the adhesive performance of the adhesive pads and thus the prey-capture success of the beetles.

Our work now offers an opportunity to study the influence of antimicrobial substances, such as the alkaloids stenusine and norstenusine produced by the abdominal pygidial glands of *Stenus* beetles, on the overall composition of the bacteria fauna on the outer cuticular surface. *Stenus* beetles show extensive grooming behavior (Betz 1999, Lusebrink, Dettner & Seifert 2008), whereby they cover their cuticle with these

antimicrobial alkaloids. Since the grooming behavior of the beetles does not include the adhesive pads at the tip of the labium (personal observation), these pads are probably not protected against microbial infestation, which might lead to a higher and qualitatively different bacterial diversity in the adhesive secretion compared with that on the outer cuticle.

Acknowledgements

16s RNA sequencing was performed by Hanh Witte, Deptartment for Evolutionary Biology and the microbiological experiments were carried out by Stephanie Helbig, Deptartment of Protein Evolution, both Max Planck Institute for Developmental Biology, Tübingen. Theresa Jones corrected the English. This work was supported by a grant from the German Research Foundation (DFG No. PAK 478) to Oliver Betz.

References

Betz, O. (1996): Function and evolution of the adhesion-capture apparatus of *Stenus* species (Coleoptera, Staphylinidae). – Zoomorphology **116:** 15–34.

Betz, O. (1998a): Life forms and hunting behaviour of some Central European *Stenus* species (Coleoptera, Staphylinidae). – Applied Soil Ecology **9:** 69–74.

Betz, O. (1998b): Comparative studies on the predatory behaviour of *Stenus* spp. (Coleoptera: Staphylinidae): the significance of its specialized labial apparatus. – Journal of Zoology **244:** 527–544.

Betz, O. (1999): A behavioural inventory of adult *Stenus* species (Coleoptera: Staphylinidae). – Journal of Natural History **33:** 1691–1712.

Betz, O. (2002): Performance and adaptive value of tarsal morphology in rove beetles of the genus *Stenus* (Coleoptera, Staphylinidae). – Journal of Experimental Biology **205:** 1097–1113.

Betz, O., Koerner, L. & Gorb, S. (2009): An insect's tongue as the model for two-phase viscous adhesives? – adhesion Adhesives & Sealants **3:** 32–35.

Enders, D., Tiebes, J., De Kimpe, N., Keppens, M., Stevens, C., Smagghe, G. & Betz, O. (1993): Enantioselective synthesis and determination of the configuration of stenusine, the spreading agent of the beetle *Stenus comma*. – Journal of Organic Chemistry **58:** 4881–4884.

Kölsch, G. (2000): The ultrastructure of glands and the production and function of the secretion in the adhesive capture apparatus of *Stenus* species (Coleoptera: Staphylinidae). – Canadian Journal of Zoology **78:** 465–475.

Koerner, L., Gorb, S. & Betz, O. (2011): Adhesive performance of the stick-capture apparatus of rove beetles of the genus *Stenus* (Coleoptera, Staphylinidae) toward various surfaces. – Journal of Insect Physiology **58:** 155–163.

Koerner, L., Gorb, S. & Betz, O. (2012): Functional morphology and adhesive performance of the stick-capture apparatus of the rove beetles *Stenus* spp. (Coleoptera, Staphylinidae). – Zoology **115:** 117–127.

Lane, D.J. (1991): 16S/23S rRNA sequencing. – In: Stackebrandt, E. & Goodfellow, M. (eds): Nucleic acid techniques in bacterial systematics. – John Wiley & Sons, 184–189.

Lusebrink, I., Dettner, K. & Seifert, K. (2008): Stenusine, an antimicrobial agent in the rove beetle genus *Stenus* (Coleoptera, Staphylinidae). – Naturwissenschaften **95:** 751–755.

Marzo de, L. (1994): Simbiosi batterica in *Stenus comma peroculatus* Putz (Coleoptera. Staphylinidae). – Atti XVII Congresso nationale italiano di Entomologia, 335–338.

Puthz, V. (2010): *Stenus* Latreille, 1797 aus dem Baltischen Bernstein nebst Bemerkungen über andere fossile *Stenus*-Arten (Coleoptera, Staphylinidae). – Entomologische Blätter **106:** 265–287.

Puthz, V. (2013): Übersicht über die orientalischen Arten der Gattung *Stenus* Latreille 1797 (Coleoptera, Staphylinidae). 330. Beitrag zur Kenntnis der Steninen. – Linzer biologische Beiträge **45/2:** 1279–1470.

Robinson, D.G., Ehlers, U., Herken, R., Hermann, B., Mayer, F. & Schürmann, F.-W. (1985): Präparationsmethodik in der Elektronenmikroskopie. – Springer, Berlin.

Sambrook, J., Fritsch, E.F. & Maniatis, T. (1989): Molecular Cloning: A Laboratory Manual. – Cold Spring Harbor Press, New York.

Schildknecht, H., Berger, D., Krauss, D., Connert, J., Gehlhaus, J. & Essenbreis, H. (1976): Defense chemistry of *Stenus comma* (Coleoptera: Staphylinidae). LXI. – Journal of Chemical Ecology **2** (1): 1–11.

Schmitz, G. (1943): Le labium et les structures bucco-pharyngiennes du genre *Stenus* Latreille. – Cellule **49:** 291–334.

Weinreich, E. (1968): Über den Klebfangapparat der Imagines von *Stenus* Latr. (Coleopt., Staphylinidae) mit einem Beitrag zur Kenntnis der Jugendstadien dieser Gattung. – Zeitschrift für Morphologie und Ökologie der Tiere **62:** 162–210.

Manuscript received: 10 October 2015
Accepted: 14 January 2016

Publikation V

Loss of the sticky harpoon—COI sequences indicate paraphyly of *Stenus* with respect to *Dianous* (Staphylinidae, Steninae)

Lars Koerner, Michael Laumann, Oliver Betz, Michael Heethoff

Zoologischer Anzeiger 252 (2013): 337–347

Zoologischer Anzeiger 252 (2013) 337–347

Contents lists available at SciVerse ScienceDirect

Zoologischer Anzeiger

journal homepage: www.elsevier.de/jcz

Zoologischer Anzeiger

Loss of the sticky harpoon – COI sequences indicate paraphyly of *Stenus* with respect to *Dianous* (Staphylinidae, Steninae)

Lars Koerner*, Michael Laumann, Oliver Betz, Michael Heethoff*

Department of Evolutionary Biology of Invertebrates, Institute for Evolution and Ecology, University Tübingen, Auf der Morgenstelle 28E, 72076 Tübingen, Germany

ARTICLE INFO

Article history:
Received 16 April 2012
Received in revised form 7 September 2012
Accepted 20 September 2012
Available online 16 October 2012
Corresponding Editor: Michael Ohl.

Keywords:
Cytochrome oxidase I
mtDNA
Phylogeny
Labium

ABSTRACT

The speciose staphylinid subfamily Steninae comprises more than 2700 species of the two genera *Stenus* and *Dianous*. Whereas the labium of *Dianous* beetles is short and unspecialized, the members of *Stenus* are characterized by a protruding elongated labium that functions as a prey-capture apparatus. This is considered the derived state and the most prominent apomorphic character for *Stenus*. To elucidate the phylogenetic relationship of *Stenus* and *Dianous*, we analyzed 807 bp of the mitochondrial cytochrome c oxidase I (COI) gene in 30 *Stenus* and 12 *Dianous* species. Our analysis indicates the evolutionary origin of *Dianous* within *Stenus*, suggesting a secondary loss of the specialized prey-capture apparatus. Whereas the derived phylogenetic position of *Dianous* within *Stenus* is supported by maximum parsimony, neighbor joining, maximum likelihood, and Bayesian analyses, the resolution of COI seems to be insufficient to consistently resolve basal relationships of *Stenus* species.

1. Introduction

The Steninae is a subfamily of the staphylinine group (i.e. subfamily groups of Lawrence and Newton, 1982) within the Staphylinidae (rove beetles), containing only two genera, i.e. *Stenus* Latreille 1797 and *Dianous* Leach 1819. The monophyly of Steninae is supported by many larval and adult autapomorphies (Puthz, 1981; Hansen, 1997; Leschen and Newton, 2003; Thayer, 2005; Grebennikov and Newton, 2009; Clarke and Grebennikov, 2009) and suggested also by molecular analysis (Grebennikov and Newton, 2009). The subfamily Steninae might also include a third, as yet undescribed genus possessing a prey-capture apparatus similar to that in *Stenus* (Leschen and Newton, 2003; Betz and Kölsch, 2004; Clarke and Grebennikov, 2009).

With almost 2500 species (Puthz, 2010), *Stenus* is one of the largest beetle genera and, with the exception of New Zealand, is distributed worldwide (Puthz, 1971, 2010). The most obvious autapomorphic character defining *Stenus* is a harpoon-like protruding elongated labium with the paraglossae being modified into sticky (adhesive) pads (Fig. 1A and B; Weinreich, 1968; Puthz, 1981; Betz, 1996, 2006). This prey-capture apparatus can be rapidly protruded toward the potential prey by increased haemolymph pressure (Bauer and Pfeiffer, 1991; Betz, 1996; Kölsch and Betz, 1998; Heethoff et al., 2011a; Heethoff and Raspotnig, 2012; Koerner et al., 2012a,b). In *Dianous* species, the labium is also slightly protrudable but much shorter and does not form an adhesive prey-capture apparatus, i.e. the paraglossae are not modified into adhesive pads (Fig. 1C and D; Weinreich, 1968; Puthz, 1981). Accordingly, *Dianous* beetles catch their prey solely using their mandibles.

The genus *Stenus* is classified into five subgenera, i.e. *Stenus* s.str., *Hemistenus* Motschulsky 1860, *Hypostenus* Rey 1884, *Metatesnus* Adam 1987 and *Tesnus* Rey 1884 (Puthz, 2001, 2008). This classification is based on the morphology of the 4th segments of the metatarsi (simple or bi-lobed), the relative length of the 1st and 5th segment of the metatarsi, the relative length of the metatarsi and metatibiae and the presence or the absence of abdominal paratergites (e.g. Cameron, 1930; Freude et al., 1964; Zhao and Zhou, 2004). This subgeneric classification of *Stenus* seems to be artificial and does probably not reflect the true phylogenetic relationships among species (e.g. Puthz, 1972, 2003). Therefore, a more elaborate classification of *Stenus* species into monophyletic species groups has been suggested (summarized in Puthz, 2008).

Although the genus *Stenus* has been considered monophyletic on the basis of its possession of the labial adhesive capture apparatus and several other adult (mostly related to the prey-capture apparatus) and larval characters, the genus *Dianous* is not defined by any autapomorphies (Puthz, 1981; Clarke and Grebennikov, 2009). Grebennikov and Newton (2009) have suggested three autapomorphic characters for the genus *Dianous*, but their analysis was based only on one *Dianous* species. Since some members of the species groups of *Dianous* greatly differ morphologically (Puthz, 1981, 2000; Shi and Zhou, 2011), they may even represent several

* Corresponding authors.
E-mail addresses: larskoerner3@hotmail.com (L. Koerner), michael@heethoff.de (M. Heethoff).

0044-5231/$ – see front matter © 2012 Elsevier GmbH. All rights reserved.
http://dx.doi.org/10.1016/j.jcz.2012.09.002

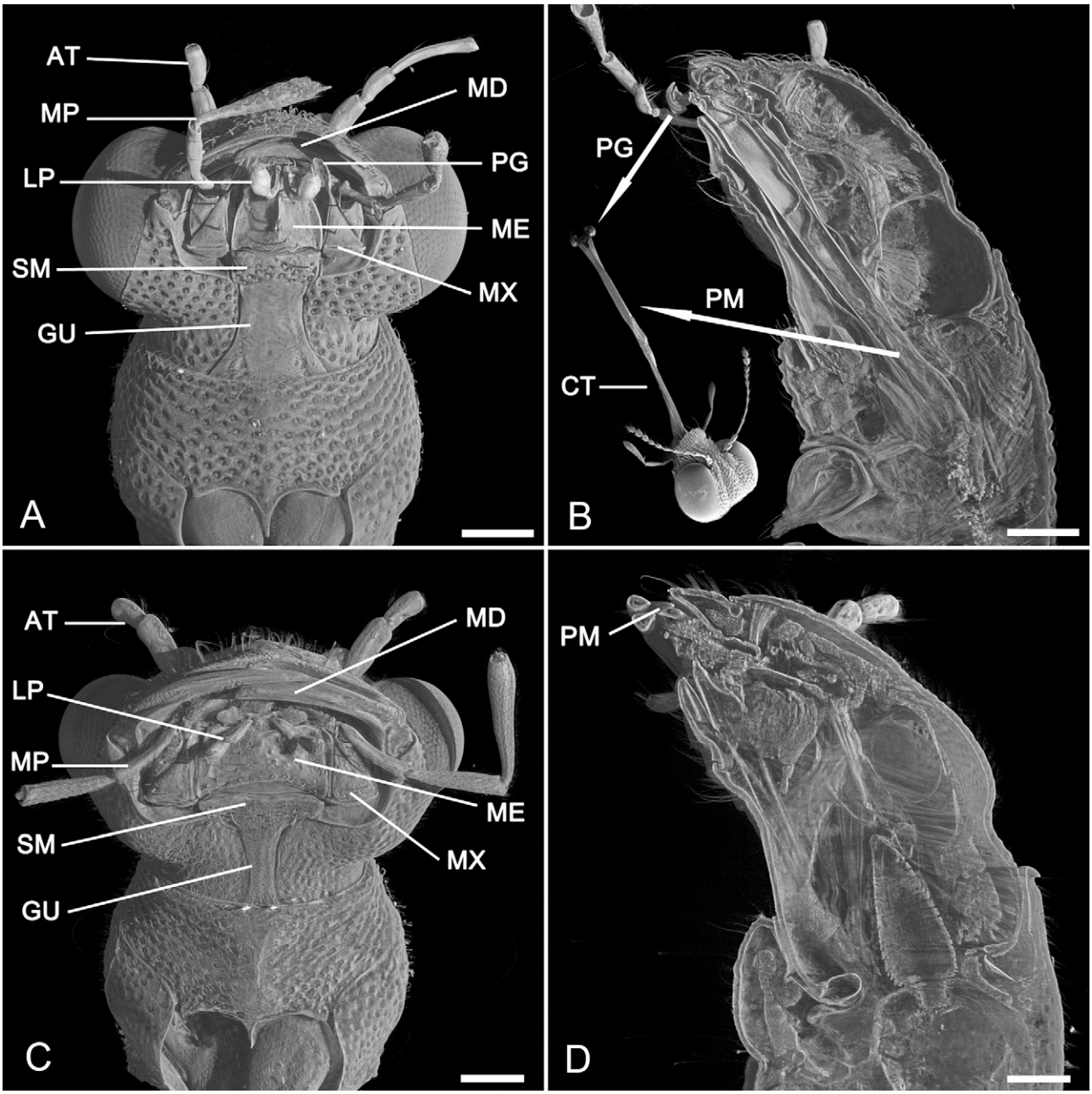

Fig. 1. Head morphology of *Stenus cicindeloides* in the resting position (A, B) and *Dianous coerulescens* (C, D) as investigated by Synchrotron μCT. (A, C) Three-dimensional model of the head (ventral aspect); (B, D) sagittal virtual section through the head. The inset in (B) is a scanning electron micrograph of the head with the protruded labium. Scale bars = 0.2 mm, inset not to scale. *Abbreviations*: AT, antenna; CT, connecting labial tube; GU, gula; LP, labial palp; MD, mandible; ME, mentum; MP, maxillary palp; MX, maxilla; PG, paraglossa modified into adhesive pad; PM, prementum; SM, submentum.

genera (Puthz, 1981). According to Puthz (1981), the genus *Dianous* forms a 'plesiomorphic, perhaps paraphyletic group and continues to represent a taxonomic unit which must be used as long as this genus cannot be defined phylogenetically'.

The genus *Dianous* comprises more than 210 species (e.g. Shi and Zhou, 2009, 2011) and is distributed in the Oriental, the Palaearctic and the Nearctic regions with its main distribution in Asia (India, China and Southeast Asia). According to the morphology of the frons (frontal area of the head), it can be categorized into species groups I and II (Puthz, 1981, 2000; Shi and Zhou, 2011; Tang et al., 2011). In contrast to *Dianous* group II (e.g. Fig. 1C), the members of *Dianous* group I (about 30% of all *Dianous* species) have large "*Stenus*"-like eyes and were traditionally considered to belong to the genus *Stenus*, until it was recognized that they do not possess the typical prey-capture apparatus of this genus (Puthz, 1981).

The aim of the current study was to clarify the phylogenetic relationships of *Stenus* and *Dianous* on the basis of a molecular phylogeny using the barcoding gene cytochrome oxidase I. Our results indicate that *Stenus* is paraphyletic with respect to *Dianous* species group II, suggesting that the labial morphology of *Dianous* reflects a process of secondary reduction of the formerly more complex prey-capture apparatus rather than its precursor.

2. Materials and methods

2.1. Material examined

Molecular analyses were conducted with 21 species of the genus *Stenus* and one representative of the genus *Dianous* (Table 1). The species were collected in Germany and identified according to

Table 1
Taxonomic coverage of species, species groups (*Stenus*; Puthz, 2008) or species complexes (*Dianous*; Shi and Zhou, 2011) and subgenera of Steninae used in the phylogenetic analysis.

Genus	Subgenus	Species group/ species complex	Species	Collecting locality	GenBank accession no.
Ingroup					
Stenus	*Stenus* s.str.	*ater*	*bimaculatus* Gyllenhal, 1810	Germany, Schleswig-Holstein, Kiel	JQ085757
				Germany, Schleswig-Holstein, Friedrichsruh	JQ085758
			juno (Paykull, 1789)	Germany, Schleswig-Holstein, Kiel	JQ085760
				Canada, Alberta	JQ085761
			lustrator Erichson, 1839	Germany, Bavaria, Bayreuth area	JQ085766
				Germany, Baden-Württemberg, Tübingen	JQ085767
		clavicornis	*clavicornis* (Scopoli, 1763)	Germany, Baden-Württemberg, Tübingen	JQ085764
				Germany, Schleswig-Holstein, Kiel	JQ085765
			providus Erichson, 1839	Germany, Baden-Württemberg, Tübingen	JQ085762
				Germany, Baden-Württemberg, Tübingen	JQ085763
		comma	*comma* Leconte, 1863	Germany, Baden-Württemberg, Tübingen	JQ085769
				Canada, Alberta	JQ085771
				China	EU546120[a]
			biguttatus (Linnaeus, 1758)	Germany, Schleswig-Holstein, Strande	JQ085772
				Germany, Schleswig-Holstein, Strande	JQ085773
			insignatus Puthz, 1981	China, Hainan Prov., Qiongzhong County, Limu shan	EU546116[a]
				China, Hainan Prov., Qiongzhong County, Limu shan	EU546122[a]
			tenuipes Sharp, 1874	China, Shanghai City	EU546121[a]
				China, Shanghai City	EU546124[a]
		guttula	*guttula* Müller, 1831	Germany, Schleswig-Holstein, Strande	JQ085774
				Germany, Baden-Württemberg, Tübingen	JQ085775
			fossulatus Erichson, 1840	Germany, Schleswig-Holstein, Strande	JQ085776
				Germany, Schleswig-Holstein, Strande	JQ085777
		boops	*boops* Ljungh, 1804	Germany, Baden-Württemberg, Tübingen	JQ085778
				Germany, Baden-Württemberg, Tübingen	JQ085779
			melanarius Stephens, 1883	China, Shanghai City	EU546113[a]
				China, Shanghai City	EU546115[a]
		canaliculatus	*canaliculatus* Gyllenhal, 1827	Germany, Baden-Württemberg, Tübingen	JQ085780
				Germany, Baden-Württemberg, Tübingen	JQ085781
			nitens Stephens, 1833	Germany, Baden-Württemberg, Tübingen	JQ085782
		humilis	*humilis* Erichson, 1839	Germany, Baden-Württemberg, Tübingen	JQ085783
				Germany, Baden-Württemberg, Tübingen	JQ085784
			proclinatus L. Benick, 1922	China, Shanghai City	EU546110[a]
	Tesnus	*crassus*	*pilosiventris* Bernhauer, 1915	China, Guizhou Prov., Tongren City, Mayanghe N. R.	EU546114[a]
	Hypostenus	*similis*	*similis* (Herbst, 1784)	Germany, Bavaria, Limmersdorfer Forst	JQ085788
				United Kingdom	DQ155964[a]
			cicindeloides (Schaller, 1783)	Germany, Schleswig-Holstein, Flintbek	JQ085785
				Hainan Prov.	EU546123[a]
			solutus Erichson, 1840	Germany, Schleswig-Holstein, Strande	JQ085789
				Germany, Schleswig-Holstein, Strande	JQ085790
		tarsalis	*tarsalis* Ljungh, 1804	Germany, Schleswig-Holstein, Flintbek	JQ085794
				Germany, Bavaria, Limmersdorfer Forst	JQ085795
	Metatesnus	*bifoveolatus*	*bifoveolatus* Gyllenhal, 1827	Germany, Schleswig-Holstein, Kiel	JQ085796
				Germany, Schleswig-Holstein, Kiel	JQ085797
		picipes	*nitidiusculus* Stephens, 1833	Germany, Schleswig-Holstein, Langwedel	JQ085801
				Germany, Baden-Württemberg, Tübingen	JQ085802
		pubescens	*pubescens* Stephens, 1833	Germany, Baden-Württemberg, Tübingen	JQ085803
	Hemistenus	*impressus*	*impressus* Germar, 1824	Germany, Schleswig-Holstein, Kiel	JQ085804
		tenuimargo	*rugipennis* Sharp, 1874	China, Zhejiang	EU546118[a]
		abdominalis	*coronatus* L. Benick, 1928	China, Beijing	EU546127[a]
		indubius	*paradecens* Tang and Li, 2005	China, Anhui	EU546128[a]
		tenuimargo	*tenuimargo* Cameron, 1913	China, Yunnan Prov., Jinghong City, Nabanhe N. R.	GU214744[a]
Dianous	Group II	*coerulescens*	*coerulescens* (Gyllenhal, 1810)	Germany, Bavaria, Röslau, Eger Falls	JQ085805
				United Kingdom	DQ156046[a]
		calceatus	*srivichaii* Rougemont, 1981	Yunnan Prov., Jinghong City, Nabanhe N. R.	GU214729[a]
			alternans Zheng, 1993	Yunnan Prov., Jinghong City, Nabanhe N. R.	GU214730[a]
			punctiventris Champion, 1919	Yunnan Prov., Jinghong City, Nabanhe N. R.	GU214731[a]
			obliquenotatus Champion, 1921	Yunnan Prov., Jinghong City, Nabanhe N. R.	GU214732[a]
			elegantulus Zheng, 1993	Guizhou Prov., Tongren City, Mayanghe N. R.	EU546129[a]
		ocellatus	*pseudacutus* Puthz, 2009	Yunnan Prov., Jinghong City, Nabanhe N. R.	GU214733[a]
			ocellifer Puthz, 2000	Yunnan Prov., Jinghong City, Nabanhe N. R.	GU214734[a]
			verticosus Eppelsheim, 1895	Yunnan Prov., Jinghong City, Nabanhe N. R.	GU214735[a]
		aereus-andrewesi	*vietnamensis* Puthz, 1980	Yunnan Prov., Jinghong City, Nabanhe N. R.	GU214736[a]
			andrewesi Cameron, 1914	Yunnan Prov., Jinghong City, Nabanhe N. R.	GU214743[a]
		chinensis	*banghaasi* Bernhauer, 1916	Guizhou Prov., Tongren City, Mayanghe N. R.	GU214741[a]
Outgroup					
Euaesthetus (Euaesthetinae)			*ruficapillus*		DQ155946[a]
Euconnus (Scydmaeninae)			sp.		DQ221972[a]

[a] Sequences taken from GenBank.

Freude et al. (1964). Canadian species were kindly provided by Dr. Inka Lusebrink and identified by Dr. Volker Puthz. Two individuals per species (if available: from different locations) were analyzed. Abdomens of the investigated specimens are kept in 70% ethanol in the collection of the Department of Evolutionary Biology of Invertebrates at the University of Tuebingen, Germany. Sequences of additional 9 *Stenus* and 11 *Dianous* species were taken from GenBank (Table 1). We used the following species as outgroups (sequences from GenBank; Table 1): *Euaesthetus ruficapillus* (Staphylinidae, Euaesthetinae) and *Euconnus* sp. (Staphylinidae, Scydmaeninae).

2.2. Sample preparation, PCR and sequencing

All specimens were stored in 70% ethanol at −20 °C until preparation. Prior to the extraction, the abdomen was removed to prevent contamination by DNA of food remains or parasites (Maus et al., 2001). For extraction of total genomic DNA, the DNeasy Tissue Kit (Qiagen, Hilden, Germany) was used. DNA was extracted according to the manufacturer's protocol. The polymerase chain reaction (PCR) was performed with GoTaq® PCR Core System I (Promega, Madison, USA); the total reaction of 20 μl contained 1.5 mM $MgCl_2$, 200 μM of each dNTP, 100 pmol of each primer and 1.25 Units of GoTaq® DNA polymerase. A fragment of approximately 800 bp of the mitochondrial cytochrome c oxidase I (COI) gene including the tRNA leucine gene was amplified using the primers C1-J-2183 (alias Jerry) and TL2-N-3014 (alias Pat; Simon et al., 1994). PCR conditions were: an initial denaturation step at 95 °C for 2 min, followed by 9 cycles of 95 °C (30 s) denaturation, 46 °C (1 min) annealing and 72 °C (45 s) extension and subsequently 34 cycles of 95 °C (30 s) denaturation, 51 °C (1 min) annealing and 72 °C (45 s). The PCR was terminated at 72 °C (5 min) for the final extension. Purification of the amplified DNA was performed using a silica membrane (MinElute PCR Purification Kit, Qiagen, Hilden, Germany). Sequencing reaction was carried out in both directions directly on the purified PCR product by Macrogen Inc. (Korea).

All sequences were submitted to GenBank (see Table 1 for accession numbers, www.ncbi.nlm.nih.gov).

2.3. Sequence analysis

Sequences were aligned manually without ambiguous positions. Phylogenetic analyses were based on Maximum Parsimony (MP), Neighbor Joining (NJ) and Maximum Likelihood (ML) algorithms using PAUP* (Swofford, 1999). For ML and NJ in PAUP*, the best-fit models of sequence evolution were estimated using the BIC criterion with ModelTest (Posada and Crandall, 1998) and ModelTest Server (Posada, 2006). The best-fit model was TVM + I + G (I: 0.311, G: 0.297) with base frequencies: freqA = 0.4073, freqC = 0.0796, freqG = 0.0431, freqT = 0.47 and substitution rates: R(a) = 0.3808, R(b) = 9.5773, R(c) = 0.4732, R(d) = 3.3755, R(e) = 9.5773 and R(f) = 1.0. MP and ML analyses in PAUP* were performed with the starting tree resulting from stepwise addition and 100 replicates of random order. The TBR swapping was used for heuristic tree search. Reliability of nodes was ascertained from 100 bootstrap replicates with identical search strategies as for the original tree for MP, and with ML-parameters and NJ as tree-reconstruction method for NJ and ML. Bayesian phylogeny estimation (BA) was calculated with MrBayes 3.1.2 (Ronquist and Huelsenbeck, 2003). Two runs were performed for 3 million generations to reach a standard deviation below 0.01. Trees were sampled every 1000 generations with a burn-in of 25%. The analyses were initiated using the default random tree option, and the substitution model was set to GTR + G + I, the most closely related model to the modeltest suggestion TVM + G + I. Posterior probabilities were estimated and trees were combined to a 50% majority rule consensus tree.

3. Results

3.1. Sequence characteristics and variation

The aligned matrix of 67 sequences from 44 species (12 species of *Dianous* group II, 30 *Stenus*, 2 outgroup) included in the analyses consisted of 807 nucleotide positions, 422 of them being variable and 382 parsimony-informative. The highest uncorrected sequence p-distance within the ingroup (Steninae) was 22.7% between *Stenus tarsalis* and *Stenus pilosiventris*. The within-group mean p-distance for taxa within *Stenus* was 15.5% and 11.0% for taxa within *Dianous*. The between-group mean distance of *Stenus* and *Dianous* was 15.7%.

3.2. Phylogenetic analysis and assessment of node support

We used different phylogenetic analysis methods to assess the phylogenetic relationships of *Stenus* and *Dianous*. Consistent topologies from different analyses are most likely robust, since they are independent of the assumptions of the phylogenetic inference method.

The most important result of our analysis is that all trees (Figs. 2–5) consistently recover the analyzed *Dianous* species of group II as a monophyletic group (Bayesian posterior probability (BPP) = 1.0 bootstrap of MP (BS_{MP}) = 81; bootstrap of ML/NJ ($BS_{ML/NJ}$) = 83), always clustering within a paraphyletic *Stenus*. There is strong Bayesian, but low MP and ML/NJ support (BPP, BS_{MP}, $BS_{ML/NJ}$ = 0.93, 21, 33) for a lineage that includes *Dianous* and one cluster of the subgenus *Stenus* s.str. (*S. ater*-, *clavicornis*-, *humilis*- and *guttula*-group).

Consistent tree topologies that appear in all phylogenetic analyses are highlighted in gray in Figs. 2–5. All trees consistently recover the cluster consisting of the *S. ater*-, *clavicornis*- and *humilis*-group (BPP, BS_{MP}, $BS_{ML/NJ}$ = 0.99, 78, 94) and the *S. guttula*-group (BPP, BS_{MP}, $BS_{ML/NJ}$ = 1.0, 100, 100) with high support values. Additionally, the only investigated species of the subgenus *Tesnus*, *S. pilosiventris*, forms a monophyletic cluster with the *Stenus canaliculatus*- and *boops*-group of the subgenus *Stenus* s.str. (BPP, BS_{MP}, $BS_{ML/NJ}$ = 1.0, 83, 78).

Our analyses further support a monophyletic relationship of the five investigated species of the subgenus *Hemistenus* (BPP, BS_{MP}, $BS_{ML/NJ}$ = 1.0, 89, 84), whereas the subgenera *Stenus* s.str., *Hypostenus* and *Metatesnus* appear as para- or polyphyletic. All analyses confirm the placement of *Stenus paradecens* within the subgenus *Hemistenus* (Tang and Yun-Long, 2008), which was originally described as belonging to *Hypostenus* (Tang and Li, 2005). Our data do not resolve relationships among the subgenera *Hypostenus* and *Metatesnus*, although the MP- and NJ-analysis indicate a monophyly of the investigated species belonging to both these subgenera.

The basal arrangement of the members of the subgenera *Hypostenus* and *Metatesnus* is supported by BA. However, basal arrangements within the Steninae based on MP, ML and NJ are inconsistently recovered and show only low bootstrap support (values below 50). Analyses based on ML and BA (Figs. 2 and 5) revealed species of the subgenera *Hypostenus* and *Metatesnus* as the basal groups of the Steninae. In contrast, MP and NJ analyses (Figs. 3 and 4) revealed members of the *Stenus comma*-group as basal groups (NJ: *S. biguttatus*, MP: *S. comma*).

Our analysis supports a close relationship of the following species, which belong to same species group of *Stenus* as defined

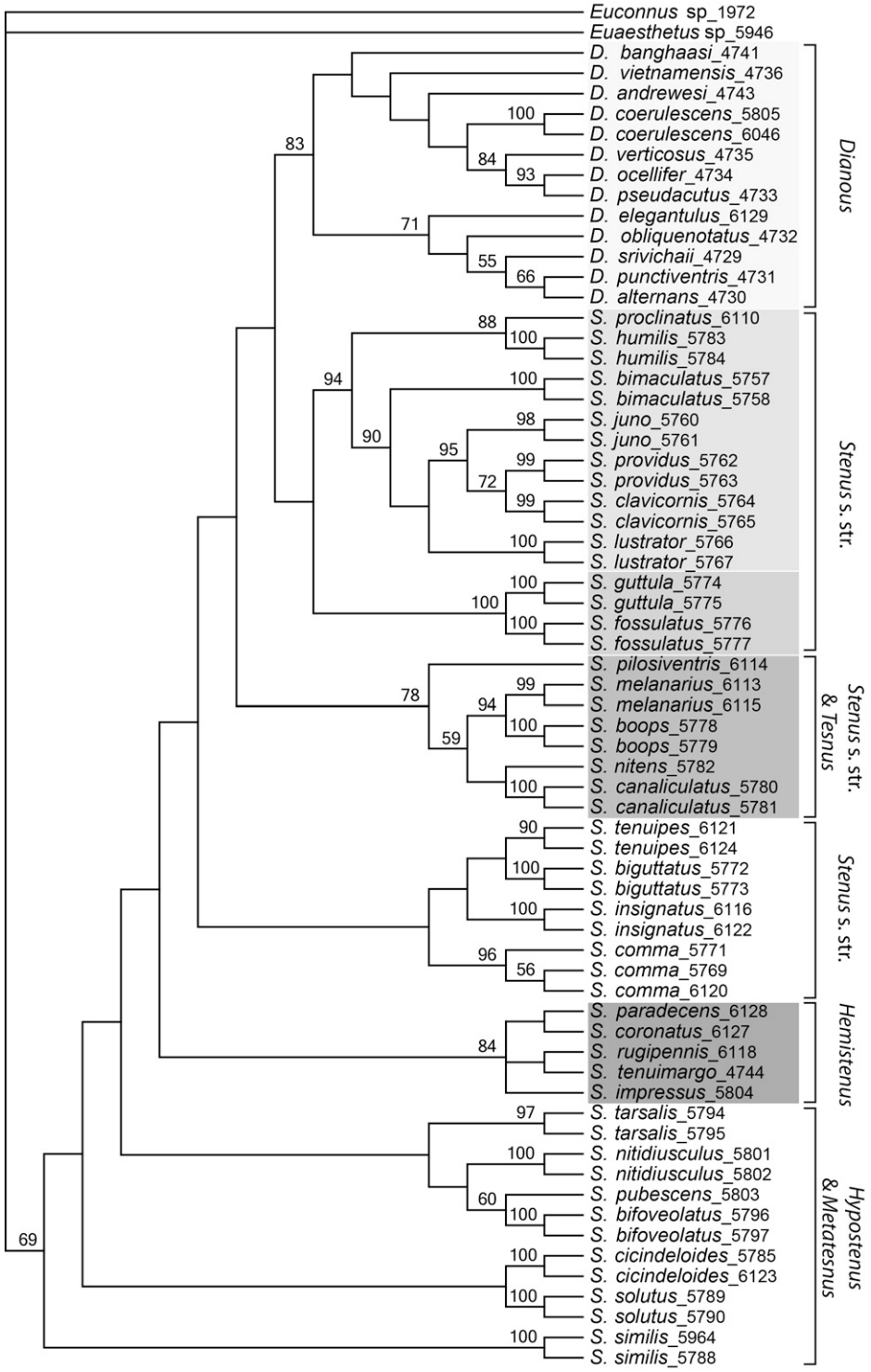

Fig. 2. Strict consensus tree resulting from the maximum-likelihood analysis (−ln *L* = 12,334.76; three trees found). The four numbers after the species name indicate the last four numbers of the accession number in GenBank (see Table 1 for species details). The numbers above the branches are bootstrap values from 100 replicates (indicated if greater than 50%). Consistent tree topologies that appear in all phylogenetic analyses (Figs. 2–5) are highlighted in gray.

by Puthz (2001, 2008): (1) *S. guttula* and *S. fossulatus*, (2) *S. humilis* and *S. proclinatus*, and (3) *S. boops* and *S. melanarius*. Additionally, the paraphyletic *S. ater* group (*S. lustrator*, *S. bimaculatus*, *S. juno*) together with the *S. clavicornis* group (*S. providus*, *S. clavicornis*) is recovered in all trees as a monophylum. A close relationship of these species is also supported on the basis of morphology (V. Puthz, pers. comm.). The monophyly of the *S. comma* group (*S. comma*, *S. biguttatus*, *S. insignatus*, *S. tenuipes*) is supported only by the BA (BPP = 0.88) and ML (Figs. 2 and 5).

The analyzed species of *Dianous* (all belonging to species group II) form a monophyletic cluster with high bootstrap support (Figs. 2–5). The *Dianous* group II is currently divided into eight

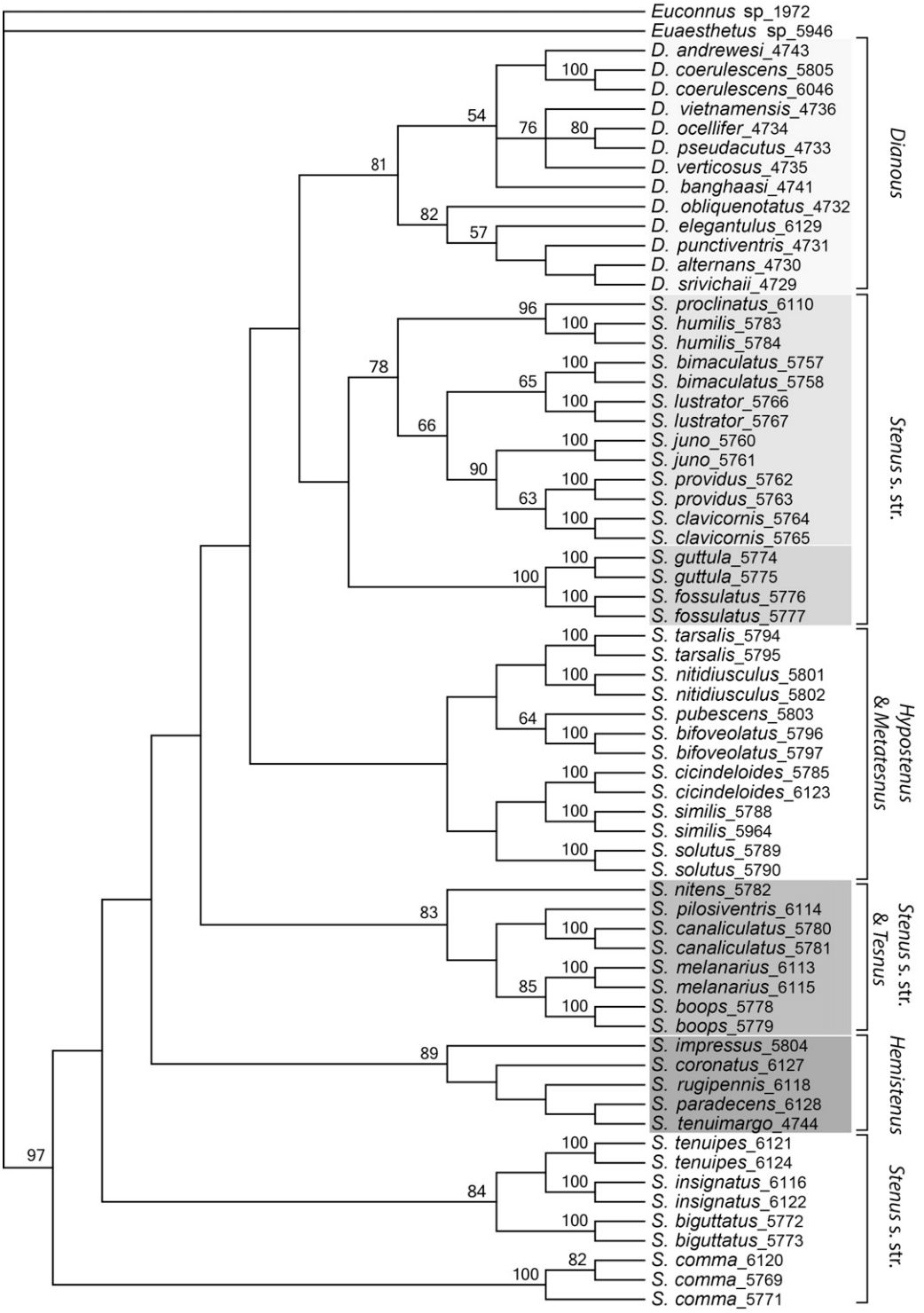

Fig. 3. Strict consensus tree resulting from three most-parsimonious trees of a length of 2781 steps (CI: 0.26, RI: 0.6). The four numbers after the species name indicate the last four numbers of the accession number in GenBank (see Table 1 for species details). The numbers above the branches are bootstrap values from 100 replicates (indicated if greater than 50%). Consistent tree topologies that appear in all phylogenetic analyses (Figs. 2–5) are highlighted in gray.

species complexes (Puthz, 2000, 2005), of which five were included in our analyses (two groups with one species and three with at least two species; Table 1). Our results support the *ocellatus*-complex (*Dianous ocellifer*, *D. verticosus*, *D. pseudacutus*) (BPP, $BS_{ML/NJ}$ = 1.0, 84) and the *calceatus*-complex (*D. alternans*, *D. elegantulus*, *D. obliquenotatus*, *D. punctiventris*, *Dianous srivichaii*) (BPP, BS_{MP}, $BS_{ML/NJ}$ = 1.0, 82, 71), but not the *aereus-andrewesi*-complex (*D. andrewesi*, *D. vietnamensis*).

4. Discussion

4.1. General considerations

The COI gene is widely used as a taxonomic barcode for species identification and biogeographic analysis (e.g. Folmer et al., 1994; Hebert et al., 2003; Ribera et al., 2003, 2004; Pons et al., 2006; Hunt et al., 2007; Heethoff et al., 2011b). This gene is used as a standard

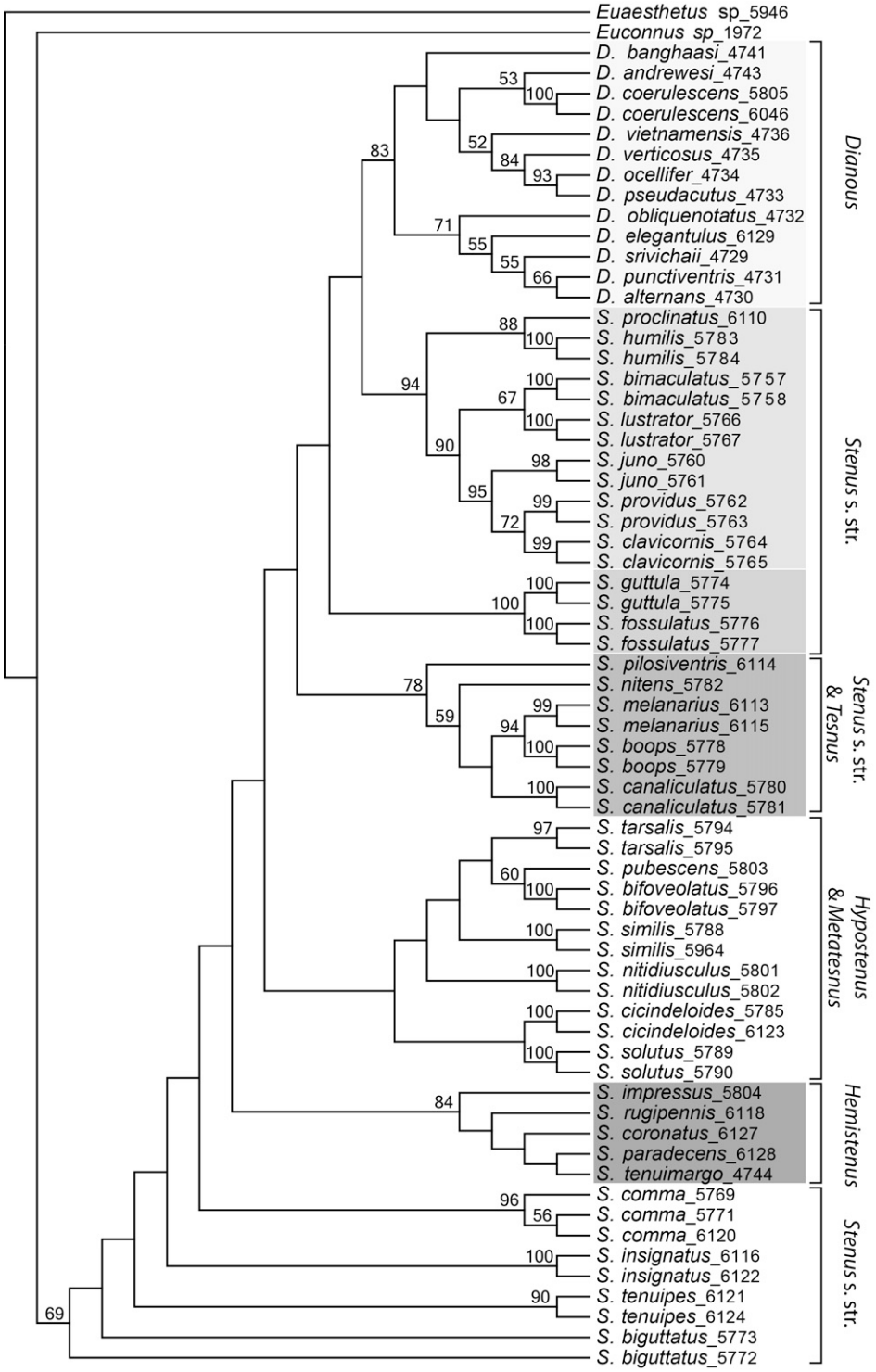

Fig. 4. Neighbor-joining tree based on ML-distances. The four numbers after the species name indicate the last four numbers of the accession number in GenBank (see Table 1 for species details). The numbers above the branches are bootstrap values from 100 replicates (indicated if greater than 50%). Consistent tree topologies that appear in all phylogenetic analyses (Figs. 2–5) are highlighted in gray.

barcode, because (1) the universal primers are extremely robust and (2) it possesses a greater range of phylogenetic signal than any other mitochondrial gene (Hebert et al., 2003).

Our results show that COI is also suitable for resolving the phylogenetic relationships within the subfamily of Steninae. The trees obtained by the different phylogenetic methods used revealed many consistent features of the tree topology. However, the basal phylogenetic arrangement of the Steninae lacks resolution. This lack of resolution of basal relationships may result from multiple divergence events over a short time frame (Maddison, 1989). Similar to the Steninae, the reason for the lack of basal resolution in the staphylinid genus *Aleochara* probably resulted not from

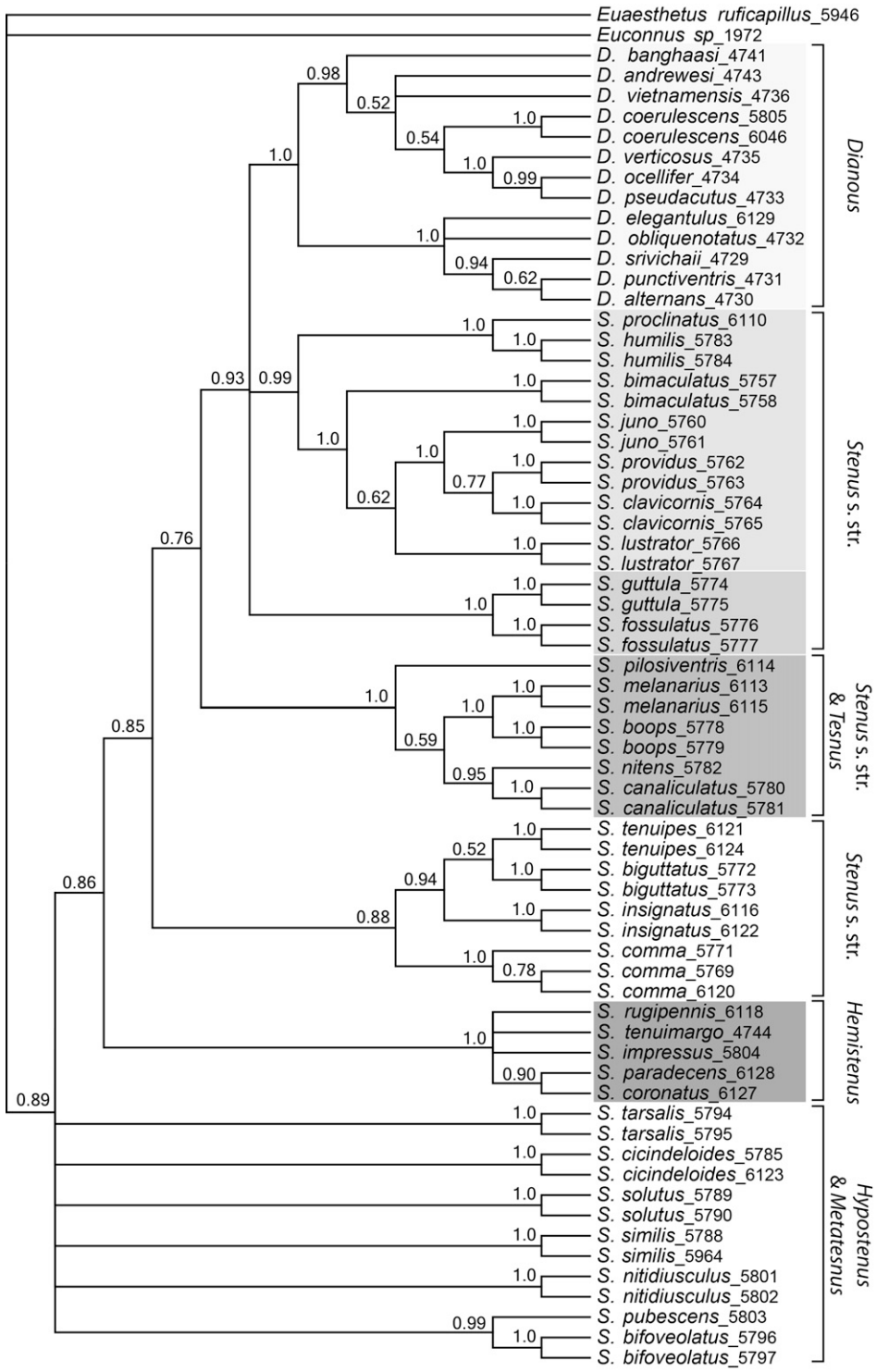

Fig. 5. Maximum a posterior (MAP) tree from Bayesian analysis. The four numbers after the species name indicate the last four numbers of the accession number in GenBank (see Table 1 for species details). The numbers above the branches indicate Bayesian posterior probabilities. Consistent tree topologies that appear in all phylogenetic analyses (Figs. 2–5) are highlighted in gray.

the unsuitability of the cytochrome oxidase genes, but might also reflect a phase of rapid evolution in which case the branching events took place in a short time (Maus et al., 2001). Further investigations with a higher taxon sampling and other genes with a higher degree of conservation are needed to resolve the basal phylogenetic arrangement of the Steninae, as the COI might be evolving too fast to detect the more basal relationships.

4.2. Molecular phylogeny of Steninae as supported by chemotaxonomical aspects

The most important result of our study is the consistent position of the *Dianous* species of group II originating within *Stenus*, therefore rendering *Stenus* paraphyletic. All gene trees recovered a derived position of *Dianous* as a sister clade to one cluster

of the subgenus *Stenus* s.str. (*S. ater*, *clavicornis*-, *humilis*- and *guttula*-group). The paraphyly of *Stenus* with respect to *Dianous* also agrees with previous results based on genomic 18S rDNA reported by Grebennikov and Newton (2009). According to them, the two analyzed *Stenus* species are more closely related to *Dianous nitidulus* (belonging to *Dianous* group II) than to a third *Stenus* species.

A close relationship of *Dianous* and *Stenus* is also supported by chemotaxonomy (Lusebrink, 2007) and the morphology of the paired pygidial glands (Jenkins, 1957), which are considered a synapomorphic character for Steninae (Clarke and Grebennikov, 2009). These pygidial glands release a spreading-active secretion (Jenkins, 1960; Betz, 1999; Lusebrink et al., 2007) that propels the beetle over the water with high velocities (Darlington, 1929; Jenkins, 1957, 1960; Betz, 1999; Lusebrink et al., 2007). This "skimming" behavior is known from *Dianous coerulescens* (Jenkins, 1957, 1960), *D. nitidulus* (Darlington, 1929) and several species of *Stenus* (Jenkins, 1960; Betz, 1999). The chemical component responsible for this movement is the alkaloid stenusine (*N*-ethyl-3-(2-methylbutyl)-piperidine), which is known solely from the subfamily of Steninae (Kanehisa and Tsumuki, 1996); it was found building the major component of the pygidial glands in many *Stenus* species and in *D. coerulescens* (Lusebrink, 2007). The other components of the pygidial glands of *D. coerulescens* are also identical to those found in *Stenus* species (Lusebrink, 2007).

4.3. Implications for the evolution of the labial prey-capture apparatus within Steninae

The genus *Stenus* has been hypothesized to be monophyletic based on the possession of its protruding elongated labium (e.g. Weinreich, 1968; Puthz, 1981; Clarke and Grebennikov, 2009). The labium of *Dianous* is much shorter and lacks the adhesive pads of *Stenus* but is also slightly eversible (Weinreich, 1968). Because of its simple labium and the developed paratergites at the abdomen, *Dianous* has always been considered more primitive than *Stenus* (Naomi, 1988; Shi and Zhou, 2011). However, according to our phylogenetic analyses, we conclude that *Dianous* and *Stenus* might be congeneric and that the simple labial morphology of *Dianous* probably reflects a process of secondary reduction of a formerly more complex prey-capture apparatus.

Interestingly, the secondary reduction (vestigialization) of the labial prey-capture apparatus seems to have also occurred in at least one other phylogenetic lineage within the genus *Stenus*, since most species of the *S. canaliculatus* group possess simplified labia that are largely shortened and have only minute paraglossae (Lars Koerner, unpublished data; Betz, 1996: Fig. 11, 1998, 2006: Fig. 13). This assumption is supported by our phylogenetic analyses, because both *Dianous* and the *S. canaliculatus* group (*Stenus nitens*, *S. canaliculatus*) cluster within species groups possessing complex labia. In *S. canaliculatus*, the labium has lost its original function as a prey-capture apparatus (Betz, 1996, 1998, 2006). Instead, these beetles seize their prey solely by means of their somewhat modified long saber-like mandibles that are well suited to grasping large prey. Similar selective demands might be responsible for the reduction of the labial prey-capture apparatus in *Dianous*. Betz (1998) reports that most *Stenus* species cannot seize quickly moving prey (e.g. collembolans) precisely and rapidly enough with their mandibles and concludes that mandibles are principally useful in catching sluggish prey. For *D. coerulescens*, Pfeiffer (1989) showed that these beetles mainly feed on slow-moving prey, such as soft-bodied arthropods and their larvae (e.g. larval Diptera and Coleoptera) that are captured by means of their mandibles. If this is a general pattern for *Dianous*, similar to some *Stenus* species, the specialization of *Dianous* with regard to the mandible attack type might have entailed their labium eventually becoming vestigial.

4.4. Intrageneric phylogeny of Stenus and Dianous

Our results do not support the traditional classification of *Stenus* in five subgenera (e.g. Cameron, 1930; Freude et al., 1964; Zhao and Zhou, 2004), since the subgenera *Stenus* s.str., *Hypo*- and *Metatesnus* appear as para- or polyphyletic. Instead, our phylogenetic data agree with the classification of *Stenus* into several monophyletic species groups as suggested by Puthz (2001, 2008). The morphological characters used for the traditional subgeneric classification are of little value for the phylogeny of *Stenus* (Puthz, 1972, 2003). For example, the *Stenus indubius* group (e.g. *S. paradecens*) traditionally fits into the subgenus *Hypostenus*, because of the absence of abdominal paratergites. Contrarily it is evidenced by the apomorphic character of the spermatheca in addition to some external structures that the *S. indubius* group has a close relationship with some *Hemistenus* species (Naomi, 2006; Tang and Yun-Long, 2008). Our molecular analysis also supports this positioning of *S. paradecens* within *Hemistenus*, giving further support that the presence or the absence of the abdominal paratergites is of low phylogenetic relevance. The validity of this conclusion is also strengthened by the finding of individuals with or without abdominal paratergites even within a single species (e.g. *S. crassus*; Benick, 1935).

According to Puthz (1968), the species of the traditional subgenus *Tesnus* actually belong to at least six monophyletic groups, with the *S. crassus* group (e.g. *S. pilosiventris*) being closely related to the subgenus *Stenus* s.str. (incl. *S. fuscipes* and *S. argus* that were formerly classified in the subgenus *Nestus*). This assumption is confirmed by our phylogenetic analysis, since the analyzed species *S. pilosiventris* of the subgenus *Tesnus* is included within the subgenus *Stenus* s.str. (*S. boops*- and *S. canaliculatus*-group) with high support values.

Our MP, NJ and ML analyses suggest a close relationship of the investigated species of *Hypostenus* and *Metatesnus*. This assumption is also supported on chemotaxonomic basis, since (i) the pygidial gland component (*Z*)- and (*E*)-3-(2′-Methyl-1′-butenyl)-pyridine is exclusively abundant in most *Hypostenus* species and *Stenus pubescens* and *Stenus binotatus* of *Metatesnus*, and (ii) the alkaloid 3-(1-isobutenyl)-pyridine, which is restricted to *Stenus solutus* and *Stenus cicindeloides* of *Hypostenus* and to *S. pubescens* and *S. binotatus* of *Metatesnus* (Lusebrink et al., 2009).

5. Conclusion

Our results indicate that the analyzed *Dianous* species of group II form a monophyletic group within *Stenus*. The phylogeny within *Dianous* remains largely unknown, however, whether *Dianous* group I and II represent sister-groups or not will not influence our conclusion that *Stenus* is not monophyletic. The internal phylogeny and the basal phylogenetic arrangement of the Steninae remain to be elucidated in detail by the analysis of other genes and by means of a broader taxon sampling scheme, in particular since the center of origin of this staphylinid subfamily presumably lies in Asia (Puthz, 2010). However, our data strongly support the inclusion of at least the *Dianous* group II into *Stenus* and therefore the paraphyly of *Stenus*.

Conflict of interest statement

The authors declare no conflicts of interests.

Acknowledgments

We wish to thank Dr. Inka Lusebrink (University of Southampton, UK), Dr. Liang Tang (Shanghai Normal University, China), Daniela Weide and Gerwin Gold for their valuable discussions, for providing beetles and for reviewing the manuscript. We also thank Dr. P. Cloetens and Dr. L. Helfen (both ESRF, Grenoble, France) for their support at the beamline ID 19 (ESRF-project SC-2127 of MH). We thank Dr. Theresa Jones for linguistic editing. This study was financed by a Grant from the Wilhelm-Schuler-Stiftung to MH.

References

Bauer, T., Pfeiffer, M., 1991. 'Shooting' springtails with a sticky rod: the flexible hunting behaviour of *Stenus comma* (Coleoptera Staphylinidae) and the counter-strategies of its prey. Animal Behaviour 41, 819–828.

Benick, L., 1935. *Stenus crassus* Scholzianus nov. var. Entomologische Blätter 31, 100–103.

Betz, O., 1996. Function and evolution of the adhesion-capture apparatus of *Stenus* species (Coleoptera Staphylinidae). Zoomorphology 116, 15–34.

Betz, O., 1998. Comparative studies on the predatory behaviour of *Stenus* spp. (Coleoptera: Staphylinidae): the significance of its specialized labial apparatus. Journal of Zoology 244, 527–544.

Betz, O., 1999. A behavioural inventory of adult *Stenus* species (Coleoptera: Staphylinidae). Journal of Natural History 33, 1691–1712.

Betz, O., 2006. Der Anpassungswert morphologischer Strukturen: Integration von Form Funktion und Ökologie am Beispiel der Kurzflügelkäfergattung *Stenus* (Coleoptera Staphylinidae). Entomologie heute 18, 3–26.

Betz, O., Kölsch, G., 2004. The role of adhesion in prey capture and predator defence in arthropods. Arthropod Structure & Development 33, 3–30.

Cameron, M., 1930. The Fauna of British India including Ceylon and Burma. Coleoptera: Staphylinidae, Vol. 1 (Micropeplinae, Oxytelinae, Oxyporinae, Steninae and Enaesthetinae). Taylor & Francis, London.

Clarke, D.J., Grebennikov, V.V., 2009. Monophyly of Euaesthetinae (Coleoptera: Staphylinidae): phylogenetic evidence from adults and larvae, review of austral genera, and new larval descriptions. Systematic Entomology 34, 346–397.

Darlington Jr., P.J., 1929. Habits of the staphylinid beetle *Dianous nitidulus*. Psyche 36, 386.

Folmer, O., Black, M., Hoeh, W., Lutz, R., Vrijenhoek, R., 1994. DNA primers for amplification of mitochondrial cytochrome c oxidase subunit I from diverse metazoan invertebrates. Molecular Marine Biology and Biotechnology 3, 294–297.

Freude, H., Harde, K.W., Lohse, G.A., 1964. Die Käfer Mitteleuropas, Bd. 4, Staphylinidae I. (Micropeplinae bis Tachyporinae). Goecke & Evers, Krefeld.

Grebennikov, V.V., Newton, A.F., 2009. Good-bye Scymaenidae, or why the ant-like stone beetles should become megadiverse Staphylinidae sensu latissimo (Coleoptera). European Journal of Entomology 106, 275–301.

Hansen, M., 1997. Phylogeny and classification of the staphyliniform beetle families (Coleoptera). Biologiske Skrifter 48, 1–339.

Hebert, P.D.N., Cywinska, A., Ball, S.L., deWaard, J.R., 2003. Biological identifications through DNA barcodes. Proceedings of the Royal Society of London Series B 270, 313–321.

Heethoff, M., Koerner, L., Norton, R.A., Raspotnig, G., 2011a. Tasty but protected – first evidence of chemical defense in oribatid mites. Journal of Chemical Ecology 37, 1037–1043.

Heethoff, M., Laumann, M., Weigmann, G., Raspotnig, G., 2011b. Integrative taxonomy: combining morphological, molecular and chemical data for species delineation in the parthenogenetic *Trhypochthonius tectorum* complex (Acari Oribatida, Trhypochthoniidae). Frontiers in Zoology 8, 2.

Heethoff, M., Raspotnig, G., 2012. Expanding the 'enemy-free space' for oribatid mites: evidence for chemical defense of juvenile *Archegozetes longisetosus* against the rove beetle *Stenus juno*. Experimental and Applied Acarology 56, 93–97.

Hunt, T., Bergsten, J., Levkanicova, Z., Papadopoulou, A., John, O.S., Wild, R., Hammond, P.M., Ahrens, D., Balke, M., Caterino, M.S., Gómez-Zurita, J., Ribera, I., Barraclough, T.G., Bocakova, M., Bocak, L., Vogler, A.P., 2007. A comprehensive phylogeny of beetles reveals the evolutionary origins of a superradiation. Science 318, 1913–1916.

Jenkins, M.F., 1957. The morphology and anatomy of the pygidial glands of *Dianous coerulescens* Gyllenhal (Coleoptera: Staphylinidae). Proceedings of the Royal Entomological Society of London. Series A, General Entomology 32, 159–167.

Jenkins, M.F., 1960. On the method by which *Stenus* and *Dianous* (Coleoptera: Staphylinidae) return to the banks of a pool. Transactions of the Royal Entomological Society of London 112, 1–14.

Kanehisa, K., Tsumuki, H., 1996. Pygidial secretion of *Stenus* rove beetles (Coleoptera: Staphylinidae). Bulletin of the Research Institute for Bioresources Okayama University 4, 25–31.

Kölsch, G., Betz, O., 1998. Ultrastrucure and function of the adhesion-capture apparatus of *Stenus* species (Coleoptera Staphylinidae). Zoomorphology 118, 263–272.

Koerner, L., Gorb, S.N., Betz, O., 2012a. Adhesive performance of the stick-capture apparatus of rove beetles of the genus *Stenus* (Coleoptera Staphylinidae) toward various surfaces. Journal of Insect Physiology 58, 155–163.

Koerner, L., Gorb, S.N., Betz, O., 2012b. Adhesive performance and functional morphology of the stick-capture apparatus of the rove beetles *Stenus* spp. (Coleoptera Staphylinidae). Zoology 115, 117–127.

Lawrence, J.F., Newton, A.F., 1982. Evolution and classification of beetles. Annual Review of Ecology and Systematics 13, 261–290.

Leschen, R.A.B., Newton, A.F., 2003. Larval description, adult feeding behaviour, and phylogenetic placement of *Megalopinus* (Coleoptera: Staphylinidae). Coleopterists Bulletin 57, 469–493.

Lusebrink, I., 2007. Stereoisomerie, Biosynthese und biologische Wirkung des Stenusins sowie weitere Inhaltsstoffe der Pygidialdrüsen der Kurzflügelkäfer Gattung *Stenus* (Staphylinidae, Coleoptera). Inaugural-Dissertation. University of Bayreuth, Bayreuth, Germany.

Lusebrink, I., Burkhardt, D., Gedig, T., Dettner, D., Mosandl, A., Seifert, K., 2007. Intrageneric differences in the four stereoisomers of stenusine in the rove beetle genus, *Stenus* (Coleoptera Staphylinidae). Naturwissenschaften 94, 143–147.

Lusebrink, I., Dettner, K., Müller, T., Seifert, K., Daolio, C., Schneider, B., Schmidt, J., 2009. New pyridine alkaloids from rove beetles of the genus *Stenus* (Coleoptera: Staphylinidae). Zeitschrift für Naturforschung 64, 271–278.

Maddison, W.P., 1989. Reconstructing character evolution on polytomous cladograms. Cladistics – The International Journal of the Willi Hennig Society 5, 365–377.

Maus, C., Peschke, K., Dobler, S., 2001. Phylogeny of the genus *Aleochara* inferred from mitochondrial cytochrome oxidase sequence (Coleoptera: Staphylinidae). Molecular Phylogenetics and Evolution 18, 202–216.

Naomi, S.-I., 1988. Studies on the subfamily Steninae (Coleoptera, Oxyporidae) from Japan I. New or little known species of the genus *Dianous* Leach (Coleoptera Oxyporidae). Transactions of the Shikoku Entomological Society 19, 47–54.

Naomi, S.-I., 2006. Taxonomic revision of the genus *Stenus* Latreille, 1797 (Coleoptera Staphylinidae, Steninae) of Japan: species group of *S. indubius* Sharp. Japanese Journal of Systematic Entomology 12, 39–120.

Pfeiffer, M., 1989. Augenbau und Beutefang bei *Stenus comma*, Leconte, 1863 und *Dianous coerulescens*, Leach, 1891. Diploma Thesis. University of Tübingen, Tübingen, Germany.

Pons, J., Barraclough, T.G., Gomez-Zurita, J., Cardoso, A., Duran, D.P., Hazell, S., Kamoun, S., Sumlin, W.D., Vogler, A.P., 2006. Sequence-based species delimitation for the DNA taxonomy of undescribed insects. Systematic Biology 55, 595–609.

Posada, D., Crandall, K.A., 1998. ModelTest: testing the model of DNA substitution. Bioinformatics 14, 817–818.

Posada, D., 2006. ModelTest server: a web-based tool for the statistical selection of models of nucleotide substitution online. Nucleic Acids Research 34, 700–703.

Puthz, V., 1968. Die *Stenus*- und *Megalopinus*-Arten Motschulskys und Bemerkungen über das Subgenus *Tesnus* Rey, mit einer Tabelle der paläarktischen Vertreter (Coleoptera, Staphylinidae) (54. Beitrag zur Kenntnis der Steninen). Notulae Entomologicae 48, 197–219.

Puthz, V., 1971. Revision der afrikanischen Steninenfauna und Allgemeines über die Gattung *Stenus* Latreille (Coleoptera Staphylinidae) (56 Beitrag zur Kenntnis der Steninen). Annales du Musée Royal de l' Afrique Centrale, Tervuren, Série In-8°, Sciences Zoologiques 187, 1–376.

Puthz, V., 1972. Das Subgenus "*Hemistenus*" (Col., Staphylinidae) (86. Beitrag zur Kenntnis der Steninen). Annales Entomologici Fennici 38, 75–92.

Puthz, V., 1981. Was ist *Dianous* Leach, 1819, was ist *Stenus* Latreille, 1796? Oder: Die Aporie des Stenologen und ihre taxonomischen Konsequenzen (Coleoptera, Staphylinidae). Entomologische Abhandlungen, Staatliches Museum für Tierkunde, Dresden 44, 87–132.

Puthz, V., 2000. The genus *Dianous* Leach in China (Coleoptera: Staphylinidae) 261. Contribution to the knowledge of Steninae. Revue Suisse de Zoologie 107, 419–559.

Puthz, V., 2001. Beiträge zur Kenntnis der Steninen CCLXIX Zur Ordnung in der Gattung *Stenus* Latreille, 1796 (Staphylinidae, Coleoptera). Philippia 10, 31–41.

Puthz, V., 2003. Neue und alte Arten der Gattung *Stenus* Latreille aus China (Insecta: Coleoptera: Staphylinidae: Steninae). Entomologische Abhandlungen. Staatliches Museum fiir Tierkunde Dresden 60, 139–159.

Puthz, V., 2005. Notes on Chinese *Dianous* Leach (Coleoptera: Staphylinidae). Entomological Review of Japan 60, 137–152.

Puthz, V., 2008. *Stenus* LATREILLE und die segenreiche Himmelstochter (Coleoptera Staphylinidae). Linzer Biologische Beiträge 40, 137–230.

Puthz, V., 2010. *Stenus* Latreille 1797 aus dem Baltischen Bernstein nebst Bemerkungen über andere fossile *Stenus*-Arten (Coleoptera, Staphylinidae). Entomologische Blätter 106, 265–287.

Ribera, I., Bilton, D.T., Vogler, A.P., 2003. Mitochondrial DNA phylogeography and population history of *Meladema* diving beetles on the Atlantic Islands and in the Mediterranean basin (Coleoptera, Dytiscidae). Molecular Ecology 12, 153–167.

Ribera, I., Nilsson, A.N., Vogler, A.P., 2004. Phylogeny and historical biogeography of Agabinae diving beetles (Coleoptera) inferred from mitochondrial DNA sequences. Molecular Phylogenetics and Evolution 30, 545–562.

Ronquist, F., Huelsenbeck, J.P., 2003. MrBayes 3: Bayesian phylogenetic inference under mixed models. Bioinformatics 19, 1572–1574.

Shi, K., Zhou, H.Z., 2009. A new *Dianous* species (Coleoptera, Staphylinidae Steninae) from China, with a key to Chinese species of the *coerulescens* complex. Deutsche Entomologische Zeitschrift 56, 289–294.

Shi, K., Zhou, H.-Z., 2011. Taxonomy of the genus *Dianous* (Coleoptera: Staphylinidae: Steninae) in China and zoogeographic patterns of its distribution. Insect Science 18, 363–378.

Simon, C., Frati, F., Beckenbach, A., Crespi, B., Liu, H., Flook, P., 1994. Evolution, weighting, and phylogenetic utility of mitochondrial gene sequences and a

compilation of conserved polymerase chain reaction primers. Annals of the Entomological Society of America 87, 651–701.
Swofford, D.L., 1999. PAUP*. Phylogenetic Analysis Using Parsimony (* and other Methods). Version 4. Sinauer Associates, Sunderland, MA.
Tang, L., Li, L.-Z., 2005. Two new species of *Stenus* from Anhui Province, East China (Coleoptera: Staphylinidae). In: Ren, G.D. (Ed.), Classification and Diversity of Insects in China. China Agriculture Science and Technology Press, Beijing, pp. 106–109.
Tang, L., Li, L.-Z., Cao, G.-H., 2011. On Chinese species of *Dianous* group I (Coleoptera, Staphylinidae Steninae). ZooKeys 111, 67–85.
Tang, L., Yun-Long, Z., 2008. Three new Stenus species of the *indubius* group (Coleoptera Staphylinidae) from China. Zootaxa 1741, 51–58.
Thayer, M.K., 2005. Staphylinidae. In: Beutel, R.G., Leschen, R.A.B. (Eds.), Handbook of Zoology, Coleoptera, vol. 1. De Gruyter, Berlin, pp. 296–344.
Weinreich, E., 1968. Über den Klebfangapparat der Imagines von *Stenus* Latr. (Coleopt., Staphylinidae) mit einem Beitrag zur Kenntnis der Jugendstadien dieser Gattung. Zeitschrift für Morphologie und Ökologie der Tierey 62, 162–210.
Zhao, C.Y., Zhou, H.Z., 2004. Five new species of the subgenus *Hemistenus* (Coleoptera: Staphylinidae, Steninae) from China. Pan-Pacific Entomologist 80, 93–108.